

Topics in Current Chemistry 310

Timothy Deming *Editor*

# Peptide-Based Materials

 Springer

**310**

## **Topics in Current Chemistry**

**Editorial Board:**

**K.N. Houk • C.A. Hunter • M.J. Krische • J.-M. Lehn**

**S.V. Ley • M. Olivucci • J. Thiem • M. Venturi • P. Vogel**

**C.-H. Wong • H. Wong • H. Yamamoto**

# Topics in Current Chemistry

## Recently Published and Forthcoming Volumes

### **Peptide-Based Materials**

Volume Editor: Timothy Deming  
Vol. 310, 2012

### **Alkaloid Synthesis**

Volume Editor: Hans-Joachim Knölker  
Vol. 309, 2012

### **Fluorous Chemistry**

Volume Editor: István T. Horváth  
Vol. 308, 2012

### **Multiscale Molecular Methods in Applied Chemistry**

Volume Editors: Barbara Kirchner, Jadran Vrabec  
Vol. 307, 2012

### **Solid State NMR**

Volume Editor: Jerry C. C. Chan  
Vol. 306, 2012

### **Prion Proteins**

Volume Editor: Jörg Tatzelt  
Vol. 305, 2011

### **Microfluidics: Technologies and Applications**

Volume Editor: Bingcheng Lin  
Vol. 304, 2011

### **Photocatalysis**

Volume Editor: Carlo Alberto Bignozzi  
Vol. 303, 2011

### **Computational Mechanisms of Au and Pt Catalyzed Reactions**

Volume Editors: Elena Soriano,  
José Marco-Contelles  
Vol. 302, 2011

### **Reactivity Tuning in Oligosaccharide Assembly**

Volume Editors: Bert Fraser-Reid,  
J. Cristóbal López  
Vol. 301, 2011

### **Luminescence Applied in Sensor Science**

Volume Editors: Luca Prodi, Marco Montalti,  
Nelsi Zaccheroni  
Vol. 300, 2011

### **Chemistry of Opioids**

Volume Editor: Hiroshi Nagase  
Vol. 299, 2011

### **Electronic and Magnetic Properties of Chiral Molecules and Supramolecular Architectures**

Volume Editors: Ron Naaman,  
David N. Beratan, David H. Waldeck  
Vol. 298, 2011

### **Natural Products via Enzymatic Reactions**

Volume Editor: Jörn Piel  
Vol. 297, 2010

### **Nucleic Acid Transfection**

Volume Editors: Wolfgang Bielke,  
Christoph Erbacher  
Vol. 296, 2010

### **Carbohydrates in Sustainable Development II**

Volume Editors: Amélia P. Rauter,  
Pierre Vogel, Yves Queneau  
Vol. 295, 2010

### **Carbohydrates in Sustainable Development I**

Volume Editors: Amélia P. Rauter,  
Pierre Vogel, Yves Queneau  
Vol. 294, 2010

### **Functional Metal-Organic Frameworks: Gas Storage, Separation and Catalysis**

Volume Editor: Martin Schröder  
Vol. 293, 2010

### **C-H Activation**

Volume Editors: Jin-Quan Yu, Zhangjie Shi  
Vol. 292, 2010

# Peptide-Based Materials

Volume Editor: Timothy Deming

With Contributions by

A. Aggeli · A. Altunbas · J. Cheng · U.-J. Choe · R.P.W. Davies ·  
T.J. Deming · M.B. van Eldijk · S.A. Harris · J.C.M. van Hest ·  
D.T. Kamei · K.L. Kiick · P.J. Kocienski · B. Liu · S. Maude ·  
C.L. McGann · D.J. Pochan · V.Z. Sun · L.R. Tai · J.-K.Y. Tan

 Springer

*Editor*

Prof. Timothy Deming  
Department of Bioengineering  
University of California  
Los Angeles, CA 90095  
USA  
demingt@seas.ucla.edu

ISSN 0340-1022 e-ISSN 1436-5049  
ISBN 978-3-642-27138-0 e-ISBN 978-3-642-27139-7  
DOI 10.1007/978-3-642-27139-7  
Springer Heidelberg Dordrecht London New York

Library of Congress Control Number: 2011943757

© Springer-Verlag Berlin Heidelberg 2012

This work is subject to copyright. All rights are reserved, whether the whole or part of the material is concerned, specifically the rights of translation, reprinting, reuse of illustrations, recitation, broadcasting, reproduction on microfilm or in any other way, and storage in data banks. Duplication of this publication or parts thereof is permitted only under the provisions of the German Copyright Law of September 9, 1965, in its current version, and permission for use must always be obtained from Springer. Violations are liable to prosecution under the German Copyright Law.

The use of general descriptive names, registered names, trademarks, etc. in this publication does not imply, even in the absence of a specific statement, that such names are exempt from the relevant protective laws and regulations and therefore free for general use.

Printed on acid-free paper

Springer is part of Springer Science+Business Media ([www.springer.com](http://www.springer.com))

---

## Volume Editor

Prof. Timothy Deming

Department of Bioengineering  
University of California  
Los Angeles, CA 90095  
USA  
*demingt@seas.ucla.edu*

## Editorial Board

Prof. Dr. Kendall N. Houk

University of California  
Department of Chemistry and Biochemistry  
405 Hilgard Avenue  
Los Angeles, CA 90024-1589, USA  
*houk@chem.ucla.edu*

Prof. Dr. Christopher A. Hunter

Department of Chemistry  
University of Sheffield  
Sheffield S3 7HF, United Kingdom  
*c.hunter@sheffield.ac.uk*

Prof. Michael J. Krische

University of Texas at Austin  
Chemistry & Biochemistry Department  
1 University Station A5300  
Austin TX, 78712-0165, USA  
*mkrische@mail.utexas.edu*

Prof. Dr. Jean-Marie Lehn

ISIS  
8, allée Gaspard Monge  
BP 70028  
67083 Strasbourg Cedex, France  
*lehn@isis.u-strasbg.fr*

Prof. Dr. Steven V. Ley

University Chemical Laboratory  
Lensfield Road  
Cambridge CB2 1EW  
Great Britain  
*Svl1000@cus.cam.ac.uk*

Prof. Dr. Massimo Olivucci

Università di Siena  
Dipartimento di Chimica  
Via A De Gasperi 2  
53100 Siena, Italy  
*olivucci@unisi.it*

Prof. Dr. Joachim Thiem

Institut für Organische Chemie  
Universität Hamburg  
Martin-Luther-King-Platz 6  
20146 Hamburg, Germany  
*thiem@chemie.uni-hamburg.de*

Prof. Dr. Margherita Venturi

Dipartimento di Chimica  
Università di Bologna  
via Selmi 2  
40126 Bologna, Italy  
*margherita.venturi@unibo.it*

**Prof. Dr. Pierre Vogel**

Laboratory of Glycochemistry  
and Asymmetric Synthesis  
EPFL – Ecole polytechnique fédérale  
de Lausanne  
EPFL SB ISIC LGSA  
BCH 5307 (Bat.BCH)  
1015 Lausanne, Switzerland  
*pierre.vogel@epfl.ch*

**Prof. Dr. Chi-Huey Wong**

Professor of Chemistry, Scripps Research  
Institute  
President of Academia Sinica  
Academia Sinica  
128 Academia Road  
Section 2, Nankang  
Taipei 115  
Taiwan  
*chwong@gate.sinica.edu.tw*

**Prof. Dr. Henry Wong**

The Chinese University of Hong Kong  
University Science Centre  
Department of Chemistry  
Shatin, New Territories  
*hncwong@cuhk.edu.hk*

**Prof. Dr. Hisashi Yamamoto**

Arthur Holly Compton Distinguished  
Professor  
Department of Chemistry  
The University of Chicago  
5735 South Ellis Avenue  
Chicago, IL 60637  
773-702-5059  
USA  
*yamamoto@uchicago.edu*

# Topics in Current Chemistry Also Available Electronically

*Topics in Current Chemistry* is included in Springer's eBook package *Chemistry and Materials Science*. If a library does not opt for the whole package the book series may be bought on a subscription basis. Also, all back volumes are available electronically.

For all customers with a print standing order we offer free access to the electronic volumes of the series published in the current year.

If you do not have access, you can still view the table of contents of each volume and the abstract of each article by going to the SpringerLink homepage, clicking on "Chemistry and Materials Science," under Subject Collection, then "Book Series," under Content Type and finally by selecting *Topics in Current Chemistry*.

You will find information about the

- Editorial Board
- Aims and Scope
- Instructions for Authors
- Sample Contribution

at [springer.com](http://springer.com) using the search function by typing in *Topics in Current Chemistry*.

*Color figures* are published in full color in the electronic version on SpringerLink.

## Aims and Scope

The series *Topics in Current Chemistry* presents critical reviews of the present and future trends in modern chemical research. The scope includes all areas of chemical science, including the interfaces with related disciplines such as biology, medicine, and materials science.

The objective of each thematic volume is to give the non-specialist reader, whether at the university or in industry, a comprehensive overview of an area where new insights of interest to a larger scientific audience are emerging.



Thus each review within the volume critically surveys one aspect of that topic and places it within the context of the volume as a whole. The most significant developments of the last 5–10 years are presented, using selected examples to illustrate the principles discussed. A description of the laboratory procedures involved is often useful to the reader. The coverage is not exhaustive in data, but rather conceptual, concentrating on the methodological thinking that will allow the non-specialist reader to understand the information presented.

Discussion of possible future research directions in the area is welcome.

Review articles for the individual volumes are invited by the volume editors.

In references *Topics in Current Chemistry* is abbreviated *Top Curr Chem* and is cited as a journal.

Impact Factor 2010: 2.067; Section “Chemistry, Multidisciplinary”: Rank 44 of 144

# Preface

These are exciting times for peptide based materials. The number of investigators in this field and consequently the number of publications in this area have increased tremendously in recent years. Not since the middle of the past century has there been so much activity focused on the physical properties of peptidic materials. Then, efforts were focused on determination of the fundamental elements that make up protein structures, leading to the discoveries of the  $\alpha$ -helix and the  $\beta$ -sheet. Many years of study followed where the propensities of individual and combinations of amino acids to adopt and stabilize these structures were investigated. Now, this knowledge is being applied to the preparation, assembly, and use of peptide based materials with designed sequences. This volume summarizes recent developments in all these areas.

Natural evolutionary processes have produced structural proteins that can surpass the performance of man-made materials: e.g. mammalian elastin in the cardiovascular system that lasts half a century without loss of function, and spider webs composed of silk threads that are tougher than most synthetic fibers. These biological polypeptides are all complex copolymers that derive their phenomenal properties from the precisely controlled sequences and compositions of their constituent amino acid monomers. Peptide polymers have many advantages over conventional synthetic polymers since they are able to hierarchically assemble into stable ordered conformations. Depending on the amino acid side chain substituents, polypeptides are able to adopt a multitude of conformationally stable regular secondary structures (helices, sheets, turns), tertiary structures (e.g. the  $\beta$ -strand-helix- $\beta$ -strand unit found in  $\beta$ -barrels), and quaternary assemblies (e.g. collagen microfibrils). The peptide materials field is nearing the point of being able to develop synthetic routes for preparation of these natural polymers as well as *de novo* designed polypeptide sequences to make candidate materials for applications in biotechnology (artificial tissues, implants), biomineralization (resilient, lightweight, ordered inorganic composites), and analysis (biosensors, medical diagnostics).

Synthetic peptide based polymers are not new materials: homopolymers of polypeptides have been available for many decades and yet have only seen limited use as materials. However, new methods in chemical synthesis have made possible the preparation of increasingly complex polypeptide sequences of controlled molecular weight that display properties far superior to earlier ill-defined homopolypeptides. Chapter 1 describes the state of the art methods for polypeptide synthesis via ring-opening polymerization of aminoacid-N-carboxyanhydrides, which is an attractive, economical route when exact sequence control is not necessary. Recent work in this area has led to preparation of polypeptides of unprecedented functionality. In cases where precise sequence control is desired, for example to replicate a specific folding motif found in nature, solid-phase synthesis (Chapter 2) and recombinant DNA (Chapter 3) methodologies are required. Chapter 2 focuses on design of sequences that assemble into fibril forming  $\beta$ -sheet motifs, and Chapter 3 describes use of biosynthesis to prepare elastomeric mimics of elastin and resilin proteins.

Peptides and polypeptides are well suited for applications where polymer assembly and presentation of functionality need to be at length scales ranging from nanometers to microns. In recent years, synthetic peptide materials have been used extensively for the preparation of self-assembled fibrils and membranes. These materials typically employ amphiphilic residues in combination with ordered chain conformations that are easily accessed using the peptide backbone. Peptidic vesicles are intriguing encapsulants that lie in a realm between liposomes and viral capsids. Chapter 4 discusses recent work in this area covering preparation of these assemblies, their properties, and their uses in drug delivery. Natural peptidic fibrils have been studied for many years, but now these are being designed to incorporate distinct self-assembly characteristics that allow them to form 3D hydrogel networks. The preparation, properties, and potential biomedical uses of peptide hydrogels are reviewed in Chapter 5. A key discerning feature of these peptidic materials are their regular secondary structures that provide opportunities for hierarchical self-assembly unobtainable with typical block copolymers or small-molecule surfactants.

With such improvements in synthesis and processing, as well as the emergence of distinct classes of materials with predictable properties (i.e. vesicles, elastomers, gels), the field of peptidic materials has come a long way. As should be expected, considerable challenges remain for this field, especially if these materials are to solve real biomedical problems. Our understanding of peptidic folding and assembly is still rather limited, especially when considering the possibilities for formation of designer tertiary (3D) structures. Efficient methods to synthesize more complex peptidic materials, such as those with post-translational modifications or branched structures are still much in need. While bioconjugation methods are better than ever, broadly applicable, high yielding methods for combining biological and chemical synthesis would open up many new areas of study. I believe that peptidic materials need to encode multiple levels of functionality and structure in their

sequences in order to succeed in biomedical applications. Since these applications present many constraints, some which vary from patient to patient, the ability to reliably tune properties via many handles is also essential. There are numerous obstacles ahead, but I, like many others, cannot ignore the opportunities presented by the unique properties of the peptide bond.

Los Angeles  
Winter 2011

Timothy Deming



# Contents

<b>Synthesis of Polypeptides by Ring-Opening Polymerization of <math>\alpha</math>-Amino Acid <i>N</i>-Carboxyanhydrides</b> .....	1
Jianjun Cheng and Timothy J. Deming	
<b>Peptide Synthesis and Self-Assembly</b> .....	27
S. Maude, L.R. Tai, R.P.W. Davies, B. Liu, S.A. Harris, P.J. Kocienski, and A. Aggeli	
<b>Elastomeric Polypeptides</b> .....	71
Mark B. van Eldijk, Christopher L. McGann, Kristi L. Kiick, and Jan C.M. van Hest	
<b>Self-Assembled Polypeptide and Polypeptide Hybrid Vesicles: From Synthesis to Application</b> .....	117
Uh-Joo Choe, Victor Z. Sun, James-Kevin Y. Tan, and Daniel T. Kamei	
<b>Peptide-Based and Polypeptide-Based Hydrogels for Drug Delivery and Tissue Engineering</b> .....	135
Aysegul Altunbas and Darrin J. Pochan	
<b>Index</b> .....	169



# Synthesis of Polypeptides by Ring-Opening Polymerization of $\alpha$ -Amino Acid *N*-Carboxyanhydrides

Jianjun Cheng and Timothy J. Deming

**Abstract** This chapter summarizes methods for the synthesis of polypeptides by ring-opening polymerization. Traditional and recently improved methods used to polymerize  $\alpha$ -amino acid *N*-carboxyanhydrides (NCAs) for the synthesis of homopolypeptides are described. Use of these methods and strategies for the preparation of block copolypeptides and side-chain-functionalized polypeptides are also presented, as well as an analysis of the synthetic scope of different approaches. Finally, issues relating to obtaining highly functional polypeptides in pure form are detailed.

**Keywords** Amino acid · Block copolymer · *N*-Carboxyanhydride · Polymerization · Polypeptide

## Contents

1	Introduction .....	2
2	Polypeptide Synthesis Using NCAs .....	4
2.1	Conventional Methods .....	4
2.2	Transition Metal Initiators .....	6
2.3	Recent Developments .....	8
3	Copolypeptide and Functional Polypeptide Synthesis via NCA Polymerization .....	14
3.1	Block Copolypeptides .....	14
3.2	Side-Chain-Functionalized Polypeptides .....	16
4	Polypeptide Deprotection and Purification .....	19
5	Conclusions and Future Prospects .....	22
	References .....	23

---

J. Cheng

Department of Materials Science and Engineering, University of Illinois at Urbana-Champaign,  
Champaign, IL 61801, USA

T.J. Deming (✉)

Department of Bioengineering, University of California, Los Angeles, CA 90095, USA  
e-mail: demingt@seas.ucla.edu



## Abbreviations

AM	Activated monomer
Bn-Glu	$\gamma$ -Benzyl-L-glutamate
bpy	2,2'-Bipyridyl
CD	Circular dichroism
COD	1,4-Cyclooctadiene
DMF	Dimethylformamide
DMSO	Dimethyl sulfoxide
EDTA	Ethylenediamine tetraacetic acid
EG	Ethylene glycol
FTIR	Fourier transform infrared spectroscopy
GPC	Gel permeation chromatography
GTP	Group transfer polymerization
HMDS	Hexamethyldisilazane
MS	Mass spectroscopy
NACE	Non-aqueous capillary electrophoresis
NCA	$\alpha$ -Amino acid- <i>N</i> -carboxyanhydride
PBLG	Poly( $\gamma$ -benzyl L-glutamate)
PDMS	Poly(dimethylsiloxane)
PEG	Poly(ethylene glycol)
TFA-Lys	$\epsilon$ -Trifluoroacetyl-L-lysine
THF	Tetrahydrofuran
TMS	Trimethylsilyl
TMSDC	Trimethylsilyl dimethylcarbamate
Z-Lys	$\epsilon$ -Carbobenzyloxy-L-lysine

## 1 Introduction

Biological systems produce proteins that possess the ability to self-assemble into complex, yet highly ordered structures [1]. These remarkable materials are polypeptide copolymers that derive their properties from precisely controlled sequences and compositions of their constituent amino acid monomers. There has been recent interest in developing synthetic routes for preparation of these natural polymers as well as de novo designed polypeptide sequences to make products for applications in biotechnology (e.g., artificial tissues and implants), biomineralization (e.g., resilient, lightweight and ordered inorganic composites), and analysis (e.g., biosensors and medical diagnostics) [2, 3].

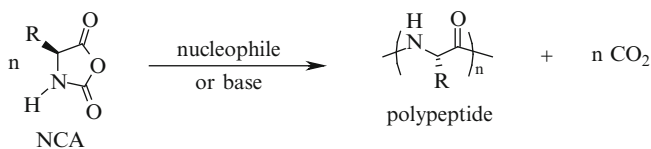
To be successful in these applications, it is important that materials can self-assemble into precisely defined structures. Peptide-based polymers have many advantages over conventional synthetic polymers since they are able to hierarchically assemble into stable, ordered conformations [4]. Depending on the substituents of the amino acid side chain, polypeptides are able to adopt a multitude of

conformationally stable, regular secondary structures (e.g., helices, sheets, and turns), tertiary structures (e.g., the  $\beta$ -strand-helix- $\beta$ -strand unit found in  $\beta$ -barrels), and quaternary assemblies (e.g., collagen microfibrils) [4]. The synthesis of polypeptides that can assemble into non-natural structures is an attractive challenge for polymer chemists.

Synthetic peptide-based polymers are not new materials: homopolymers of polypeptides have been available for many decades but have only seen limited use as structural materials [5, 6]. However, new methods in chemical synthesis have made possible the preparation of increasingly complex polypeptide sequences of controlled molecular weight that display properties far superior to ill-defined homopolypeptides [7]. These polymers are well suited for applications where polymer assembly and functional domains need to be at length scales ranging from nanometers to micrometers. These block copolymers are homogeneous on a macroscopic scale, but dissimilarity between the block segments typically results in microphase heterogeneity yielding materials useful as surfactants, micelles, membranes, and elastomers [8]. Synthesis of simple hydrophilic/hydrophobic hybrid diblock copolymers, when dispersed in water, allows formation of peptide-based micelles and vesicles potentially useful in drug and gene delivery applications [9, 10]. The regular secondary structures obtainable with the polypeptide blocks provide opportunities for hierarchical self-assembly that are unobtainable with typical block copolymers or small-molecule surfactants.

Upon examining the different methods for polypeptide synthesis, the limitations of these techniques for preparation of well-defined copolymers readily become apparent. Conventional solid-phase peptide synthesis is neither useful nor practical for direct preparation of large polypeptides ( $> 100$  residues) due to unavoidable deletions and truncations that result from incomplete deprotection and coupling steps. The most economical and expedient process for synthesis of long polypeptide chains is the polymerization of  $\alpha$ -amino acid-*N*-carboxyanhydrides (NCAs) (Scheme 1) [11, 12]. This method involves the simplest reagents, and high molecular weight polymers can be prepared in both good yield and large quantity with no detectable racemization at the chiral centers. The considerable variety of NCAs that have been synthesized ( $> 200$ ) allows exceptional diversity in the types of polypeptides that can be prepared [11, 12].

Since the late 1940s, NCA polymerizations have been the most common technique used for large scale preparation of high molecular weight polypeptides [13]. However, these materials have primarily been homopolymers, random copolymers, or graft copolymers that lack the sequence specificity and monodispersity of natural



**Scheme 1** Polymerization of  $\alpha$ -amino acid-*N*-carboxyanhydrides (NCA)

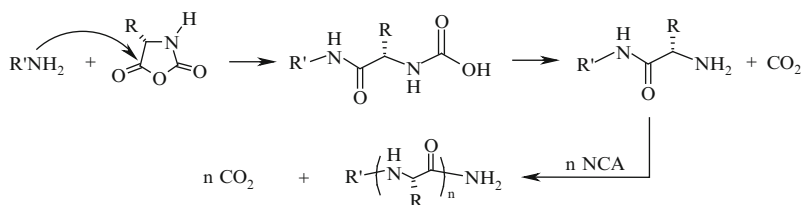
proteins. Until recently, the level of control in NCA polymerizations has not been able to rival that attained in other synthetic polymerizations (e.g., vinyl addition polymerizations) where sophisticated polymer architectures have been prepared (e.g., stereospecific polymers and block copolymers) [14]. Attempts to prepare block copolypeptides and hybrid block copolymers using conventional NCA polymerization has usually resulted in polymers whose compositions did not match monomer feed compositions and that contained significant homopolymer contaminants [15–17]. Block copolymers could only be obtained in pure form by extensive fractionation steps, which significantly lowered the yield and efficiency of this method. The limitation of NCA polymerizations has been the presence of side reactions (chain termination and chain transfer) that restrict control over molecular weight, give broad molecular weight distributions, and prohibit formation of well-defined block copolymers [18]. Recent progress in elimination of these side reactions has been a major breakthrough for the polypeptide materials field. A variety of metal- and organo-catalysts have been developed and utilized in recent years for the formation of multiblock polypeptides or polypeptide-containing hybrid materials with well-defined structures via controlled polymerization of NCAs [19–22].

## 2 Polypeptide Synthesis Using NCAs

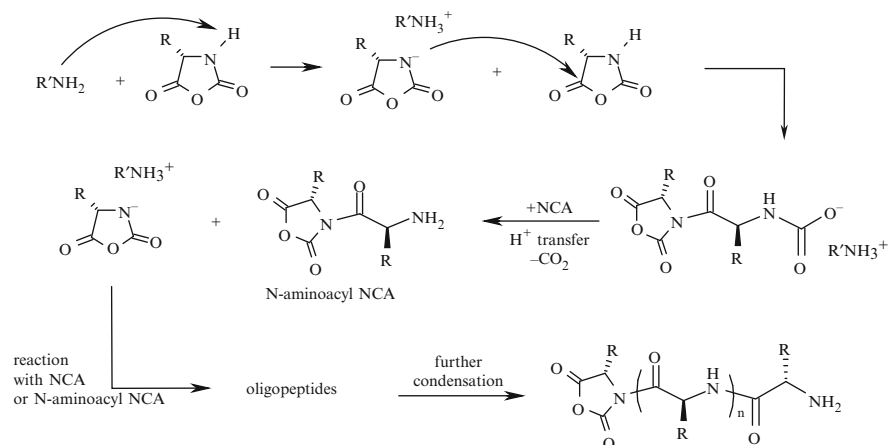
### 2.1 *Conventional Methods*

NCA polymerizations are traditionally initiated using many different nucleophiles and bases, the most common being primary amines and alkoxide anions [11, 12]. Primary amines, being more nucleophilic than basic, are good general initiators for polymerization of NCA monomers. Tertiary amines, alkoxides, and other initiators that are more basic than nucleophilic have found use since they are in some cases able to prepare polymers of very high molecular weights where primary amine initiators cannot. Optimal polymerization conditions have often been determined empirically for each NCA and thus there have been no universal initiators or conditions by which to prepare high molecular weight polymers from any monomer. This is in part due to the different properties of individual NCAs and their polymers (e.g., solubility and reactivity) but is also strongly related to the side reactions that occur during polymerization.

The most likely pathways of NCA polymerization are the so-called “amine” and the “activated monomer” (AM) mechanisms [11, 12]. The amine mechanism is a nucleophilic ring-opening chain growth process where the polymer could grow linearly with monomer conversion if side reactions were absent (Scheme 2). On the other hand, the AM mechanism is initiated by deprotonation of an NCA, which then becomes the nucleophile that initiates chain growth (Scheme 3). It is important to note that a given system can switch back and forth between the amine and AM mechanisms many times during a polymerization: a propagation step for one



**Scheme 2** Proposed mechanism for NCA polymerization initiated by nucleophilic amines



**Scheme 3** Proposed mechanism for NCA polymerization initiated by activated monomers

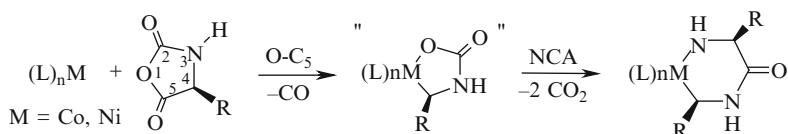
mechanism is a side reaction for the other, and vice versa. It is because of these side reactions that block copolypeptides and hybrid block copolymers prepared from NCAs using amine initiators often have structures different to those predicted by monomer feed compositions and most likely have considerable homopolymer contamination. These side reactions also prevent control of chain-end functionality, which is crucial for preparation of hybrid copolymers.

One inherent problem in conventional NCA polymerizations is that there is no control over the reactivity of the growing polymer chain-end during the course of the polymerization. Once an initiator reacts with a NCA monomer, it is no longer active in the polymerization and the resulting primary amine, carbamate, or NCA anion end group is free to undergo a variety of undesired side reactions. Another problem is associated with the purity of NCA monomers. Although most NCAs are crystalline compounds, they typically contain minute traces of acid, acid chlorides, or isocyanates that can quench propagating chains. The presence of other adventitious impurities, such as water, can cause problems by acting as chain-transfer agents or even as catalysts for side reactions. Overall, the sheer abundance of potential reactions present in reaction media make it difficult to achieve a living polymerization system where only chain propagation occurs.

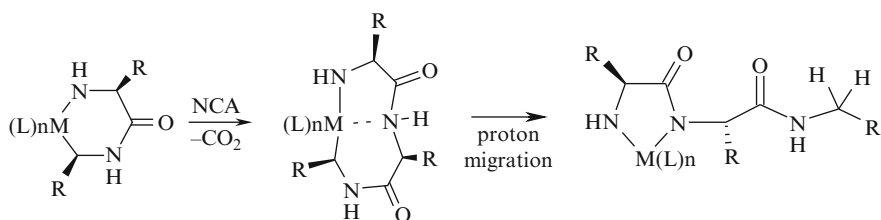
## 2.2 Transition Metal Initiators

One strategy for eliminating side reactions in NCA polymerizations is the use of transition metal complexes as active species to control addition of NCA monomers to polymer chain-ends. The use of transition metals to control reactivity has been proven in organic and polymer synthesis as a means to increase both reaction selectivity and efficiency [23]. Using this approach, substantial advances in controlled NCA polymerization have been realized in recent years. Highly effective zerovalent nickel and cobalt initiators (i.e.,  $(\text{PMe}_3)_4\text{Co}$  [24], and  $\text{bpyNi}(\text{COD})$ , where  $\text{bpy} = 2,2'$ -bipyridine and  $\text{COD} = 1,5$ -cyclooctadiene [19]) were developed by Deming that allow the living polymerization of NCAs into high molecular weight polypeptides via an unprecedented activation of the NCAs into covalent propagating species. The metal ions can be conveniently removed from the polymers by simple precipitation or dialysis of the samples after polymerization.

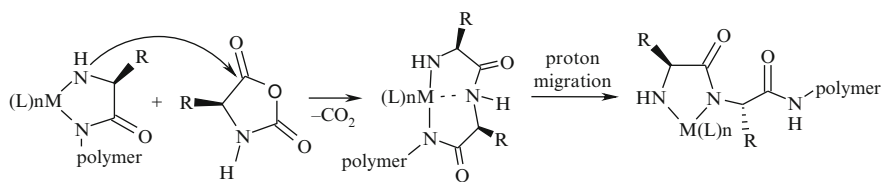
Mechanistic studies on the initiation process showed that both these metals react identically with NCA monomers to form metallacyclic complexes by oxidative addition across the anhydride bonds of NCAs [19, 24, 25]. These oxidative-addition reactions were followed by addition of a second NCA monomer to yield complexes identified as six-membered amido-alkyl metallacycles (Scheme 4). These intermediates were found to further contract to five-membered amido-amidate metallacycles upon reaction with additional NCA monomers. This ring contraction is thought to occur via migration of an amide proton to the metal-bound carbon, which liberates the chain-end from the metal (Scheme 5) [26]. The resulting amido-amidate complexes were thus proposed as the active polymerization intermediates. Propagation through the amido-amidate metallacycle was envisioned to occur by initial attack of the nucleophilic amido group on the electrophilic  $\text{C}_5$  carbonyl of an NCA monomer (Scheme 6). This reaction would result in a large metallacycle that



**Scheme 4** Oxidative-addition of NCAs to zerovalent cobalt and nickel complexes



**Scheme 5** Metallacycle ring contraction mediated by NCA addition

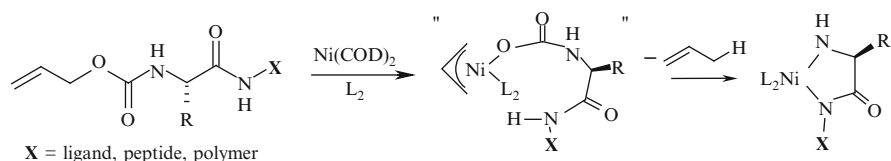


**Scheme 6** Chain propagation in transition-metal-mediated NCA polymerization

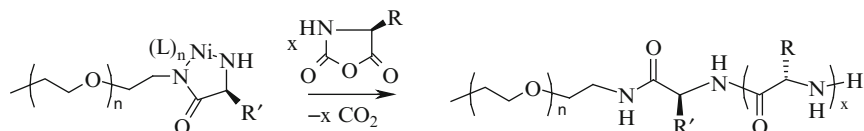
could contract by elimination of  $CO_2$ . Proton transfer from the free amide to the tethered amidate group would further contract the ring to give the amido-amidate propagating species, while in turn liberating the end of the polymer chain and becoming available for reaction with the next incoming NCA molecule.

In this manner, the metal is able to migrate along the growing polymer chain, while being held by a robust chelate at the active end. The formation of these chelating metallacyclic intermediates appears to be a general requirement for obtaining living NCA polymerizations using transition metal initiators. These cobalt and nickel complexes are able to produce polypeptides with narrow chain length distributions (given by the polydispersity index, i.e., the weight-average molecular weight divided by the number-average molecular weight,  $M_w/M_n$ , which in this case is  $< 1.2$ ) and controlled molecular weights ( $500 < M_n < 500,000$  g/mol) [26]. This polymerization system is very general, and gives controlled polymerization of a wide range of NCA monomers as pure enantiomers (D- or L-configuration) or as racemic mixtures. By addition of different NCA monomers, the preparation of block copolypeptides of defined sequence and composition is feasible [7, 27].

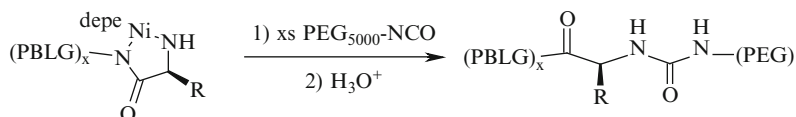
The transition metal initiators for NCA polymerization described above should provide a means for controlled synthesis of polypeptide hybrid block copolymers. However, a limitation of this methodology when using zerovalent metal complexes as initiators is that the active propagating species are generated in situ, where the C-terminal end of the polypeptide is derived from the first NCA monomer. Consequently, this method does not allow attachment of functionality (e.g., polymer or small molecule) to the carboxyl chain-end of the polypeptides. To facilitate control over the C-terminal chain-end, Deming and coworkers pursued alternative methods for direct synthesis of the amido-amidate metallacycle propagating species and developed allyloxycarbonylaminoamides as universal precursors to amido-amidate nickelacycles. These simple amino acid derivatives undergo tandem oxidative additions to nickel(0) to give active NCA polymerization initiators (Scheme 7) [28]. These complexes were found to initiate polymerization of NCAs yielding polypeptides with defined molecular weights, narrow molecular weight distributions, and with quantitative incorporation of the initiating ligand as a C-terminal end-group. This chemistry provides a very facile way to incorporate diverse molecules such as polymers, peptides, oligosaccharides, or other ligands onto the carboxyl chain-ends of polypeptides via a robust amide linkage (Scheme 8), and was further elaborated by Menzel's group to grow polypeptides off polystyrene particles [29].



**Scheme 7** Formation of chain-end functionalized nickelacycle initiators



**Scheme 8** Preparation of PEG-polypeptide diblock copolymers by macroinitiation



**Scheme 9** Preparation of PEG-polypeptide diblock copolymers by isocyanate end-capping

As an extension of this work, Deming also developed a means to end-cap living polypeptide chains with electrophilic reagents. When a macromolecular electrophile is used, the resulting product is a polypeptide hybrid block copolymer. It is well known that in NCA polymerizations the electrophiles, such as isocyanates, act as chain-terminating agents by reaction with the propagating amine chain-ends [11, 12]. Deming and coworkers reported that the reactive living nickelacycle polypeptide chain-ends could be quantitatively capped by reaction with excess isocyanate, isothiocyanate, or acid chloride [30]. Using this chemistry, they prepared isocyanate end-capped poly(ethylene glycol) (PEG) and reacted this, in excess, with living poly( $\gamma$ -benzyl L-glutamate) (PBLG) to obtain PBLG-PEG diblock copolymers (Scheme 9). Reaction with living ABA triblock copolymers (*vide infra*) gave the corresponding PEG-capped CABAC hybrid pentablock copolymers, where A was PBLG; B was polyoctenamer, PEG or PDMS; and C was PEG. Since excess PEG was used to end-cap the living polypeptide chains, the pentablock copolymers required purification, which was achieved by repeated precipitation from THF into methanol. Overall, it can be seen that the use of controlled NCA polymerization allows formation of very complex hybrid block copolymer architectures that rival those prepared using any polymerization system.

### 2.3 Recent Developments

In recent years, a number of new approaches have been reported for obtaining controlled NCA polymerizations. These approaches share a common theme in that

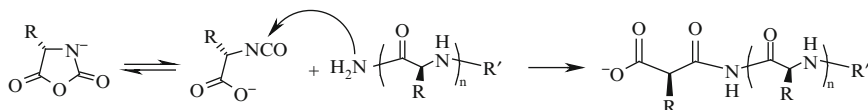
they are all improvements on the use of classical primary amine polymerization initiators. This approach is attractive since primary amines are readily available and because the initiator does not need to be removed from the reaction after polymerization. In fact, if the polymerization proceeds without any chain-breaking reactions, the amine initiator becomes the C-terminal polypeptide end-group. In this manner, there is potential to form chain-end-functionalized polypeptides or even hybrid block copolymers if the amine is a macroinitiator. The challenge in this approach is to overcome the numerous side reactions of these systems without the luxury of a large number of experimental parameters to adjust.

In 2004, the group of Hadjichristidis reported the primary-amine-initiated polymerization of NCAs under high vacuum conditions [21]. The strategy here was to determine if a reduced level of impurities in the reaction mixture would lead to fewer polymerization side reactions. Unlike the vinyl monomers usually polymerized under high vacuum conditions, NCAs cannot be purified by distillation. Consequently, it is doubtful whether the NCAs themselves can be obtained in higher purity under high vacuum recrystallization than by recrystallization under a rigorous inert atmosphere. However, the high vacuum method does allow for better purification of polymerization solvents and the *n*-hexylamine initiator. It was found that polymerizations of  $\gamma$ -benzyl-L-glutamate NCA (Bn-Glu NCA) and  $\epsilon$ -carbobenzyloxy-L-lysine NCA (Z-Lys NCA) under high vacuum in DMF solvent displayed all the characteristics of a living polymerization system [21]. Polypeptides could be prepared with control over chain length, chain length distributions were narrow, and block copolypeptides were prepared. Controlled polymerization of NCAs under high vacuum was later confirmed by Messman and coworkers [31].

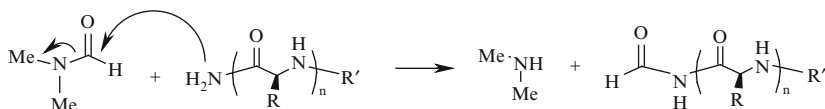
The authors concluded that the side reactions normally observed in amine-initiated NCA polymerizations are simply a consequence of impurities. Since the main side reactions in these polymerizations do not involve reaction with adventitious impurities such as water, but instead reactions with monomer, solvent, or polymer (i.e., termination by reaction of the amine-end with an ester side chain, attack of DMF by the amine-end, or chain transfer to monomer) [11, 12], this conclusion does not seem to be well justified. It is likely that the role of impurities (e.g., water) in these polymerizations is very complex. A possible explanation for the polymerization control observed under high vacuum is that the impurities act to catalyze side reactions with monomer, polymer, or solvent. In this scenario, it is reasonable to speculate that polar species such as water can bind to monomers or the propagating chain-end and thus influence their reactivity.

Further insights into amine-initiated NCA polymerizations were also reported in 2004 by the group of Giani and coworkers [32]. This group studied the polymerization of  $\epsilon$ -trifluoroacetyl-L-lysine NCA (TFA-Lys NCA) in DMF using *n*-hexylamine initiator as a function of temperature. In contrast to the high vacuum work, the solvent and initiator were purified using conventional methods and the polymerizations were conducted under a nitrogen atmosphere on a Schlenk line. After complete consumption of NCA monomer, the crude polymerization mixtures were analyzed by gel permeation chromatography (GPC) and non-aqueous capillary electrophoresis (NACE). A unique feature of this work was the use of NACE to





**Scheme 10** Polypeptide chain termination by reaction with NCA anions

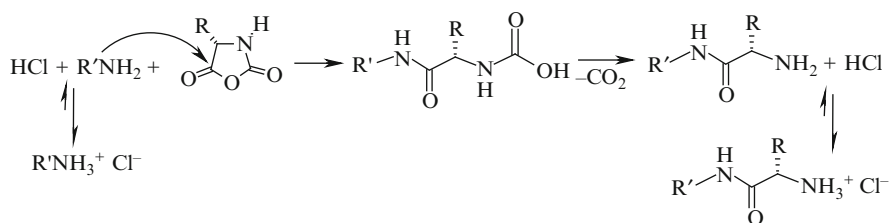


**Scheme 11** Polypeptide chain termination by reaction with DMF solvent

separate and quantify the amount of polymers with different chain-ends, which corresponded to living chains (amine end-groups) and “dead” chains (carboxylate and formyl end-groups from reaction with NCA anions and DMF solvent, respectively; see Schemes 10 and 11). Not surprisingly, at 20 °C, the polymer products consisted of 78% dead chains and only 22% living chains, which illustrates the abundance of side reactions in these polymerizations under normal conditions.

An intriguing result was found for polymerizations conducted at 0 °C where 99% of the chains had living amine chain-ends, and only 1% were found to be dead chains. To verify that these were truly living polymerizations, additional NCA monomer was added to these chains at 0 °C, resulting in increased molecular weight and no increase in the amount of dead chains. Although this was only a preliminary study and further studies need to be conducted to explore the scope of this method, this work clearly shows that the common NCA polymerization side reactions can also be eliminated by lowering the temperature. The effect of temperature is not unusual, as similar trends can be found in cationic and anionic vinyl polymerizations [33]. At elevated temperature, the side reactions have activation barriers similar to chain propagation. When the temperature is lowered, it appears that the activation barrier for chain propagation becomes lower than that of the side reactions and chain propagation dominates kinetically. A remarkable feature of this system is that the elevated levels of impurities, as compared to the high vacuum method, do not seem to cause side reactions at low temperature. This result further substantiates the idea that the growing chains do not react with the adventitious impurities, but that they mainly affect these polymerizations by altering the rates of discrete reaction steps. The same group reported recently that addition of urea in the polymerization solution could also improve the polymerization and minimize the tendency of formation of bimodal molecular weight distribution [34].

Another innovative approach to controlling amine-initiated NCA polymerizations was reported in 2003 by Schlaad and coworkers [20]. Their strategy was to avoid formation of NCA anions, which cause significant chain termination after rearranging to isocyanocarboxylates [11, 12], through use of primary amine hydrochloride salts as initiators. The reactivity of amine hydrochlorides with NCAs was first explored by the group of Knobler, who found that they could react



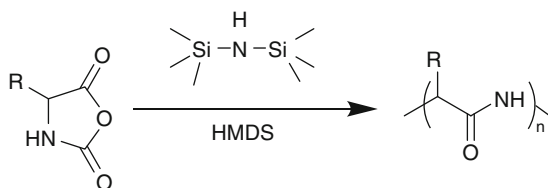
**Scheme 12** Polypeptide synthesis using amine-hydrochloride initiators

hydrochlorides with NCAs to give single NCA addition products [35, 36]. Use of the hydrochloride salt takes advantage of its diminished reactivity as a nucleophile compared to the parent amine, which effectively halts the reaction after a single NCA insertion by formation of an inert amine hydrochloride in the product. The reactivity of the hydrochloride presumably arises from formation of a small amount of free amine by reversible dissociation of HCl (Scheme 12). This equilibrium, which lies heavily toward the dormant amine hydrochloride species, allows for only a very short lifetime of reactive amine species. Consequently, as soon as a free amine reacts with an NCA, the resulting amine end-group on the product is immediately protonated and is prevented from further reaction. The acidic conditions also assist elimination of  $\text{CO}_2$  from the reactive intermediate and, more importantly, suppress formation of unwanted NCA anions.

To obtain controlled polymerization, and not just single NCA addition reactions, Schlaad's group increased the reaction temperature (from 40 to 80 °C), which was known from Knobler's work to increase the equilibrium concentration of free amine, as well as increase the exchange rate between amine and amine hydrochloride [35, 36]. Using primary amine hydrochloride end-capped polystyrene macroinitiators to polymerize *Z*-Lys NCA in DMF, Schlaad's group obtained polypeptide hybrid copolymers in 70–80% yield after 3 days at elevated temperature. Although these polymerizations are slow compared to amine-initiated polymerizations, the resulting polypeptide segments were well defined with very narrow chain length distributions ( $M_w/M_n < 1.03$ ). These distributions were much narrower than those obtained using the free amine macroinitiator, which argues for diminished side reactions in the polypeptide synthesis. The molecular weights of the resulting polypeptide segments were found to be approximately 20–30% higher than would be expected from the monomer-to-initiator ratios. This result was attributed to termination of some fraction of initiator species by traces of impurities in the NCA monomers, although the presence of unreacted polystyrene chains was not reported.

Although more studies need to be performed to study the scope and generality of this system, the use of amine hydrochloride salts as initiators for controlled NCA polymerizations shows tremendous promise. Fast, reversible deactivation of a reactive species to obtain controlled polymerization is a proven concept in polymer chemistry, and this system can be compared to the persistent radical effect employed in all controlled radical polymerization strategies [37]. Like those systems, success of this method requires a carefully controlled matching of the

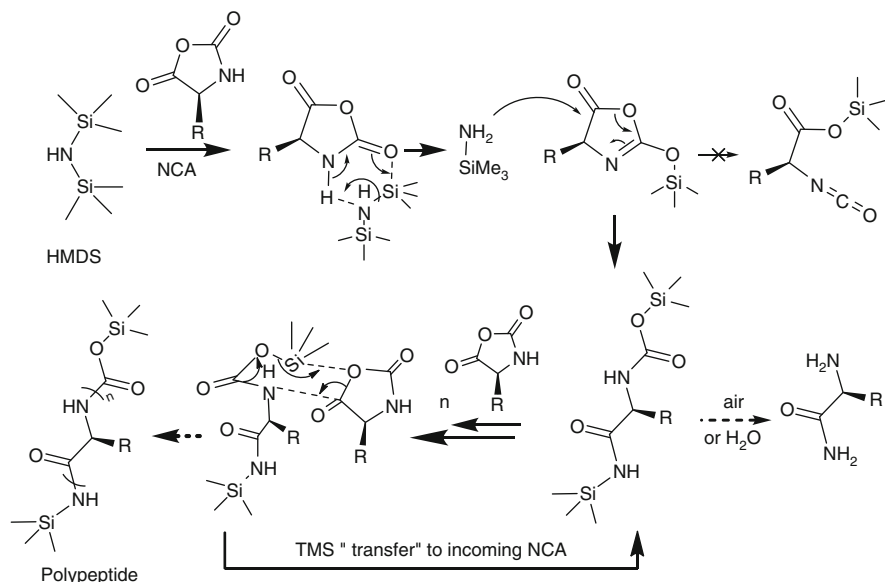
**Scheme 13** Polypeptide synthesis using HMDS initiator



polymer chain propagation rate constant, the amine/amine hydrochloride equilibrium constant, and the forward and reverse exchange rate constants between amine and amine hydrochloride salt. This means that it is likely that reaction conditions (e.g., temperature, halide counterion, solvent) will need to be optimized to obtain controlled polymerization for each different NCA monomer, as is the case for most vinyl monomers in controlled radical polymerizations. Within these constraints, it is possible that controlled NCA polymerizations utilizing simple amine hydrochloride initiators can be obtained.

A new approach of controlling NCA polymerization was reported by the Cheng group in 2007 [22]. In a screen of amine initiators for the polymerization of Bn-Glu NCA, they found that hexamethyldisilazane (HMDS) showed remarkable control of polymerizations and led to formation of PBLG with excellent chain length control, with less than 22% deviation from the expected molecular weights, and narrow molecular weight distributions ( $M_w/M_n < 1.2$ ) (Scheme 13). The NCA polymerizations initiated with HMDS differed greatly from those initiated with conventional secondary amine initiators, e.g., diethylamine, in which elevated PBLG molecular weights (three to four times higher than the expected molecular weights) and broad molecular weight distributions were observed.

The controlled NCA polymerizations observed with HMDS suggested that their initiation and chain propagation mechanisms differ from either the “amine” (Scheme 2) or the “AM” mechanism (Scheme 3), typically observed with amine initiators. As a secondary amine, HMDS can either function as nucleophile to open the NCA ring at C<sub>5</sub>, or act as a base to deprotonate the NH group [11]. Previous studies showed that secondary amines with bulky alkyl groups (e.g., diisopropylamine) exclusively deprotonated NCAs [38]. Therefore, it is unlikely that HMDS, a secondary amine containing two bulky TMS groups, attacks the C<sub>5</sub> of Bn-Glu NCA. If the first step involves the deprotonation of the NCA NH group by HMDS, an N-TMS NCA would form that should undergo rapid rearrangement to form an  $\alpha$ -isocyanatocarboxylic acid [39]. However, no isocyanate stretch ( $\sim 2,230$ – $2,270$   $\text{cm}^{-1}$ ) was observed when a mixture of equimolar Bn-Glu NCA and HMDS was analyzed by FTIR. Interestingly, it was observed that the Si–N absorption band of HMDS at  $932$   $\text{cm}^{-1}$  in FTIR disappeared, indicating the cleavage of an Si–N bond during initiation. It therefore seems likely that a TMS group is transferred to C<sub>2</sub> from HMDS in a coordinated manner (Scheme 14). Instead of forming an isocyanate, the NCA-TMS intermediate instead undergoes rapid ring-opening by the in-situ-generated TMS-amine to form a TMS-carbamate. Cheng and coworkers confirmed the formation of TMS-carbamates through a combination of  $^{13}\text{C}$  NMR and mass spectroscopy (MS) analysis of an equimolar

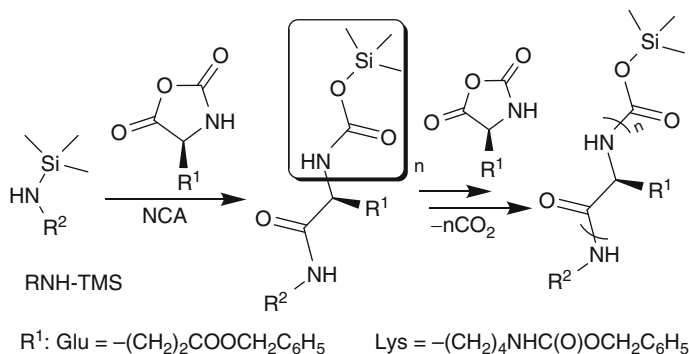


**Scheme 14** Proposed mechanism for polypeptide synthesis using HMDS initiator

mixture of Bn-Glu NCA and HMDS in DMSO- $d_6$ . The MS analysis of a mixture of Bn-Glu NCA and HMDS (at a 5:1 molar ratio) further showed peaks corresponding to the molecular weights of the dimer through the pentamer containing the TMS-carbamate end-group. This suggests that polypeptide chains were indeed propagated through the transfer of the TMS group from the terminal TMS-carbamate to the incoming monomer to form a new TMS-carbamate terminal propagating group (Scheme 14). To demonstrate that controlled NCA polymerizations can be mediated by the TMS-carbamate group, Cheng synthesized trimethylsilyl dimethylcarbamate (TMSDC), a TMS-carbamate compound, and used it as the initiator for Bn-Glu NCA polymerization. Polymerizations using this initiator yielded PBLG chains with controllable molecular weights and narrow molecular weight distributions, as in the HMDS-mediated polymerizations.

These TMS-carbamate-mediated NCA polymerizations resemble to some extent the group-transfer polymerization (GTP) of acrylic monomers initiated by organosilicon compounds [40]. Unlike GTPs that typically require Lewis acid activators or nucleophilic catalysts to facilitate the polymerization [41], TMS-carbamate-mediated NCA polymerizations do not appear to require any additional catalysts or activators. However, it is still unclear whether the TMS transfer proceeds through an anionic process as in GTP [41] or through a concerted process as illustrated in Scheme 14.

As the polypeptide chains are propagated only at the amine-end through the transfer of the terminal TMS-carbamate to the incoming monomer to form a new TMS-carbamate terminal propagating group, Cheng and his team reasoned that use of a N-TMS amine as the initiator will generate an amine and a TMS group



**Scheme 15** Polypeptide synthesis using TMS-amine initiators

(Scheme 15) that can subsequently form a corresponding amide at the C-terminus and a TMS-carbamate at the N-terminus after NCA ring opening. Thus, chain propagation should proceed in the same manner as HMDS-mediated polymerization. Because a large variety of N-TMS amines are readily available, this method should allow facile functionalization at the C-terminal ends of polypeptides. It has been demonstrated that a variety of primary amines, ranging from small molecules to polymers or containing a variety of functional groups (e.g., norbornene, alkyne, azide, PEG, etc.), could be readily introduced to the C-terminal ends of polypeptides via N-TMS amine-mediated, controlled NCA polymerization [42].

The polymerizations initiated by HMDS and N-TMS amines usually complete within 24 h at ambient temperature with quantitative monomer consumption. These polymerizations in general are slower than those mediated by Deming's Ni(0) or Co(0) initiators (about 30–60 min at ambient temperature) [19, 24, 25], but are much faster than those initiated by amines at low temperature or using amine hydrochloride initiators [20]. These HMDS and N-TMS amine-mediated NCA polymerizations can also be applied to the preparation of block copolypeptides of defined sequence and composition [22]. This organosilicon-mediated NCA polymerization, which was also shown by Zhang and coworkers to be useful for controlled polymerization of  $\gamma$ -3-chloropropanyl-L-Glu NCA [43], offers an advantage for the preparation of polypeptides with defined C-terminal end-groups.

### 3 Copolypeptide and Functional Polypeptide Synthesis via NCA Polymerization

#### 3.1 Block Copolypeptides

For the examination of model protein–protein interactions and the assembly of novel three-dimensional structures, block copolypeptides are required that have

structural domains (i.e., amino acid sequences) whose size and composition can be precisely adjusted. Such materials have proven elusive using conventional techniques. NCA polymerizations initiated by a strong base are very fast. These polymerizations are poorly understood and block copolymers generally cannot be prepared. NCA polymerizations initiated by primary amines are also not free of side reactions. Even after fractionation of the crude preparations, the resulting polypeptides are relatively ill-defined, which may complicate unequivocal evaluation of their properties and potential applications. Nevertheless, there are many reports on the preparation of block copolypeptides using conventional primary amine initiators [44]. Examples include many hydrophilic–hydrophobic and hydrophilic–hydrophobic–hydrophilic di- and triblock copolypeptides (in which hydrophilic residues were glutamate and lysine, and hydrophobic residues were leucine [28, 29], valine [45], isoleucine [46], phenylalanine [30], and alanine [47]) prepared to study conformations of the hydrophobic domain in aqueous solution. These conformational preferences of different amino acid residues were used as the basis for early models for predicting protein conformations from sequence. Consequently, these copolypeptides were studied under conditions favoring isolated single chains (i.e., high dilution), and self-assembly of the polymers was not investigated. These copolymers were often subjected to only limited characterization (e.g., analysis of amino acid composition) and, as such, their structures, and the presence of homopolymer contaminants, were not conclusively determined. Some copolymers, which had been subjected to chromatography, showed polymodal molecular weight distributions containing substantial high and low molecular weight fractions [30]. The compositions of these copolymers were found to be very different from the initial monomer feed compositions and varied widely for different molecular weight fractions. It appears that most, if not all, block copolypeptides prepared using amine initiators have structures different to those predicted by monomer feed compositions and probably have considerable homopolymer contamination due to the side reactions described above.

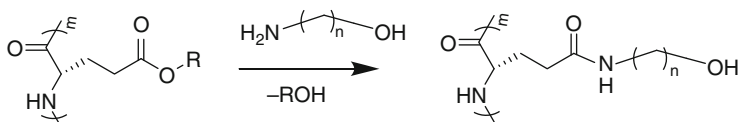
Polypeptide block copolymers prepared via transition-metal-mediated NCA polymerization are well-defined, with the sequence and composition of block segments controlled by the order and quantity of monomer, respectively, added to initiating species. These block copolypeptides can be prepared with the same level of control found in anionic and controlled radical polymerizations of vinyl monomers, which greatly expands the potential of polypeptide materials. The unique chemistry of these initiators and NCA monomers also allows NCA monomers to be polymerized in any order, which is a challenge in most vinyl copolymerizations, and the robust chain-ends allow the preparation of copolypeptides with many block domains (e.g., more than four). The self-assembly of these block copolypeptides has also been investigated (e.g., to direct the biomimetic synthesis of ordered silica structures [48]) for formation of polymeric vesicular membranes [49–51], or for preparation of self-assembled polypeptide hydrogels [52] and nanoscale emulsion droplets [53]. Furthermore, poly(L-lysine)-*block*-poly(L-cysteine) block copolypeptides have been used to generate hollow, organic–inorganic hybrid microspheres composed of a thin inner layer of gold nanoparticles surrounded by a thick layer of

silica nanoparticles [54]. Using the same procedure, hollow spheres could also be prepared, which consisted of a thick inner layer of core-shell CdSe/CdS nanoparticles and thicker silica nanoparticle outer layer [55]. The latter spheres are of interest because they allow for microcavity lasing without the use of additional mirrors, substrate spheres, or gratings.

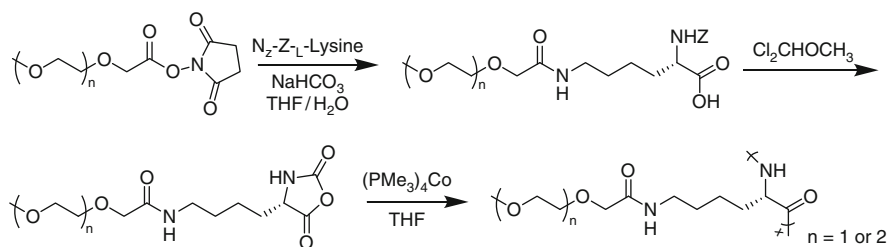
### 3.2 *Side-Chain-Functionalized Polypeptides*

There have been many examples in which polypeptides were chemically modified to improve their properties for delivery applications. Typically, this strategy involves the hydrophobic modification of poly(lysine) or poly(glutamate/aspartate) side chains by covalent attachment of lipophilic groups [5, 6]. These modifications are akin to polymer grafting reactions and thus result in random placement of these hydrophobic substituents (typically long alkyl chains) along the polypeptide chains. These modifications were performed in order to increase the polypeptide's ability to bind hydrophobic drugs, aggregate in aqueous solution, and/or penetrate the lipid bilayers of cell walls. The random placement of the hydrophobes along the chain means that they cannot act as a distinct domain in supramolecular assembly, as in a block copolymer, thus limiting their ability to organize.

Other types of chemical polypeptide modification include addition of sugars, or sugar-binding groups [27, 43, 56–58], to increase functionality, and the addition of nonionic, polar groups to increase solubility and blood circulation lifetime [8]. Increasing bioavailability is a major concern for drug delivery using synthetic polypeptides. The amino acid functionalities that provide water solubility (e.g., the amino group of lysine, or the carboxylate groups of glutamate and aspartate) are also detrimental in that their polymers behave as polyelectrolytes. As such, they bind strongly to oppositely charged biomolecules (i.e., proteins, polynucleic acids, polysaccharides, lipids) resulting in aggregation and either rapid removal from the bloodstream or rapid digestion within cells [59]. To circumvent this problem, nonionic, water-solubilizing polypeptide residues have been sought. Following the discovery that optically pure polyserine is not water-soluble at chain lengths greater than 20 residues [21], there have been many attempts to prepare chemically modified residues that would impart these desired features. The simplest of these approaches is the grafting of PEG chains ( $1,000 < M_n < 5,000$ ) onto side-chain functionalities, as described above, which results in highly heterogeneous materials that retain considerable charge [9]. A more sophisticated solution was the development of hydroxyalkylglutamine polymers, prepared by the reaction of poly(alkylglutamate) esters with  $\alpha,\omega$ -amino alcohols (Scheme 16). These polypeptides, particularly poly(hydroxypropylglutamine) and poly(hydroxybutylglutamine), were found to be nonionic and soluble in water over a wide pH range [32]. As such, these polymers should be useful as solubilizing domains in polypeptide-based drug delivery systems. The major detriments of these materials, however, are that they are recognized as foreign entities and rapidly degraded in vivo, they are



**Scheme 16** Synthesis of water-soluble poly(hydroxyalkyl glutamines)



**Scheme 17** Synthesis of water-soluble EG-grafted poly(L-lysine)s

difficult to prepare without significantly degrading the polypeptide chains, and they lack ordered secondary structure in solution [32]. The last property is important since one of the main reasons for using polypeptide scaffolds in biomedical applications is to take advantage of their ordered chain conformations to mimic protein structures.

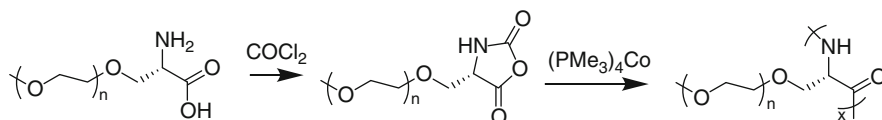
Deming and, more recently, Klok have taken a different approach toward the development of nonionic, water-soluble polypeptides. They incorporated the solubilizing and protective properties of PEG into polypeptides by conjugation of short ethylene glycol (EG) repeats onto amino acid monomers, as opposed to the well-documented approach of grafting PEG to the ends or side chains of polypeptides [60]. Deming has also recently extended this work by attaching nonionic monosaccharides to amino acid monomers to give nonionic, sugar-functionalized polypeptides [57] (Scheme 17). The functionalized NCA approach avoids the need for expensive amino- or carboxylato-functionalized PEG molecules necessary for coupling, and avoids difficulties associated with derivatization of polymers that are usually associated with polypeptide chain cleavage and broadening of molecular weight distributions. In particular, the presence of short EG repeats or saccharides on every residue resulted in a high density of hydrophilic moieties around the polymer chain. In effect, the polypeptides are surrounded by an EG or saccharide sheath that should mimic the physical properties of PEG or polysaccharides [33], respectively, yet not deleteriously affect the secondary structure of the polypeptide core. For instance, circular dichroism (CD) analysis revealed that EG-grafted poly(L-lysine) is essentially 100%  $\alpha$ -helical in pH 7 water at 25 °C. This conformation was unaffected by many environmental factors. Its helical structure was stable in water over an examined pH range of 2–12. EG-grafted poly(L-lysine) was also stable in solutions containing various denaturing agents, such as up to 3 M NaCl, 1 M urea, or 1 M guanidinium-HCl. The thermal stability of the helical



conformation of EG-grafted poly(L-lysine) was also very high, and as much as 75% of its helicity is retained at 85 °C. This polymer is also soluble and helical in many organic solvents (e.g., THF, MeOH, and CHCl<sub>3</sub>), and was not digested by hydrolytic enzymes that readily digest poly(L-lysine) (e.g., papain, trypsin) [7], indicative of the PEG-like properties imparted by the EG sheath. The polymer has surface properties similar to unstructured PEG, but also possesses a rod-like backbone due to its  $\alpha$ -helical conformation. Similar monomers and polymers were prepared by Klok using succinate linkages between the EG segments and lysine [61]. In these polymers, the ester linkages to the EG segments are potentially degradable in water, and the polymers were found to prevent nonspecific protein adsorption when used to coat surfaces.

Recently, Deming and coworkers also reported glycopolypeptides via living polymerization of glycosylated-L-lysine NCAs [57], demonstrating the feasibility of synthesizing water-soluble, highly helical (ca. 88% helicity) polypeptides via monosaccharide-functionalized NCA monomers. Measurement of CD spectra from 4 to 90 °C revealed that the  $\alpha$ -helical conformation of poly(galactosyl-L-lysine) was gradually disrupted as temperature was increased, with roughly 40% helicity being retained at 90 °C. This behavior is probably due to disruption of amide H-bonding by interactions with water molecules [6]. These disordered polypeptides remained water-soluble, and their  $\alpha$ -helical conformations were completely regained upon cooling, showing that this process is reversible. The molecular weights of these rod-like “PEG-mimic” [60] or “polysaccharide-mimic” [57] polymers could also be easily adjusted by varying the NCA-to-Co(0) initiator ratios.

Similar oligo-EG modifications to the  $\beta$ -sheet preferring amino acids L-serine and L-cysteine were found to allow facile aqueous processing of their corresponding  $\beta$ -forming polymers. The EG side chains were found to provide good water solubility to the polymers, which could then form  $\beta$ -sheet structures upon solvent evaporation or by controlled addition of a solvent that stabilizes the  $\beta$ -conformation. The synthesis of EG-modified polyserine is shown in Scheme 18, where the EG repeats were coupled onto the amino acid using an ether linkage [62]. The modified amino acids were then converted to their corresponding NCA monomers to allow subsequent polymerization. CD analysis of the water-soluble polymer in deionized water at pH 7 revealed that it was in a disordered chain conformation [35, 36]. The CD spectra of this polymer were also invariant with solution pH and buffer strength, consistent with this result. However, films cast from aqueous solutions of this polymer from a variety of buffers all gave CD spectra indicative of the  $\beta$ -sheet conformation. The transformation from disordered conformation to  $\beta$ -sheet was also achieved in water by addition of increased percentages of methanol or



**Scheme 18** Synthesis of water-soluble EG-grafted poly(L-serine)s

acetonitrile. Wide-angle X-ray scattering data from films of oligo-EG-grafted poly (L-serine) revealed reflections that were also commensurate with the antiparallel  $\beta$ -sheet structure. Overall, these EG-modified polypeptides provide “PEG-like”  $\alpha$ -helix and  $\beta$ -sheet forming segments that can be incorporated into block copolypeptide delivery agents. Such domains provide not only improved solubility and bioavailability, but allow incorporation of secondary structure to control self-assembly of the drug complexes.

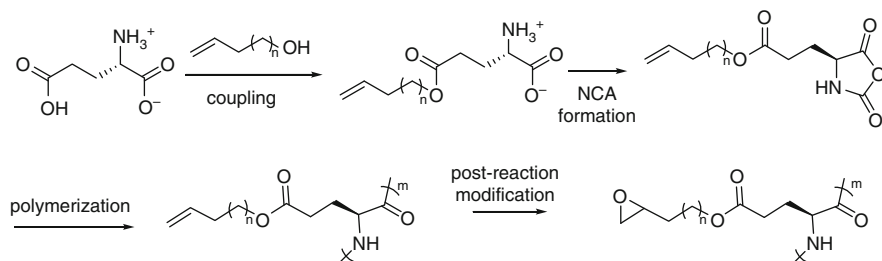
## 4 Polypeptide Deprotection and Purification

Although quite complex copolypeptide architectures can now be synthesized, obtaining these materials in a state of high purity typically requires additional measures. As discussed above, many of the copolypeptides synthesized using conventional methods contain homopolymer impurities, which must be removed by selective solvent extractions or fractional precipitation, when possible. Since conventional NCA polymerizations also usually give polypeptide segments with large chain length distributions, these samples are ideally also fractionated to give samples of well-defined composition. An additional purification issue arises from the amphiphilic nature of many of these copolymers, e.g., PEG-PBLG. Such polymers tend to associate in most solvents, leading to trapped solvents or solutes in the copolymer sample, which can complicate analytical studies. In the case of polymerizations initiated by a transition metal, removal of the metal from the sample is also important for most applications. For rigorous purification of these amphiphilic copolymers, Deming's group has found that exhaustive dialysis of the samples against deionized water is very effective at removing small molecule contaminants. In cases where a polymer segment can bind strongly to metals such as  $\text{Co}^{2+}$  and  $\text{Ni}^{2+}$ , the addition of a potent metal chelator, such as EDTA, in the early stages of dialysis was found to be sufficient to remove all traces of the metal ions.

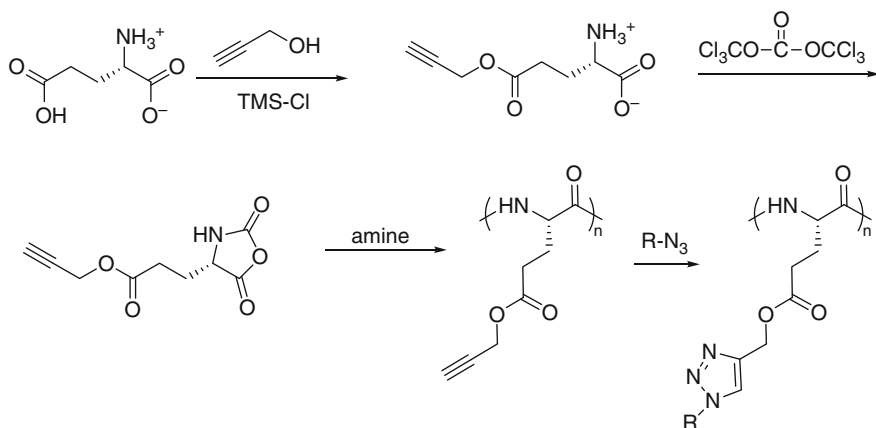
A highly useful feature of copolypeptide materials is their functionality. The common naturally occurring amino acids contain numerous acidic and basic functional groups that provide interesting pH-responsive character to these materials. These functional groups are masked by protecting groups before synthesis of the NCA monomers, since they will typically interfere with polypeptide synthesis or NCA stability [11, 12]. Consequently, these protecting groups must be removed after polymerization if the functional group chemistry is to be used. The first concern with polypeptide deprotection is whether or not all the protecting groups have been removed. Small amounts of residual protecting groups can significantly influence the resulting polypeptide properties, especially since the protecting groups are typically hydrophobic and the deprotected chain is typically hydrophilic. Fortunately, most of the common protecting groups are removed without difficulty, and deprotection levels greater than 97% are readily attained. The second, and more serious, consequence of deprotection is cleavage of the peptide chain, or racemization of the optically pure amino acid residues.

Basic polypeptides, such as polylysine or polyarginine, are readily deprotected [11, 12, 48]. Acidic polypeptides, such as polyglutamic acid or polyaspartic acid, require more care in deprotection reactions due to an abundance of potential side reactions. PBLG, for example, can be debenzylated using strong acid, aqueous base, or catalytic hydrogenation. Use of strong acid (e.g., gaseous HBr or HBr in acetic acid) avoids any racemization, but is known to lead to significant chain cleavage arising from protonation of side-chain ester groups that react with the amide backbone [49]. Basic conditions avoid this reaction, but can lead to significant racemization unless the amount of base is carefully controlled [50, 51]. Hydrogenation would appear to be the most attractive method, however, it is only effective for chains less than 10 kDa in mass. Larger PBLG chains adopt stable helical conformations that prevent access of the hydrogenation catalyst to the ester groups [50, 51]. Ester cleavage using trimethylsilyl iodide was found to give clean conversion to the readily hydrolyzed trimethylsilyl ester, without any racemization or chain cleavage [52]. The major drawbacks of this reagent are its expense as well as its reactivity with most other functional groups, such as the ether linkages in PEG. The deprotection of poly( $\beta$ -benzyl-L-aspartate) shows less side reactions under acidic conditions compared to PBLG. However, it has been reported that the polymer backbone undergoes partial rearrangement to  $\beta$ -peptide linkages under basic conditions, presumably through an imide intermediate [54]. The degree of racemization in these samples was not discussed.

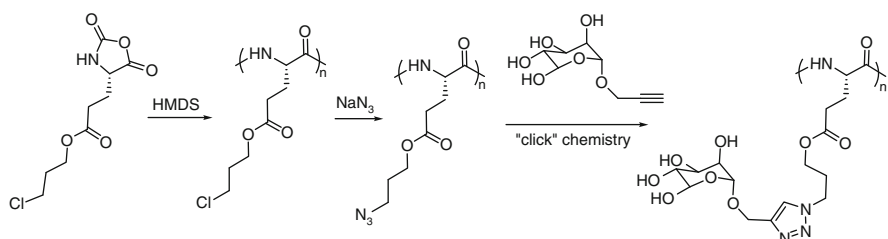
To avoid the issues of deprotection chemistry and to allow facile side-chain functionalization, an emerging field is focused on the development of new NCA monomers bearing side-chain functional groups that stay intact during polymerization and can be used for highly efficient conjugation of functional moieties after polymerization. The synthesis of  $\gamma$ -alkenyl-L-glutamate NCAs was reported by Poché et al. in 1997, and these were utilized for preparing poly(L-glutamate)s containing pendant alkene functional groups that were modified by a variety of reactions (Scheme 19) [63]. In the past few years, a number of other NCAs bearing conjugation-amenable side-chain functional groups, as well as their polymerizations, have been reported. These include  $\gamma$ -propargyl-L-glutamate NCA by Hammond [64] and Chen [56] (Scheme 20),  $\gamma$ -3-chloropropyl-L-glutamate NCA by Zhang (Scheme 21) [43], propargyl-DL-glycine NCA by Heise (Scheme 22) [65],



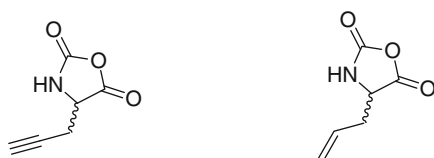
**Scheme 19** Synthesis and derivatization of alkene-terminated poly(glutamates)



**Scheme 20** Synthesis and derivatization of alkyne-terminated poly(glutamates)



**Scheme 21** Synthesis and derivatization of azido-terminated poly(glutamates)

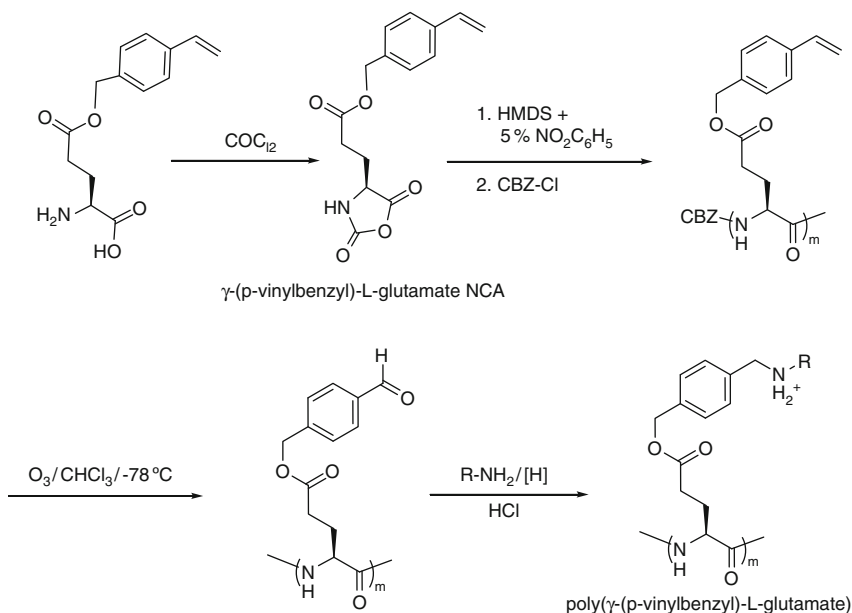


**Scheme 22** Alkene and alkyne bearing NCAs

propargyl-DL-glycine NCA

allyl-DL-glycine NCA

allyl-DL-glycine NCA by Schlaad (Scheme 22) [58] and  $\gamma$ -(*p*-vinylbenzyl)-L-glutamate NCA by Cheng (Scheme 23) [66]. Through a variety of azide-alkyne, thiol-ene and other chemistries, these functionalized polypeptides were modified with a variety of functional moieties including monosaccharides and PEG chains. These reactive polypeptides have the potential for generation of a large library of functional polymers from a single precursor. For instance, conversion of alkene groups in poly( $\gamma$ -(*p*-vinylbenzyl)-L-glutamate) to aldehydes, followed by reductive amination with primary amines was used to generate poly(L-glutamate) analogs with charged groups distally situated on their side chains (Scheme 23) [66]. These



**Scheme 23** Synthesis and derivatization of aldehyde-terminated poly(glutamates)

side-chain charged poly(L-glutamate) analogs were found to be water-soluble and able to adopt stable  $\alpha$ -helical conformations over a wide range of pH (pH 1–12), in contrast to poly(L-lysine) or poly(L-glutamic acid) that are known for their pH-dependent helix–coil transitions.

## 5 Conclusions and Future Prospects

The synthesis of polypeptides by ring-opening polymerization of NCAs is an area that has been under study for more than six decades. Initially, this field suffered from limitations in the synthesis of the polypeptide components, which required excessive sample purification and fractionation to obtain well-defined copolymers. In recent years, vast improvements in NCA polymerizations, either using metal initiators [19, 67] or improved conventional initiators [21, 22, 68] now allow the synthesis of hybrid and block copolymers of controlled dimensions (molecular weight, sequence, composition, and molecular weight distribution). Such materials will greatly assist in the development and identification of new self-assembled structures made possible with ordered polypeptide segments, as well as yield new materials with a wide range of tunable properties.

There are still many challenging issues that remain to be addressed in the field of synthetic polypeptides. NCA purification has been one of the bottlenecks limiting the availability and scale-up of NCA monomers. Recrystallization has long been the

only practical method for obtaining NCA monomers with satisfactory purity for polymerization. Recently, Deming and coworkers reported the purification of NCA monomers using flash chromatography, which may substantially improve the purity of NCAs and potentially make it possible to purify NCA monomers that do not crystallize [69]. Polymerizations of NCAs are usually conducted in anhydrous organic solvents, which are not environmentally friendly. As an alternative approach, Mori and coworkers recently attempted the use of ionic liquids for the polymerization of Bn-Glu NCA, underscoring an effort to integrate green chemistry with the synthesis of polypeptides [70].

## References

1. Branden C, Tootz J (1991) Introduction to protein structure. Garland, New York
2. Cha JN, Stucky GD, Morse DE, Deming TJ (2000) Biomimetic synthesis of ordered silica structures mediated by block copolypeptides. *Nature* 403:289–292
3. van Hest JCM, Tirrell DA (2001) Protein-based materials, toward a new level of structural control. *Chem Commun* 1897–1904
4. Voet D, Voet JG (1995) Biochemistry, 2nd edn. Wiley, New York, Chap 32
5. Fasman G (1989) Prediction of protein structure and the principles of protein conformation. Plenum Press, New York
6. Fasman GD (1967) Poly-alpha-amino acids. Dekker, New York
7. Deming TJ (2000) Living polymerization of alpha-amino acid-N-carboxyanhydrides. *J Polym Sci Polym Chem* 38:3011–3018
8. Discher DE, Eisenberg A (2002) Polymer vesicles. *Science* 297:967–973
9. Kwon GS, Naito M, Kataoka K, Yokoyama M, Sakurai Y, Okano T (1994) Block copolymer micelles as vehicles for hydrophobic drugs. *Colloids Surf B* 2:429–434
10. Takae S, Miyata K, Oba M, Ishii T, Nishiyama N, Itaka K, Yamasaki Y, Koyama H, Kataoka K (2008) PEG-detachable polyplex micelles based on disulfide-linked block cationomers as bioresponsive nonviral gene vectors. *J Am Chem Soc* 130:6001–6009
11. Kricheldorf H (1990) Polypeptides. In: Pencze S (ed) Models of biopolymers by ring opening polymerization. CRC, Boca Raton, pp 1–132
12. Kricheldorf HR (1987)  $\alpha$ -Amino acid-N-carboxyanhydrides and related materials. Springer, New York
13. Woodward RB, Schramm CH (1947) Synthesis of protein analogs. *J Am Chem Soc* 69:1551–1552
14. Webster OW (1991) Living polymerization methods. *Science* 251:887–893
15. Kubota S, Fasman GD (1975) Beta-conformation of polypeptides of valine, isoleucine, and threonine in solution and solid-state - optical and infrared studies. *Biopolymers* 14:605–631
16. Howard JC, Cardinaux F, Scheraga HA (1977) Block copolymers of amino-acids. 2. Physico-chemical data on copolymers containing L-alanine or L-phenylalanine. *Biopolymers* 16:2029–2051
17. Cardinaux F, Howard JC, Taylor GT, Scheraga HA (1977) Block copolymers of amino-acids. 1. Synthesis and structure of copolymers of L-alanine or L-phenylalanine with D, L-lysine-D7 or D, L-lysine. *Biopolymers* 16:2005–2028
18. Sekiguchi H (1981) Mechanism of N-carboxy-alpha-amino acid anhydride (Nca) polymerization. *Pure Appl Chem* 53:1689–1714
19. Deming TJ (1997) Facile synthesis of block copolypeptides of defined architecture. *Nature* 390:386–389

20. Dimitrov I, Schlaad H (2003) Synthesis of nearly monodisperse polystyrene-polypeptide block copolymers via polymerization of N-carboxyanhydrides. *Chem Commun* 2944–2945
21. Aliferis T, Iatrou H, Hadjichristidis N (2004) Living polypeptides. *Biomacromolecules* 5:1653–1656
22. Lu H, Cheng JJ (2007) Hexamethyldisilazane-mediated controlled polymerization of alpha-amino acid N-carboxyanhydrides. *J Am Chem Soc* 129:14114–14115
23. Collman JP, Hegedus LS, Norton JR, Finke RG (1987) Principles and applications of organotransition metal chemistry, 2nd edn. University Science, Mill Valley
24. Deming TJ (1999) Cobalt and iron initiators for the controlled polymerization of alpha-amino acid-N-carboxyanhydrides. *Macromolecules* 32:4500–4502
25. Deming TJ (1998) Amino acid derived nickelacycles: intermediates in nickel-mediated polypeptide synthesis. *J Am Chem Soc* 120:4240–4241
26. Deming TJ, Curtin SA (2000) Chain initiation efficiency in cobalt- and nickel-mediated polypeptide synthesis. *J Am Chem Soc* 122:5710–5717
27. Deming TJ (2005) Polypeptide hydrogels via a unique assembly mechanism. *Soft Matter* 1:28–35
28. Curtin SA, Deming TJ (1999) Initiators for end-group functionalized polypeptides via tandem addition reactions. *J Am Chem Soc* 121:7427–7428
29. Witte P, Menzel H (2004) Nickel-mediated surface grafting from polymerization of alpha-amino acid-N-carboxyanhydrides. *Macromol Chem Phys* 205:1735–1743
30. Brzezinska KR, Curtin SA, Deming TJ (2002) Polypeptide end-capping using functionalized isocyanates: preparation of pentablock copolymers. *Macromolecules* 35:2970–2976
31. Pickel DL, Politakos N, Avgeropoulos A, Messman JM (2009) A mechanistic study of alpha-(amino acid)-N-carboxyanhydride polymerization: comparing initiation and termination events in high-vacuum and traditional polymerization techniques. *Macromolecules* 42:7781–7788
32. Vayaboury W, Giani O, Cottet H, Deratani A, Schue F (2004) Living polymerization of alpha-amino acid N-carboxyanhydrides (NCA) upon decreasing the reaction temperature. *Macromol Rapid Commun* 25:1221–1224
33. Odian G (2004) Principles of polymerization, 4th edn. Wiley-Interscience, New York
34. Vayaboury W, Giani O, Cottet H, Bonaric S, Schue F (2008) Mechanistic study of alpha-amino acid N-carboxyanhydride (NCA) polymerization by capillary electrophoresis. *Macromol Chem Phys* 209:1628–1637
35. Knobler Y, Bittner S, Frankel M (1964) Reaction of N-carboxy-alpha-amino-acid anhydrides with hydrochlorides of hydroxylamine O-alkylhydroxylamines + amines syntheses of amino-hydroxamic acids amido-oxy-peptides + alpha-amino-acid amides. *J Chem Soc* 3941
36. Knobler Y, Bittner S, Virov D, Frankel M (1969) Alpha-aminoacyl derivatives of aminobenzoic acid and of amino-oxy-acids by reaction of their hydrochlorides with amino-acid N-carboxyanhydrides. *J Chem Soc C* 1821
37. Fischer H (2001) The persistent radical effect: a principle for selective radical reactions and living radical polymerizations. *Chem Rev* 101:3581–3610
38. Peggion E, Cosani A, Mattucci AM, Scoffone E (1964) Polymerization of gamma-ethyl-L-glutamate-N-carboxyanhydride initiated by Di-N-butyl and Di-isopropyl amine. *Biopolymers* 2:69–78
39. Kricheldorf HR, Greber G (1971) N-silylated amino acid N-carboxylic acid anhydrides (oxazolidine-2,5-diones). *Chem Ber* 104:3131
40. Webster OW, Hertler WR, Sogah DY, Farnham WB, Rajanbabu TV (1983) Group-transfer polymerization. 1. A New concept for addition polymerization with organo-silicon initiators. *J Am Chem Soc* 105:5706–5708
41. Webster OW (2004) Group transfer polymerization: mechanism and comparison with other methods for controlled polymerization of acrylic monomers. In: *New synthetic methods. Advances in polymer science*, vol 167. Springer, Berlin, pp 1–34

42. Lu H, Wang J, Lin Y, Cheng J (2009) One-pot synthesis of brush-like polymers via integrated ring-opening metathesis polymerization and polymerization of amino acid N-carboxyanhydrides. *J Am Chem Soc* 131:13582–13583
43. Tang HY, Zhang DH (2010) General route toward side-chain-functionalized alpha-helical polypeptides. *Biomacromolecules* 11:1585–1592
44. Lutz JF, Schutt D, Kubowicz S (2005) Preparation of well-defined diblock copolymers with short polypeptide segments by polymerization of N-carboxy anhydrides. *Macromol Rapid Commun* 26:23–28
45. Brzezinska KR, Deming TJ (2001) Synthesis of ABA triblock copolymers via acyclic diene metathesis polymerization and living polymerization of alpha-amino acid-N-carboxyanhydrides. *Macromolecules* 34:4348–4354
46. Brzezinska KR, Deming TJ (2004) Synthesis of AB diblock copolymers by atom-transfer radical polymerization (ATRP) and living polymerization of alpha-amino acid-N-carboxyanhydrides. *Macromol Biosci* 4:566–569
47. Kros A, Jesse W, Metselaar GA, Cornelissen JJLM (2005) Synthesis and self-assembly of rod-rod hybrid poly(gamma-benzyl L-glutamate)-block-polyisocyanide copolymers. *Angew Chem Int Ed* 44:4349–4352
48. Ben-Ishai D, Berger A (1952) Cleavage of N-carbobenzoxy groups by dry hydrogen bromide and hydrogen chloride. *J Org Chem* 17:1564–1570
49. Blout ER, Idelson M (1956) Polypeptides VI. Poly-alpha-glutamic acid: preparation and helix-coil conversions. *J Am Chem Soc* 78:497–498
50. Hanby WE, Waley SG, Watson J (1948) Synthetic polyglutamic acid. *Nature* 161:132
51. Hanby WE, Waley SG, Watson J (1950) 632. Synthetic polypeptides. Part II. Polyglutamic acid. *J Chem Soc* 3239–3249
52. Subramanian G, Hjelm RP, Deming TJ, Smith GS, Li Y, Safinya CR (2000) Structure of complexes of cationic lipids and poly(glutamic acid) polypeptides: a pinched lamellar phase. *J Am Chem Soc* 122:26–34
53. Hanson JA, Chang CB, Graves SM, Li ZB, Mason TG, Deming TJ (2008) Nanoscale double emulsions stabilized by single-component block copolypeptides. *Nature* 455:85–U54
54. Saudek V, Pivcova H, Drobnik J (1981) NMR-study of poly(aspartic acid). 2. Alpha-peptide and beta-peptide bonds in poly(aspartic acid) prepared by common methods. *Biopolymers* 20:1615–1623
55. Kim KT, Vandermeulen GWM, Winnik MA, Manners I (2005) Organometallic-polypeptide block copolymers: synthesis and properties of poly(ferrocenyldimethylsilane)-b-poly(gamma-benzyl-L-glutamate). *Macromolecules* 38:4958–4961
56. Xiao CS, Zhao CW, He P, Tang ZH, Chen XS, Jing XB (2010) Facile synthesis of glycopolypeptides by combination of ring-opening polymerization of an alkyne-substituted N-carboxyanhydride and click “glycosylation”. *Macromol Rapid Commun* 31:991–997
57. Kramer JR, Deming TJ (2010) Glycopolypeptides via living polymerization of glycosylated-L-lysine N-carboxyanhydrides. *J Am Chem Soc* 132:15068–15071
58. Sun J, Schlaad H (2010) Thiol-Ene clickable polypeptides. *Macromolecules* 43:4445–4448
59. Deming TJ (2002) Methodologies for preparation of synthetic block copolypeptides: materials with future promise in drug delivery. *Adv Drug Delivery Rev* 54:1145–1155
60. Yu M, Nowak AP, Deming TJ, Pochan DJ (1999) Methylated mono- and diethyleneglycol functionalized polylysines: nonionic, alpha-helical, water-soluble polypeptides. *J Am Chem Soc* 121:12210–12211
61. Wang J, Gibson MI, Barbey R, Xiao SJ, Klok HA (2009) Nonfouling polypeptide brushes via surface-initiated polymerization of N-epsilon-oligo(ethylene glycol)succinate-L-lysine N-carboxyanhydride. *Macromol Rapid Commun* 30:845–850
62. Hwang JY, Deming TJ (2001) Methylated mono- and di(ethylene glycol)-functionalized beta-sheet forming polypeptides. *Biomacromolecules* 2:17–21
63. Poche DS, Thibodeaux SJ, Rucker VC, Warner IM, Daly WH (1997) Synthesis of novel gamma-alkenyl L-glutamate derivatives containing a terminal C-C double bond to produce polypeptides with pendant unsaturation. *Macromolecules* 30:8081–8084



64. Engler AC, Lee HI, Hammond PT (2009) Highly efficient “grafting onto” a polypeptide backbone using click chemistry. *Angew Chem Int Ed* 48:9334–9338
65. Huang J, Habraken G, Audouin F, Heise A (2010) Hydrolytically stable bioactive synthetic glycopeptide homo- and copolymers by combination of NCA polymerization and click reaction. *Macromolecules* 43:6050–6057
66. Lu H, Wang J, Bai Y, Lang JW, Liu S, Lin Y, Cheng J (2011) Ionic polypeptides with unusual helical stability. *Nat Commun* 2:206
67. Peng YL, Lai SL, Lin CC (2008) Preparation of polypeptide via living polymerization of Z-Lys-NCA initiated by platinum complexes. *Macromolecules* 41:3455–3459
68. Schlaad H, Smarsly B, Losik M (2004) The role of chain-length distribution in the formation of solid-state structures of polypeptide-based rod-coil block copolymers. *Macromolecules* 37:2210–2214
69. Kramer JR, Deming TJ (2010) General method for purification of alpha-amino acid-N-carboxyanhydrides using flash chromatography. *Biomacromolecules* 11:3668–3672
70. Mori H, Iwata M, Ito S, Endo T (2007) Ring-opening polymerization of gamma-benzyl-L-glutamate-N-carboxyanhydride in ionic liquids. *Polymer* 48:5867–5877

# Peptide Synthesis and Self-Assembly

S. Maude, L.R. Tai, R.P.W. Davies, B. Liu, S.A. Harris, P.J. Kocienski,  
and A. Aggeli

**Abstract** Peptides and proteins are the most diverse building blocks in biomolecular self-assembly in terms of chemistry, nanostructure formation and functionality. Self-assembly is an intrinsic property of peptides. In this chapter, we attempt to address the following issues: How can we synthesize a self-assembling peptide? What are the fundamental physical and chemical principles that underpin peptide self-assembly? How can we learn to finely control peptide self-assembly? The merits of answering these questions are inspiring both for biology and medicine in terms of new opportunities for understanding, preventing and curing of diseases, and for nanotechnology in terms of new prescribed routes to achieving peptide-based nanostructures with a range of properties appropriate for specific applications.

**Keywords** Co-assembly · Functionalization · Molecular dynamics · Self-assembly · Solid phase synthesis

## Contents

1	Introduction .....	29
2	Solid Phase Peptide Synthesis .....	30
	2.1 Protection Strategies in SPPS .....	31
	2.2 Coupling Methods in SPPS .....	32
	2.3 Known Problems in SPPS .....	34
3	Peptide Self-Assembly .....	36
	3.1 Model Self-Assembling Peptides .....	36
	3.2 Hierarchical Self-Assembly .....	38

---

S. Maude, L.R. Tai, R.P.W. Davies, P.J. Kocienski and A. Aggeli (✉)  
Centre for Molecular Nanoscience, School of Chemistry, University of Leeds, Leeds LS2 9JT, UK  
e-mail: [a.aggeli@leeds.ac.uk](mailto:a.aggeli@leeds.ac.uk)

B. Liu and S.A. Harris  
Centre for Molecular Nanoscience, School of Chemistry, University of Leeds, Leeds LS2 9JT, UK  
School of Physics & Astronomy, University of Leeds, Leeds LS2 9JT, UK

3.3	pH- and Ionic Strength-Triggered and Switchable Self-Assembly .....	40
3.4	In Silico Design of Self-Assembling Peptides .....	43
4	Self-Assembling Peptides as Frameworks for Other Functional Molecules .....	46
4.1	Assemblies Formed from Modified Self-Assembling Monomers .....	46
4.2	Modification of Self-Assembled Structures .....	56
5	Conclusions .....	66
	References .....	67

## Abbreviations

AFM	Atomic force microscopy
Boc	<i>tert</i> -Butoxycarbonyl
BOP	<i>O</i> -Benzotriazol-1-yloxytris(dimethylamino)phosphonium hexafluorophosphate
CD	Circular dichroism
DCC	Dicyclohexylcarbodiimide
Fmoc	9-Fluorenylmethoxycarbonyl
HATU	2-(7-Aza-1H-benzotriazole-1-yl)-1,1,3,3-tetramethyluronium hexafluorophosphate
HBTU	2-(1H-Benzotriazole-1-yl)-1,1,3,3-tetramethyluronium hexafluorophosphate
HCTU	2-(6-Chloro-1H-benzotriazole-1-yl)-1,1,3,3-tetramethylaminium hexafluorophosphate
HOAt	1-Hydroxy-7-azabenzotriazole
HOBt	1-Hydroxybenzotriazole
HOSu	<i>N</i> -Hydroxysuccinimide
HPLC	High performance liquid chromatography
IR	Infrared
MALDI	Matrix-assisted laser desorption/ionisation
MD	Molecular dynamics
MDC	Monodansylcadaverine
PEG	Poly(ethylene glycol)
PyAOP	7-Azabenzotriazol-1-yloxytris(pyrrolidino)phosphonium hexafluorophosphate
PyBOP	<i>O</i> -Benzotriazol-1-yloxytris(pyrrolidino)phosphonium hexafluorophosphate
SANS	Small angle neutron scattering
SPPS	Solid phase peptide synthesis
TBTU	2-(1H-Benzotriazole-1-yl)-1,1,3,3-tetramethyluronium tetrafluoroborate
TEM	Transmission electron microscopy
TFA	Trifluoroacetic acid
TGase	Tissue transglutaminase
UV	Ultraviolet

## 1 Introduction

Biomolecular self-assembly is an intensely studied research area worldwide and interest in the field is predicted to increase even further in the future. There are a number of factors that constantly drive attention to this topic. First, biomolecular self-assembly is the main underlying mechanism for the production of most important structures in nature, from the cell membrane and the various cell organelles to the extracellular matrix and structures with extraordinary properties such as silk and muscle fibres. Second, molecular self-assembly is one of the two main approaches for the production of well-defined, functional nanostructures essential for the fast growing field of nanotechnology; in particular, molecular self-assembly is seen as the main bottom-up approach in nanoscience and nanotechnology. It is a neat concept with great potential that is based on individual molecules acting as molecular bricks held together by a “glue” of noncovalent intermolecular interactions. A wide range of biological and synthetic molecules can act as molecular bricks. In biomolecular self-assembly, the most diverse building blocks in terms of chemistry, nanostructure formation and functionality are peptides and proteins. A very promising initial observation is that, in principle, self-assembly is an intrinsic property of peptides, since all peptides by definition have a peptide backbone full of complementary hydrogen bond donor and acceptor sites. However, the next big questions that research efforts are trying to answer are:

1. What are the fundamental physical and chemical principles that underpin peptide self-assembly?
2. How can we learn to finely control peptide self-assembly?

The merits of answering these questions are inspiring both for biology and medicine, in terms of new opportunities for understanding, preventing and curing of diseases, and for nanotechnology in terms of new prescribed routes to achieving peptide-based nanostructures with a range of properties appropriate for specific applications.

In order to attempt to tackle either of the two questions above, the first hurdle that needs to be overcome in most cases is to make a peptide; luckily an advantage of peptides as building blocks is that they can be made using a variety of different approaches. Genetic engineering has established itself as an indispensable route to the manufacture of a wide range of proteinaceous materials, e.g. allowing affordable production of bulk quantities of versatile, monodisperse long polypeptides. At the same time, the chemical, synthetic approach is still the preferred route for peptide production in a large number of cases, especially for shorter peptides, because it provides an easy, fast method for the reliable production of an unlimited number of high quality peptides with no risk of infection from transmissible diseases. A short introduction to the main method of chemical peptide synthesis, the solid phase method, is described in Sect. 2, with comments on some peculiarities that are encountered in peptides with high propensity for self-assembly.

Peptide self-assembly is a complex phenomenon driven by thermodynamic and kinetic considerations. Thus, answering question 1 is not a trivial task. Section 3 presents an example of an analytical way of describing peptide self-assembly and demonstrates the unique opportunities it creates for a quantitative and thorough understanding of this phenomenon, as well as for peptide design. Finally, Sect. 4 attempts to address question 2 by demonstrating the opportunities for design of ever-more complex peptide building blocks with the aim of controlling their assembly and suitability for functionalisation. This section deliberately concentrates on the molecular and self-assembly levels rather than touching upon the types of applications of self-assembling peptides, which is a topic covered by other reviews.

## 2 Solid Phase Peptide Synthesis

The original concept of solid phase peptide synthesis (SPPS) was introduced by Merrifield in 1963 [1]. The concept entails the stepwise elongation of polypeptides covalently attached to insoluble polymeric resins. There are several distinct advantages to SPPS over traditional solution phase peptide synthesis. These include: (1) the use of excess reagents to drive coupling reactions to completion, (2) simplified isolation and purification steps, and (3) the ease of automation. In addition, SPPS has also overcome the problem of poor intermediate solubility often encountered in conventional solution phase synthesis. The anchoring of the first residue to the resin (Fig. 1) requires the use of resin-linker functionalities, typically esters or amides [2]. Peptide synthesis can then continue by repetitive cycles of deprotection of the N-terminus protecting group on the peptide and of coupling of the following amino acid. Isolation of the resin by filtration and purification by means of washing is executed between each stage [3]. Once the sequence is complete, the peptide is cleaved from the resin [4].

The nature of the SPPS technique limits the range of chemistries used for peptide assembly, and all resin-bound intermediates are precursors to the final product. The two primary areas of consideration are the protection strategies and the coupling methods [5]. At least two types of orthogonal protecting groups are employed during a linear peptide elongation to differentiate the reactive functionalities of the amino acid side chains. The protecting groups prevent side reactions from occurring during peptide couplings. Efficient coupling of each incoming amino acid is required to achieve product homogeneity. In particular, an inefficient early coupling will result in deletion sequences on all subsequent elongations. Amino acid couplings also require care so that configurational integrity is preserved. This criterion has fuelled the development of numerous carboxylic activating agents to reduce problems such as low yields, racemisation, degradation etc. [3]. Together with advances in high performance liquid chromatography (HPLC) and mass spectrometry, SPPS has become a routine method for polypeptide synthesis [6].

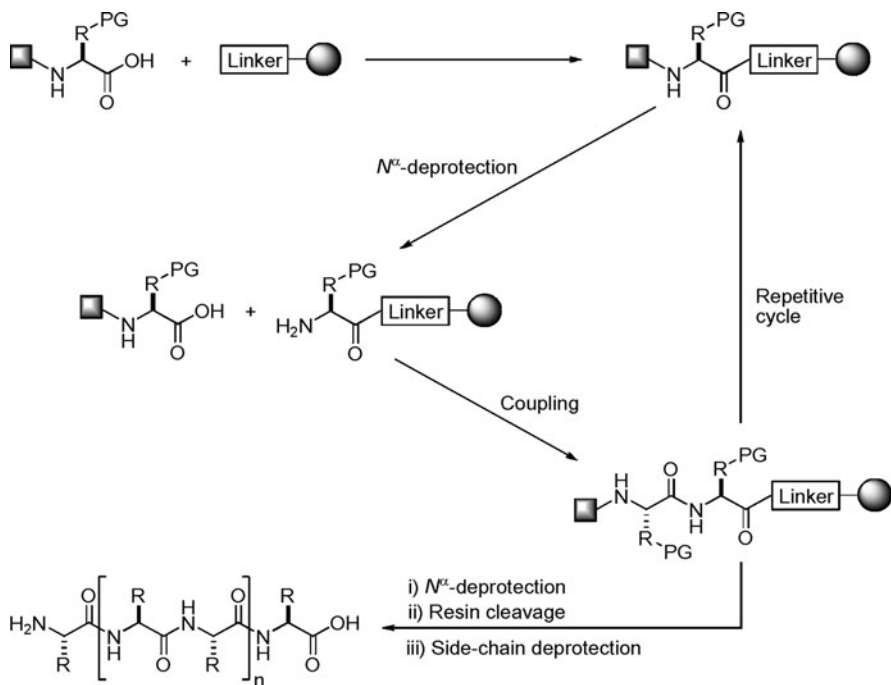
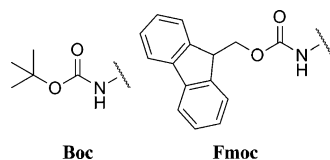


**Fig. 1** Linear solid phase peptide synthesis

**Fig. 2** Two common  $N^\alpha$ -protecting groups



## 2.1 Protection Strategies in SPPS

In SPPS, there are two main protecting groups commonly used for  $N^\alpha$ -protection [3]: *tert*-butoxycarbonyl (Boc) [7] and 9-fluorenylmethoxycarbonyl (Fmoc) [8] (Fig. 2).

In the Boc protection approach, benzyl groups are used to protect the reactive amino acid side-chain functionalities because they are more acid-stable than the Boc groups. Trifluoroacetic acid (TFA) is sufficient to remove the Boc groups while leaving the benzyl groups intact (Fig. 3).

In the Fmoc protection approach, the acid-labile *tert*-butyl groups are often used for side-chain protection. The base-labile Fmoc groups can be easily removed during a synthesis using piperidine (Fig. 4). The final global deprotection together with cleavage from the polymeric support is achieved with TFA.

Developments of protection strategies in peptide synthesis have led to the introduction of a wider variety of protecting groups for different functionalities and provide orthogonal protection to specific side chains (Table 1).

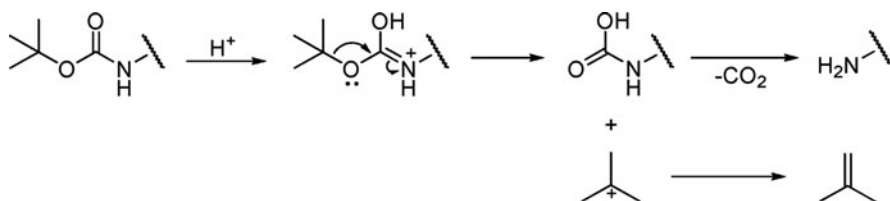


Fig. 3 Removal of *tert*-butoxycarbonyl (*Boc*) group

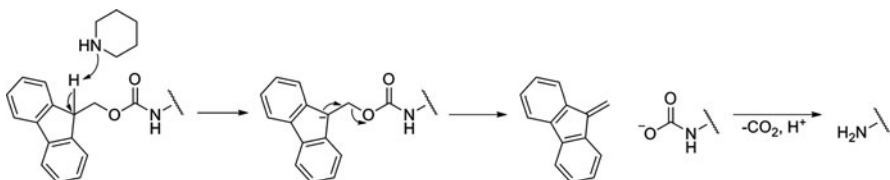


Fig. 4 Removal of 9-fluorenylmethoxycarbonyl (*Fmoc*) group

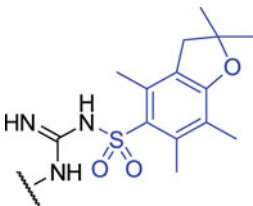
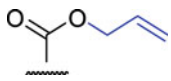
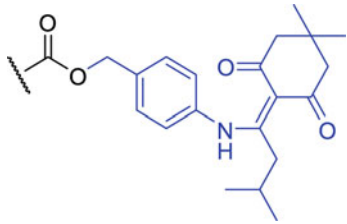
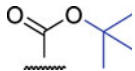
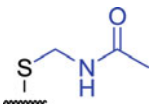
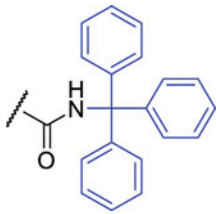
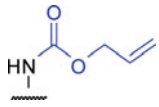
## 2.2 Coupling Methods in SPPS

Efficient and unambiguous peptide-bond formation requires chemical activation of the carboxyl component of the  $N^\alpha$ -protected amino acid. An ideal coupling reagent must be able to achieve high coupling efficiency and prevent racemisation or detrimental side reactions. Racemisation sometimes occurs during the coupling reaction where the epimerisation of stereogenic centres in building blocks leads to diastereomeric sequences in the peptide chain.

One of the earliest reagents for peptide elongation, dicyclohexylcarbodiimide (DCC) forms a highly reactive intermediate of *O*-acylisourea during the in-situ activation of a carboxyl group [9]. This intermediate can undergo intramolecular cyclisation to give an oxazolone compound that eventually leads to racemisation (Fig. 5). Investigations of the racemisation mechanism enabled the development of additives to suppress racemisation in coupling reactions and promote efficiency [10].

The first additive designed for peptide elongation was *N*-hydroxysuccinimide (HOSu) [11] but it has been superseded by 1-hydroxybenzotriazole (HOBT) [12] and 1-hydroxy-7-azabenzotriazole (HOAt) (Fig. 6). These compounds, when used in conjunction with a range of coupling reagents, can suppress racemisation and accelerate reaction rates to provide optimal coupling yields. The phosphonium and uronium salts are also among the most effective and widely used reagents for coupling reactions. Extensive developments in this class of compounds have led to a variety of activating agents that possess superior coupling reactivity and reduce side reactions.

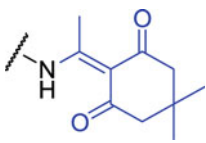
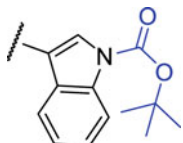
**Table 1** Common side-chain protecting groups

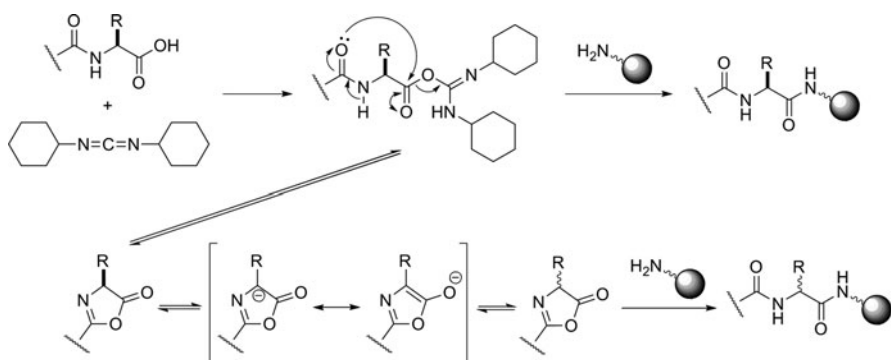
Amino acid residue	Molecular structure of protecting group	Abbreviation for protecting group
Arginine		Pbf
Aspartic acid/glutamic acid		All
Aspartic acid/glutamic acid		ODmab
Aspartic acid/glutamic acid		OtBu
Cysteine		Acm
Glutamine		Trt
Lysine		Alloc

(continued)



**Table 1** (continued)

Amino acid residue	Molecular structure of protecting group	Abbreviation for protecting group
Lysine		Dde
Tryptophan		Boc

**Fig. 5** Racemisation as a consequence of the oxazolone formation

### 2.3 Known Problems in SPPS

Side reactions in SPPS can still occur even though global protection strategies are used. These side reactions can be residue- or sequence-specific and their intervention depends upon many factors.

#### 2.3.1 Incomplete $N^\alpha$ Deprotection and Coupling Reactions

The failure to completely remove the  $N^\alpha$ -protecting group and incomplete coupling reactions are among the most frequent problems observed in SPPS and result in

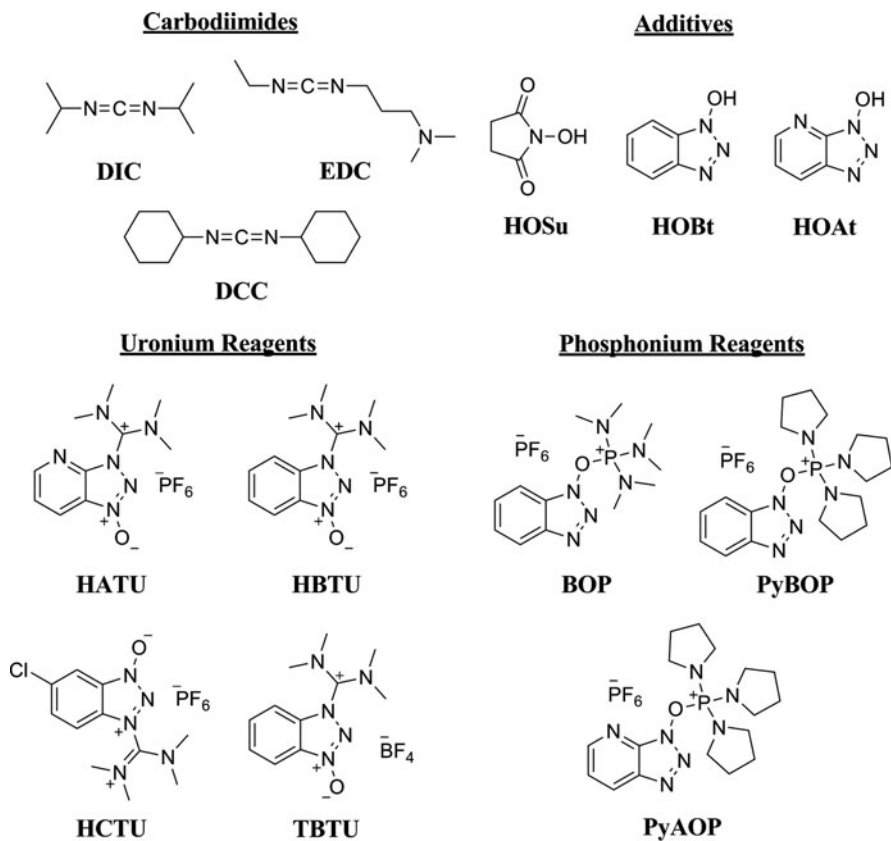


**Fig. 6** Commonly used additives and coupling reagents. *DCC* dicyclohexylcarbodiimide, *HOSu* *N*-hydroxysuccinimide, *HOBt* 1-hydroxybenzotriazole, *HOAt* 1-hydroxy-7-azabenzotriazole

deletion peptides, which are lacking one or more amino acid residues at the end of the synthesis. A truncated sequence or capping stems from the irreversible blocking of the N-terminus of a peptide chain. Further elongation is thus prevented.

### 2.3.2 Difficult Sequences

On-resin intermolecular association of protected peptide intermediates can cause sluggish deprotection and coupling reactions [13]. The aggregation and formation of  $\beta$ -sheets or other secondary structures prevent the N-terminus of the peptide chain from reaching the reagents necessary for elongation. This problem can possibly be overcome by using a convergent solid-phase approach.

### 2.3.3 Undesired Cyclisations

Cyclic structures can form as a result of side reactions. One of the most common examples is the formation of diketopiperazines during the coupling of the third amino acid onto the peptide chain (Fig. 7). Intramolecular amide bond formation gives rise to a cyclic dipeptide of a six-membered ring structure, causing losses to the sequence and regeneration of the hydroxyl sites on the resin. The nucleophilic group on the resin can lead to further unwanted reactions [14].

This problem can be suppressed by introducing a bulky steric group, such as the trityl-based resins (Fig. 8), at the C-terminal peptide-anchorage.

Another competing cyclisation during peptide synthesis is the formation of aspartimides from aspartic acid residues [15]. This problem is common with the aspartic acid–glycine sequence in the peptide backbone and can take place under both acidic and basic conditions (Fig. 9). In the acid-catalysed aspartimide formation, subsequent hydrolysis of the imide-containing peptide leads to a mixture of the desired peptide and a  $\beta$ -peptide. The side-chain carboxyl group of this  $\beta$ -peptide will become a part of the new peptide backbone. In the base-catalysed aspartimide formation, the presence of piperidine used during Fmoc group deprotection results in the formation of piperidines.

## 3 Peptide Self-Assembly

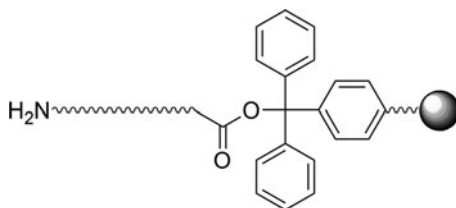
### 3.1 Model Self-Assembling Peptides

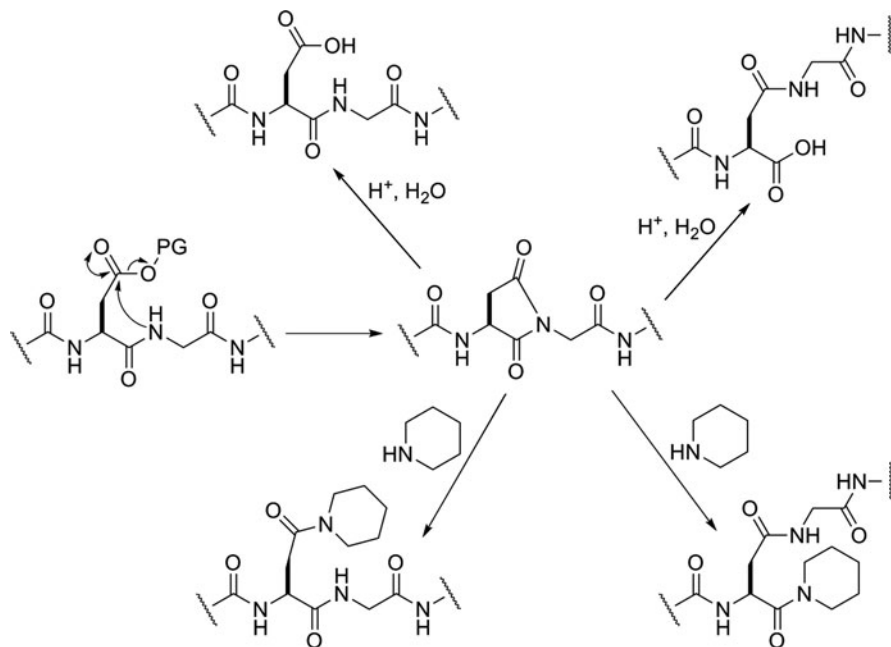
In order to explore systematically the main principles that guide peptide self-assembly, a useful approach is to study model self-assembling peptides. In this way, the natural chemical and conformational complexity of biological peptides



Fig. 7 Formation of diketopiperazines

Fig. 8 Trityl-based resin





**Fig. 9** Consequences of an aspartimide formation

can be minimised. An example of this approach is the design of peptide  $P_{11-2}$  (Ac-QQRFQWQFEQQ-Am) [16]. Several principles were applied by the researchers to the successful design of this  $\beta$ -strand-forming sequence. Alternating hydrophilic and hydrophobic residues in the core lend themselves to a  $\beta$ -strand-favoured conformation [17]. An odd number of amino acid residues were selected in order to encourage a complete register of the adjacent amphiphilic peptide strands in an antiparallel  $\beta$ -sheet tape. Side-chain interactions are another important factor in driving strand assembly. Dimethylene groups on the glutamine residues provide hydrophobic side-chain interactions, while the aromatic residues, also hydrophobic, additionally interact via  $\pi$ - $\pi$  stacking interactions. Aqueous solubility of peptide tapes is promoted through the hydrophilic ends of the side chains of glutamine, glutamic acid and arginine. Acetylation and amidation removes the charges normally present at peptide termini to prevent unwanted interaction between  $COO^-$  and  $NH_3^+$ . This modification can also help reduce proteolysis [18]. Finally, the positively charged arginine and the negatively charged glutamic acid residues are positioned such that the complementary charges of arginine and glutamic acid on neighbouring strands are adjacent to each other if the peptide is in an anti-parallel  $\beta$ -sheet configuration.

$P_{11-2}$  was found to form self-supporting gels at a concentration of approximately  $15 \text{ mg mL}^{-1}$  in pH-neutral water. In water, circular dichroism (CD) spectra of the

peptide up to 40  $\mu\text{M}$  were indicative of a random coil conformation, but above that concentration the peptide becomes predominantly  $\beta$ -sheet [19]. Further evidence of a  $\beta$ -sheet conformation was found on analysis of the amide I' band of the infrared (IR) spectrum of aqueous P<sub>11-2</sub>. A nucleated, surfactant-like, self-assembly mechanism was suggested; for aggregates of a certain critical size or higher, the loss of entropy during self-assembly is compensated for by the enthalpy gain of peptide strands associating in a tape [19].

### 3.2 Hierarchical Self-Assembly

Expanding on this idea, Aggeli et al. progressed to develop a model describing P<sub>11-2</sub> self-assembly [20]. In this treatment (Fig. 10), peptide monomers in a  $\beta$ -strand conformation are considered to be chiral rods with chemically distinct faces and complementary donor and acceptor groups aligned on opposite sides.

For a random coil monomer to change to a  $\beta$ -strand, the free energy increase is  $\epsilon_{\text{trans}}$ , reflecting mainly a loss of configurational entropy. On formation of a  $\beta$ -sheet tape, there is a free energy of intermolecular association for each interacting pair of monomers  $\epsilon_{\text{tape}}$ . Because  $\beta$ -sheets with a right-hand twist as viewed down the polypeptide chain are lower in free energy [21],  $\beta$ -sheet tapes have an inherent left-hand twist viewed down the tape axis. Tapes contain two distinct faces: one of

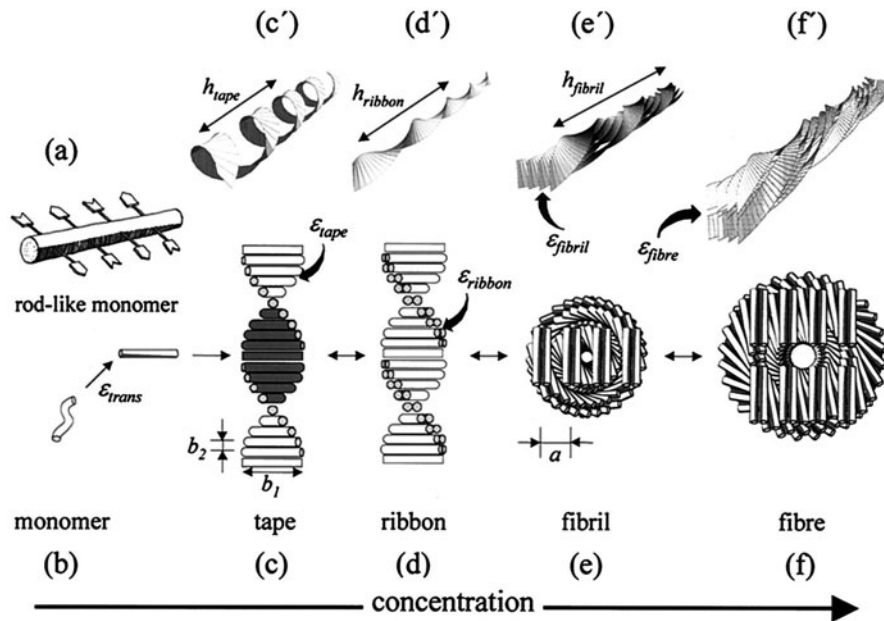


**Fig. 10** (a–f) Hierarchical self-assembly model for chiral rod-like units. A curly tape (c'), a twisted ribbon (d'), a fibril (e') and a fibre (f'). Adapted from Aggeli et al. [20]. Copyright 2001 National Academy of Sciences, USA

which may interact more favourably with itself, and the other more favourably with the solvent. Tapes therefore adopt a helical form. As one side of the tape is more soluble than the other, tapes pair into twisted ribbons to exclude their less-soluble surfaces, with an associated free energy change of  $\epsilon_{\text{ribbon}}^{\text{attr}}$  per peptide. Fibrils form when ribbons stack, driven by attraction between their faces, with a free energy change  $\epsilon_{\text{fibril}}^{\text{attr}}$  per pair of interacting peptides. If the edges of fibrils are mutually attractive, they may stack into fibres, with an associated free energy change  $\epsilon_{\text{fibre}}^{\text{attr}}$ .

The twist of these aggregates determines the resulting structure. When ribbons stack into fibrils, and fibrils into fibres, packing considerations cause these twisted aggregates to bend and modify their twist with an elastic energy penalty  $\epsilon_{\text{elast}}$ . For fibrils, it can be shown that the  $\epsilon_{\text{fibril}}$  per peptide in a fibril is:

$$\epsilon_{\text{fibril}} = \frac{p-1}{2p} \epsilon_{\text{fibril}}^{\text{attr}} - \epsilon_{\text{fibril}}^{\text{elast}} \quad (1)$$

which has a maximum value for a given  $p$  (the number of ribbons in a fibril), resulting in a predominant fibril width. This is illustrated by the calculated phase diagram (Fig. 11), which shows the balance of ribbon attraction versus the relative pitch of ribbons. Ribbons do not tend to assemble further if they are highly twisted or have low attraction energies. Infinite stacks form at high attraction energies and low twist. Fibrils occur for a range of parameter combinations between these extremes.

These free energies determine the critical concentrations for observing each peptide structure. In very dilute conditions, this class of peptides exist as random coil monomers in conformational flux. Above a critical concentration,  $c_{\text{tape}}^*$ , the concentration of monomer remains constant and formation of tapes occurs:

$$c_{\text{tape}}^* = V_{\text{beta}}^{-1} \exp(\epsilon_{\text{trans}} - \epsilon_{\text{tape}}) \quad (2)$$

where  $V_{\text{beta}}^{-1}$  is the per peptide volume of chemical bonds between peptides in a tape. To see all of these possible structures as concentration increases, the criterion is that  $\epsilon_{\text{tape}} \gg k_B T \gg \epsilon_{\text{ribbon}} \gg \epsilon_{\text{fibril}} \gg \epsilon_{\text{fibre}}$ , so that the critical concentrations for each structure increase in the reverse order.

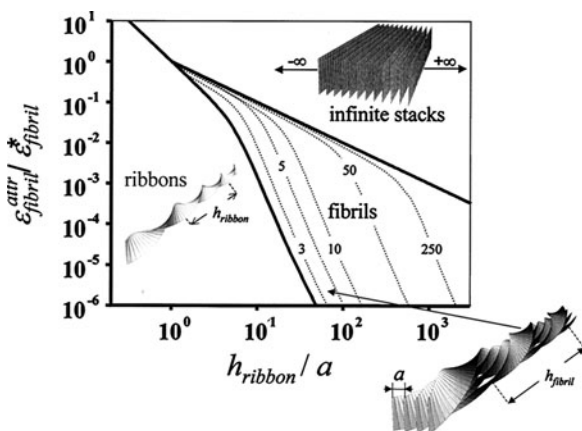


**Fig. 11** Phase diagram of a twisted ribbon solution that forms fibrils. The axes represent relative helix pitch of isolated ribbons and relative stacking attraction of ribbons. Reproduced from Aggeli et al. [20]. Copyright 2001 National Academy of Sciences, USA

For instance, P<sub>11</sub>-2 forms ribbons at concentrations  $\geq 0.1$  mM in water. At 0.6 mM, these ribbons self-assemble into fibrils and at higher concentrations into fibres. Conversely, glutamine-rich P<sub>11</sub>-1 (Ac-QQRQQQQQEQQ-Am) forms ribbons at 1 mM and does not form fibrils, even at concentrations as high as 25 mM. Association of P<sub>11</sub>-2 into ribbons is much more favourable due to it having hydrophobic aromatic residues arranged such that there is a large disparity between the hydrophobicity of each of its tape faces.

### 3.3 *pH- and Ionic Strength-Triggered and Switchable Self-Assembly*

The  $pK_a$  of amino acid side chains has been utilised in fine balancing of electrostatic interactions between peptide monomers, enabling switchable aggregation. Modification of the P<sub>11</sub>-2 design led to further designs: P<sub>11</sub>-4 (Ac-QQRFWEFEQQ-Am) and P<sub>11</sub>-5 (Ac-QQOFOWOFQQ-Am), based on the criterion of needing a charge to stabilise fibril formation [22]. P<sub>11</sub>-4 was designed with three glutamic acids so that fibrils form at low pH where these are neutralised, and it becomes monomeric at higher pH as the acids become deprotonated and exert electrostatic repulsions. Transitions between monomer and aggregate states can be carried out repeatedly, limited only by the concomitant ionic strength increase (aqueous NaCl is produced on acid–base neutralisation), eventually resulting in a flocculate. P<sub>11</sub>-5 behaves in the opposite manner. At low pH, P<sub>11</sub>-5 is monomeric, while at pH above 7.8 a fibril-containing gel is obtained, due to the positive ornithine residues becoming neutralised. Note that this pH is actually considerably lower than the  $pK_a$  of ornithine (10.8), which suggests that this  $pK_a$  reduction is due to repulsion between the positive ornithine side chains.

pH is a solution-controlled condition that can be changed to control the electrostatic charge on peptides with ionisable side chains and consequently promote or hinder their interaction and self-assembly. Ionic strength is another solution-dependent property that can adjust the effects of peptide charge, not by removing the charge, but by mitigating its effects through screening.

P<sub>11</sub>-4 and P<sub>11</sub>-8 (Ac-QQRFOWOFEQQ-Am) were examined in a study on the effect of physiological ionic strength on self-assembly at 10 mg mL<sup>-1</sup> [23]. For P<sub>11</sub>-4 solutions in 130 mM NaCl, the transition from  $\beta$ -sheet to random coil is shifted up more than 4 pD units (Fig. 12). The authors ruled out the possibility that this could be the result of a change in side-chain acidity by acid–base titration, and suggest that this change is due to a Debye length decrease. It was also discovered that the structure of the predominant fibrous structures, whether in gels, flocculates or nematic fluids, appeared to be unaffected by the presence of salt.

P<sub>11</sub>-8, like P<sub>11</sub>-5, is designed to self-assemble at high pH. Comparable shifts in properties were found when studying P<sub>11</sub>-8 solutions in 130 mM NaCl (Fig. 12). The  $\beta$ -sheet to random coil transition is lowered by 3 pD units and the pD range over which it forms nematic gels is extended down to pD 8.5 in aqueous NaCl

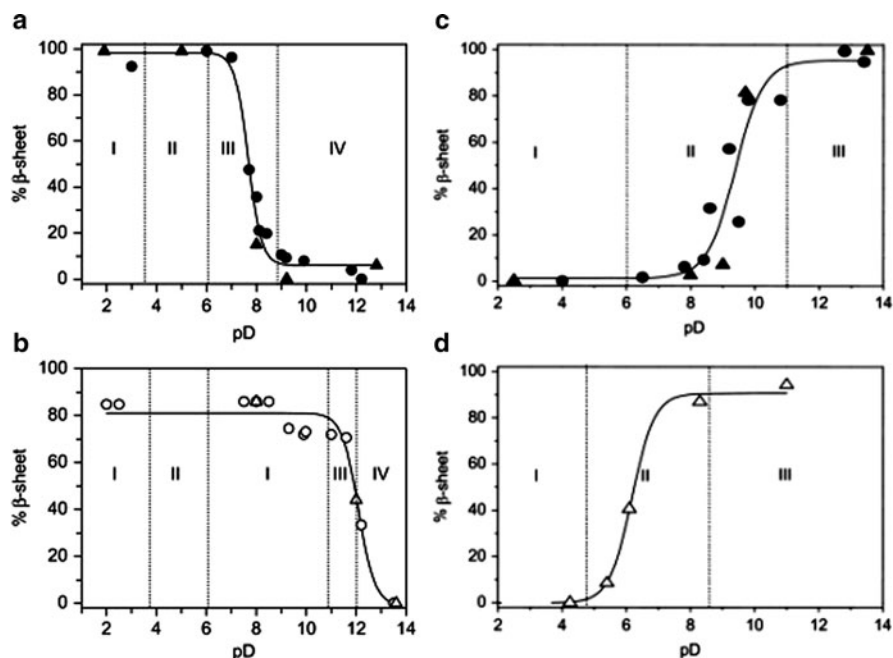


**Fig. 12** P<sub>11-4</sub> (a, b) and P<sub>11-8</sub> (c, d)  $\beta$ -sheet variation measure by IR (circles) and NMR (triangles): 10 mg mL<sup>-1</sup> peptide solutions prepared in (a, c) D<sub>2</sub>O and (b, d) 130 mM NaCl in D<sub>2</sub>O. For P<sub>11-4</sub>, I nematic gel, II flocculate, III nematic fluid, IV isotropic fluid. For P<sub>11-8</sub>, I isotropic fluid, II biphasic solution, III nematic gel. Adapted from Carrick et al. [23]. Copyright 2007, with permission from Elsevier

from pD 11 in water. Comparable effects were seen for analogues of P<sub>11-4</sub> and P<sub>11-8</sub> containing serines in place of glutamines to increase hydrophilicity.

These two studies in particular are important. They demonstrate that not only can P<sub>11</sub> peptide self-assembly be adjusted by sequence modification to suit a particular ionic strength and pH (e.g. conditions found *in vitro* or *in vivo*) but that it can be also made reversible and responsive. This raises the possibility that these peptides can be used in drug delivery, or as therapeutics that self-assemble post-injection.

Many other researchers have developed self-assembling peptide designs featuring pH- and/or ionic strength-dependent behaviour. The discovery by Zhang et al. of the self-assembling  $\beta$ -sheet EAK16-II peptide Ac-(AEAEAKAK)<sub>2</sub>-Am [24], originating from a yeast protein, has inspired the design of other related sequences. KFE12, (FKFE)<sub>3</sub>, is one of those. It does not gelate at low pH (due to charged lysines) nor high pH (due to glutamic acids), but does so at neutral pH. At low pH, where the peptide has a net positive charge, it was found that the presence of anions induces gelation. The critical coagulation concentration decreased strongly when using ions of increased valence, in some agreement with the Schulze–Hardy rule [25]. A later study used KFE12 as a basis for examining the influence of the number of sequence repeats, side-chain hydrophobicity and charge on the critical coagulation concentration [26].



The RAD16-I peptide, Ac-(RADA)<sub>4</sub>-Am is another EAK16-II-derived peptide that also displays pH-dependent behaviour. Nanofibres form at pH 1 and pH 4, but amorphous aggregates are seen at pH 7–9.5, despite the  $\beta$ -sheet content under these conditions being comparable to that at pH 1. Smaller, round aggregates are present at pH 13 [27]. The RATEA16 peptide, with sequence Ac-(RATARA EA)<sub>2</sub>-Am, is a modification of RAD16-I that can undergo a reversible transition from hydrogel (neutral pH) to either a solution containing shorter fibres (at low pH) or a precipitate containing amorphous material (at high pH) [28].

Schneider and colleagues have studied lysine-rich,  $\beta$ -hairpin peptides. MAX1 (VKVKVKVKV<sup>D</sup>PPTKVKVKVKV-NH<sub>2</sub>) exists as a random coil under conditions where the lysines are protonated [29]. Switching to basic pH neutralises these charges and favours a conformational transition to  $\beta$ -sheet and subsequent self-assembly and gelation. Acidifying the gel results in MAX1 reverting to a random coil and hence the gel breaks down. This pH responsiveness was fine-tuned by replacing lysines with glutamic acids, reducing both the net positive charge and the pH at which such a transition occurs [30]. Moreover, MAX1 is susceptible to ionic strength triggering. MAX1 gelation does not occur at neutral pH and low ionic strength, but increasing the ionic strength screens the charged lysines, permitting self-assembly and gelation [31].

Self-assembly mechanisms triggered by pH and ionic strength can also be applied to non- $\beta$ -sheet peptide motifs. Hartgerink's group created an  $\alpha$ -helical coiled-coil from peptides whose charged glutamic acid groups prevent their association into fibres at high pH. Placing the peptide under acidic conditions enables gelation; this is reversible using NH<sub>4</sub>OH vapour [32]. Zimenkov and co-workers successfully created a pH-responsive, fibril-forming coiled-coil peptide, TZ1H, basing their design on the isoleucine zipper peptide, GCN4-pII [33]. Inclusion of histidines at positions such that they are present at the interfaces of coils, provides a pH switching mechanism. At pH 6.5–8, the peptide is  $\alpha$ -helical, but at pH 4–5.6, the peptide becomes random coil, presumably destabilised by the proximity of the histidines that are protonated in the more acidic conditions.

Stupp and colleagues have developed peptide amphiphiles featuring a peptide head and alkyl tail, one of which is soluble to 50 mg mL<sup>-1</sup> in water. On reducing the pH to below 4, gelation occurs at just 2.5 mg mL<sup>-1</sup>, primarily driven by self-assembly into fibres, allowing the hydrophobic tails to be excluded from the aqueous solution [34]. Self-assembly was shown to be reversible with the addition of KOH. A novel feature of this design is the inclusion of cysteines, whose oxidation to form disulphide bridges has the benefit of making the fibres no longer susceptible to pH-induced breakdown; this too can be reversed by reduction using dithiothreitol (DTT). The pH switching behaviour of a larger range of amphiphiles were explored in a subsequent report [35], which additionally discussed the use of Ca<sup>2+</sup> ions as a self-assembly trigger. Adding EDTA allows ion-induced amphiphile assembly to be reversed [36]. The choice of counterion influences the minimum concentration of peptide required for gelation; although it decreases with increasing ion valence, it does not depend on valence alone [36].

A current trend is the use of very short peptide sequences. Ulijn and co-workers reported several pH-responsive Fmoc-protected dipeptides. One of these was Fmoc-<sup>D</sup>Ala-<sup>D</sup>Ala, which reversibly gels at pH 3 and undergoes dissolution at pH 6. Jayawarna and co-workers later screened several other Fmoc-dipeptides to find those suitable for use under physiological conditions as potential cell scaffolds [37]. Of these, Fmoc-FF was the most promising, it is a clear solution at high pH, but gels below pH 8 [37]. Gazit and co-workers also independently reported on Fmoc-FF gels at around the same time [38, 39]. Adams and co-workers monitored the kinetics of gelation of several Fmoc-dipeptides, including Fmoc-FF, via rheology while solution pH was slowly decreased [40].

pH not only triggers peptide self-assembly, but can also influence the resulting morphology. Gazit and Reches observed that the diphenylalanine peptide, a sequence present in  $\beta$ -amyloid, could form nanotubes [41]. Kumaraswamy and co-workers established that the dimensions of the FF nanotubes is dependent on both pH and media conditions [42]. The research groups of Lynn and Hamley both studied closely related A $\beta$ -derived peptides: Ac-KLVFFAE-NH<sub>2</sub> (A $\beta$ <sub>16-22</sub>) forms fibres at pH 7, but nanotubes at pH 2 [43], whereas the modified variant YYKLVFFC produces short, twisted fibrils at pH 11, but longer and straighter fibrils at pH 4.7 [44].

Capes et al. discuss the surfactant-like peptide Ac-IIEENDD-OH, which forms twisted  $\beta$ -sheet fibrils under acidic conditions (pH 3). As pH increases these are disrupted by the increasingly deprotonated acidic residues, resulting in the formation of nanospheres at higher pH [45]. The Ac-K<sub>n</sub>(QL)<sub>m</sub>K<sub>n</sub> block peptides of Dong and colleagues incorporate a central QL amphiphilic repeat that favours a  $\beta$ -sheet conformation. The flanking lysines enhance the solubility of aggregates such that (QL)<sub>6</sub> is completely insoluble at pH 2–12, but lysine repulsion between chains can restrict self-assembly [46]. The peptide K<sub>2</sub>(QL)<sub>6</sub>K<sub>2</sub> was found to balance these constraints, producing soluble fibres at pH 7.4. At pH 12, where the lysines are predominantly uncharged, the peptide precipitates with the precipitate consisting of fibres that are much longer than those formed at pH 7.4. A high NaCl concentration (1 M) leads to viscous solutions that also have increased fibre lengths compared with those prepared at 150 mM NaCl. Subtle changes in peptide properties can result by reordering a peptide's sequence: EAK16-II forms fibrillar structures over a wide range of pH, but EAK16-IV (Ac-AEAEAEAEAKAKAKAK-Am) forms globules, instead of fibrils, at neutral pH, perhaps as a result of this peptide preferring to fold such that the glutamic acid and lysine residues are in close contact [47].

### 3.4 *In Silico Design of Self-Assembling Peptides*

For technological applications it is highly desirable to be able to design self-assembling systems to have particular physico-chemical properties under a given set of experimental conditions. Using computer simulation, it is possible to construct an atomistic model of tapes, ribbons and fibrils to study all of the interatomic interactions within the system in a quantitative manner. Figure 13 shows atomistic

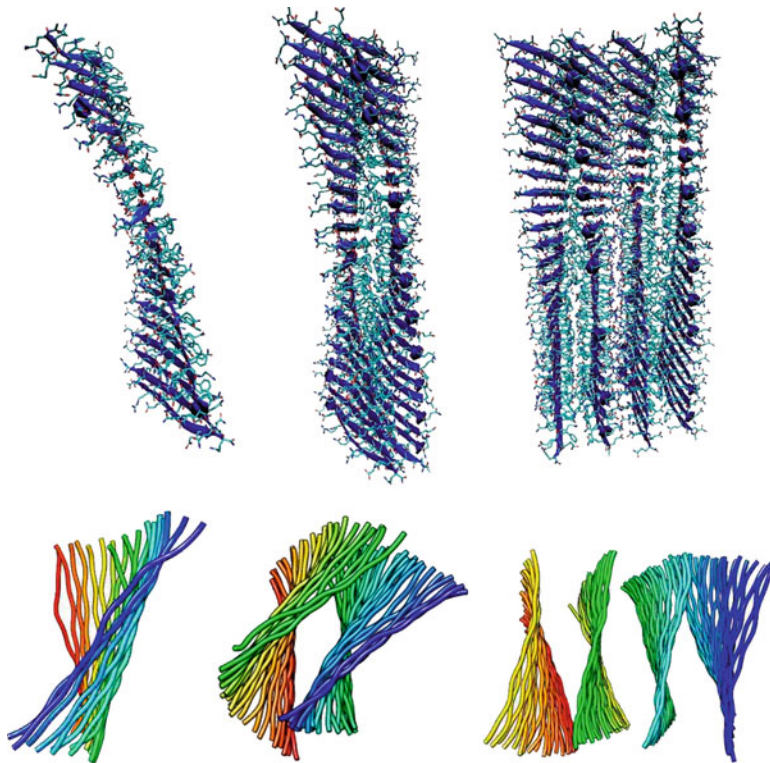


**Fig. 13** Structures resulting from atomistic molecular dynamics simulations of  $P_{11-2}$  tapes (*left*), ribbons (*middle*) and fibrils (*right*) viewed perpendicular to (*top*) and along (*bottom*) the long axis of the tape. Hydrogen atoms and solvent molecules are not shown for clarity

models of a  $P_{11-2}$  tape (left), a ribbon (centre) and a fibril (right). To construct these models, it is necessary to know the peptide sequence and how the  $\beta$ -strands are arranged within the self-assembled structure (i.e. anti-parallel and in register). Using a molecular building tool such as NAB [48], and a rotamer library to optimise the side-chain conformations [49], it is then possible to construct a starting model for the atomistic structure of the self-assembled peptides. This model is then read into a molecular modelling package such as AMBER [50].

For a detailed but accessible description of molecular modelling techniques, see Leach [51]. In brief, atomistic molecular modelling software uses an empirical force field to calculate the forces between each pair of atoms within the system. All covalent bonds are treated as simple harmonic springs (and therefore cannot break during the simulation). The force-field also contains bond angle and dihedral terms, which maintain the correct chemical shape of the polypeptides. In addition, the force field ascribes van der Waals forces and electrostatic interactions between all pairs of atoms in the system so that salt-bridge interactions, hydrogen bonding interactions and dispersion forces are all included in the calculation. It is also possible

to simulate different pH environments by changing the protonation state of any titratable amino acids in the starting structure. The initial starting structure is then surrounded by water molecules and counterions to mimic the solvent environment. Although such a detailed model is desirable to represent the self-assembled peptides as accurately as possible, these calculations are extremely computationally expensive. Even with the most sophisticated supercomputing facilities, simulations containing more than 100  $\beta$ -strands of an 11-mer peptide are sufficiently large to be technically challenging. Therefore, it is far easier to study tapes, ribbons and fibrils with computer simulation than it is to study fibres, which contain many stacks of  $\beta$ -sheets.

Once the initial starting structure has been associated with an appropriate force field, this structure is energy-minimised to relieve local steric clashes. Restrained molecular dynamics (MD) simulation is then used to equilibrate the system. MD uses classical mechanics in conjunction with the force field to evolve the positions of all atoms in the system over time [51]. The technique provides a “movie” of the changing shape of the molecular assembly as it undergoes thermal fluctuations, and in principle also allows an initial “guess” at an atomistic structure of a self-assembled peptide aggregate to relax into a more realistic conformation. For example, the initial starting structures for the aggregates shown in Fig. 13 were completely flat, and the twist emerges spontaneously as a prediction from the MD. To achieve this requires a very careful equilibration procedure in which artificial restraints are used to hold the individual  $\beta$ -strands in the correct position within the peptide assembly as the system is heated to 300 K. These restraints are then slowly removed, and the final equilibrated structure is subjected to MD for timescales of around 20 ns. If the equilibration procedure has been successful, then the peptides remain in an ordered aggregated structure throughout the simulation, as in Fig. 13. If unsuccessful, then the aggregated  $\beta$ -sheet structure will start to disassemble into individual polypeptide strands. In practise, the *in silico* design procedure is iterative, and may require several rounds of initial structure optimisation and equilibration before  $\beta$ -strand assemblies remain in an ordered aggregated state during the final MD calculation.

Once a self-assembled structure has been obtained that remains in an ordered state during 20 ns of MD, there is a wealth of structural, energetic and dynamic information that can be extracted. First, the simulations provide an estimate of structural quantities such as the twist of the  $\beta$ -sheets, which are useful parameters for input into the hierarchical model of self-assembly described in Sect. 3.2. Second, the computer model can be used to calculate the relative energies of the stabilising interactions both within individual  $\beta$ -sheets and between stacked  $\beta$ -sheets and how these might change with amino acid sequence, pH or the solution conditions. MD simulation also provides information about the flexibility of the self-assembled peptide aggregates, which can be combined with energy measurements to give an estimate of free energies. However, calculating dynamic quantities, such as entropies, from MD simulations is extremely challenging for systems of this size due to the computational expense of the calculations. Nevertheless, as supercomputer resources and computer codes continue to improve so will the predictive power of *in silico* design methods. Computer modelling is

therefore expected to become increasingly important in extending our understanding at the molecular level and in designing self-assembling and switchable systems.

## 4 Self-Assembling Peptides as Frameworks for Other Functional Molecules

The way that P<sub>11</sub> peptides self-assemble is important for polypeptides and proteins: amyloid-type structures are believed to have the same core structure, and in fact the propensity to self-assemble in this manner is hypothesized to be a general property of polypeptides [52]. It is therefore unsurprising that systems featuring this motif are common. In recent years, a push towards the use of peptide-based self-assembled materials has led to increasing interest in extending their functionality by derivatising them.

Derivatised fibrils are of interest for several reasons. As seen with the P<sub>11</sub> peptides, they can have regular sizes, making the formation of well-defined nanoscaffolds a possibility. Size adjustment at the nanoscale is possible, e.g. by adjusting the tape width or number of tapes in a fibril, in turn tunable by altering the primary sequence. It may be possible to arrange functional molecules attached to fibrils regularly on the external fibril surface, giving a “bottom-up” route to nanoscale arrays. Finally, adding other moieties to these systems may also reveal hitherto unknown aspects of their self-assembly pathways, for example, what features promote or prevent assembly?

Woolfson and Mahmoud have classified the routes to preparation of decorated self-assembling peptide materials [53] as (1) co-assembly, where the functional part is already attached to a self-assembling component prior to assembly, and (2) post-assembly, where a non-functionalised self-assembled structure is modified by covalent or non-covalent means. This discussion adheres to this classification. A third route, beyond the scope of this review, is the use of structured peptides as templates for inorganic materials. Section 4.1 discusses functionalised self-assemblies formed from co-assembly-type approaches, while post-assembly modifications of self-assembled structures are considered in Sect. 4.2.

### 4.1 Assemblies Formed from Modified Self-Assembling Monomers

#### 4.1.1 Mixed Fibrils

Self-assembly is not restricted to merely a mixture of functionalised and non-functionalised, but otherwise identical, sequences. It is possible to use distinct sequences in mixtures and combine functionality. The formation of modified fibrils

from a mixture of peptides with distinct amino acid sequences was demonstrated by MacPhee and Dobson [54]. Two fibril-forming sections of the highly  $\beta$ -sheet protein transthyretin were selected for use ( $TTR_{10-19}$  and  $TTR_{105-115}$ ), and coupled to fluorescent groups, giving the modified forms fluorescein-5-maleimide (F5M- $TTR_{10-19}$ ) and dansyl chloride (dansyl- $TTR_{105-115}$ ). Upon inclusion in fibrils, as the fluorescent emission peak shifts (due to a more hydrophobic environment for the probe) and anisotropy changes (due to the molecule becoming part of a slowly rotating complex) these fluorescent groups make detection of their inclusion possible. CD spectroscopy and transmission electron microscopy (TEM) of labelled peptides showed that these modifications had no effect on self-assembly; fibrils of these modified peptides were found to contain large amounts of  $\beta$ -sheet character.

Preparation of mixed peptide fibrils was similar for both of these labelled peptides: 1% (by weight) was incubated at 37 °C with the other, unlabelled peptide in 10%  $CH_3CN/H_2O$  at pH 2. For  $TTR_{10-19}$  with 1% dansyl- $TTR_{105-115}$ , a blue shift and dansyl anisotropy increase were observed, indicating the inclusion of dansyl- $TTR_{105-115}$  into fibrils. CD spectroscopy proved that the structure was primarily  $\beta$ -sheet.

For  $TTR_{105-115}$  with 1% F5M- $TTR_{10-19}$ , the  $\beta$ -sheet signature was again observed via CD, although this time there was some additional turn character compared with pure  $TTR_{10-19}$ , indicating some structural change. With this mixture, only a small fluorescein red shift was observed, but its anisotropy increase, comparable to the previous case, implied that cofibrils had again formed. The TEM images in Fig. 14 show the change resulting from mixing fibrils, the mixed fibrils having a periodic twist.

Distinguishing the two fibril components in TEM was achieved by attaching an antibody that binds to the fluorescent site, before adding another, gold-labelled,

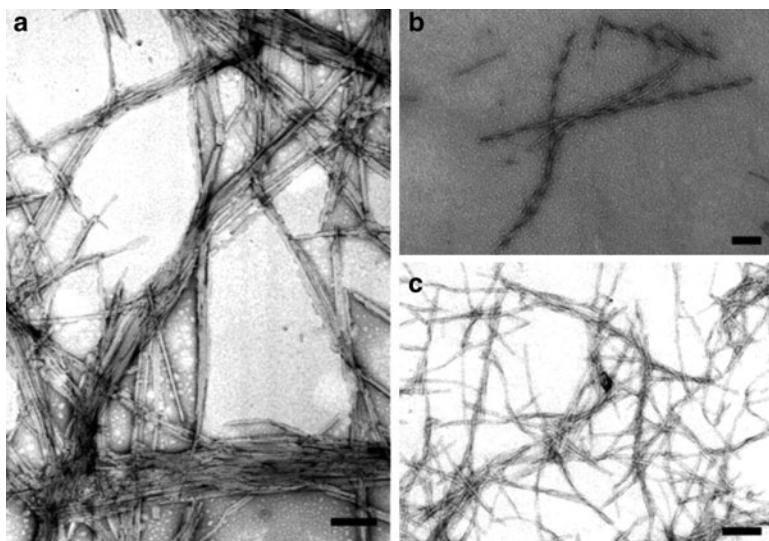
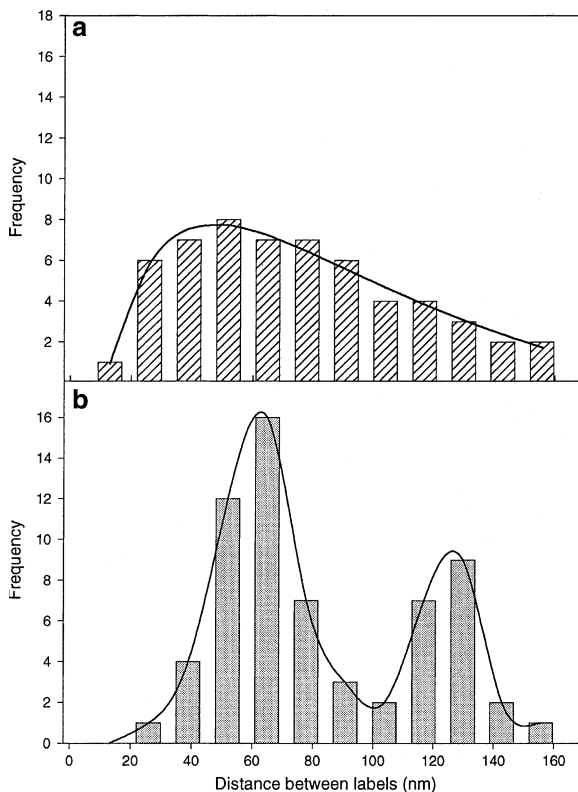


**Fig. 14** (a)  $TTR_{105-115}$  fibrils, (b, c)  $TTR_{105-115}$  fibrils containing 1% F5M- $TTR_{10-19}$ . Scale bars: 200 nm. Reprinted with permission from MacPhee and Dobson [54]. Copyright 2000 American Chemical Society

**Fig. 15** Distance between colloidal gold particles: (a) particles are attached to TTR<sub>105–115</sub> fibrils containing F5M-TTR<sub>10–19</sub>; (b) particles are attached to insulin fibrils containing F5M-TTR<sub>10–19</sub>. Reprinted from MacPhee and Dobson [54]. Copyright 2000 American Chemical Society



antibody specific to the first. Derivatised peptides were found to be inserted randomly into the fibrils with an average spacing of the order of 50 nm (Fig. 15).

An attempt to incorporate these fluorescent peptide derivatives into insulin fibrils saw similar success, despite the insulin fibrils being comprised of longer monomers (51 residues) than the TTR variants. Evidence for these TTR peptides being incorporated in mixed TTR/insulin fibrils included a transition to  $\beta$ -sheet structure observed via CD spectra as time elapsed modification of fluorescent properties, and immunogold TEM imaging. In this case, a more periodic spacing between gold particles along insulin fibrils was observed (approximately 60 and 125 nm, see Fig. 15). The authors state that TTR inclusion in mixed fibrils is likely to be random. However, the difference here could be caused by a regular structural repeat, such as the 60 nm insulin helical twist, which exposes the fluorescent group to solvent at a regular spacing.

Fluorescently modified fibrils are a useful probe. Furthermore, MacPhee and Dobson have shown that it may be possible to bind other non-peptidic functional groups, provided they can be covalently linked during synthesis. They also demonstrate that utilizing intrinsic fibril structural features might be one approach to the production of peptide scaffolds with well-defined ligand spacings.

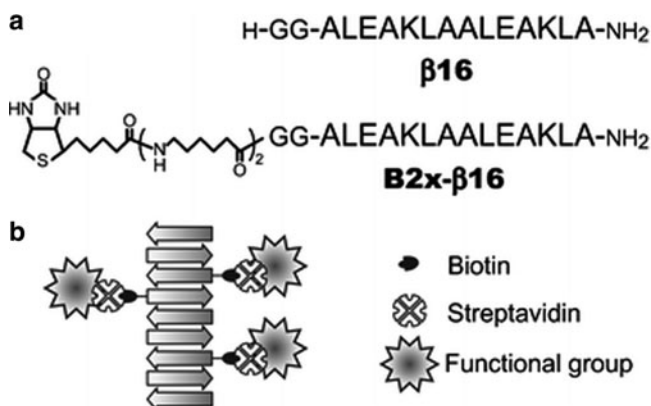


**Fig. 16** (a) Sequences of peptides  $\beta 16$  and B2x- $\beta 16$ . (b) Biotin-derivatised cofibrils binding to a functionalised streptavidin with a functional group. Reproduced by permission of The Royal Society of Chemistry from Kodama et al. [56]

Here, two different sequences from transthyretin were successfully combined into mixed fibrils [54]. This is not always the case, however. For amyloidogenic proteins, the ability of other fibrils to act as cross-seeds for growth is known to depend on sequence similarity [55]. Seeding hen lysozyme solutions with seeds formed from closely related sequences (e.g. hen and other lysozymes) led to the largest increases in the rate of formation of fibrils. Consequently, there may be some restrictions on the selection of distinct peptide sequences to produce scaffolds.

Mihara's group used a co-assembly route to produce peptide fibrils containing biotin using the individual peptides in an initially random coil state (Fig. 16) [56]. The residues were sequenced such that neighbouring hydrophilic (E, K) and hydrophobic (L, A) residues were on opposing faces in a  $\beta$ -strand arrangement. Halfway along the sequence, these faces were switched such that an antiparallel arrangement was favoured (satisfying demands of complementary electrostatic interactions between E and K residues, and placing hydrophobic residues near to each other in adjacent strands).

CD, TEM and a thioflavin binding assay (binding to fibrils results in a characteristic fluorescence emission) were used to confirm the existence of mixed fibrils (width roughly 20 nm, lengths ranging from hundreds of nanometres to several micrometres) prepared from the two peptides ( $\beta 16$  and B2x- $\beta 16$ ) and consisting of  $\beta$ -sheets.

Streptavidin with attached gold particles was added to mixtures of  $\beta 16$  and B2x- $\beta 16$ , starting with no biotin and increasing the molar ratio up to 1% of B2x- $\beta 16$ . This increased the amount of streptavidin attached to fibrils, demonstrating that the amount of biotin present in the fibrils was dependent on this ratio.

It was also observed at 1% B2x- $\beta 16$  that gold particles had a tendency to be found with an approximate 50 nm spacing (Fig. 17), implying that binding occurs regularly. This is not fully understood: this distance is equivalent to approximately 100–120 peptides along a single sheet filament, but as fibrils consist of several



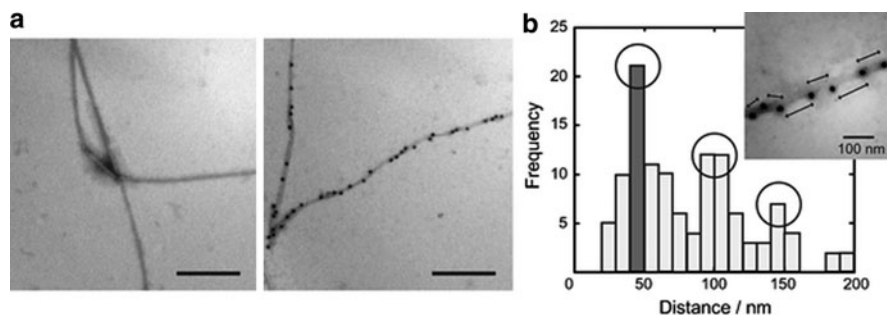


**Fig. 17** (a) TEM images of  $\beta 16$  fibrils (*left*) and cofibrils with 1% B2x- $\beta 16$  (*right*), with added gold-labelled streptavidin. *Scale bars*: 500 nm. (b) Histogram showing the distance between gold particles on  $\beta 16$  fibrils. *Inset*: TEM image of labelled  $\beta 16$  fibrils indicating the distances measured. Reproduced by permission of The Royal Society of Chemistry from Kodama et al. [56]

filaments, the spacing would be expected to be shorter simply based on the molar ratio. One proposed explanation is that streptavidin binds to multiple biotin sites, which may place a lower limit on the distance between bound streptavidin. Another explanation, as MacPhee and Dobson suggested for their insulin fibrils, is that the fibril structural periodicity causes biotin to be exposed to solution at regular intervals. Despite the lack of understanding of this mechanism, ordered arrays can be produced using this method. Modification of streptavidin is routine, making this strategy especially useful; indeed Kodama et al. also reported that they had used a fluorescently labelled avidin in this manner.

An earlier work by Mihara's group extended the idea of mixing peptides to the use of mixtures of complementary amino acid sequences to form fibrils [57]. A base peptide sequence (Fig. 18) consisting of two identical chains joined by a disulphide bond between cysteine residues was used, with residues  $X_1$ – $X_4$  being either glutamic acid (negatively charged at neutral pH) or lysine (positively charged at neutral pH). The general peptide sequence was developed on the basis of known coiled-coil-forming sequences of proteins. One particular example of this peptide class, with EKEK as residues  $X_1$ – $X_4$ , was already known to undergo a spontaneous  $\alpha$ -helix (the two linked peptide chains initially forming  $\alpha$ -helices) to  $\beta$ -sheet transition, resulting in fibrils [58].

Mixtures of three peptides were also screened for their ability to form fibrils containing all three. Rather than testing all possibilities, carefully selected mixtures were used. Peptides in the equimolar mixtures were charged, but the overall sum of the peptide charges was zero, to build in chain–chain electrostatic attractions. If individual peptides or a peptide pair in a mixture formed fibrils, the mixture was not studied. Application of these criteria led to six possible mixtures: these were mixed at 4  $\mu\text{M}$  each at pH 7.4 and left for several days at room temperature to self-assemble.

Thioflavin binding indicated fibrils formed for two of these three mixtures (EEEK, EKEE, KKKK and EEKE, KEEE, KKKK). The requirement of all three peptides to produce fibrils was further demonstrated by testing individual peptides

**a**

Entry	Peptide	X <sub>1</sub>	X <sub>2</sub>	X <sub>3</sub>	X <sub>4</sub>	Total charge at neutral pH	Amyloid fibril formation
1	EEEE	E	E	E	E	-8	-
2	EEEK	E	E	E	K	-4	-
3	EEKE	E	E	K	E	-4	-
4	EKEE	E	K	E	E	-4	-
5	KEEE	K	E	E	E	-4	-
6	EEKK	E	E	K	K	0	++
7	EKEK	E	K	E	K	0	+++
8	EKKE	E	K	K	E	0	-
9	KEEK	K	E	E	K	0	-
10	KEKE	K	E	K	E	0	+++
11	KKEE	K	K	E	E	0	+
12	EKKK	E	K	K	K	+4	-
13	KEKK	K	E	K	K	+4	-
14	KKEK	K	K	E	K	+4	-
15	KKKE	K	K	K	E	+4	-
16	KKKK	K	K	K	K	+8	-

**Fig. 18** Peptide library used for studying complementary peptides. Reproduced from Takahashi et al. [57] with permission. Copyright Wiley-VCH

and peptide pairs, which gave negative results in the thioflavin test. CD spectra showed that the secondary structure in these two mixtures was  $\alpha$ -helix prior to it changing to  $\beta$ -sheet after 2 days. Fibrils were also seen under TEM. Additionally, this was extended even further. A screening process applied to mixtures of four peptide sequences found that two of the eight mixtures tested resulted in fibrils.

One model proposed to explain why specific mixtures form fibrils is a lateral arrangement of strands in an antiparallel  $\beta$ -sheet (Fig. 19). This permits favourable contacts between both hydrophobic and oppositely charged side chains.

An alternative possibility is a vertical stacking structure where the  $\beta$ -strands are arranged on top of each other, again satisfying electrostatic and hydrophobic packing considerations (Fig. 20). Whichever is more likely, this is still far from a complete picture because the exact arrangement of the two disulphide-linked peptide chains is not yet known.

In this instance, adamantane was present to promote interaction of peptides through its hydrophobicity, but its attachment did not hinder fibril formation. It might be possible to chemically or biologically derivatise this group before being introduced to the peptide, or to select another hydrophobic component that could be suitably modified and attached to the peptide. This research also highlights the feasibility of creating peptide arrays comprised of several different sequences.

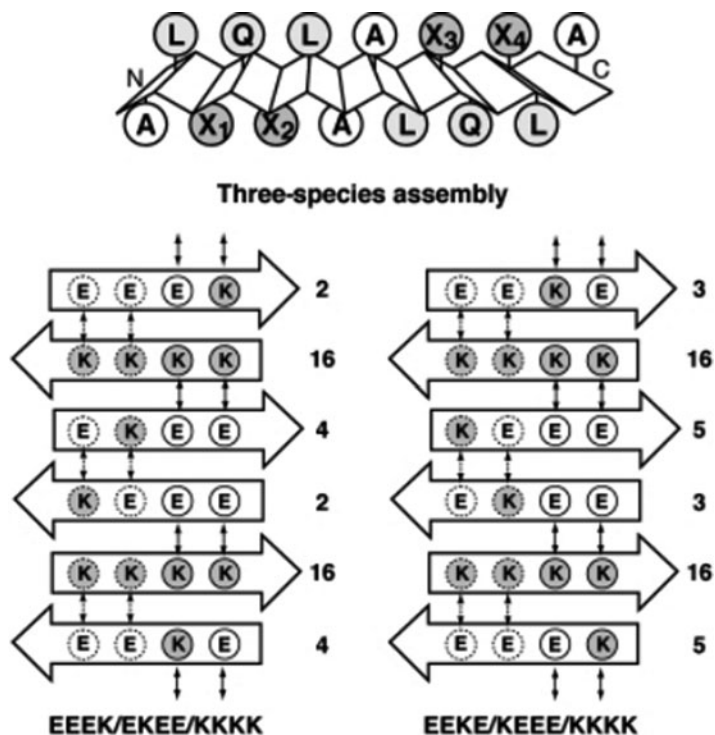


**Fig. 19** Lateral model for assembly of peptide mixtures producing laminated  $\beta$ -sheets. Residues in *solid circles* are on the upper face, residues in *dashed circles* are on the lower face of the  $\beta$ -sheet. Reproduced from Takahashi et al. [57] with permission. Copyright Wiley-VCH. Numbers refer to the peptide entries in Fig. 18. Arrows are directions of the (antiparallel) beta sheet strands; beginning and end of arrow correspond to N- and C-peptide termini respectively

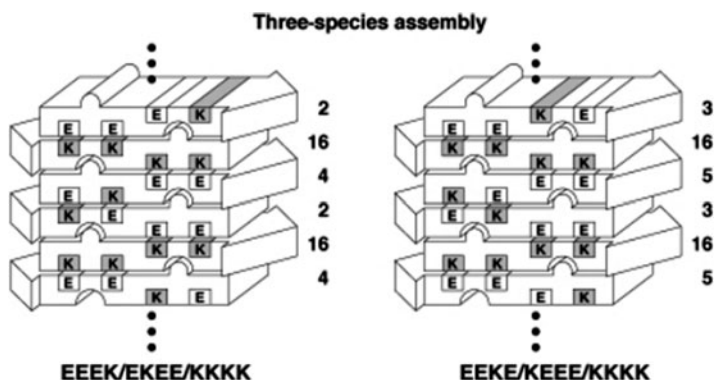


**Fig. 20** Vertical model of complementary assembly of peptide mixtures. Hydrophobic interactions are represented by the interlocking of raised sections and holes. The axis is indicated by *dots*. Reproduced from Takahashi et al. [57] with permission. Copyright Wiley-VCH. Numbers refer to the peptide entries in Fig. 18. Positively charged residues are dark shaded in contrast with the negatively charged residues which are light shaded

### 4.1.2 Poly(ethylene glycol) Derivatives

Poly(ethylene glycol) (PEG) is a polymer of considerable interest due to several properties, including solubility in both water and many organic solvents, non-toxicity and ability to induce cell fusion, and it has found many biological applications [59]. Despite its poor mechanical strength, attaching PEG chains onto mechanically strong materials, such as fibrils [60], is one way to harness its properties [61].

Lynn and co-workers carried out studies of the  $A\beta_{(10-35)}$  peptide – derived from residues 10–35 of the  $\beta$ -amyloid responsible for Alzheimer’s disease – which forms fibrils composed of parallel  $\beta$ -sheets [62]. The peptide was compared to its C-terminal PEG-derivatised analogue. TEM experiments showed that both formed fibrils [63] (Fig. 21) but the uranyl acetate stain was not found inside the peptide-PEG fibrils, indicating that PEG was at the outer edge of the fibril.

Small angle neutron scattering (SANS) experiments also helped establish the location of PEG [64]: the radius of the  $A\beta_{(10-35)}$ -PEG fibril was found to be about 40% larger than that of the peptide alone, and when the effect of scattering due to PEG was removed (using contrast matching, i.e. using a proportion of  $D_2O$  such that PEG-scattering matched that of the solvent), the observed fibril radius agreed with that of peptide alone, further supporting the idea of a PEG-coated fibril.

The lack of lateral aggregation of  $A\beta_{(10-35)}$ -PEG fibrils is striking compared with the dense networks of fibrils seen in pure  $A\beta_{(10-35)}$ . A 1:1 ratio mixture produced fibrils that exhibited association somewhere between these two extremes (Fig. 22). The change in morphology implies that the two species are forming mixed fibrils. It is thought that the PEG block prevents fibrils from lateral aggregation because

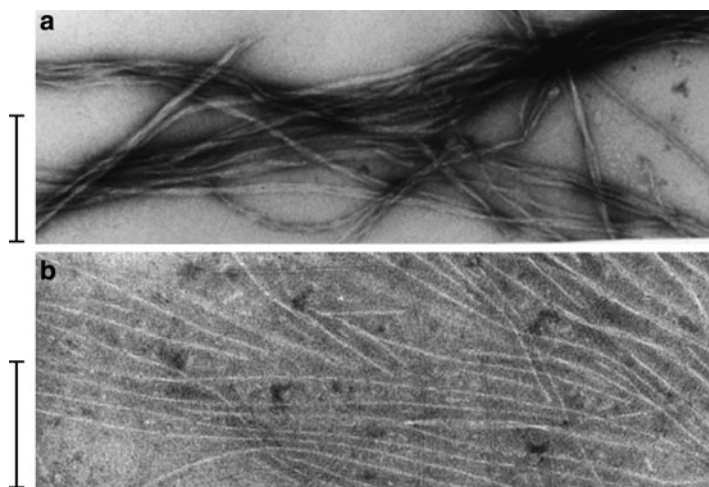


**Fig. 21** TEM images of (a)  $A\beta_{(10-35)}$  and (b)  $A\beta_{(10-35)}$ -PEG fibrils, both prepared at pH 7.4. Reprinted with permission from Burkoth et al. [63]. Copyright 1998 American Chemical Society

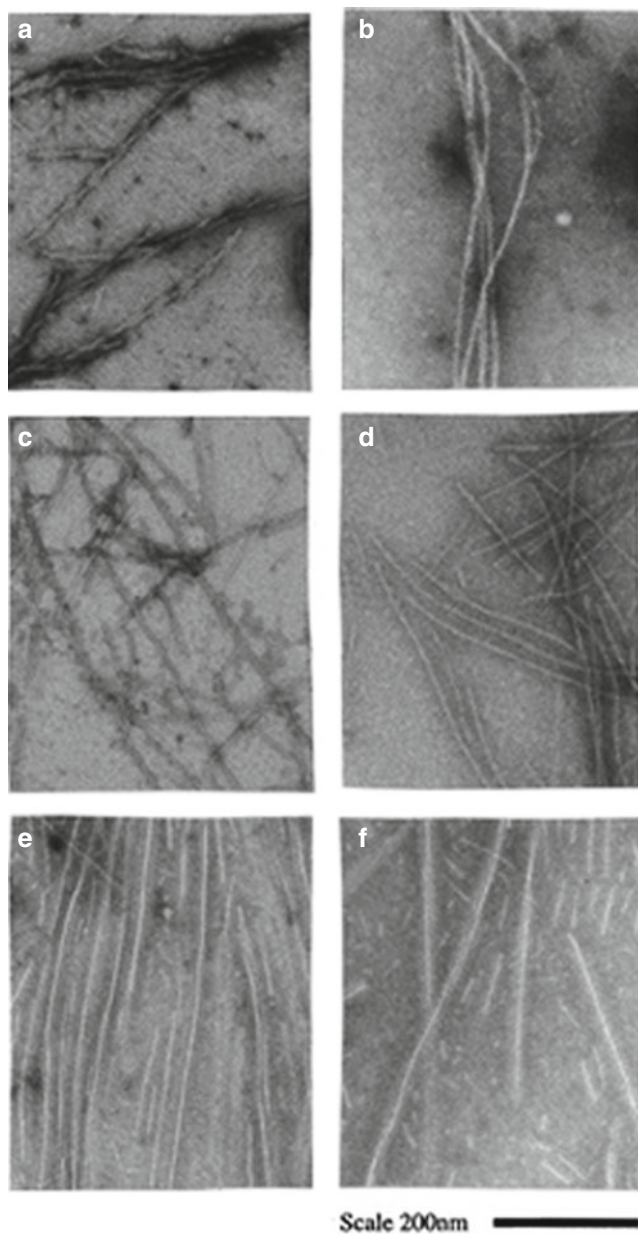


**Fig. 22** TEM images of  $A\beta_{(10-35)}$ -PEG titrated with  $A\beta_{(10-35)}$  at pH 5.7: (a) 100%  $A\beta_{(10-35)}$ , (b) 10:1  $A\beta_{(10-35)}$ : $A\beta_{(10-35)}$ -PEG, (c) 6:3  $A\beta_{(10-35)}$ : $A\beta_{(10-35)}$ -PEG, (d) 1:1  $A\beta_{(10-35)}$ : $A\beta_{(10-35)}$ -PEG, (e) 1:4  $A\beta_{(10-35)}$ : $A\beta_{(10-35)}$ -PEG, and (f) 100%  $A\beta_{(10-35)}$ -PEG. Reproduced with permission from Burkoth et al. [62]. Copyright 2000 American Chemical Society

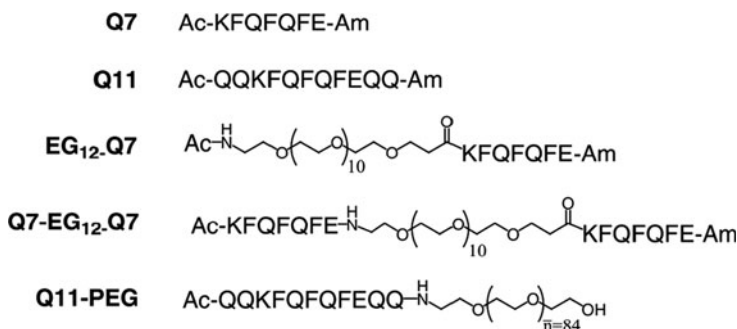


**Fig. 23** Sequences of various peptides and PEG-derivatised peptides. Reproduced with permission from Collier and Messersmith [68]. Copyright Wiley-VCH

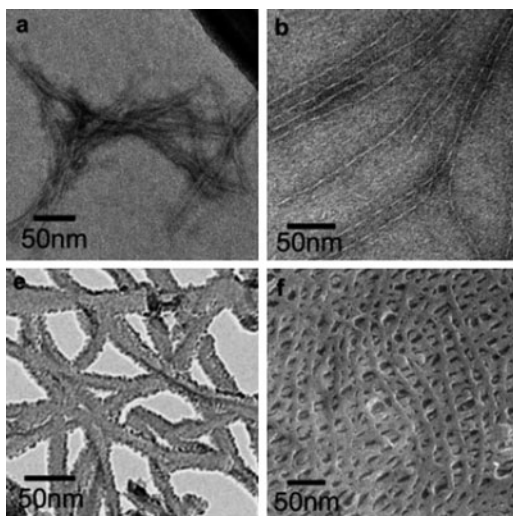
the hydrophilic PEG shields the hydrophobic residues present at the C-terminus, which would ordinarily drive this process [63].

Other fibril-PEG systems have also been studied. Earlier work by Hamley and co-workers examined PEG/de novo  $\beta$ -strand peptide block copolymers using wide and small angle X-ray scattering techniques [65]. Peptides with PEG attached still formed fibrillar aggregates similarly to the unmodified peptide, and yet were also stabilized against pH changes that normally cause the peptide to undergo secondary structure changes. More recent research by Hamley, Krysmann and others has investigated the effects of PEGylating fragments derived from amyloid peptides (e.g. KLVFF and longer variants) [66, 67].

Collier and Messersmith prepared two peptides [68]: Q11, already known to form  $\beta$ -sheet fibrils (see transglutaminase experiment discussed below) and Q7 (comprised of the middle seven Q11 residues). These had PEG blocks attached either at peptide termini or between two residues (Fig. 23). Salt-containing solutions of each were prepared. Q7 and Q11 formed gels, as was expected. By contrast, EG<sub>12</sub>-Q7 produced more fractured structures. Q11-PEG was soluble and did not gel, but was found to form fibrils. Q7-EG<sub>12</sub>-Q7 could not be solubilized in aqueous solution. CD and IR spectra measured from the four remaining self-assembling peptides indicated that all but EG<sub>12</sub>-Q7 were likely to be antiparallel, although IR absorptions also indicated some helicity.

Despite these secondary structure similarities, TEM enabled clearer distinctions between the different peptide-PEG systems. Both Q7-based materials tended to form ribbons. Q11 and Q11-PEG were predominantly fibrils, although there was a marked difference in how they packed (Fig. 24). Q11-PEG fibrils characteristically had greater lengths and smaller thickness than Q11 fibrils. Fibrils of Q11-PEG in TEM study also tended to avoid crossing, and ran adjacent to each other with a regular spacing of 10–15 nm. Quick-freeze, deep-etch (QFDE) TEM images in Fig. 24 also highlight how Q11-PEG fibrils display less fibril interaction and exhibit avoidance. Exactly how PEG prevents aggregation has not been elucidated, but this work shows that it is possible to control the macromolecular ordering of fibrils.

**Fig. 24** TEM images of Q11 (top left) and Q11-PEG (top right) fibrils. QFDE-TEM images of Q11 (bottom left) and Q11-PEG (bottom right) fibrils. Reproduced with permission from Collier and Messersmith [68]. Copyright Wiley-VCH



Work on longer polypeptides conjugated to PEG blocks has been conducted by Smeenk et al. who investigated block copolymers containing a central alanylglycine motif: PEG-[(AG)<sub>3</sub>(EG)]<sub>n</sub>-PEG [69]. A long, alanylglycine-based central polypeptide (Fig. 25), a sequence found in silk fibroin, was prepared by protein expression in *Escherichia coli*. Inclusion of cysteines at both ends of this sequence meant that PEG could be attached by reacting with a maleimide-functionalised PEG. PEG was attached with the idea of inhibiting large scale crystallization of the  $\beta$ -sheet fibrils and this proved successful, with individual fibrils discernable in TEM. Both TEM and atomic force microscopy (AFM) (Fig. 26) measurements suggest that the polymer with  $n = 20$  produced longer structures in the direction of the  $\beta$ -sheet hydrogen bonds than for  $n = 10$ , as expected, but with AFM-measured heights for both closely matching (explained by the proposed packing model in Fig. 26).

## 4.2 Modification of Self-Assembled Structures

Functionalised peptide fibrils could be used as a scaffold to place constraints on the attached groups, before carrying out chemical modification. This is exemplified by the supramolecular polymers prepared by Jahnke et al. [70] (Fig. 27) where a diacetylene component was crosslinked by exposure to ultraviolet (UV) light post-assembly. These polymers have several distinct regions. The tetra-alanine segment is a  $\beta$ -sheet-forming segment. Interestingly, structure **2** adopts a parallel  $\beta$ -sheet structure, as elucidated by IR, in contrast to the predominantly anti-parallel structure of **1**. Hydrogen bonding of the end  $\text{NHCOCH}_3$  group presumably drives this; the importance of the end group in this polymer will be discussed below.

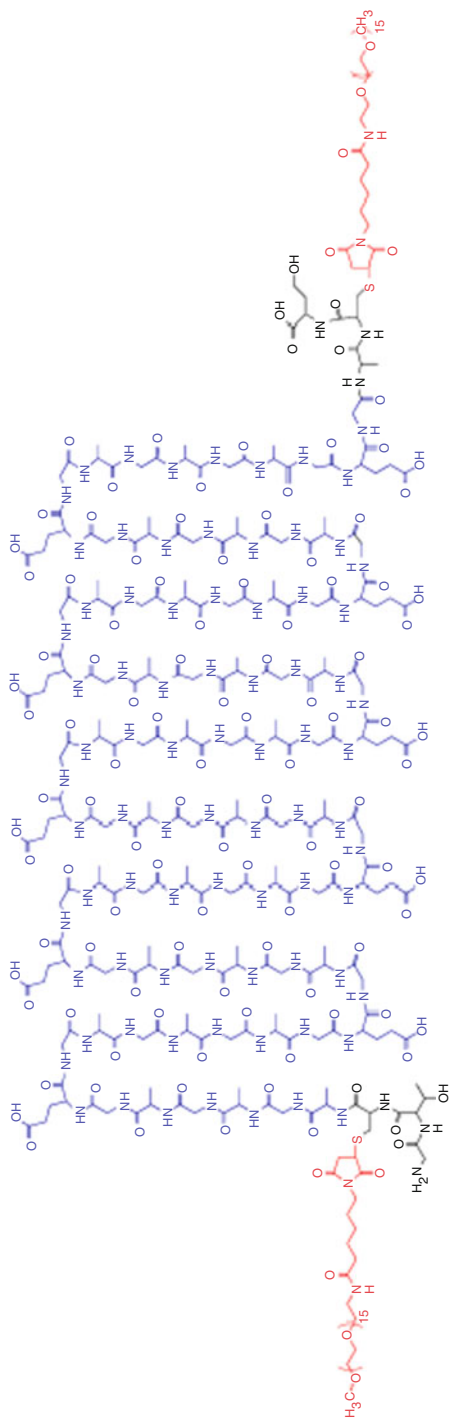


**Fig. 25** ABA-type block copolymer formed by reaction of maleimide-functionalised PEG with cysteine-flanked [(AG)<sub>3</sub>EG]<sub>n</sub> β-sheet element. Reproduced with permission from Smeenk et al. [69]. Copyright Wiley-VCH



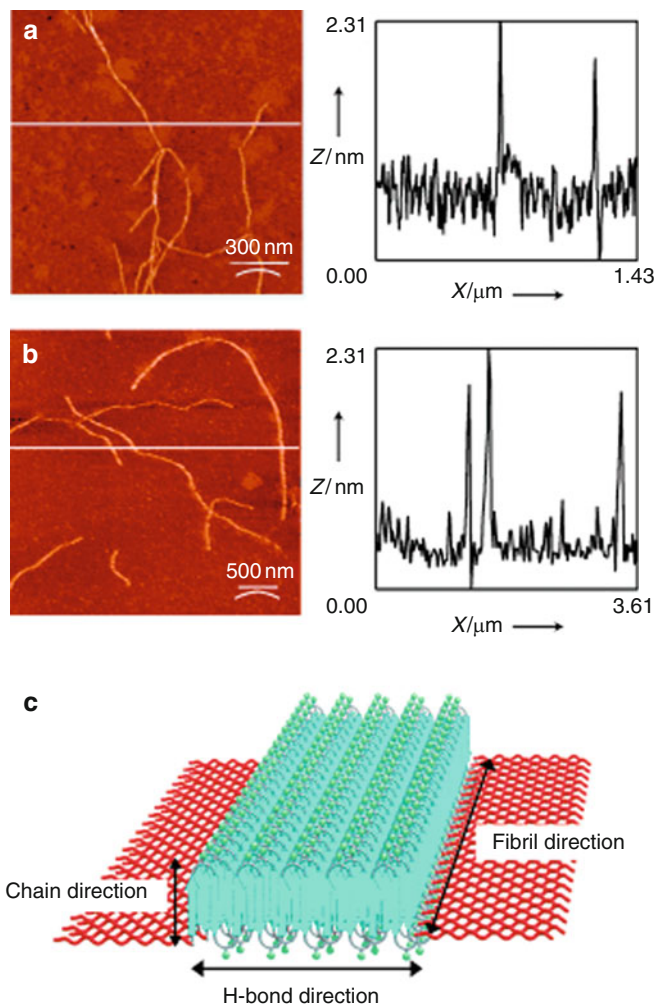


**Fig. 26** Tapping-mode AFM images of fibrils on mica (*left*) and corresponding height profiles (across the white lines in the AFM images) (*right*): (a) PEG-[(AG)<sub>3</sub>EG]<sub>10</sub>-PEG, (b) PEG-[(AG)<sub>3</sub>EG]<sub>20</sub>-PEG. (c) Proposed  $\beta$ -sheet fibril packing. Reproduced with permission from Smeenk et al. [69]. Copyright Wiley-VCH

The alkyl chains allow the molecule to be dissolved in organic solvents, while the  $\text{NHCOCH}_3$  was found necessary for UV diacetylene polymerisation because of the possibility of hydrogen bonding between the  $\text{NHCOCH}_3$  groups on adjacent chains (structure  **$\beta$ 2**). This locks the polymers into a conformation where diacetylene crosslinking can take place, yielding a poly(diacetylene) (structure **P2**) with strong UV absorption bands. Without the  $\text{NHCOCH}_3$  group, this specific crosslinking could not be performed.

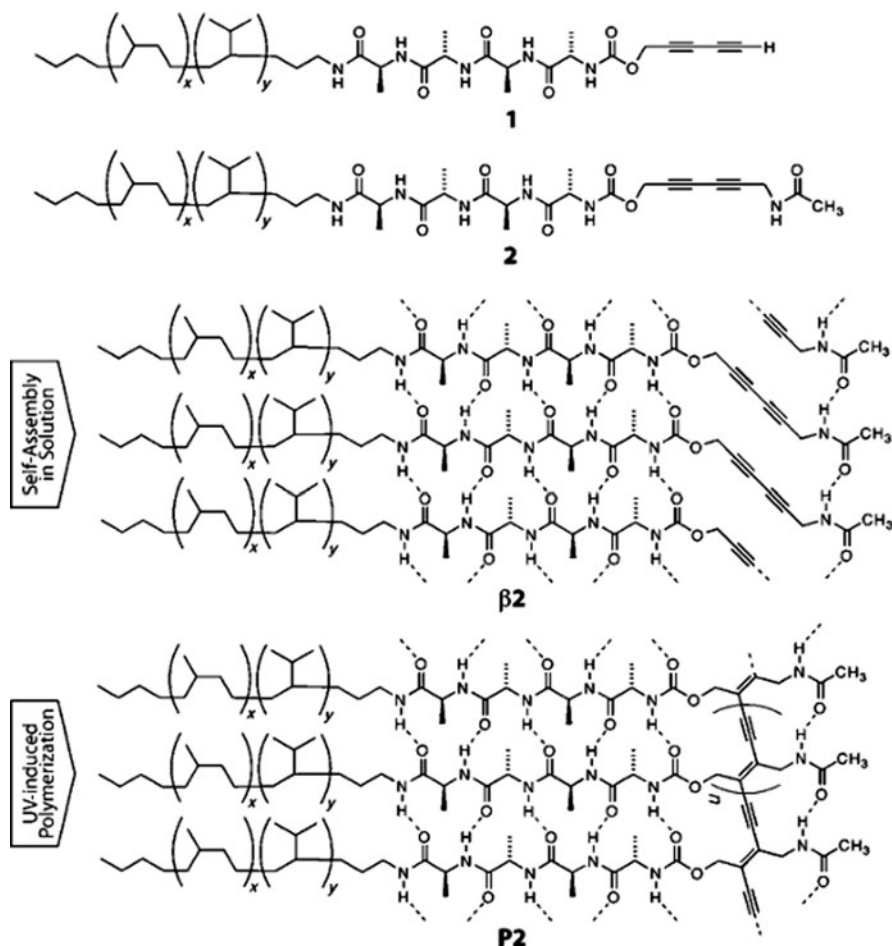


**Fig. 27** Peptide-diacetylene  $\beta$ -sheet (formed by self-assembly of **2**) before ( $\beta 2$ ) and after (**P2**) polymerisation. Reproduced with permission from Jahnke et al. [70]. Copyright Wiley-VCH

X-ray diffraction measurements of the assemblies of structure **2** gave a spacing comparable to those measured in studies of other  $\beta$ -sheet fibrils (4.59 Å). TEM and AFM observations before polymerisation indicated that fibrils of uniform widths and heights had formed. AFM imaging also shows that these double helical fibrils (Fig. 28) are formed from two ribbons. Ribbon widths were found to be approximately double the length of one peptide-diacetylene, so each ribbon was thought to be two  $\beta$ -sheets. Pairs of ribbons are assumed to form a double helical fibril, with the peptide shielded from the organic solvent by the hydrophobic coils (Fig. 30). The two polymerised diacetylene chains are thought to be aligned along the centre of each ribbon.

**Fig. 28** AFM image of self-assembled peptide-diacetylene **2**. Reproduced with permission from Jahnke et al. [70]. Copyright Wiley-VCH

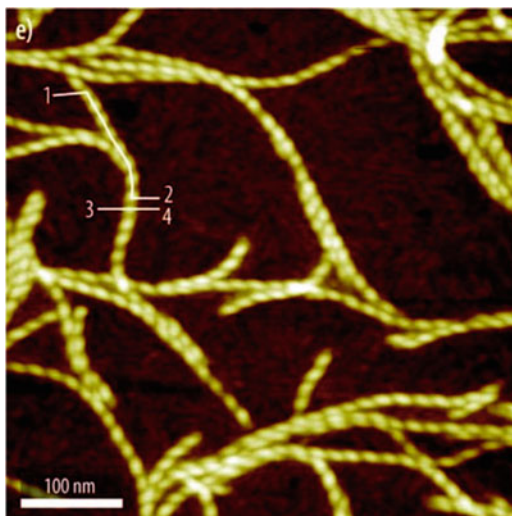
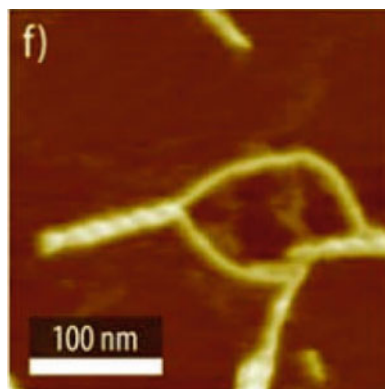


**Fig. 29** AFM image of peptide-diacetylene **2** showing the constituent ribbons at the ends of a double helix. Reproduced with permission from Jahnke et al. [70]. Copyright Wiley-VCH



From this work, the same group progressed to attaching a variety of end groups, in place of the  $\text{NHCOCH}_3$ , to the diacetylene [71]. This allows further control over the resulting supramolecular structure in organic solvents. Thin tapes, rigid tapes with a figure-of-eight cross-section, and helical bundles of double tapes were produced. The self-assembly model developed by Aggeli and co-workers described in Sect. 3.2 was used to explain these findings. Structures are governed by the number and spacing of hydrogen bonds that end groups can form between adjacent  $\beta$ -strands. As previously, only structures with sufficient ordering could be successfully photopolymerised into poly(diacetylene). Unlike the prepolymerised peptide aggregates, conjugated polymers could be exposed to hexafluoroisopropanol (HFIP) without disaggregating, and could also be handled directly with an AFM tip without breaking the structures (Fig. 31). The ability to make subtle adjustments to intermolecular packing may help these materials to find applications in organic electronics.

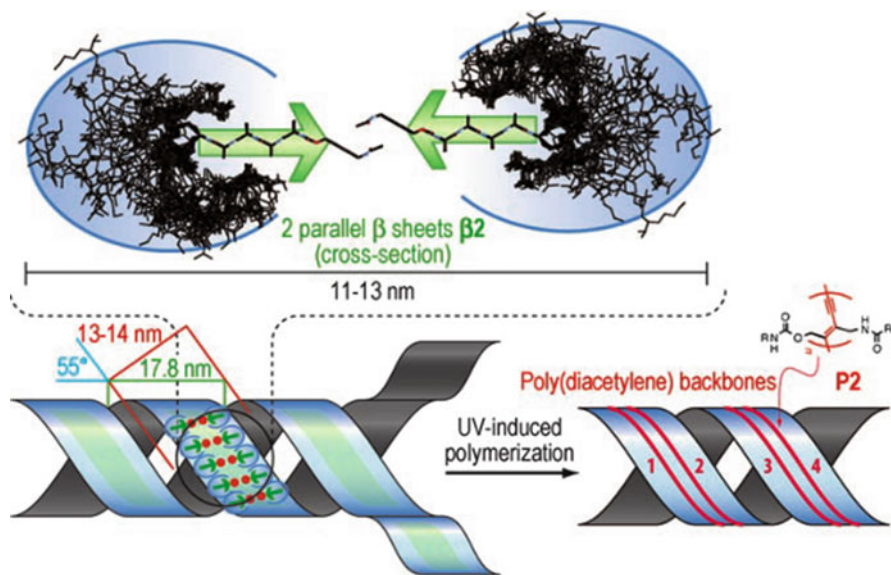


**Fig. 30** Model for the self-assembly of structure 2 into a double helix comprised of two ribbons, each of which consists of two parallel sheets. Reproduced with permission from Jahnke et al. [70]. Copyright Wiley-VCH

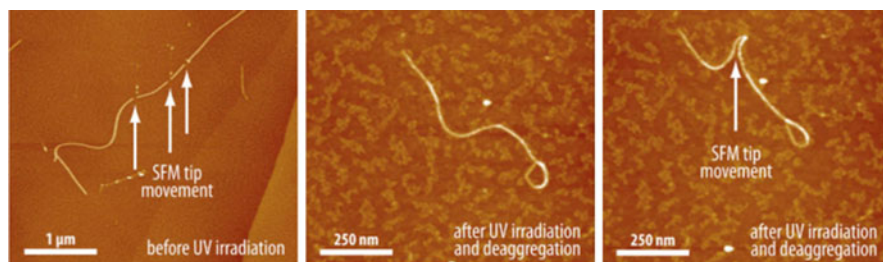


**Fig. 31** Interaction of a peptide-diacetylene (as structure 2 above, but with the  $\text{NHCOCH}_3$  replaced by  $\text{NHCOCH}_2\text{CH}_2\text{COOCH}_3$ ) with an AFM tip. *Left*: The AFM tip has broken a fibril that had no UV crosslinked diacetylenes while trying to move it. *Middle and right*: UV crosslinking allows manipulation with the AFM tip without damaging the fibril. Adapted with permission from Jahnke et al. [71]. Copyright Wiley-VCH

An alternative to modifying the functional group attached to fibrils is to utilise the chemistry present in the amino acid side chains. Furthermore, as peptides often undergo specific modification by enzymes *in vivo*, these could be harnessed for synthetic purposes. Q11 ( $\text{Ac-QQKFQFQFEQQ-Am}$ , a fibril-forming peptide based on P<sub>11</sub>-2), was coupled to lysine-based molecules by treatment with an enzyme (tissue transglutaminase, TGase) which results in a reaction between lysine and glutamine side chains [72] (Fig. 32).

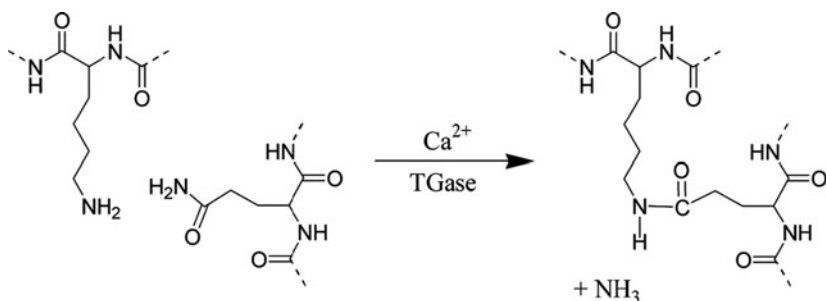
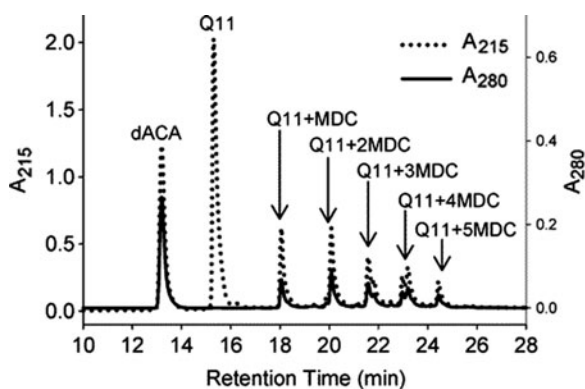


**Fig. 32** Transglutaminase (*TGase*)-mediated coupling between lysine and glutamine residues. Adapted with permission from Collier and Messersmith [72]. Copyright 2003 American Chemical Society

**Fig. 33** HPLC analysis for (previously self-assembled) Q11 reacting with monodansylcadaverine (*MDC*), with peaks assigned to the various adducts. Reprinted with permission from Collier and Messersmith [72]. Copyright 2003 American Chemical Society



A dansyl-containing lysine analogue, monodansylcadaverine (*MDC*), was used in initial *TGase* linking, because the dansyl UV absorption peak allowed quantification by reverse-phase HPLC using the absorbance at 280 nm. The reacted Q11 was dissolved in TFA along with a known dansyl standard. Peak areas of the standard were then compared with product to establish the amount of *MDC* present into Q11. Six Q11 peaks were measured and ascribed to Q11 with zero to five *MDC*s attached (Fig. 33).

Repeated addition of *MDC* to Q11 did occur, but the dominant product was Q11 with a single *MDC*. The fraction of Q11 with higher numbers of attached *MDC* decreased for increasing *MDC* number. Separately, a lysine peptide that contained the bioactive RGD [73] sequence (*n*-dansyl-GLKGGRGDS-Am) was successfully *TGase* crosslinked with self-assembled Q11: five distinct Q11-dansyl RGD were detected by mass spectrometry.

An interesting point raised by the authors is that Q11 was not observed to crosslink with itself, despite containing both lysine and glutamine residues. This could be explained by the lysine side chain being inaccessible to *TGase* within  $\beta$ -sheet aggregates; Q11 potentially exists as small aggregates even when prepared in fresh dilute solution. Because crosslinking between peptides could enhance the

material's mechanical properties, the authors state that producing a peptide that deliberately forms crosslinks could be of future interest.

If attachment of a particular constituent is incompatible with peptide synthesis, or detrimental to self-assembly, an alternative approach would be to add a functional group that selectively binds this molecule. After synthesis and self-assembly of the peptide, the difficult molecule could be introduced to the binding site included on the peptide.

A recent advance in this area is that of Buell and co-workers, who published a method to modify protein fibrils under physiological conditions via the use of Traut's reagent (2-iminothiolane) [74]. When reacted with Traut's reagent, the primary amines of the peptides are modified to sulphhydryl groups. This sulphur modification was used to covalently attach fibrils of  $\alpha$ -synuclein and A $\beta$ (1–42) peptide to gold surfaces under physiological conditions. When incubated with monomeric solution, it was found that this modification does not limit their behaviour as seeds for further growth. It is not inconceivable that this type of modification could be used to attach fibrils to functionalised gold nanoparticles [75]. Changing the functionalised groups on the nanoparticle, rather than the self-assembled peptide, could be a route to using the peptide as a customisable scaffold.

Another example of the use of binding for functionalisation is the "recruiting" of coiled-coil peptides developed by Ryadnov and Woolfson [76]. These incorporate complementary sticky ends so that they grow into fibres [77], and contain a component that will selectively bind a target molecule (Fig. 34). This concept was demonstrated using biotin (itself capable of binding a gold-labelled streptavidin) or a short peptide antigen (the FLAG epitope, sequence DYKDDDDK) used to bind a corresponding antibody that was biotin-labelled, and could in turn be detected by gold-labelled streptavidin. In both cases, fibres could be formed, just as with unmodified peptides, and gold nanoparticles were detected on the surface (Fig. 35). Biotinylated self-assembling fibres SAF-p1 and SAF-p2 mixed with their non-biotinylated complement, or even mixed together, produced fibres that were successfully coated with gold-labelled streptavidin. Binding of streptavidin was around three times greater for the biotinylated fibres when compared with a control test of gold streptavidin on unmodified SAF-p1 or SAF-p2 fibres. Although the fibres of SAF-p1-biotin formed on mixing it with SAF-p2 were similar to those of unmodified peptides, self-assembly of antigen-containing fibres (produced by mixing SAF-p1-FLAG with SAF-p2) was disrupted to some degree. Fibres were seen less frequently and when observed were found to have shorter lengths. This is thought to be a result of the extra negative charge of the antigen, and highlights the necessity for groups added to self-assembling systems to not interfere with the assembly process.

Mahmoud et al. extended this concept by using the peptide itself to bind a tagged component, obviating the need for biotin or an antigen to be attached to the self-assembling component. Positively charged coiled-coil peptide fibres, with regions of arginine present on their exterior, can bind short, negatively charged peptide-based tags [78]. The short peptides tested had sequences of the form R-GG-(xy)<sub>n</sub>-GYG where xy was either DE (negative), KR (positive) or AQ (neutral) (*n* was typically

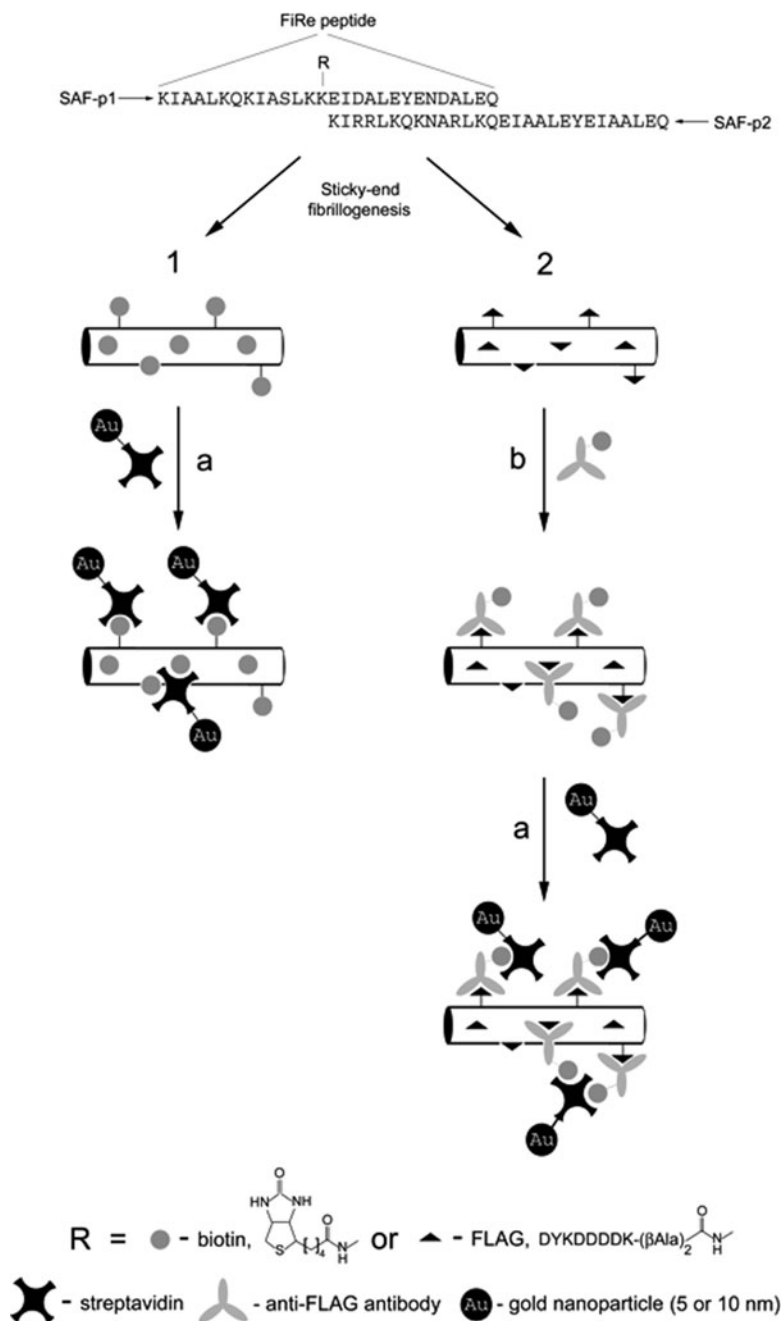


**Fig. 34** Functionalisation of bait peptides. 1 Gold-labelled streptavidin is attached directly. 2 Biotin-labelled anti-FLAG antibody is bound to the FLAG on the peptide (reaction *b*) and this is used to attach gold-labelled streptavidin (reaction *a*). Reprinted with permission from Ryadnov and Woolfson [76]. Copyright 2004 American Chemical Society

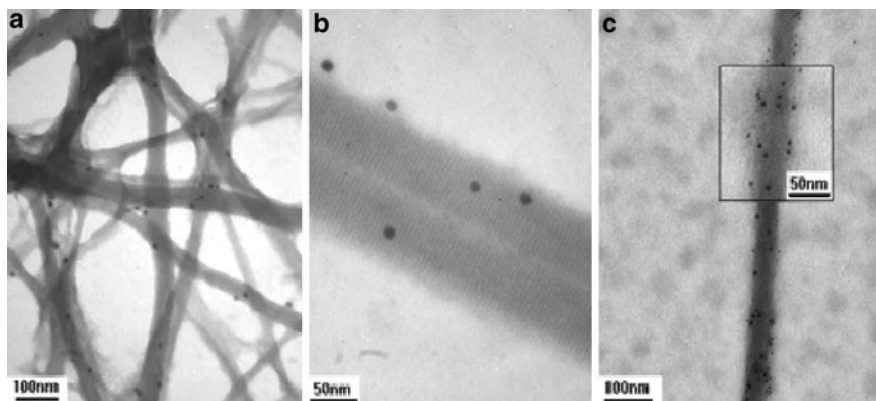


**Fig. 35** TEM image of peptide fibres coated with streptavidin-gold nanoparticles. (a, b) Peptides with biotin directly attached (using SAF-p1-biotin); particles are 10 nm, (c) Peptide fibre with biotinylated anti-FLAG antibody attached that was then bound to gold-labelled streptavidin; particles are 5 nm. Reprinted with permission from Ryadnov and Woolfson [76]. Copyright 2004 American Chemical Society

3), with biotin, linked by a glycine spacer, as the R group. Self-assembled coiled-coil fibres, formed by the complementary 28 amino acid peptides SAF-p1 and SAF-p2a, were mixed separately with each of these biotinylated peptides. TEM experiments utilising gold-labelled streptavidin, which binds to the tagged peptide in these experiments, showed that only the DE negatively charged tag was bound by fibres. Additionally, increasing the tag peptide concentration led to a greater proportion of particles binding to the peptide. In further testing with other fibre-forming peptide variants, the DE tag was found to bind to fibres with clusters of charge on the surface, but not to fibres with just a single exposed positive charge. The authors conclude that this implies that the density of charge, not just charge complementarity, on the surface is important.

This result leads us further towards the goal of creating more modular systems. A well-established self-assembling peptide system can be left unchanged while its customisation can be achieved by changing the tag on the binding peptide (e.g. biotin), or even by changing the complement to the tag on the binding peptide (e.g. replacing the gold attached to streptavidin with another ligand). Generalisation of this idea does not seem too unreasonable given that the researchers successfully used rhodamine-B as the R group, demonstrating its binding by fluorescence microscopy.

Finally, in somewhat of an inversion of the theme of this discussion – modifying self-assembled structures – it is notable that *removal* of a component initially added to peptides can be used to trigger conformational change. Koga and co-workers demonstrated this process using a core  $\beta$ -sheet-forming peptide ( $L_4K_8L_4$ ) that forms fibres at pH 9 [79]. By adding an enzyme-cleavable PEG chain to the peptide, self-assembly could be inhibited until the chain was removed. They studied both  $L_4K_8L_4$ -VPRGS-PEG, containing the thrombin-cleavable VPRGS tag, and a non-



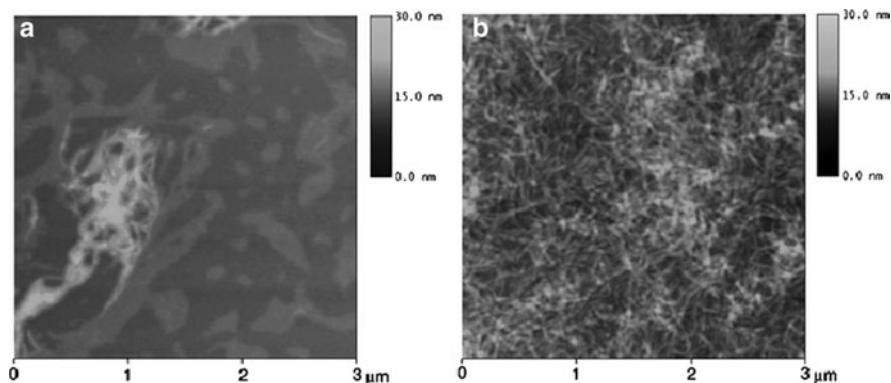


**Fig. 36** Tapping mode AFM images of  $L_4K_8L_4$ -VPRGS-PEG (a) before and (b) after thrombin digestion (at pH 9). Fibres in (b) have diameters of about 5–6 nm. Adapted by permission of The Royal Society of Chemistry from Koga et al. [79]

cleavable  $L_4K_8L_4$ -SGRPVL-PEG control peptide. (PEG had a molecular weight of approximately 3,000 Da.)

Following thrombin treatment, matrix assisted laser desorption/ionisation (MALDI) mass spectra found that only the peptide with the RG sequence lost PEG. CD spectra showed that the RG peptide underwent a swift change from  $\alpha$ -helix and random coil to  $\beta$ -sheet after cleavage, but this was not observed for non-cleaved peptides. A control  $L_4K_8L_4$ -VPR peptide also underwent rapid conformational transition to  $\beta$ -sheet, similarly to the cleaved  $L_4K_8L_4$ -VPRGS-PEG. For the thrombin-inactive peptide, no secondary structure change was observed. Examination of AFM images (Fig. 36) confirmed these findings: before digestion, non-uniform aggregates were observed, but the species present after digestion were thin fibrils with consistent thickness. It is suggested that an increase in peptide aqueous solubility by, and/or steric bulk of, the PEG are responsible for the restriction of  $\beta$ -sheet formation by PEG modification. This work contrasts the PEG studies outlined in Sect. 4.1.2, in which PEGylated peptides still self-assembled.

In this case, the restriction of peptide self-assembly was both desired, and by design. More generally, when looking to modify peptides and retain their self-assembly, where modifications are incompatible with assembly, post-assembly strategies will be necessary.

## 5 Conclusions

The work reviewed here demonstrates the tremendous versatility, promise and importance of peptides as building blocks in molecular self-assembly. However, in order to fully harness their potential in nanotechnology, more systematic work

needs to be carried out to understand the precise way in which they interact, determine their exact conformation within their self-assembling states, and grasp in a more quantitative manner the basic scientific rules that underpin peptide self-assembly.

**Acknowledgments** S. Maude and L.R. Tai acknowledge the financial support of EU FP6 BASE grant. L.R.Tai also thanks the School of Chemistry, University of Leeds for a part studentship. R.P.W. Davies and B.Liu are grateful to the Dutch Polymer Institute (DPI) for financial contribution. The work was also partly supported by the Leeds Centre of Excellence in Medical Engineering funded by the Wellcome Trust and EPSRC, WT088908/z/09/z.

## References

1. Merrifield RB (1963) *J Am Chem Soc* 85:2149
2. Bodanszky M (1993) *Principles of peptide synthesis*. Springer, Berlin
3. Lloyd-Williams P, Albericio F, Giralte E (1997) *Chemical approaches to the synthesis of peptides and proteins*. CRC, Boca Raton
4. Chan WC, White PD (2000) *Fmoc solid phase peptide synthesis, a practical approach*. Oxford University Press, New York
5. Seebach D, Kimmerlin T (2005) *J Pept Res* 65:229
6. Albericio F (2004) *Curr Opin Chem Biol* 8:211
7. Carpino LA (1957) *J Am Chem Soc* 79:4427
8. Carpino LA, Han GY (1970) *J Am Chem Soc* 92:5748
9. Sheehan JC, Hess GP (1955) *J Am Chem Soc* 77:1067
10. Han S-Y, Kim Y-A (2004) *Tetrahedron* 60:2447
11. Drees F, Wuensch E (1966) *Chem Ber* 99:110
12. Koenig W, Geiger R (1970) *Chem Ber* 103:788
13. Atherton E, Woolley V, Sheppard RC (1980) *J Chem Soc Chem Commun*:970
14. Merrifield RB, Gisin BF (1972) *J Am Chem Soc* 94:3102
15. Merrifield RB, Tam JP, Riemen MW (1988) *Pept Res* 1:6
16. Aggeli A, Bell M, Boden N, Keen JN, Knowles PF, McLeish TCB, Pitkeathly M, Radford SE (1997) *Nature* 386:259
17. Xiong HY, Buckwalter BL, Shieh HM, Hecht MH (1995) *Proc Natl Acad Sci USA* 92:6349
18. Maillère B, Mourier G, Hervé M, Ménez A (1995) *Mol Immunol* 32:1377
19. Aggeli A, Bell M, Boden N, Keen JN, McLeish TCB, Nyrkova I, Radford SE, Semenov A (1997) *J Mater Chem* 7:1135
20. Aggeli A, Nyrkova IA, Bell M, Harding R, Carrick L, McLeish TCB, Semenov AN, Boden N (2001) *Proc Natl Acad Sci USA* 98:11857
21. Chothia C (1973) *J Mol Biol* 75:295
22. Aggeli A, Bell M, Carrick LM, Fishwick CWG, Harding R, Mawer PJ, Radford SE, Strong AE, Boden N (2003) *J Am Chem Soc* 125:9619
23. Carrick LM, Aggeli A, Boden N, Fisher J, Ingham E, Waigh TA (2007) *Tetrahedron* 63:7457
24. Zhang S, Holmes T, Lockshin C, Rich A (1993) *Proc Natl Acad Sci USA* 90:3334
25. Caplan MR, Moore PN, Zhang SG, Kamm RD, Lauffenburger DA (2000) *Biomacromolecules* 1:627
26. Caplan MR, Schwartzfarb EM, Zhang SG, Kamm RD, Lauffenburger DA (2002) *Biomaterials* 23:219
27. Ye ZY, Zhang HY, Luo HL, Wang SK, Zhou QH, Du XP, Tang CK, Chen LY, Liu JP, Shi YK, Zhang EY, Ellis-Behnke R, Zhao XJ (2008) *J Pept Sci* 14:152
28. Zhao Y, Yokoi H, Tanaka M, Kinoshita T, Tan TW (2008) *Biomacromolecules* 9:1511

29. Schneider JP, Pochan DJ, Ozbas B, Rajagopal K, Pakstis L, Kretsinger J (2002) *J Am Chem Soc* 124:15030
30. Rajagopal K, Lamm MS, Haines-Butterick LA, Pochan DJ, Schneider JP (2009) *Biomacromolecules* 10:2619
31. Ozbas B, Kretsinger J, Rajagopal K, Schneider JP, Pochan DJ (2004) *Macromolecules* 37:7331
32. Dong H, Paramonov SE, Hartgerink JD (2008) *J Am Chem Soc* 130:13691
33. Zimenkov Y, Dublin SN, Ni R, Tu RS, Breedveld V, Apkarian RP, Conticello VP (2006) *J Am Chem Soc* 128:6770
34. Hartgerink JD, Beniash E, Stupp SI (2001) *Science* 294:1684
35. Hartgerink JD, Beniash E, Stupp SI (2002) *Proc Natl Acad Sci USA* 99:5133
36. Stendahl JC, Rao MS, Guler MO, Stupp SI (2006) *Adv Funct Mater* 16:499
37. Jayawarna V, Ali M, Jowitt TA, Miller AF, Saiani A, Gough JE, Ulijn RV (2006) *Adv Mater* 18:611
38. Reches M, Gazit E (2005) *Isr J Chem* 45:363
39. Mahler A, Reches M, Rechter M, Cohen S, Gazit E (2006) *Adv Mater* 18:1365
40. Adams DJ, Mullen LM, Berta M, Chen L, Frith WJ (2010) *Soft Matter* 6:1971
41. Reches M, Gazit E (2003) *Science* 300:625
42. Kumaraswamy P, Lakshmanan R, Sethuraman S, Krishnan UM (2011) *Soft Matter* 7:2744
43. Mehta AK, Lu K, Childers WS, Liang Y, Dublin SN, Dong JJ, Snyder JP, Pingali SV, Thiyagarajan P, Lynn DG (2008) *J Am Chem Soc* 130:9829
44. Hamley IW, Castelletto V, Moulton C, Myatt D, Siligardi G, Oliveira CLP, Pedersen JS, Abutbul I, Danino D (2010) *Macromol Biosci* 10:40
45. Capes JS, Kiley PJ, Windle AH (2010) *Langmuir* 26:5637
46. Dong H, Paramonov SE, Aulisa L, Bakota EL, Hartgerink JD (2007) *J Am Chem Soc* 129:12468
47. Hong YS, Legge RL, Zhang S, Chen P (2003) *Biomacromolecules* 4:1433
48. Brown RA, Case DA (2006) *J Comput Chem* 27:1662
49. Canutescu AA, Shelenkov AA, Dunbrack RL (2003) *Protein Sci* 12:2001
50. Case DA, Cheatham TE, Darden T, Gohlke H, Luo R, Merz KM, Onufriev A, Simmerling C, Wang B, Woods RJ (2005) *J Comput Chem* 26:1668
51. Leach AR (2001) *Molecular modelling: principles and applications*, 2nd edn. Pearson Education EMA, London
52. Chiti F, Dobson CM (2006) *Annu Rev Biochem* 75:333
53. Woolfson DN, Mahmoud ZN (2010) *Chem Soc Rev* 39:3464
54. MacPhee CE, Dobson CM (2000) *J Am Chem Soc* 122:12707
55. Krebs MRH, Morozova-Roche LA, Daniel K, Robinson CV, Dobson CM (2004) *Protein Sci* 13:1933
56. Kodama H, Matsumura S, Yamashita T, Mihara H (2004) *Chem Commun*:2876
57. Takahashi Y, Ueno A, Mihara H (2002) *Chembiochem* 3:637
58. Takahashi Y, Ueno A, Mihara H (1998) *Chemistry* 4:2475
59. Harris JM (ed) (1992) *Poly(ethylene glycol) chemistry: biotechnical and biomedical applications*. Plenum, New York
60. Fukuma T, Mostaert AS, Jarvis SP (2006) *Tribol Lett* 22:233
61. Lim K, Herron JN (1992) *Poly(ethylene glycol) chemistry: biotechnical and biomedical applications*. Plenum, New York
62. Burkoth TS, Benzinger TLS, Urban V, Morgan DM, Gregory DM, Thiyagarajan P, Botto RE, Meredith SC, Lynn DG (2000) *J Am Chem Soc* 122:7883
63. Burkoth TS, Benzinger TLS, Jones DNM, Hallenga K, Meredith SC, Lynn DG (1998) *J Am Chem Soc* 120:7655
64. Burkoth TS, Benzinger TLS, Urban V, Lynn DG, Meredith SC, Thiyagarajan P (1999) *J Am Chem Soc* 121:7429
65. Hamley IW, Ansari IA, Castelletto V, Nuhn H, Rosler A, Klok HA (2005) *Biomacromolecules* 6:1310

66. Hamley IW, Krysmann MJ (2008) *Langmuir* 24:8210
67. Hamley IW, Krysmann MJ, Kellarakis A, Castelletto V, Noirez L, Hule RA, Pochan DJ (2008) *Chemistry* 14:11369
68. Collier JH, Messersmith PB (2004) *Adv Mater* 16:907
69. Smeenk JM, Otten MBJ, Thies J, Tirrell DA, Stunnenberg HG, Van Hest JCM (2005) *Angew Chem Int Ed* 44:1968
70. Jahnke E, Lieberwirth I, Severin N, Rabe JP, Frauenrath H (2006) *Angew Chem Int Ed* 45:5383
71. Jahnke E, Severin N, Kreutzkamp P, Rabe JP, Frauenrath H (2008) *Adv Mater* 20:409
72. Collier JH, Messersmith PB (2003) *Bioconjug Chem* 14:748
73. Ruoslahti E (1996) *Annu Rev Cell Dev Biol* 12:697
74. Buell AK, White DA, Meier C, Welland ME, Knowles TPJ, Dobson CM (2010) *J Phys Chem B* 114:277
75. Daniel M, Astruc D (2004) *Chem Rev* 104:293
76. Ryadnov MG, Woolfson DN (2004) *J Am Chem Soc* 126:7454
77. Pandya MJ, Spooner GM, Sunde M, Thorpe JR, Rodger A, Woolfson DN (2000) *Biochemistry* 39:8728
78. Mahmoud ZN, Grundy DJ, Channon KJ, Woolfson DN (2010) *Biomaterials* 31:7468
79. Koga T, Kitamura K, Higashi N (2006) *Chem Commun*:4897

# Elastomeric Polypeptides

Mark B. van Eldijk, Christopher L. McGann, Kristi L. Kiick,  
and Jan C.M. van Hest

**Abstract** Elastomeric polypeptides are very interesting biopolymers and are characterized by rubber-like elasticity, large extensibility before rupture, reversible deformation without loss of energy, and high resilience upon stretching. Their useful properties have motivated their use in a wide variety of materials and biological applications. This chapter focuses on elastin and resilin – two elastomeric biopolymers – and the recombinant polypeptides derived from them (elastin-like polypeptides and resilin-like polypeptides). This chapter also discusses the applications of these recombinant polypeptides in the fields of purification, drug delivery, and tissue engineering.

**Keywords** Elastin · Elastin-like polypeptides · Elastomeric polypeptides · Resilin · Resilin-like polypeptides

## Contents

1	Introduction .....	72
2	Elastin and Elastin-Like Polypeptides .....	73
2.1	Elastin Biosynthesis .....	73
2.2	General Properties of Elastin and Tropoelastin .....	76
2.3	Development and Properties of Recombinant Elastins .....	78
2.4	Applications of Elastin-Like Polypeptides .....	80
3	Resilin and Resilin-Like Polypeptides .....	94
3.1	Resilin Occurrence and Biosynthesis .....	94

---

M.B. van Eldijk and J.C.M. van Hest (✉)  
Institute for Molecules and Materials, Radboud University Nijmegen, 6525 AJ Nijmegen, The Netherlands  
e-mail: [j.vanhest@science.ru.nl](mailto:j.vanhest@science.ru.nl)

C.L. McGann and K.L. Kiick (✉)  
Department of Materials Science and Engineering, University of Delaware, Newark, DE 19716, USA  
e-mail: [kiick@udel.edu](mailto:kiick@udel.edu)

3.2	General Properties of Resilin .....	100
3.3	Development and Properties of Recombinant Resilins .....	104
3.4	Applications of Resilin-Like Polypeptides .....	106
4	Conclusions .....	109
	References .....	110

## 1 Introduction

Elastomeric polypeptides are a class of very interesting biopolymers and are characterized by rubber-like elasticity, large extensibility before rupture, reversible deformation without loss of energy, and high resilience upon stretching. Their useful properties have motivated their use in a wide variety of materials and biological applications. Here, we focus on two elastomeric proteins and the recombinant polypeptides derived thereof.

The first elastomeric protein is elastin, this structural protein is one of the main components of the extracellular matrix, which provides structural integrity to the tissues and organs of the body. This highly crosslinked and therefore insoluble protein is the essential element of elastic fibers, which induce elasticity to tissue of lung, skin, and arteries. In these fibers, elastin forms the internal core, which is interspersed with microfibrils [1, 2]. Not only this biopolymer but also its precursor material, tropoelastin, have inspired materials scientists for many years. The most interesting characteristic of the precursor is its ability to self-assemble under physiological conditions, thereby demonstrating a lower critical solution temperature (LCST) behavior. This specific property has led to the development of a new class of synthetic polypeptides that mimic elastin in its composition and are therefore also known as elastin-like polypeptides (ELPs).

Resilin is the second elastomeric polypeptide that is discussed here. This protein, found in specialized regions of the insect cuticle, similarly demonstrates extraordinary extensibility and elasticity; its role as an elastic spring in insect organs provides clear illustration of its characteristic fatigue resistance and resilience. In fact, its mechanical properties are in near-agreement with classic rubber-elasticity theory, a remarkable feature for a hydrophilic biopolymer network. Apart from the outstanding mechanical properties, resilin provides an interesting comparison to other protein elastomers due to its hydrophilicity, but also due to the fact that resilin shares certain compositional characteristics. In particular, the high number of proline and glycine residues found in resilin as well as other protein elastomers could indicate some sort of structural importance. While silks and elastin have received the most attention from the scientific community over the past few decades, the development of recombinant resilins, facilitated by advances made in recombinant DNA technologies and protein engineering, has provided invaluable opportunities for the application of resilin as a biomaterial. Recombinant resilin could potentially see application in a variety of fields, including tissue engineering, drug delivery, biosensors, and nanobiotechnology.

This chapter will discuss the basic aspects of elastin and resilin and will address their biological role, biochemical processing, and properties. The materials inspired by elastin and resilin, such as elastin-like polypeptides and resilin-like polypeptides, and applications thereof, will also be covered.

## 2 Elastin and Elastin-Like Polypeptides

### 2.1 Elastin Biosynthesis

Elastin is a heavily crosslinked biopolymer that is formed in a process named elastogenesis. In this section, the role of elastin and the different steps of elastin production will be described, starting with transcription of the genetic code and processing of the primary transcript, followed by translation into the elastin precursor protein and its transport to the extracellular matrix. Finally, the crosslinking and fiber formation, which result in the transition from tropoelastin to elastin, are described.

Tropoelastin is the soluble precursor of elastin and consists of alternating hydrophobic and hydrophilic peptide domains. The most common amino acids in the hydrophobic domains are Gly, Val, Ala, and Pro, which are often present in repeats of tetra-, penta-, and hexapeptides, such as Gly-Gly-Val-Pro, Gly-Val-Gly-Val-Pro, Gly-Val-Pro-Gly-Val, and Gly-Val-Gly-Val-Ala-Pro, respectively [3, 4]. The hydrophilic domains are mainly composed of lysines interspersed by alanines.

Tropoelastin is encoded by a single copy gene and the alternating hydrophobic and hydrophilic domains are generally encoded by different expressed regions, or exons (Fig. 1). Those exons are alternated by introns (intragenic regions), which are



**Fig. 1** Primary structure of human tropoelastin isoform 3 (EBI accession no. P15502). The highlighted regions correspond to the signal peptide and hydrophobic and hydrophilic domains. Based on [2]

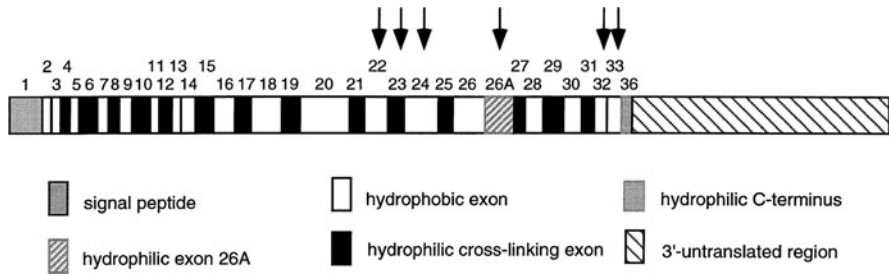


**Fig. 2** cDNA structure of human tropoelastin. The alternating hydrophobic and hydrophilic domains are generally encoded by different exons, shown in *white* and *black*, respectively. The *arrows* indicate the six exons that are subject to alternative splicing in a cassette-like fashion. Reproduced from [8] with permission from John Wiley and Sons, copyright 1998

not present in the final transcript. Even though a single gene is coding for tropoelastin, various types (isoforms) of tropoelastin exist due to extensive alternative splicing [5, 6]. Six exons were shown to be subject to this process in a cassette-like fashion in which an exon is either included or excluded, and this results in at least 11 human isoforms (Fig. 2, arrows) [7]. The elastin genes of human, bovine, chick, and rat have been sequenced and the amino acid sequences were determined [8]. Even though a strong similarity was found between tropoelastins from different sources, some variation does exist. Some exons are specific for a certain species, for example exon 26A is only present in human elastin. This exon is rich in charged and polar amino acids and is thought to influence the structural and biological functions of elastin [6].

After mRNA splicing, the tropoelastin mRNA is translated at the surface of the rough endoplasmic reticulum (RER) in a variety of cells: smooth muscle cells, endothelial and microvascular cells, chondrocytes and fibroblasts. The approximately 70 kDa precursor protein (depending on isoform) is synthesized with an N-terminal 26-amino-acid signal peptide. This nascent polypeptide chain is transported into the lumen of the RER, where the signal peptide is removed cotranslationally [9].

Very few post-translational modifications have been found on tropoelastin. However, hydroxylation of 25% of the proline residues is observed [10]. The enzymatic modification of proline to hydroxyproline (Hyp) is performed by prolyl hydroxylase [11]. The purpose of this hydroxylation remains unclear and it is even proposed that Hyps in tropoelastin are a by-product of collagen hydroxylation as this occurs in the same cellular compartment [8].

Once the tropoelastin is synthesized, it is bound by the elastin-binding protein (EBP). This binding of EBP to tropoelastin is believed to prevent intracellular aggregation and to protect it from proteolytic degradation [12]. EBP is a 67 kDa multifunctional peripheral membrane protein and is part of the elastin receptor [13]. The two other subunits of the receptor complex are transmembrane proteins of 61 kDa and 55 kDa [14]. EBP is also equipped with a binding site for  $\beta$ -galactosaccharides, and binding of these sugars allosterically leads to reduced affinity for tropoelastin and results in dissociation of EBP from the 61 kDa and 55 kDa



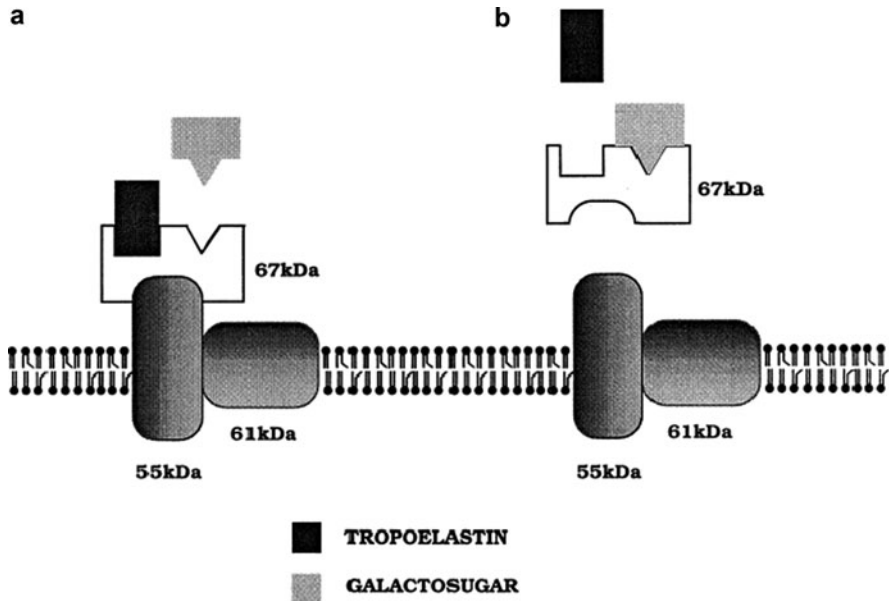


**Fig. 3** Binding and release of tropoelastin. The elastin receptor consists of a 67 kDa peripheral subunit (EBP) with two transmembrane proteins of 61 and 55 kDa. The 67 kDa protein binds tropoelastin and galactosugars through two separate sites. (a) Tropoelastin binds to the intact EBP complex. (b) Upon binding of a galactosugar, the EBP loses its affinity for both tropoelastin and the membrane-bound protein, which leads to the release of tropoelastin. Reproduced from [8] with permission from John Wiley and Sons, copyright 1998

membrane proteins. While complexed with EBP, elastin is transported from the RER to the cell surface via the Golgi apparatus. Upon reaching the cell surface, it is secreted from the cell. Galactosugar moieties on microfibrils at the cell surface are then bound by EBP, which leads to release of tropoelastin (Fig. 3).

The microfibrils act as a scaffold onto which the tropoelastin molecules are deposited. In order for tropoelastin to be incorporated into the elastic fibers it needs to be crosslinked. To facilitate the crosslinking, these elastin precursors must associate and align. This alignment is thought to proceed via the process of coacervation. This process occurs via an inverse temperature transition, which induces the aggregation of tropoelastin. At low temperatures tropoelastin is soluble in aqueous solutions; upon raising the temperature the solution becomes cloudy because the tropoelastin molecules aggregate and become ordered by the interactions between their hydrophobic domains. This phenomenon is completely reversible (by cooling) and is thermodynamically controlled. This process is also known as lower critical solution temperature (LCST) behavior and can be influenced by protein concentration, salt concentration, and pH.

After the self-assembly process, the tropoelastin molecules are enzymatically crosslinked via the lysine residues in the hydrophilic domains. In this last step of the elastogenesis, the amines of the lysine residues are enzymatically converted

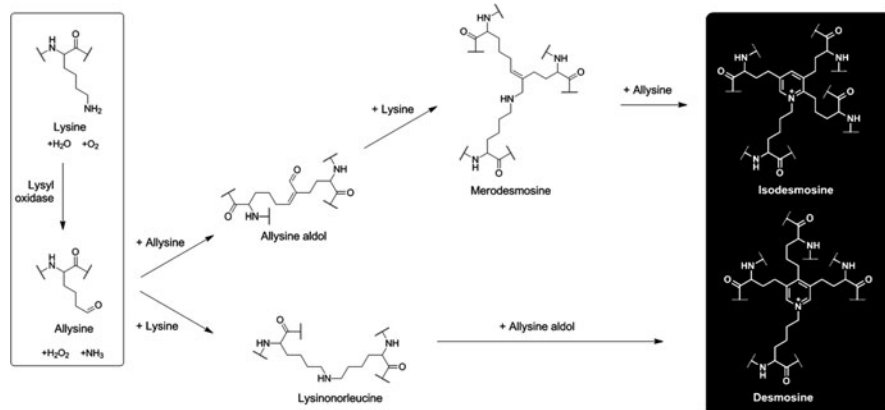


**Fig. 4** Structures and formation routes of crosslinks in elastin. In the first step, lysine is catalytically converted to allysine by lysyl oxidase; all subsequent condensation steps are spontaneous

to aldehydes (allysine) by lysyl oxidase via oxidative deamination (Fig. 4). Lysyl oxidase is a copper-dependent amine oxidase. In the following spontaneous condensations, allysine can react with another allysine or with lysine to form di-, tri- and tetrafunctional crosslinks, to eventually yield desmosine and isodesmosine linkages [15]. The interchain crosslinking and the high number of hydrophobic residues immediately lead to insolubility of the elastin.

## 2.2 General Properties of Elastin and Tropoelastin

Research into elastin, its properties, and the fiber formation was for a considerable period of time hindered due to its insolubility. However, discovery of the soluble tropoelastin precursor made new investigations possible. The tropoelastin protein can be isolated from copper-deficient animals. However, this is a very animal-unfriendly and low yielding process [2]. Therefore, it is preferred to obtain tropoelastin from overexpression in microbial hosts such as *Escherichia coli* (*E. coli*). Most studies are thus based on tropoelastin obtained via bacterial production.

The main biological function of elastin is to provide elasticity to organs and tissues. However, it has been shown that elastin and peptides derived from elastin also have additional biological properties. Elastin can be degraded by several protein-degrading enzymes, such as elastases, matrix metalloproteinases, and cathepsins. The resulting elastin-derived peptides (EDP) can interact with other extracellular matrix proteins to induce a broad range of biological activities. EDPs are chemotactic for various cells, such as fibroblasts and monocytes, by binding to the EBP [16, 17]. The consensus sequence GXXPG (X being any natural amino acid) of EDPs was proposed to be crucial for the interaction with the EBP.

The coacervation of tropoelastin plays a crucial role in the assembly into elastic fibers. This coacervation is based on the LCST behavior of tropoelastin, which causes tropoelastins structure to become ordered upon raising the temperature. The loss of entropy of the biopolymer is compensated by the release of water from its chain [2, 18, 19]. This release of water results in dehydration of the hydrophobic side chains, and this is the onset of the self-assembly leading to the alignment of tropoelastin molecules.

Weiss and coworkers intensively investigated the coacervation behavior of a single isoform of tropoelastin. They produced tropoelastin by overexpression in *E. coli*, and the coacervation was then assayed by monitoring turbidity while varying protein concentration, NaCl concentration, and pH. All these factors influence the temperature at which the coacervation is initiated. A typical tropoelastin coacervation curve is shown in Fig. 5. Increasing tropoelastin concentration resulted in a shift towards lower temperatures and a reduction of the temperature range over which coacervation took place. A lowering of coacervation temperature was also found upon increasing NaCl concentration. It is suggested that this is caused by NaCl decreasing the effective concentration of water by binding it in hydration shells, which therefore leads to an increase in protein concentration. Impurities that are able to bind the hydrophobic domains of the tropoelastin also had a major influence on the coacervation [20].

This coacervation process forms the basis for the self-assembly, which takes place prior to the crosslinking. The assembly of tropoelastin is based on an ordering process, in which the polypeptides are converted from a state with little order to a more structured conformation [8]. The insoluble elastic fiber is formed via the enzymatic crosslinking of tropoelastin (described in Sect. 2.1). Various models have been proposed to explain the mechanism of elasticity of the elastin fibers.

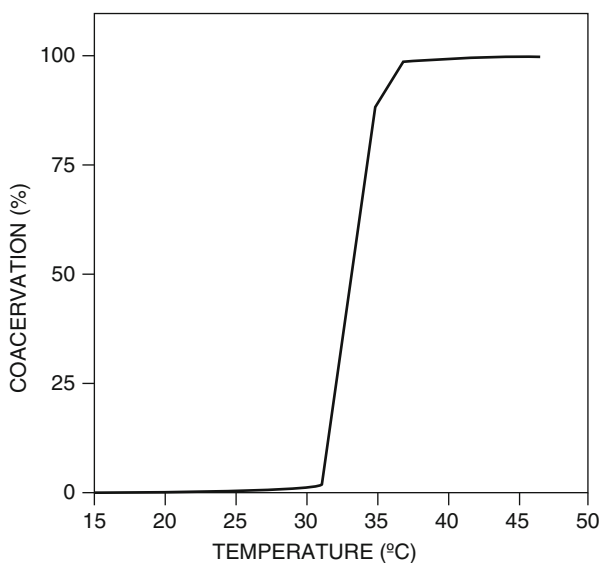


**Fig. 5** Coacervation curve of 40 mg/mL tropoelastin in 10 mM sodium phosphate pH 7.4, containing 150 mM NaCl. Maximal coacervation was obtained at 37 °C. Reproduced from [20] with permission from John Wiley and Sons, copyright 1997

The main models are described in a review by Vrhovski and Weiss [8]. For ideal elastomers in the extended mode, all the energy resides on the backbone and can therefore be recovered upon relaxation [18]. Generally, it is believed that the mechanism of elasticity is entropy-driven, thus the stretching decreases the entropy of the system and the recoil is then induced by a spontaneous return to the maximal level of entropy [8].

### 2.3 Development and Properties of Recombinant Elastins

In order to obtain a better understanding of the origin of the interesting characteristics of elastin and its precursor, several groups have investigated model polymers with elastin-based sequences. Urry and coworkers performed pioneering work in this field. They were the first to synthesize the repetitive peptides, their oligomers, and the polymers that were found in the hydrophobic domains of elastin. Via this approach they determined the conformation and interactions of these domains. Of particular interest proved to be the repeat sequence of Val-Pro-Gly-Xaa-Gly (VPGXG), where the fourth residue can be any natural amino acid except proline. They observed that polymers of this pentapeptide repeat coacervate in a similar way to tropoelastin. Polypeptides containing this type of sequence were coined elastin-like polypeptides [21]. In some articles and reviews the terms elastin-mimetic polypeptides or elastin-like recombinamers are used instead of elastin-like polypeptides, however in this chapter we will refer to these polymers as elastin-like polypeptides.

Poly(VPGVG) (Fig. 6) has been studied most thoroughly and it was shown that it exhibits an inverse phase transition. The biopolymer undergoes phase separation from solution upon increasing temperature, resulting in a  $\beta$ -spiral structure and simultaneous release of water molecules associated with the polymer chain (Fig. 7).

**Fig. 6** Chemical structure of poly(Val-Pro-Gly-Val-Gly)

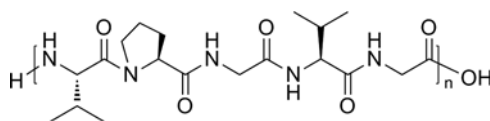
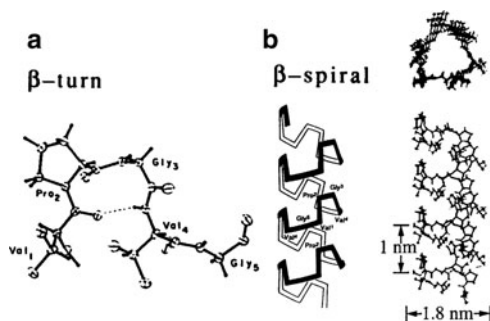


**Fig. 7** (a) Recurring  $\beta$ -turn found in poly(VPGVG). (b)  $\beta$ -spiral structure adopted by the poly(VPGVG) upon raising the temperature above the inverse transition temperature. Reprinted from [22] with permission from Elsevier, copyright 1992



The effects of varying the fourth amino acid and the biopolymer length have been extensively investigated and models have been proposed [23–26]. ELP constructs are usually described using the notation ELP[ $X_iY_jZ_k-n$ ], where the capital letters between the brackets indicate the single letter amino acid code for the Xaa-replacing residue in the pentapeptide Val-Pro-Gly-Xaa-Gly. The subscript stands for the ratio of the guest residues and the  $n$  represents the total number of pentapeptide repeats.

Figure 8a shows the turbidity measurements for different guest residues in ELP [ $V_8X_2$ ]. Lower transition temperatures ( $T_t$ ) correlate with increased hydrophobicity of the guest residue [24, 25]. This data was extrapolated to other ratios of Val:Xaa (Fig. 8b). The transition temperature could also be influenced by the molecular weight of the ELP. The  $T_t$  was shown to increase with decreasing polymer length (Fig. 8c) [23, 26].

ELPs can be produced via chemical synthesis and biosynthetically. For chemical synthesis via solid phase peptide synthesis, the attainable polymer length is limited, and if long polymers with a defined length are required then the biosynthetic approach is more appropriate. An advantage of chemical synthesis is, however, that it enables the facile introduction of functional residues in the polypeptide [27].

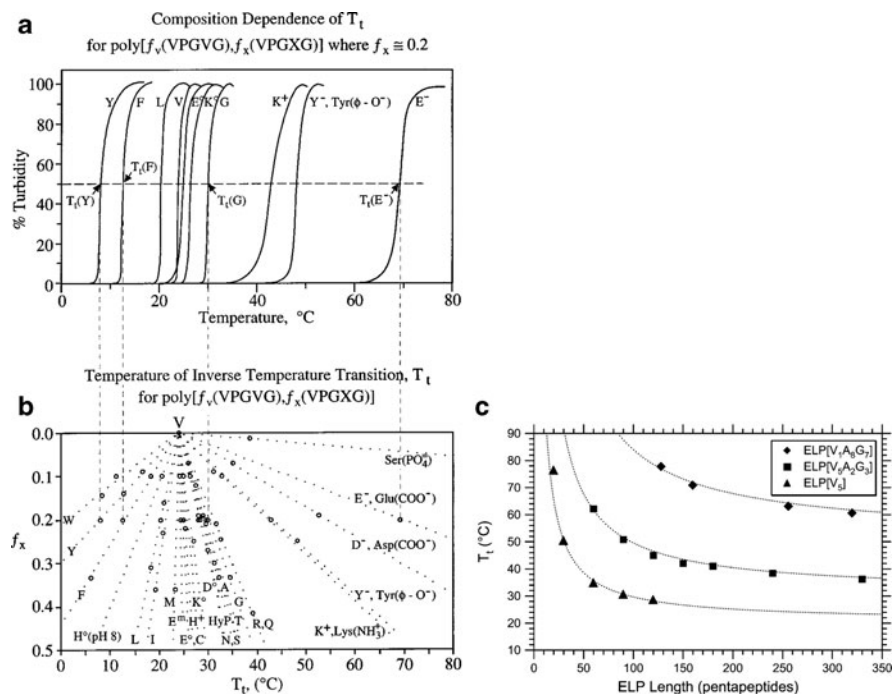


**Fig. 8** (a) Effects of varying the amino acid at fourth position in ELP[ $V_8X_2$ ]. (b) Extrapolation of transition temperature for other ratios of Val:Xaa. (a) and (b) Reprinted from [24] with permission from American Chemical Society, copyright 1993 (c) Molecular weight dependence of transition temperature. Reprinted from [23] with permission from Elsevier, copyright 2002

In the biosynthetic approach, protein expression in *E. coli* [27], yeast [28, 29], and plants [30, 31] have been employed. This approach requires the construction of genes encoding for these repetitive polypeptides. Different methods for gene construction have been published: multimerization [32], recursive directional ligation [33], and recursive directional ligation via plasmid reconstruction [23, 34].

Several studies were performed on the optimization of expression levels of ELP proteins in *E. coli*. In a recent example, the expression protocol was optimized for an ELP fusion with green fluorescent protein (GFP). This fusion protein was expressed and purified in a yield of 1.6 g/L of bacterial culture, which finally yielded ~400 mg GFP/L bacterial culture. This extremely high yield was found after uninduced expression in nutrient-rich medium supplemented with phosphate, glycerol and certain amino acids, such as proline and alanine [234]. The influence of fusion order was also examined and it was found that positioning the ELP at the C-terminus of target protein resulted in significantly higher expression levels [35].

## 2.4 Applications of Elastin-Like Polypeptides

### 2.4.1 Temperature-Triggered Purification

After expression of poly(VPGXG) genes, the biopolymer can easily be purified from a cellular lysate via a simple centrifugation procedure, because of the inverse temperature transition behavior. This causes the ELPs to undergo a reversible phase transition from being soluble to insoluble upon raising the temperature above the  $T_t$  and then back to soluble by lowering the temperature below  $T_t$  (Fig. 9). The insoluble form can be induced via addition of salt [27]. The inverse transition can

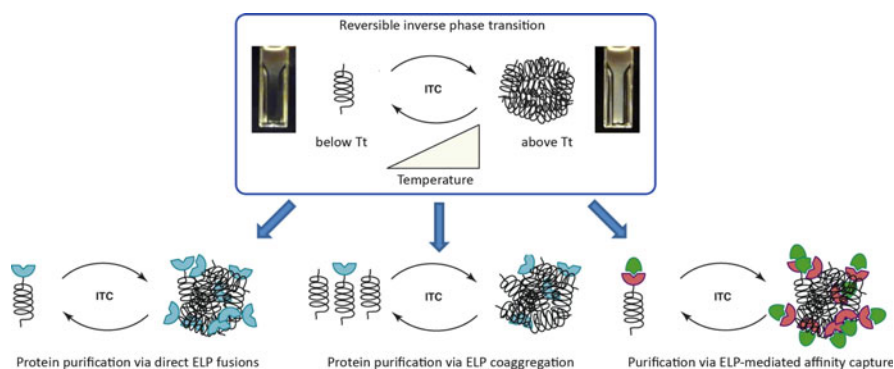


**Fig. 9** Purification of ELPs by ITC is based on the reversible inverse phase transition. *Left*: Protein purification via direct ELP fusions. A soluble ELP fused to a target protein becomes reversibly insoluble upon increasing temperature above  $T_t$ . *Center*: Protein purification via ELP coaggregation. An excess of free ELPs enhances the aggregation of trace quantities of ELP-fusions. *Right*: Purification via ELP-mediated affinity capture (EMAC). ELPs are fused to capture proteins, which bind specifically and reversibly to a target protein. This target protein can then be aggregated at temperatures above the  $T_t$ . Adapted from [38] with permission from Elsevier, copyright 2010

be assayed by monitoring the solution turbidity as function of temperature. The complete purification process is called inverse transition cycling (ITC), which is achieved by repeated centrifugation while alternating the temperature above and below the  $T_t$  [33].

The inverse transition temperature of the elastomeric polypeptide motivated Meyer and Chilkoti to design ELP fusion proteins. They hypothesized that the temperature-dependent inverse transition of the free biopolymer could be transferred to the fusion protein and would allow nonchromatographic separation of recombinant fusion proteins via the ITC procedure [33]. This hypothesis was furthermore supported by the results of previous studies on protein conjugates of poly(*N*-isopropylacrylamide), a synthetic polymer that undergoes a similar thermally driven phase transition, which showed that the transition behavior of the free polymer is retained in the conjugate [36, 37]. This founded the use of ELPs for purification of primarily recombinant proteins but also other molecules. The ELP-mediated purification procedures can be sorted into three categories: protein purification via direct ELP fusions (Fig. 9, left), protein purification via ELP coaggregation (Fig. 9, center), and purification via ELP-mediated affinity capture (EMAC) (Fig. 9, right).

### Protein Purification via Direct ELP Fusion

As an example of purification via the ELP fusion approach Meyer and Chilkoti (Fig. 9, left), purified the proteins thioredoxin and tendamistat. For this purpose these target proteins and ELP were genetically fused via a short peptide sequence that included a thrombin cleavage site, which allows the removal of the ELP tag after the purification is completed. The general outline of the purification procedure

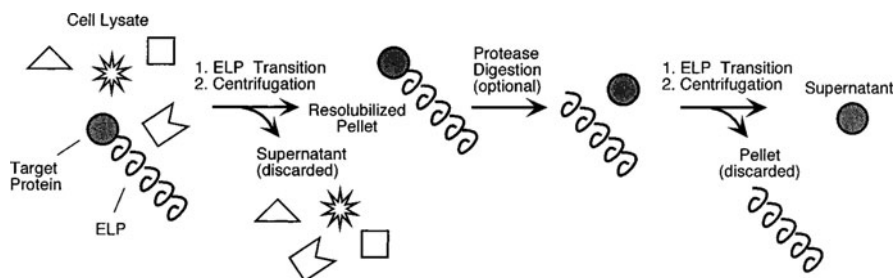


**Fig. 10** Inverse transition cycling (ITC) purification. The target proteins are genetically fused to an ELP via a short peptide linker that includes a protease cleavage site. After expression, the fusion protein is separated from the other proteins in the cellular lysate by inducing the ELP inverse temperature phase transition. The solution is then centrifuged at elevated temperature to pellet the aggregated fusion protein. The pellet is resolubilized by cooling below the  $T_t$  and the solution is centrifuged at low temperature to remove the remaining insoluble matter. This cycle of heated and cooled centrifugation is repeated several times to obtain higher purity. The target protein can then be liberated from the ELP via proteolytic cleavage and the cleaved ELP is then removed with another round of ITC. Reproduced from [39] with permission from John Wiley and Sons, copyright 2001

is depicted in Fig. 10. They showed that ELPs could be used for purification of target proteins with technical simplicity, low cost, ease of scale-up, and capacity for multiplexing [33].

In a subsequent study, the effect of reducing the ELP molecular weight on the expression and purification of a fusion protein was investigated. Two ELPs, ELP [V-20] and ELP[V<sub>5</sub>A<sub>2</sub>G<sub>3</sub>-90], both with a transition temperature at ~40°C in phosphate-buffered saline (PBS) containing 1 M NaCl, were applied for the purification of thioredoxin. Similar yields were observed for both fusion proteins, resulting in a higher thioredoxin yield for the ELP[V-20] fusion, since the ELP fraction was smaller. However, a more complex phase transition behavior was observed for this ELP and therefore a selection of an appropriate combination of salt concentration and solution temperature was required [39].

The ELP expression system was compared to the conventional oligohistidine fusion, which is traditionally applied for purification by immobilized metal affinity chromatography (IMAC). Both techniques were shown to have a similar yield of the recombinant protein. The temperature-triggered approach offers a fast and inexpensive nonchromatographic separation with the possibility for larger scale purification. Although the ELP expression system may not be applicable to all types of recombinant proteins, numerous examples have already been shown [40].

In the previous examples, protease-dependent cleavage was used to remove the ELP tag and to obtain the purified target protein. However, several problems are associated with the use of a protease-dependent cleavage: additional cost of the purification process, an additional purification step to separate the protease from the target protein and possible cleavage sites in the target protein. Therefore, the methodology was optimized by introducing self-cleaving inteins for protease-independent cleavage of the target protein. Both Wood and coworkers [41] and the research groups of Chilkoti and Filipe [42] simultaneously reported on this self-cleaving ELP tag. The latter demonstrated this approach by the use of the mini-intein from *Mycobacterium xenopi* GyrA gene (Mxe) to purify thioredoxin [42]. Wood and coworkers published several extensive protocols describing every aspect of how to use cleavable elastin-like polypeptide tags [43, 44]. Some other proteins were also expressed as a direct ELP fusion protein and were then purified by ITC [45, 46].

### Protein Purification via ELP Coaggregation

The previous ELP fusions all are examples of protein purification in which the ELP is covalently connected to the protein of choice. This approach is suitable for the purification of recombinant proteins that are expressed to high levels, but at very low concentrations of ELP the recovery becomes limited. Therefore this approach is not applicable for proteins expressed at micrograms per liter of bacterial culture, such as toxic proteins and complex multidomain proteins. An adjusted variant of ITC was designed to solve this problem. This variant makes use of coaggregation of free ELPs with ELP fusion proteins. In this coaggregation process, an excess of free ELP is added to a cell lysate to induce the phase transition at low concentrations of



ELP fusion protein (Fig. 9, center). It was shown that picomolar levels of ELP fusion proteins could be purified via ELP coaggregation [47, 48]. The value of this technique was shown by the purification of low levels of ELP fused to an anti-atrazine antibody [49].

### Purification via ELP-Mediated Affinity Capture

The third purification procedure is based on the combination of temperature-triggered aggregation and affinity capture and has been used to not only purify proteins [50–54] but also other molecules [55, 56], and for the removal of pollutants from a solution [57–59]. For this procedure, ELP is conjugated to a capture reagent, which can be done either genetically or chemically. This procedure eliminates the need for cleavage of ELP after purification and introduces the potential to recycle the ELP.

Various purification systems of this type were developed by Chen and coworkers, such as a new plasmid purification method. This system is based on the interaction between a DNA-binding protein and its cognate DNA sequence harbored on the target plasmid. Thus, an ELP is genetically fused to a DNA-binding protein. After binding of the fusion protein to the plasmid via the recognition sequence, the complex can be collected by triggering the inverse phase transition of ELP. Subsequently, the plasmid can be eluted from the DNA-binding protein by heating to  $\sim 60^{\circ}\text{C}$ , after which the ELP-DNA binding protein is removed and recycled via centrifugation to obtain the purified plasmid in solution. A schematic overview of the plasmid purification via temperature-triggered affinity capture is depicted in Fig. 11 [55, 56].

Proteins have been purified in a similar way, for example antibodies. For this purpose, ELPs were combined with antibody-binding domains, such as Protein G, Protein L, or Protein A [50–52, 54]. The antibodies can be bound via the ELP-antibody binding domain fusion and then those complexes can be purified via temperature-triggered precipitation. Also histidine-tagged proteins were purified by temperature-triggered purification. An ELP with repeating sequences of  $[(\text{VPGVG})_2(\text{VPGKG})(\text{VPGVG})_2]_{21}$  was chemically modified by reacting the amino groups of the lysines with imidazole-2-carboxaldehyde to introduce metal-binding ligands. Subsequently, the biopolymer was charged with  $\text{Ni}^{2+}$  to enable binding of histidine-tagged proteins. This combined the advantages of histidine-tag purification with inverse transition cycling [53].

The last example of EMAC also makes use of metal-binding groups, although here they are used to remove heavy metal contaminants. The first report on temperature-triggered removal of cadmium made use of histidine-tagged ELPs, because they strongly bind  $\text{Cd}^{2+}$  [57]. In a later report, ELP was fused to a metal-binding domain, which was shown to bind  $\text{Cd}^{2+}$  more effectively and selectively than the histidine-tagged ELPs [59]. A similar approach was followed with the construction of ELP-MerR, where an ELP was fused to the metalloregulatory protein MerR, which is responsible for regulating expression of the mercury

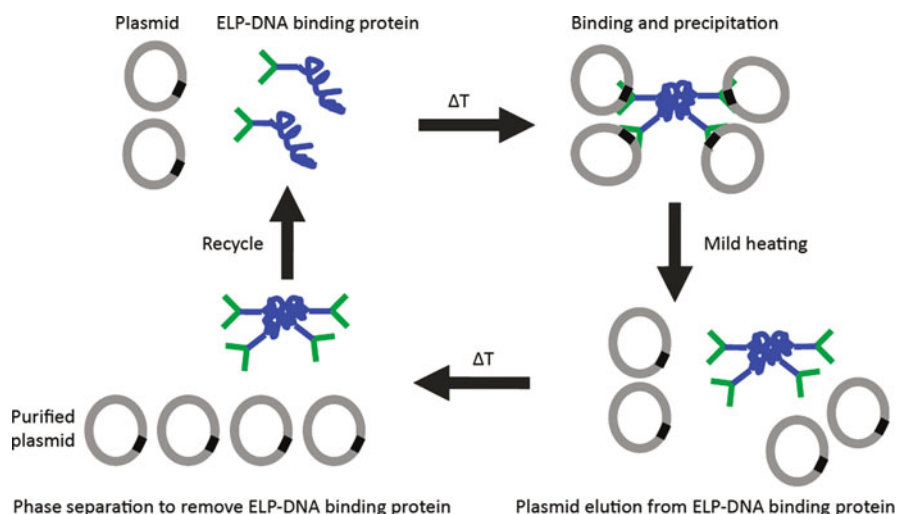


**Fig. 11** Principle of temperature-triggered affinity purification of plasmid DNA. An ELP fused to a DNA binding protein (*ELP-DNA binding protein*) was used to bind a plasmid. The ELP-DNA binding protein–plasmid complex is aggregated by increasing the temperature and is then collected by centrifugation. Subsequently, the plasmid is eluted from the DNA binding protein by mild heating, after which the ELP-DNA binding protein is removed and recycled via centrifugation to obtain the purified plasmid in solution. Adapted from [56] by permission from Macmillan Publishers Ltd: Nature Protocols, copyright 2007

detoxification pathway. This fusion protein was used for specific removal and recycling of mercury [58].

#### 2.4.2 Drug Delivery

Numerous experimental therapeutics have shown potency *in vitro*; however, when they are tested *in vivo*, they often lack significant efficacy. This is often attributed to unfavorable pharmacokinetic properties and systemic toxicity, which limit the maximum tolerated dose. These limitations can be overcome by use of drug carriers. Two general types of carrier systems have been designed: drug conjugation to macromolecular carriers, such as polymers and proteins; and drug encapsulation in nanocarriers, such as liposomes, polymersomes and micelles.

Over the past decades, ELPs have also been applied in drug delivery as both macromolecular carriers and nanocarriers. The ELP-based carrier systems combine the advantages of drug carriers with the properties of ELPs. In addition to these carrier systems, ELP-based drug depots for controlled release have been designed, such as drug releasing gels and drug-eluting films.

ELPs with different transition temperatures have been employed for drug delivery. These can typically be divided into three categories:

1. Soluble ELPs with a  $T_t$  above the body temperature
2. Stimulus-responsive ELPs with a  $T_t$  in the region where phase transition can be triggered in vivo, thus slightly above body temperature
3. Insoluble ELPs with a  $T_t$  below body temperature

This final class of ELPs is used in nanocarriers and in drug depots. In this section, the emphasis will be on systems that have already been tested in vivo, and on some recent promising developments in the area of ELP-assisted drug delivery.

### Macromolecular Carriers

In macromolecular drug delivery systems, drugs are attached to polymeric compounds, such as synthetic polymers [60], dendrimers [61], and antibodies [62], in order to enhance the delivery of the active substance to the diseased tissue and to reduce the toxicity to healthy tissue. The use of macromolecular delivery systems provides several advantages: extension of the half-life of the drug, the ability to introduce targeting moieties into the carrier, the possibility of triggered drug release, and the aforementioned reduced cytotoxicity.

In cancer treatment, passive targeting of macromolecular carriers to tumors is a commonly used approach. This passive targeting is based on the enhanced permeability and retention (EPR) effect, which leads to an accumulation of the high molecular weight carrier in the tumor tissue. The EPR effect arises from the different physiology of tumor vasculature, where the vessel walls are highly porous and lack the tight junctions that are present in healthy tissue. As a result, macromolecular carriers extravasate and accumulate preferentially in tumor tissue relative to normal tissues [63, 64].

All the aforementioned advantages and several additional features apply to ELP-based macromolecular carriers. First, ELP-based carriers are thermally responsive. Second, ELP is a biopolymer and therefore is nontoxic and biodegradable. Third, the gene-based synthesis of ELP allows the creation of genetic fusions with functional peptides and proteins, such as targeting sequences.

Recently, Chilkoti and coworkers showed the effective use of self-assembled ELP-drug conjugates in the treatment of solid tumors in mice. For this purpose, the ELP[VA<sub>8</sub>G<sub>7</sub>-160] with a transition temperature of  $\gg 37^\circ\text{C}$  was equipped with a conjugation site for hydrophobic molecules, for example therapeutics. This conjugation segment consisted of eight cysteine residues, interspersed with diglycine spacers. Doxorubicin (Dox), a hydrophobic and clinically effective drug, was modified with a terminal maleimide via an acid-labile hydrazone linker and then coupled to the thiols of the Cys residues via the maleimide–thiol reaction. This macromolecular carrier spontaneously assembled into micellar nanoparticles of  $\sim 40$  nm diameter (Fig. 12). The half-life, the maximum tolerated dose, and the anti-tumor activity of these nanoparticles in mice were evaluated by administering the drug conjugates systemically. It was found that the ELP-Dox formulation

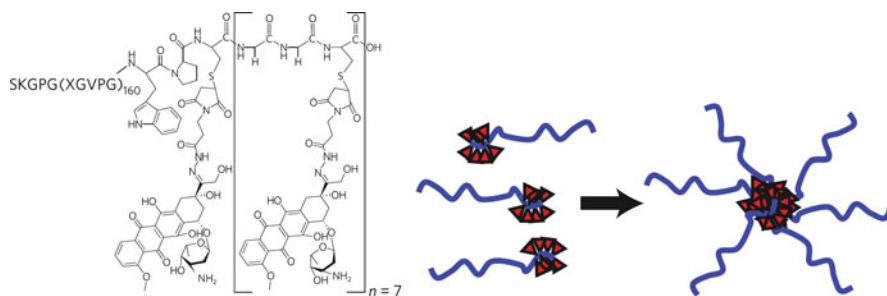


**Fig. 12** *Left*: Structure of ELP[VA<sub>8</sub>G<sub>7</sub>-160] conjugated to doxorubicin via the cysteine residues. *Right*: Self-assembly of ELP-Dox to form nanoparticles. Reprinted from [65] by permission from Macmillan Publishers Ltd: Nature Materials, copyright 2009

allowed a higher dose than the free drug, which is probably caused by the shielding of ELP to limit the toxicity of Dox to healthy tissue. With a single injection, at the maximum tolerated dose, ELP-Dox outperformed the free drug in reducing tumor volume and this led to a substantial increase in animal survival [65].

The previous example of application of ELPs in drug delivery does not exploit their thermal responsiveness. In most other examples, the ELP phase transition is used to target ELP-drug conjugates towards tumors by applying local heating of tissue (local hyperthermia). Chilkoti and coworkers were the first to employ this principle. They developed a method for targeting of intravenously injected ELPs towards solid tumors by local hyperthermia. In addition, mild hyperthermia also enhanced the delivery of drugs to solid tumors, due to the increase of vascular permeability at temperatures between 40°C and 45°C [66]. Two ELPs were synthesized: ELP[V<sub>5</sub>A<sub>2</sub>G<sub>3</sub>-150] with a  $T_t$  of 41°C, which is between the body temperature and the mild hyperthermic temperature; and the control ELP[VA<sub>8</sub>G<sub>7</sub>-160] with a  $T_t$  well above 55°C, which is unresponsive at the mild hyperthermic temperature. These biopolymers were labeled with either rhodamine or with radioactive iodine for *in vivo* fluorescence video-microscopy and radiolabel distribution studies in nude mice with implanted human tumors. Thermal targeting of ELP [V<sub>5</sub>A<sub>2</sub>G<sub>3</sub>-150] led to an increase in tumor localization compared to the control ELP with hyperthermia and to the same polymer without hyperthermia [67, 68]. In these labeling studies, the amines in the ELPs were labeled, but in another study <sup>14</sup>C radiolabels were incorporated into the backbone of both ELPs during protein expression. This was used to minimize the influence of the labeling while studying the biodistribution and pharmacokinetics and to prevent release of the radiolabel [69, 70]. Next, Dox was conjugated to ELP[V<sub>5</sub>A<sub>2</sub>G<sub>3</sub>-150] via an acid-labile hydrazone linker, but this lowered the  $T_t$  to below the body temperature, thus this ELP could not be employed for *in vivo* thermally triggered targeting [71]. In a subsequent study to minimize perturbation of the linker on the phase transition behavior and to provide an efficient and quantitative release of Dox, the chain length and the hydrophobicity of the hydrazone linker were optimized [72]. Also, the targeting of ELP towards the tumor via local hyperthermia was further

optimized by thermal cycling of the tumor. This method relies on heating and cooling cycles of the tumor tissue, whereby the hyperthermia causes an increased vascular concentration of the ELP[V<sub>5</sub>A<sub>2</sub>G<sub>3</sub>-150] aggregates adhering to the vessel walls in the tumor, which upon return to normal temperature leads to an increase in transvascular transport [73]. A recent review by Chilkoti and coworkers gives a comprehensive overview on their efforts in the field of ELP-assisted drug delivery [74].

Generally, the plasma membrane of eukaryotic cells is impermeable to macromolecular carriers. Therefore, Raucher and coworkers improved the ELP-assisted drug delivery by fusing a cell-penetrating peptide (CPP) to the ELP carrier to facilitate its cellular uptake [75, 76]. CPPs are short peptides that are capable of efficiently crossing the cellular plasma membrane and entering the cell's cytoplasm. CPPs have been shown to deliver a variety of cargos across the cell membrane [77]. Various CPPs, such as penetratin (Pen) derived from *Drosophila* transcription factor Antennapedia, the Tat peptide derived from the HIV-1 Tat protein, the hydrophobic membrane translocating sequence (MTS) from the Kaposi fibroblast growth factor, and the cationic Bac peptide derived from the bacteriocin antimicrobial peptide, were fused to the N-terminus of the ELP (for sequences see Fig. 13) [78, 79]. In addition to the use of this system for delivery of Dox, therapeutic peptides were fused to the C-terminus of the CPP-ELP (Fig. 13). This design was examined for a therapeutic peptide that inhibits the oncogenic transcription factor c-Myc [78, 80] and for cell cycle inhibitory peptides [79, 81, 82]. These types of drug delivery systems were shown to be effective in different types of cancer cells, but no *in vivo* studies have yet been reported. However, in a recent review on CPP-ELPs for therapeutic peptide delivery it is mentioned that a Bac-ELP with a therapeutic peptide for inhibition of c-Myc is currently under investigation in mouse breast cancer models and in a rat glioma model [83].

Another approach that also employs the thermal responsiveness of ELPs for drug delivery is the hyperthermia-triggered multivalency. To this end, block copolymers of two ELP regions were synthesized (ELP[VA<sub>8</sub>G<sub>7</sub>-*n*]-ELP[V<sub>5</sub>-*n*]), where one of the blocks had a transition temperature at the hyperthermic temperature of the tumor and the other block was insensitive in this temperature range. The end of the insensitive block was genetically modified with a peptidic ligand that targets a specific cellular receptor or a membrane protein that is upregulated by tumor cells. Normally, the effectiveness of this type of peptide is limited due to its

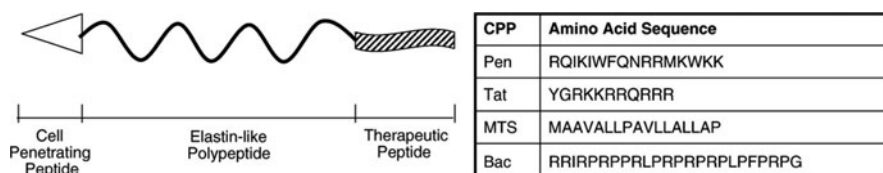


**Fig. 13** *Left:* ELP carrier N-terminally fused to a cell-penetrating peptide and C-terminally fused to a therapeutic peptide. *Right:* Amino acid sequences for several cell-penetrating peptides (see text for details). Reprinted from [83] with permission from Elsevier, copyright 2010

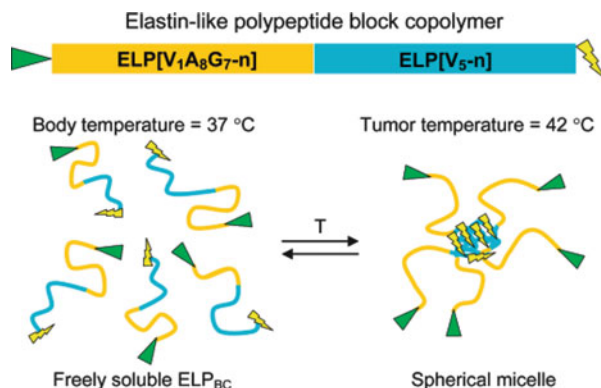


**Fig. 14** Hyperthermia-triggered multivalency. Block copolymers consisting of two ELP blocks, a hydrophilic ELP[VA<sub>8</sub>G<sub>7</sub>-*n*] block and a hydrophobic ELP[V<sub>5</sub>-*n*] block were designed. The N-terminal hydrophilic block was modified with a peptidic ligand (*triangle*) by gene fusion and the design also allows introduction of a drug or imaging agent at the C-terminus (*lightning bolt*). *T* temperature. Reprinted in part from [84] with permission from American Chemical Society, copyright 2008

systemic toxicity; however, in this approach the block copolymer was triggered by the hyperthermia in the tumor to assemble into a drug delivery vehicle displaying multiple ligands. This triggered multivalency is supposed to increase the binding affinity of the ligand-ELP in tumor tissue without increasing the accumulation in healthy tissue. A schematic overview of the design and rationale is given in Fig. 14 [84, 85].

## Nanocarriers

Micellar nanocarriers have already been applied successfully for delivery of hydrophobic drugs [86]. These carriers are usually the product of self-assembled block copolymers, consisting of a hydrophilic block and a hydrophobic block. Generally, an ELP with a transition temperature below body temperature is used as hydrophobic block and the hydrophilic block can be an ELP with a transition temperature above body temperature or another peptide or protein. The EPR effect also directs these types of carriers towards tumor tissue.

In 2000, the first example of ELP diblock copolymers for reversible stimulus-responsive self-assembly of nanoparticles was reported and their potential use in controlled delivery and release was suggested [87]. Later, these type of diblock copolypeptides were also covalently crosslinked through disulfide bond formation after self-assembly into micellar nanoparticles. In addition, the encapsulation of 1-anilinonaphthalene-8-sulfonic acid, a hydrophobic fluorescent dye that fluoresces in hydrophobic environment, was used to investigate the capacity of the micelle for hydrophobic drugs [88]. Fujita et al. replaced the hydrophilic ELP block by a polyaspartic acid chain ( $D_m$ ). They created a set of block copolymers with varying

block lengths, ELP[V- $n$ ]-D $_m$  where  $n = 40, 80, 120,$  or  $160$  and  $m = 22, 44, 88,$  or  $176$ . They investigated the self-assembled structures and they observed the formation of particles with a homogeneous size of 50–250 nm upon triggering the transition [89].

ELP-based triblock copolypeptides have also been used to produce stimulus-responsive micelles, and Chaikof and coworkers envisioned the possible application of these micelles as controlled drug delivery vehicles. These amphiphilic triblock copolymers were constructed from two identical hydrophobic ELP endblocks and a hydrophilic ELP midblock. Below the transition temperature, loose and monodispersed micelles were formed that reversibly contracted upon heating, leading to more compact micelles with a reduced size [90].

Rodríguez-Cabello and coworkers reported a modified elastin-like polypeptide, in which the glycine at the third position of the repetitive sequence was replaced by an alanine residue. These biopolymers consisting of VPAVG repeats also showed a reversible phase transition; however, strong undercooling was needed to resolubilize this ELP [91]. This biopolymer has already been used to encapsulate the model drug dexamethasone phosphate [92]. A recent study uses this type of ELP, (VPAVG) $_{220}$ , to encapsulate bone morphogenetic proteins (BMPs) in ELP-based nanoparticles for drug delivery. BMPs are signaling proteins that are capable of promoting new bone formation, and the developed delivery system was shown to be effective in an *in vitro* cell assay [93].

## Drug Depots

ELP-assisted local delivery of drugs is realized via several strategies. In the first strategy, soluble ELPs are injected and their coacervation is triggered by the body temperature. Here, the drug can be covalently attached to the ELP or it can just be mixed with the ELP. In another approach, crosslinked ELP depots containing a drug can be produced and then implanted to generate a stable release of the drug.

This first strategy was used by Setton and coworkers to trigger the *in situ* formation of an ELP-based drug depot for sustained release. Biodistribution studies of radiolabeled ELPs with a  $T_t$  below body temperature were performed after intrarticular injection in rats [94]. Later, drug depots of ELPs with covalently attached immunomodulator therapeutics [95] and anti-TNF $\alpha$  therapeutics [96] were created. Respectively, ELP[V-120] and ELP[V-60] biopolymers with a transition below body temperature were used in these studies.

The Chilkoti group applied the local injection approach for intratumoral drug delivery. ELP[V-120], with a transition at 27°C, was designed and labeled with  $^{14}\text{C}$ ,  $^{125}\text{I}$  or  $^{131}\text{I}$  for radiotherapy. The first two labels were used to monitor tumor retention of the ELP and the last label was addressed to equip the ELP with anti-tumor activity. It was found that mice treated with  $^{131}\text{I}$ -labeled ELP[V-120] experienced a significantly prolonged survival over those treated with saline [97].

For the second type of drug release from depots, ELPs were crosslinked prior to implantation. In an investigation on the controlled release of the antibiotics

cefazolin and vancomycin, ELP[KV<sub>16</sub>-102] was used. This ELP was crosslinked via the amines on the lysine residues using  $\beta$ -[tris(hydroxymethyl)phosphino]propionic acid (THPP) to enable a high degree of antibiotic entrapment. The functionality of this approach was shown *in vitro* [98]. Another very recent example of this methodology is the production of drug-loaded ELP microspheres, which are crosslinked with glutaraldehyde. The ELP temperature-responsiveness was then used to open and close the pores of these microspheres [99].

In clinical trials using adenoviral vectors for gene delivery, it was shown that selective delivery of sufficient number of therapeutic gene copies remains difficult and that the lack of this selectivity caused acute toxicity and immunogenicity for the healthy tissue. Cappello and Ghandehari applied silk-elastin-like polypeptide (SELPs) [32] hydrogels to overcome the challenges of cancer gene therapy in head and neck cancer [100]. They found that intratumoral injection of adenoviruses with SELPs enhanced gene expression in tumors up to tenfold compared to viral injection without the biopolymer [101–103]. In mouse models, the SELPs efficiently controlled the duration and extent of transfection in tumors for up to 5 weeks with no detectable spread to the liver. This resulted in a fivefold greater reduction in tumor volume compared to intra-tumoral injection of adenoviruses without the biopolymer [104, 105].

### 2.4.3 Tissue Engineering

In the field of tissue engineering, the principles of engineering and life sciences are applied for the development of functional substitutes for damaged tissue. To this end, biomaterials have been used to replace, restore, or enhance organ function. Therefore the material needs to be able to match the characteristics of the tissue it is replacing, such as shape, physical properties, and support in cellular processes [106].

The application of ELPs in tissue engineering is attractive for several reasons: first, ELPs are based on elastin, which is a main component of the extracellular matrix. As a result they are non-immunogenic, biocompatible, and biodegradable [107]. ELPs can furthermore be produced in relatively high yields in host cells, such as bacteria, and this type of polymer synthesis provides control over the exact amino acid sequence and polymer length. ELPs can also easily be purified by exploiting their inverse temperature transition. For these reasons, ELPs were used and modified to form hydrogels, films, and fibers for various tissue engineering applications, such as cartilaginous, vascular, ocular, and liver tissue regeneration.

Setton and Chilkoti applied ELPs as a three-dimensional matrix to entrap chondrocytes. In their study, ELP[V<sub>5</sub>G<sub>3</sub>A<sub>2</sub>-90] with a transition temperature of 35°C at 50 mg/mL in PBS was used. This biopolymer can be used to generate a suspension with cells, which upon injection into a defect site will form a scaffold. They showed that *in vitro* the resulting ELP gel supported the viability of chondrocytes and the synthesis and accumulation of cartilage-specific extracellular matrix material. This suggested that ELPs indeed could be used for *in situ* formation



of a scaffold for cartilaginous tissue repair [108]. Later, they also demonstrated that ELP gels could induce and support chondrocytic differentiation of human adipose-derived adult stem cells in vitro, without the addition of chondrocyte-specific growth factors [109]. Haider et al. [110] also demonstrated the potential of SELPs [32] as scaffold for the encapsulation and chondrogenesis of human mesenchymal stem cells. These SELPs irreversibly form hydrogels upon triggering the transition [110]. One significant problem is that the shear modulus of uncrosslinked ELPs is several orders lower than of articular cartilage. In order to increase the load-bearing capabilities of ELP gels, glutamine- and lysine-containing ELPs that could be enzymatically crosslinked via transglutaminase were developed [111]. Even though the shear modulus was increased and the ability to promote the synthesis and retention of cartilage tissue was retained, the crosslinking reaction proceeded over a long time, which prevented its clinical use. Therefore, a chemical crosslinking method that would proceed within a shorter time was developed. For this method, several lysine-containing ELPs were crosslinked with  $\beta$ -[tris (hydroxymethyl)phosphino]propionic acid (THPP) [112–114]. ELP[V<sub>6</sub>K<sub>1</sub>-224] was then used as an injectable scaffold for cartilage repair in a goat model of an osteochondral defect. It was shown that the ELP crosslinker solution was easily delivered and resulted in a stable, well-integrated gel that supported cell infiltration and matrix synthesis, but unfortunately this gel was prone to rapid degradation [115]. In a recent study, many lysine-containing ELPs were evaluated for their mechanical properties in an effort to optimize the ELP formulation for in vivo application [116].

Tirrell and coworkers designed artificial extracellular matrix (aECM) proteins for small-diameter vascular grafts. For vascular grafts, both mechanical integrity and biological interaction with host tissue are important properties. Therefore, the aECM proteins contained alternating CS5 binding domains and elastin-like polypeptide domains (Fig. 15, aECM 3). The fibronectin CS5 domains provide cell

**aECM 1:**

M-MASMTGGQQMG-HHHHHHHH-DDDDK(LD-YAVTGRGDSPASSKPIA((VPGIG)<sub>2</sub>VPGKG(VPGIG)<sub>2</sub>)<sub>4</sub>VP)<sub>3</sub>-LE

T7 tag His tag Cleavage site RGD cell-binding domain Elastin-like domain

**aECM 2:**

M-MASMTGGQQMG-HHHHHHHH-DDDDK(LD-YAVTGRDGSPPASSKPIA((VPGIG)<sub>2</sub>VPGKG(VPGIG)<sub>2</sub>)<sub>4</sub>VP)<sub>3</sub>-LE

T7 tag His tag Cleavage site Scrambled RGD cell-binding domain Elastin-like domain

**aECM 3:**

M-MASMTGGQQMG-HHHHHHHH-DDDDK(LD-EEIQIGHIPREDVDYHLYPG((VPGIG)<sub>2</sub>VPGKG(VPGIG)<sub>2</sub>)<sub>4</sub>VP)<sub>3</sub>-LE

T7 tag His tag Cleavage site CS5 cell-binding domain Elastin-like domain

**aECM 4:**

M-MASMTGGQQMG-HHHHHHHH-DDDDK(LD-EEIQIGHIPREVDYHLYPG((VPGIG)<sub>2</sub>VPGKG(VPGIG)<sub>2</sub>)<sub>4</sub>VP)<sub>3</sub>-LE

T7 tag His tag Cleavage site Scrambled CS5 cell-binding domain Elastin-like domain

**Fig. 15** Amino acid sequences of artificial extracellular matrix (aECM) proteins. Each protein contains a T7 tag, a histidine tag, a cleavage site, and elastin-like domains with lysine residues for crosslinking. The RGD cell-binding domain is found in aECM 1, whereas aECM 3 contains the CS5 cell-binding domain. aECM 2 and aECM 4 are the negative controls with scrambled binding domains for aECM 1 and aECM 3, respectively. Reprinted from [121] with permission from American Chemical Society, copyright 2004

adhesion signals whereas the ELP domains give these materials elasticity and mechanical integrity. The aECMs also contained lysine residues, either incorporated into the ELP domains or near the C- and N-termini, to allow crosslinking without interrupting the CS5 binding domains [117–119]. It was shown that these crosslinked films of aECMs had properties resembling those of the natural elastin [120]. In another study, aECMs with RGD binding domains were produced (Fig. 15, aECM 1) and compared to the CS5 domains. Here, it was found that the cellular response to aECM proteins can be modulated through choice of binding domain and that those with the RGD sequence showed rapid cell spreading and matrix adhesion [121]. Subsequently, variation in ligand density was accomplished by mixing two aECMs (Fig. 15, aECMs 1 and 2) in different ratios prior to crosslinking. Using this method, cell adhesion and spreading could be modulated [122].

#### 2.4.4 Hybrid Materials

In the previous sections it was demonstrated that the stimulus-responsive behavior of ELP was transferred to ELP fusion proteins and even to non-covalently bound moieties, such as proteins, plasmids, and heavy metals, mostly for biomedical and biotechnological applications. The ability of ELPs to reversibly switch their polarity is also of great interest for the development of stimulus-responsive materials. Many approaches have therefore recently been undertaken to integrate ELPs with, for example, polymers, particles, and surfaces.

In 2003, the van Hest group produced elastin-based side-chain polymers [123]. This research was motivated by the demonstration of the occurrence of an inverse temperature transition in a single repeat of VPGVG [124]. A methacrylate-functionalized VPGVG was synthesized and used as a monomer to perform atom transfer radical polymerization (ATRP) to produce homopolymers (Fig. 16b) or

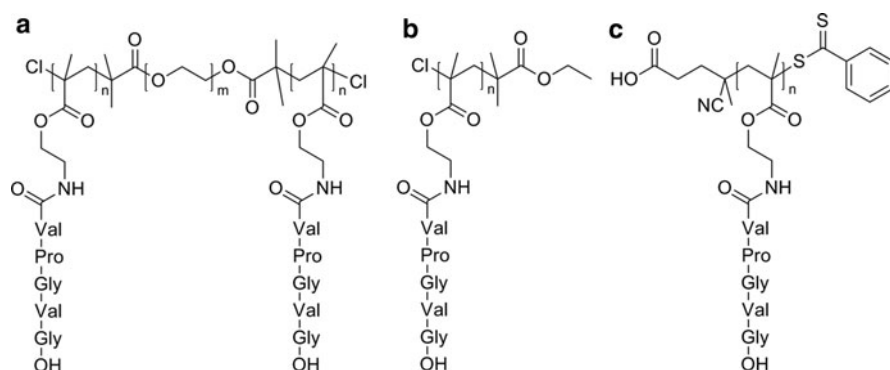


**Fig. 16** Various type of elastin-based side-chain polymers (a) ABA block copolymer produced via ATRP, (b) homopolymer produced via ATRP, (c) homopolymer produced via RAFT polymerization

ABA block copolymers (Fig. 16a), in which the A blocks are based on the methacrylate-functionalized VPGVG and the B block is a bifunctional poly(ethylene glycol) ATRP macroinitiator. It was shown that these polymers exhibited behavior similar to that of linear poly(VPGVG) [123, 125]. Later, Cameron and coworkers used another type of controlled radical polymerization (reversible addition-fragmentation chain transfer polymerization, RAFT) to produce homopolymer elastin-based side-chain polymers (Fig. 16c) [126]. They found that binary mixtures of well-defined elastin-based side-chain polymers showed a single transition temperature, which depended on the blend composition [127]. Additionally, they immobilized these elastin-based side-chain polymers on polymerized high internal phase emulsions (polyHIPE), to demonstrate the potential of this methodology to reversibly immobilize biomolecules such as enzymes [128]. Also ring-opening metathesis polymerization (ROMP) was used to prepare elastin-based oligopeptides of low molecular weight and low polydispersity [129]. More recently, random copolymers of elastin-based monomers and oligo(ethylene glycol)-based monomers were generated using ROMP [130].

Inspired by the elastin-based side-chain polymers, Lemieux et al. prepared elastin-based stimulus-responsive gold nanoparticles. To this end, they capped gold particles with a layer of a single repeat of thiol-functionalized VPGVG peptides (Fig. 17a). These nanoparticles showed LCST behavior, which was modulated by varying the pH of the solution [131].

Besides short ELPS, longer ELPs have also been conjugated to synthetic polymers. In one approach, Cu(I)-catalyzed azide-alkyne cycloaddition click chemistry was applied. For this purpose, ELPs were functionalized with azides or alkynes via incorporation of azidohomoalanine and homopropargyl glycine, respectively, using residue-specific replacement of methionine in ELP via bacterial expression [133]. More recently, an alternative way to site-selectively introduce azides into ELPs was developed. Here, an aqueous diazotransfer reaction was performed directly onto ELP[V<sub>5</sub>L<sub>2</sub>G<sub>3</sub>-90] using imidazole-1-sulfonyl azide [134].

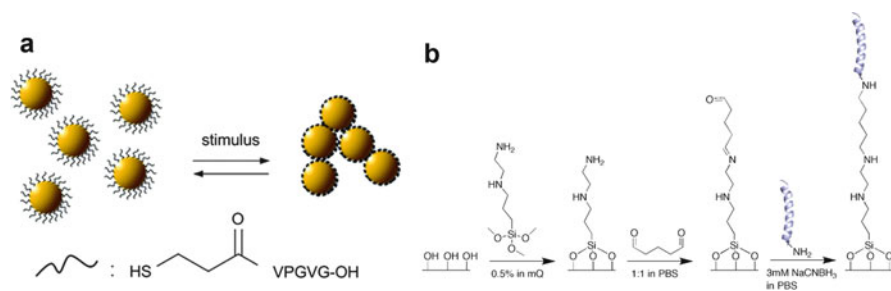


**Fig. 17** (a) Elastin-based stimulus-responsive gold nanoparticles. Reproduced from [131] by permission of The Royal Society of Chemistry (b) Functionalization of a glass surface with ELP. In the first step, the glass surface is aminosilylated with *N*-2-(aminoethyl)-3-aminopropyltrimethoxysilane, then modified with glutaraldehyde. Subsequently, the stimulus-responsive biopolymer is covalently immobilized using reductive amination. Reproduced from [132] by permission of The Royal Society of Chemistry

In another investigation, ELP[V<sub>5</sub>L<sub>2</sub>G<sub>3</sub>-90] with three lysines in the N-terminal region was immobilized on a glass surface in a microreactor to enable temperature-controlled positioning of ELP fusion proteins. For this purpose, the glass surface was first functionalized with *N*-2-(aminoethyl)-3-aminopropyltrimethoxysilane, followed by glutaraldehyde treatment and reductive amination to immobilize the biopolymer on the surface (Fig. 17b) [132].

Hybrid materials of poly(VPGVG)s and gold were also conveniently produced. ELP[V<sub>5</sub>A<sub>2</sub>G<sub>3</sub>-180] was adsorbed onto colloidal gold particles via electrostatic interactions [135]. Subsequently, these ELPs were covalently immobilized on the gold surface, by reacting the amines in the ELP with *N*-hydroxysuccinimide-activated carboxyl groups attached to gold. These stimulus-responsive particles were subsequently used to capture and release biomolecules [136].

Huang et al. were able to synthesize optically responsive hybrid materials. They used the block copolymer ELP[V-40]-ELP[V<sub>4</sub>C<sub>1</sub>-10], which was assembled onto gold nanorods via the thiol-moieties of the cysteine residues. Exposure of the ELP-functionalized gold nanorods to near-infrared light led to heating of the gold due to surface plasmon resonance (SPR). This resulted in phase transition and aggregation of the ELP-functionalized gold nanorods [137]. Also, the group of Rodriguez-Cabello reported similar hybrid materials based on ELP-functionalized gold nanoparticles [138, 139].

## 3 Resilin and Resilin-Like Polypeptides

### 3.1 Resilin Occurrence and Biosynthesis

#### 3.1.1 Occurrence

Resilin was first discovered and brought to the attention of the scientific community by Weis-Fogh in the late 1950s [140, 141]. Through studies into arthropod locomotion, certain proteinaceous patches of the insect cuticle (i.e., exoskeleton) [142] were shown to exhibit perfect long-range elasticity and superior extensibility, supporting rapid deformation in insect organs without hysteresis. The first written descriptions of resilin in 1960 [from tendons of dragonflies (Odonata) and wing hinges of locusts (Orthoptera)] described it as a colorless, swollen isotropic rubber with remarkable elastic recovery and a unique amino acid composition [141]. Resilin did not dissolve in any solvent that did not break peptide bonds and the crosslinks were described as being “extremely stable,” though the chemistry of the crosslinks was unknown at the time. Following the initial discovery and description of resilin in locusts and dragonflies, others quickly began finding the protein throughout the Arthropoda phylum [140].

The solid cuticle of the arthropod is a complex extracellular product made of chitin (a polysaccharide) and tanned or fibrous proteins, and is often hard and

colored [142]. However, in 1947, La Greca identified and described a colorless, transparent cuticle found in the wing hinges of locusts that sharply contrasted with the solid cuticle associated with insects. Later to be named “rubber-like cuticle,” these elastic hyaline structures largely went unnoticed until Weis-Fogh’s investigation of locust flight during the 1950s [141, 143]. Detailed analysis of several elastic elements of the locust flight system revealed small cuticular patches that possessed long-range elasticity; these patches, which consisted of protein and chitin, could undergo extreme deformation before quickly returning to their original shape [144]. Through careful analysis of similar rubber-like cuticle regions prepared from different insect species, it was determined that the protein was responsible for the elastic properties of the cuticle. Further, it was determined that the protein exhibited a unique amino acid composition that differed from other insect cuticle proteins as well as other structural proteins such as collagen and elastin [141, 145]. The protein was named resilin, derived from the latin *resilire*, which means “to spring back” [144, 145].

Resilin is often found in the insect cuticle as part of a relatively simple composite material containing only the protein and chitin [141, 144]. Chitin is found in nearly all types of arthropod cuticle in the form of stiff filaments that run parallel to the surface of the cuticle, but that gradually change direction to form a helicoidal pattern. The resilin-containing cuticle in locust wing-hinge ligament contains the helicoidal chitin structures and makes the ligament difficult to stretch, but capable of bending and twisting deformations [144]. It was determined that the elasticity of the rubber-like cuticle was derived from the resilin protein as the treatment of the cuticle with proteases, strong acids, or bases left only the chitinous component, which was delicate and inextensible [141].

Following the discovery of resilin in the locust and dragonfly [141, 146], resilin was more widely found in other arthropods. Resilin was discovered in the salivary pump of assassin bugs and in the feeding pump of *Rhodnius prolixus* where, in both cases, it acted as an elastic antagonist to muscle action [140, 147]. Other instances of resilin serving the function of an elastic spring in feeding/pumping mechanisms include the tsetse fly [148], reduviid bugs [149], and honey bees [150]. These elastic resilin springs act as an energy-saving mechanism for the insects by providing a passive means of emptying the pump cavities [148, 149]. In the honey bee, resilin was found to provide resistance to the power stroke of the venom-dispensing pump and also served to facilitate the stinging action by providing cushioning for the stinger apparatus [150].

Resilin has also been found to serve an important role in the sound production of arthropods, notably in the Cicadae family, but also in Pyralidae family (moths) and in scorpions [151–157]. Relatively thick patches of resilin (100–150  $\mu\text{m}$ ) are found in the tymbals, which are the sound production organs of the cicada. As seen in the feeding/pumping mechanisms, these elastic patches provide spring-like elasticity that returns the tymbal to its rest position following release of tension in the tymbal muscle. The resilin contained in these structures must operate under very rapid stress-release cycles, in the 1–10 kHz range for some cicadas, but despite these demanding mechanical requirements, it has been found that energy losses can be less than 20% [140, 151, 154, 156, 157].

The elasticity, rapid response, and low energy dissipation serve a particularly important role in the mechanically active tissues responsible for the locomotion of insects. In addition to the description of resilin in the flight systems of the locust and the dragonfly [146], the protein was found to contribute to insect flight in damselflies [158], beetles [159], and other species of the Dermapteran order [160]. Resilin was found in the components of the wing in these insects where it served to provide spring-like recovery of different wing elements following deformation, as well as to dampen the aerodynamic forces felt by the wing [158–160]. Apart from flight, resilin has been found in the ambulatory systems of cockroaches [161, 162] and house flies [163]; resilin provides elasticity to the joints and thereby facilitates rapid movement in both species [161, 162]. Resilin in insect tarsus has been indicated in additional taxa [164], including ants and bees [165]. Perhaps the most notable application of resilin-based rubber-like elasticity in the locomotion of insects is seen in the jumping mechanism of fleas [166–171] and other jumping arthropods [172–176]. Initial investigations of these jumping mechanisms suggested a spring-like model, with resilin serving as the major elastic element responsible for storing the energy required for a jump [169, 171, 174, 176]; however, competing evidence has suggested that the chitinous components are actually responsible for most of the energy storage [168, 173].

The rubber-like elasticity of resilin is only one of its outstanding mechanical properties; it also demonstrates a remarkable capacity for stretching. The extensibility of resilin can be seen in the ability of some insects to swell their abdomens to many times the original size. For example, resilin has been found in the cuticle of the physogastric queen termite, which has been shown to increase the size of its abdomen up to 50 times following fertilization [177]. Honey ants, which swell their abdomens when gorging on food, have also been shown to contain resilin [178]. The one unifying characteristic with respect to the occurrence of resilin in arthropods is that it can almost always be found when rubber-like elasticity is a prerequisite for function. However, resilin also appears in unexpected places such as the lens cuticle of the firefly, *Photinus pyralis* Linnaeus [179], and even outside of the insect community as in the case of the maxilliped flagella of crabs and crayfish [180].

### 3.1.2 Biosynthesis

Interest in the composition of resilin, specifically in its primary structure, grew in the early 1990s when Lombardi and Kaplan published the amino acid sequences of tryptic digests of cockroach resilin [181]. These sequences were found to resemble the tryptic digest sequences of locust resilin investigated by Ardell and Andersen, who subsequently used both sets of sequences to search for genes that may code for resilin in *Drosophila melanogaster*. This effort led to the discovery of two genes that produce peptides homologous to the tryptic digest sequences from both the cockroach and locust [144, 182]. One of the genes, CG15920, was suggested to encode the precursor protein for resilin. The gene product had an amino acid

composition and an isoelectric point that closely resembled resilin [182]. It contained a 17-residue signal peptide sequence at the N-terminus, indicating that it may be secreted into the extracellular space [182, 183], and it contained a sequence that resembled the R&R-2 variant of the Rebers–Riddiford consensus sequence that has been identified in the binding of proteins to chitin in the insect cuticle [182, 184]. Many cuticle proteins from evolutionary disparate species of insect were found to contain some variant of this sequence, G-X<sub>7</sub>-[DEN]-G-X<sub>6</sub>-[FY]-X-A-[DGN]-X<sub>2,3</sub>-G-[FY]-X-[AP] (X is any amino acid and the numerical subscript is the number of residues) [185], leading to the belief that the highly conserved sequence served an important biological function such as the binding to chitin in the cuticle [186]. Subsequent expression and characterization of this domain has provided convincing evidence for its role in binding to chitin [185, 187].

However, the most important indication that the CG15920 gene encoded a resilin precursor was the discovery of highly conserved repeat sequences. These resilin “motif” sequences are repeated in domains on either side of the chitin binding domain (see Fig. 18). The first motif sequence, GGRPSDSYGAPGGGN, is located in the N-terminal region (exon 1) with respect to the chitin binding domain (exon 2), while the second motif sequence, GYSGRPGGQDLG, dominates the C-terminal region (exon 3) of the CG15920 gene product [182]. As discussed in Sect. 3.3, these sequences have provided the basis for the development of recombinant resilin-like polypeptides that attempt to recreate the long-range

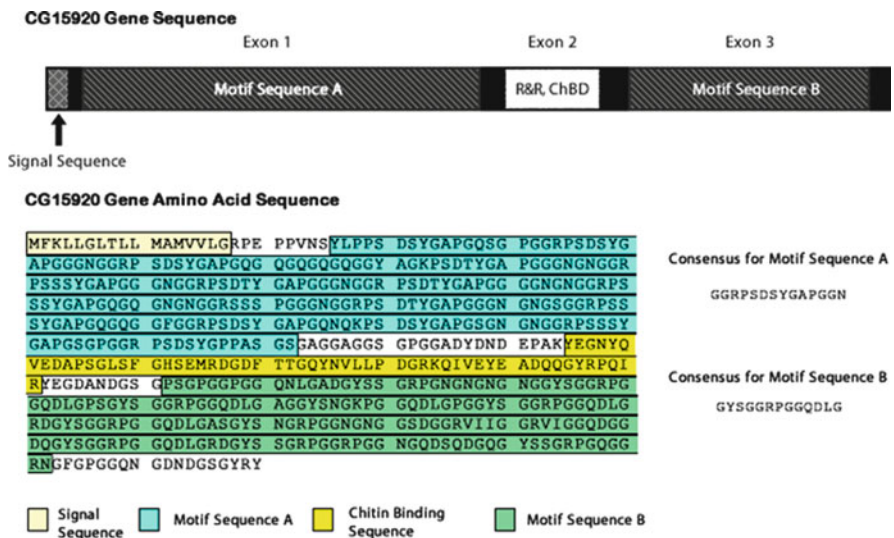


**Fig. 18** CG15920 gene sequence and primary structure. The consensus repeat sequences are also represented. The *highlighted* regions correspond to the signal sequence, R&R chitin-binding domain, and the elastomeric domains containing repeat motifs A and B. Reproduced from [182, 188] with permission from Elsevier, copyright Elsevier 2001, 2010

elasticity of natural resilin. Furthermore, the modules of the CG15920 gene appear to mirror the protein-chitin-protein morphology of the insect cuticle. Additionally, it has been shown that there are two splices of the CG15920 gene: one that contains the chitin binding domain and one where it is absent [182, 187, 188]. It is possible that the synthesis of the two variants depends on whether chitin is being synthesized in the rubber-like cuticle. For instance, the synthesis of chitin-binding resilin may be unregulated during the formation of chitin lamellae while the alternative variant is synthesized primarily to form the embedding proteinaceous matrix. Recent research into putative resilin genes has revealed a high level of conservation for the resilin genes amongst *Drosophila* species, but these putative resilin genes can vary once outside a particular genus of insect [188].

The amino acid composition of resilin was elucidated shortly after its first description and was shown to be unique among other structural proteins found in Nature; a summary of the amino acid sequence is given in Table 1.

Resilin has a greater percentage of acidic residues than collagen, elastin, and silk fibroin and contains fewer non-polar residues (i.e., Gly, Ala, Val, Ile, Leu, Pro, Met, and Phe) than silk fibroin and elastin. The significant content of acidic residues might account for resilin's hydrophilicity as well as its low isoelectric point, as indicated through swelling experiments [141, 145]. Resilin contains little to no

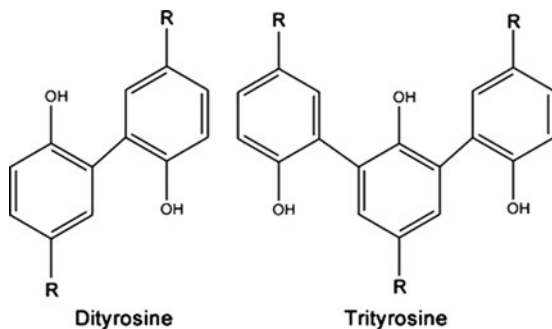
**Table 1** Amino acid composition of resilin from wing-hinge and prealar arm of locust

Amino acid	Resilin		Comparison		
	Residues/10 <sup>5</sup> g protein		Residues/10 <sup>5</sup> g protein		
	Average wing-hinge	Prealar arm	Collagen (ox-hide)	Elastin (ox ligamentum nuchae)	Silk fibroin ( <i>Bombyx mori</i> )
Asp	113	122	52	4.5	16
Thr	35	34	19	8	12
Ser	91	91	41	8	160
Glu	53	54	76	14	14
Pro	87	89	125	156	5
Gly	448	414	354	398	590
Ala	129	120	116	212	389
Val	30	36	21	148	30
Met	Nil	Nil	6.5	(<1)	Nil
iLeu	20	19	14	31	9
Leu	26	27	28	66	7
Tyr	29	35	5	9	69
Phe	30	27	14	30	8
Amide N	(102)	–	(46)	(3)	–
Lys	6	–	27	3	4
His	8.5	–	4.5	0.5	2
Arg	40	–	47	5	6
Total	1,145	1,128	1,063 <sup>a</sup>	1,093	1,321

Results of amino acid analysis performed on resilin from the locust *Schistocerca gregaria*, compared with values for collagen, elastin, and silk fibroin. Reproduced from [145] with permission from Elsevier, copyright Elsevier 1961<sup>a</sup>Includes 106 hydroxyproline and 7 hydroxylysine



**Fig. 19** Dityrosine and trityrosine crosslinks found in resilin. The R groups connect to the backbone of the polypeptide chain



methionine, cysteine, hydroxyproline, and tryptophan. Except for silk fibroin, resilin contains more tyrosine residues than the other structural proteins compared in the Table 1. The levels of tyrosine in the insect cuticle can vary from 4% to 13% (by weight) and in resilin, tyrosine accounts for approximately 5% of the total weight [145, 189, 190].

Andersen demonstrated that two novel fluorescent compounds served as the chemical crosslinks in resilin [189–192]. These aromatic  $\alpha$ -amino acids contained a phenolic group and were shown to be a diaminodicarboxylic acid and a triamino-tricarboxylic acid: dityrosine and trityrosine (see Fig. 19) [192]. Physical measurements determined the average molecular weight between junction points to be  $\sim 5,000$  Da in the case of dragonfly resilin [193], which corresponds closely to the value of  $\sim 3,000$  Da derived from the amino acid analysis, assuming that the fluorescent amino acids constitute the crosslinks in resilin. Other various forms of crosslinking, such as disulphide bridges, ester groups, amide bonds, etc., had been ruled out, leading to the conclusion that these novel fluorescent compounds were indeed the only crosslinks for the network protein [189–192, 194, 195]. The formation of di- and trityrosine or homolog crosslinks was later discovered in other elastic tissues, including those originating from higher organisms. Dityrosine has been isolated from elastin [196], collagen [197], fibroin, keratin [198], and other structural proteins and tissues [199–201]. The crosslinking of the tyrosine residues can result from the phenolic coupling of two phenoxy radicals of the residues [202]; this is initiated by a radical species (i.e.,  $\bullet\text{OH}$ ) and was shown to be mediated, *ex vivo*, by the reaction of a peroxidase and hydrogen peroxide [203].

Additionally, the crosslinking and immobilization of resilin in the insect cuticle appears to occur very quickly, perhaps as soon as it is deposited. Temperature also plays a role; it has been found that the rate and the extent to which resilin is crosslinked increases with increasing temperatures [204–206]. The exact mechanism by which resilin is actually crosslinked is still largely unknown and although peroxidase has been demonstrated to form di- and trityrosines there is no substantiated proof of this mechanism for the formation of the resilin network [144, 207]. The discovery of the resilin gene and interest in the development of recombinant resilins (discussed in Sect. 3.3) may reinvigorate the study of the crosslinking of resilin [144].

### 3.2 *General Properties of Resilin*

Crosslinked resilin is a highly stable, swollen isotropic rubber that is resistant to both high temperatures and protein coagulants. Resilin in neutral water is unaffected by heating up to 125°C and does not begin to degrade until 140–150°C. Additionally, a myriad of fixatives, and tanning and coagulating agents are virtually unsuccessful in bringing about permanent change in resilin from the rubbery state to the solid state, even with prolonged treatment [141]. Only under the most extreme conditions, outside physiological ranges, is the protein irreparably altered; for example, the protein degrades under high or low pH conditions or when incubated with proteases. In fact, resilin is quite easily digested by proteolytic enzymes including papain, various trypsins, chymotrypsin, pepsin, elastase from porcine sources, and the mixture of enzymes found in the saliva of Reduviid bugs [141]. Resilin is transparent and absent of any color; however, the refractive index of resilin cuticle exceeds 1.4 and the water content at neutral pH is 50–60%, which indicates a very concentrated material. Resilin swells in alkaline buffers and shrinks in acidic buffer, but the material remains rubbery under all conditions unless it is dried out or dehydrated in pure alcohol [141]. Dried resilin behaves like a glassy polymer, but when reintroduced to water it regains its rubbery nature and demonstrates all the properties of an amorphous polymer network above its glass transition. Nonpolar solvents have proven completely incapable of penetrating the resilin cuticle; very few polar solvents will plasticize the protein matrix, which is insoluble in all solvents. Resilin will shrink from dehydration in alcohols and also become glassy (as when dried), but the protein will swell and become rubbery in ethylene glycol, formic acid and formamide. Resilin is also capable of isotropic, reversible swelling; resilin can be swollen in alkaline buffer, shrunk in acidic buffer and then swollen once again when returned to an alkaline buffer [141]. In addition to the absolute insolubility of resilin in nonpolar solvents, the protein also proved to be resistant to chaotropic solutes such as urea, guanidine hydrochloride, and alkaline cupric ethylenediamine, the latter of which demonstrated the ability to disrupt hydrogen bonding in silk fibroin without destroying peptide bonds. Additionally, resilin was unaffected by agents that disrupt the disulphide bridges of cystine. The insolubility of resilin under all of these conditions and its remarkable resistance to heat supports the suggestion that the protein exists as a covalently crosslinked network with very chemically stable crosslinks [141, 145].

Resilin and elastin, unlike other structural proteins, fulfill both definitions of an “elastic” material. Colloquially speaking, resilin and elastin are stretchy or flexible. They also fulfill the strict definition of an elastic material, i.e., the ability to deform in proportion to the magnitude of an applied stress without a loss of energy, and the recovery of the material to its original state when that stress is removed. Resilin and elastin are alone in the category of structural proteins (e.g., collagen, silk, etc.) in that they have the correct blend of physical properties that allow the proteins to fulfill both definitions of elasticity. Both proteins have high extensibility and combine that property with remarkable resilience [208].

Resilin from dragonfly tendon is capable of stretching 3–4 times its resting length before breaking and will completely recover even after weeks of an applied tensile stress. The tensile strength was measured to be at least  $30 \text{ kg cm}^{-2}$  (2.94 MPa) and the elastic modulus has been reported to be approximately  $6 \text{ kg cm}^{-2}$  (0.588 MPa) [141, 144, 193], but the initial elastic modulus has been reported to be as high as  $20 \text{ kg cm}^{-2}$  (1.96 MPa) [146, 208]. The toughness and the resilience of dragonfly tendon has been reported to be  $4 \text{ MJ m}^{-3}$  and 92%, respectively [208]. Possibly due to the addition of stiffer elements (i.e., the chitin lamellae), the prealar arm of the wing-hinge of the locust was found to have a slightly higher elastic modulus at  $9 \text{ kg cm}^{-2}$  (0.882 MPa). The mechanical properties of resilin are dependent on pH and on the swelling of the material; resilin swelled in alkaline buffers becomes increasingly stiff. Dynamic testing of the prealar arm revealed that the loss factor, defined as the ratio of energy irreversibly lost as heat to the total change in stored elastic energy, was exceedingly low at about 3.5% per half cycle when strained at biologically relevant frequencies (15–20 cycles/s). Even at high frequencies, such as 200 cycles/s, the loss factor remained less than 10% and, as mentioned previously, the loss factor is low even in the extreme case of cicada sound production [140, 146, 151, 156, 157].

Resilin and elastin have relatively high extensibility and resilience, but as compared to the collagen and the silks, the proteins sacrifice stiffness (elastic modulus) and strength (see Table 2). Collagen and dragline silk are much stiffer materials, but lack the extensibility that is characteristic of the rubber-like proteins. On the other hand, the mussel byssus fibers and the viscid silk have the extensibility of resilin and elastin, but lack the resilience [208].

The most notable physical property of natural resilin is the near-ideal rubber elasticity it exhibits when swollen in water or other polar solvents [141]. Its long-range elasticity, insolubility in various solvents, and chemical stability of the di- and trityrosine crosslinks provided the first indications that resilin might be an ideal network [141, 193, 211]. As mentioned above for elastin, in rubber elasticity theory, the force applied to deform a network is made up of an energetic contribution and an entropic contribution; the entropic contribution accounts for much of the applied force in rubbers and therefore, drives recovery following deformation [211, 212]. In a perfect rubber, energy used to deform the network decreases the entropy of the system; little to no energy is lost in other interactions [144]. Resilin demonstrates remarkable agreement with rubber elasticity theory and, in fact, the agreement between theory and experiment was even closer than that for natural and synthetic rubbers studied at the time of the resilin experiments [193], despite the fact that resilin can undergo a variety of hydrophobic and hydrogen bonding interactions [144, 211]. This agreement suggests that the disappearance and creation of these interactions must be balanced during deformation [144].

Electron microscopy and X-ray diffraction experiments conducted on resilin-containing insect cuticle provided further support for resilin existing in the rubbery state as a crosslinked random network of protein chains. No fine structure was revealed by the electron microscopy experiments and zero crystallinity could be detected from the X-ray diffraction experiments. Furthermore, the diffraction

**Table 2** Material properties of structural proteins and synthetics

Material	Modulus, $E_{\text{init}}$ (GPa)	Strength, $\sigma_{\text{max}}$ (GPa)	Extensibility, $\varepsilon_{\text{max}}$	Toughness (MJ m <sup>-3</sup> )	Resilience (%)
Elastin (bovine ligament) <sup>a</sup>	0.0011	0.002	1.5	1.6	90
Resilin (dragonfly tendon) <sup>a</sup>	0.002	0.004	1.9	4	92
Collagen (mammalian tendon) <sup>a</sup>	1.2	0.12	0.13	6	90
Mussel byssus, distal ( <i>M. californianus</i> ) <sup>a</sup>	0.87	0.075	1.09	45	28
Mussel byssus, proximal ( <i>M. californianus</i> ) <sup>a</sup>	0.016	0.035	2.0	35	53
Dragline silk ( <i>A. diadematus</i> ) <sup>a</sup>	10	1.1	0.3	160	35
Viscid silk ( <i>A. diadematus</i> ) <sup>a</sup>	0.003	0.5	2.7	150	35
Kevlar <sup>a</sup>	130	3.6	0.027	50	–
Carbon fibre <sup>a</sup>	300	4	0.013	25	–
High-tensile steel <sup>a</sup>	200	1.5	0.008	6	–
Poly(glycerol-sebacate) <sup>b</sup>	0.00028	–	2.67	–	–
Poly(PEG-citrate) <sup>b</sup>	0.00191	0.00151	15.05	–	–
Natural rubber <sup>c</sup>	0.002	0.030	9	–	–
Chloroprene rubber <sup>c</sup>	0.003	0.022	10	–	–

Table summarizes the material properties of structural proteins, high performance synthetic materials and synthetic elastomers

<sup>a</sup>Table and material data redrawn from [208] with permission from The Royal Society, copyright 2002

<sup>b</sup>Maximum values presented. Data collected from [209]

<sup>c</sup>Unfilled, vulcanized rubber. Maximum values presented. Data collected from [210]

measurements taken for strained resilin, which might have some microcrystalline structure due to chain alignment, were little changed from the relaxed resilin measurements. The complete lack of any indication of structure from either the microscopy or diffraction experiments supports the conclusion that natural resilin lacks any regular structural pattern [213].

These remarkable mechanical properties thus probably arise owing to the flexibility of the chain, imparted by conserved amino acid sequences. A survey of the amino acid sequences of other elastomeric proteins reveals one often-conserved motif, the proline-glycine dyad. The proline-glycine motif has been found in numerous proteins possessing long range elasticity, including vertebrae elastins, molluscan byssus fibers, high molecular weight glutenin, spider flagelliform silk, and spider dragline silk (see Table 3) [188, 214, 215]. It has been suggested that the conformational features of the proline-glycine dyad, particularly the propensity of the motif to form  $\beta$ -turns, confers elastomeric behavior to these structural proteins [214, 215]. To this end, specific mechanisms have been proposed, though not without controversy, as to how the  $\beta$ -turn structure might bestow long-range

**Table 3** Sequences of repeat motifs of elastomeric domains

Protein	Repeat motif
Abductin	GGFGGMGGGX
Elastin	VPGG VPGVG APGVGV
Byssus	GPGGG
Flagelliform silk	GPGGX
Dragline silk	GPGQQ GPGGY GGYGPGS
HMW subunits of wheat gluten	PGQQQQ GYYPTSPQQ GQQ
Resilin	GGRPSDSYGAPGGGN GYSGGRPGGQDLG

Partially reproduced from [215] with permission from The Royal Society, copyright 2002

elasticity. Studies on the repeat motifs found in elastin indicated that the  $\beta$ -turn structure was the major conformational feature and that elastin might be made up of tandem  $\beta$ -turns, which form a  $\beta$ -spiral structure. The dampening of internal chain dynamics upon the extension of elastin was subsequently proposed for the mechanism of elasticity [216]. The non-crystalline regions of spider silks have also been predicted to contain repetitive proline-glycine  $\beta$ -turn structures and are believed to be responsible for the elasticity of the materials [217, 218]. The repetitive domains of glutenin have demonstrated a propensity to form  $\beta$ -turns and it has been proposed that it forms a  $\beta$ -spiral type similar to elastin. However, it has not been unequivocally established that this is the contributing factor to the material's elasticity [215].

The conservation of proline-glycine repeats in proresilin suggests some form of structural importance, as in other elastomeric proteins [182], but subsequent investigations on resilin-like motifs have provided little evidence for the  $\beta$ -spiral model [219]. More rigorous analysis on an array of resilin-like polypeptides pointed to an equilibrium between folded  $\beta$ -turns and extended structures [220]. This would suggest, in accordance with the historic evidence, that resilin behaves as an entropic spring whereby stretching the material causes the chains to shift to extended conformations and recover via entropically driven recoil. In this light, the role of proline and glycine might not be to impose a particular conformation, and therefore a repeated structure, but as recently discussed by Rausher et al. [221], the true role of these residues in elastomeric proteins might be to disrupt the occurrence of regular structures. Prolines have the tendency to disrupt secondary structure because of their rigid conformation, whereas glycines preclude the formation of secondary structure because they are simply too flexible [220, 221]. However, the one missing element is corroboration from mechanical studies. Structural studies and molecular dynamic investigations, although informative, cannot conclude a direct relationship between structure and function. Additionally, resilin exists as a swollen network and the crosslinking of the resilin sequences into a network may

alter the favored conformational states of the peptide chain. An approach that combines structural studies and mechanical testing on an array of slightly different resilin-like motifs might provide more conclusive evidence for or against a proline-glycine structure–function relationship.

### 3.3 Development and Properties of Recombinant Resilins

As highlighted throughout this volume and in the sections on elastin in this review, progress in recombinant DNA technologies over the past three decades has made the development of biosynthetic protein polymers increasingly simple and promising. These methodologies permit the straightforward design of de novo sequences that endow protein polymers with tailored properties and with applications ranging from medicine to the development of high performance materials [222]. The development of recombinant resilins has likewise benefited from the increasingly facile nature of protein engineering and biosynthetic protein polymer production [182, 187, 219, 223–230]. Following the first description of the *Drosophila* CG15920 gene, Elvin et al. cloned, expressed, and purified the first exon of the gene as a soluble protein in *E. coli*. The authors demonstrated that this soluble protein, rec1-resilin, could be cast into a highly concentrated network by reacting tyrosines using a peroxidase from *Arthomyces ramosus* or through Ru(II)-mediated photo-crosslinking. The initial yields from isopropyl  $\beta$ -D-thiogalactopyranoside (IPTG)-induced expression of the rec1-resilin gene were relatively low at about 15 mg/L culture volume, too low to be useful for many applications especially as gels could only be formed at concentrations greater than 20 wt% [226]. However, improvements in expression have permitted production of relatively pure rec1-resilin at levels as high as 300 mg/L culture volume. Expression was conducted under high cell density fermentation conditions and with a two-step induction method inspired by Studier auto-induction methods [227, 231]. Affinity chromatography was replaced by a facile non-chromatographic “salting-out and heating” method that precipitated rec1-resilin through initial ammonium sulfate precipitation, followed by heating the resolubilized precipitate. The extraordinary heat stability and hydrophilic properties of resilin allowed the protein to remain in solution while other proteins denatured, aggregated, and precipitated [227]. This non-chromatographic purification provides a possible cost-effective pathway to the scaling up of the production of recombinant resilin.

Two new resilin genes based upon the consensus repeat motifs of the *Drosophila* CG15920 gene and from an *Anopheles gambiae* (African malaria mosquito) homolog have also been constructed. The consensus sequences from *Anopheles* (AQTSSQYGAP) contain a slightly different combination of amino acids to the *Drosophila* sequence (GGRPSDSYGAPGGN), with conservation of the YGAP motif. To ensure the fidelity of the final genes, short doubled-stranded oligonucleotides were designed to contain the consensus repeat motifs and were recursively ligated to develop genes containing 2, 4, 8, 16, 32, and 64 copies of the

repeat in tandem. The genes containing 16 repeats (Dros16, from the *Drosophila* gene and An16, from the *Anopheles* gene) were expressed and purified using the non-chromatographic method [228].

Recombinant resilins appear to closely match native resilin in both physical and mechanical properties. Following the crosslinking of the first recombinant resilin, rec1-resilin, Elvin et al. were able to demonstrate the presence of dityrosine as well as the characteristic blue fluorescence [226]; the crosslinking and fluorescence of An16 and Dros16 were confirmed in a following study [229]. As with native resilin, the rec1-resilin, An16, and Dros16 recombinant proteins all demonstrated remarkable resistance to heat [227, 228]. Investigations into the structure of the An16 resilin through Raman spectroscopy, 2D-NMR and small angle X-ray scattering indicated that the protein did not form a consistent secondary structure either in concentrated crosslinked materials or as soluble protein. The results suggest that the An16 resilin is a dynamic and heterogeneous protein with possibly a small degree of order in the YGAP region of the sequence [219]. Later circular dichroism (CD) studies on all three recombinant resilins revealed that An16 and the rec1-resilin were populated with a number of conformations, including  $\beta$ -sheets, turns, and poly (L-proline II) (PPII) structures, but that approximately 60% of the protein was disordered (see Table 4). However, solutions of the An16 and rec1-resilin protein in urea, which tends to stabilize PPII structure, failed to provide any conclusive results as to whether it was a dominant structure in the recombinant resilins. It is possible that the two proteins exchange between PPII and another conformation or that the contribution of the PPII conformation is overestimated by the traditional secondary structure prediction programs employed to deconvolute the CD spectra

**Table 4** Secondary structure analysis: a comparison of resilin-like polypeptides

Resilin-like polypeptide and sequence motif	Technique	Helices (%)	Strands (%)	Turns (%)	Unordered (%) (or random coil)	Beta sheet (%)	PPII (%)
An 16 <sup>a</sup> (AQTPSSQYGAP)	CD	5	–	11	64	10	10
Dros 16 <sup>b</sup> (GGRPSDSYGAPGGGN)	CD	5.3	–	11.8	45.7	27.3	9.9
Rec1 resilin <sup>a</sup> (GGRPSDSYGAPGGGN, but irregular) <sup>c</sup>	CD	2	–	11	58	18	11
Full-length <i>Drosophila</i> Resilin (two motifs) <sup>d</sup>	FTIR	11.9	15.3	29.1	43.8	–	–
	CD	9.8	16.1	17.5	41.6	–	–
Crosslinked <i>Drosophila</i> resilin (two motifs) <sup>d</sup>	FTIR	14.2	19.9	24.4	41.4	–	–
	CD	9.3	15.7	17.9	42.7	–	–

<sup>a</sup>Data reproduced from [229] with permission from The American Chemical Society, copyright 2009

<sup>b</sup>Reported in supplementary material from Lyons et al. [229]

<sup>c</sup>Sequence derived from first exon of CG15920 gene; therefore, it contains irregularities, but consensus repeat GGRPSDSYGAPGGGN

<sup>d</sup>Sequence derived from complete CG15920 gene; contains two consensus repeat motifs: GGRPSDSYGAPGGGN and GYSGGRPGQDLG [187] with permission from The American Chemical Society, copyright 2009

[232]. Interestingly, the CD of Dros16 demonstrated a more ordered protein with more  $\beta$ -structure than the other two resilin-like polypeptides [229].

Perhaps the most important indicator of a successful recombinant resilin is whether its mechanical properties match those of native resilin. In most of the studies, tensile testing and either scanning probe microscopy (SPM) or AFM were utilized to investigate the mechanical properties of crosslinked gels of recombinant resilin. The SPM studies of rec1-resilin, An16, and Dros16 demonstrated that the crosslinked materials had negligible hysteresis and resilience of  $97\pm 3\%$ ,  $98\pm 4\%$  and  $91\pm 5\%$ , respectively. Tensile testing confirmed the resilience as well as provided elastic moduli and strain-to-break values for rec1-resilin and An16. In both cases, the recombinant polypeptides showed good extension-to-break values: up to  $250\pm 43\%$  for rec1-resilin and  $347\pm 61\%$  for An16. The rec1-resilin exhibited the greater modulus of the two, with a modulus at  $26\pm 9$  kPa as compared to the  $5.7\pm 2$  kPa for An16. The degree of crosslinking was only slightly lower in the An16 than in the rec1-resilin; however, An16 has 14.3% dityrosine content and rec1-resilin has 18.8–21% dityrosine content [226, 229].

### 3.4 Applications of Resilin-Like Polypeptides

Multiple applications for resilin-like polypeptides have garnered renewed research interest since the report of the first recombinant resilin in 2005. The excellent mechanical properties of the resilin-like polypeptides has directed investigation toward their use as high-performance materials and in tissue engineering applications. It is widely acknowledged that cells interact and take cues from their microenvironment and, therefore, the development of polymeric scaffolds to mimic the extracellular matrix and drive desired cell or tissue responses has been of wide interest. To this end, our laboratories have developed a modular resilin-like polypeptide (RLP12) (see Fig. 20) that contains not only twelve repeats of the

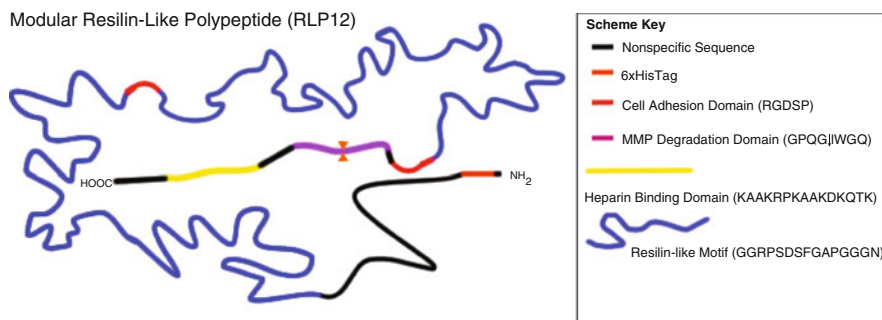


**Fig. 20** Modular resilin-like polypeptide containing domains conferring elastomeric properties, heparin molecule interaction, cell adhesion, and matrix metalloproteinase (MMP) proteolysis. Lysine residues are encoded periodically to permit crosslinking



putative resilin-like motif from the first exon of the *Drosophila* CG15920 gene, but also sequences for cell binding, proteolytic degradation, and heparin immobilization. Additionally, the tyrosine residues in the resilin motif were replaced with phenylalanine to facilitate future studies involving photochemical crosslinking using the non-natural amino acids. The well-characterized cell-binding domain from the tenth type-III domain of fibronectin, RGDSP, was included in several locations along the polypeptide chain. A matrix metalloproteinase sequence, GPQG↓IWGQ, and heparin-interacting domain, KAAKRPKAAKDKQTK, were also included to confer specific degradation and heparin immobilization properties. The heparin immobilization could potentially facilitate the sequestration of growth factors such as vascular endothelial growth factor (VEGF) or basic fibroblast growth factor (bFGF). This construct was expressed using a BL21Star(DE3)/pET28a expression system and Studier auto-induction; the protein was purified using Ni-nitrilotriacetic acid (NTA) chromatography. Structural investigations of the RLP12 using CD and Fourier transform infrared (FTIR) spectroscopy demonstrated that the recombinant protein was largely unordered, but there was evidence for a small population of  $\beta$ -turns [223]. The RLP12 construct has subsequently been recursively ligated to create higher molecular weight polypeptides that might, as they include multiple heparin-binding domains, facilitate the formation of noncovalent networks with heparin. Unlike the other recombinant resilins, the RLP12 is crosslinked through the Mannich-type reaction of lysine side chains with the hydroxyl residues of the THPP ( $\beta$ -[Tris(hydroxymethyl) phosphino] propionic acid) crosslinker. The mechanical properties of 25 wt% gels were analyzed via oscillatory rheology and tensile testing. The oscillatory rheology indicated the storage modulus was approximately 10 kPa, while the tensile testing exhibited a Young's modulus in the 30–60 kPa range and a strain-to-break ratio of 180% [223]. Recently, more thorough analysis of the properties of the RLP12 gels revealed the expected strong dependence of the mechanical properties on the extent of crosslinking and has resulted in materials with storage moduli relevant to soft tissue engineering, but with significantly increased resilience [233].

The modular design of the RLP, containing domains conferring both desired mechanical and biological properties, offers the opportunity to target specific tissues as well as providing a more complex material that better captures salient features of native extracellular matrix. Initial studies using mouse NIH 3T3 fibroblasts provided initial evidence for the adhesion and proliferation of cells on these novel matrices, but more rigorous cell culture studies are necessary [223]. In particular, the culturing of other cell lines such as those found in vocal fold or cardiac tissue; varying gel stiffness; and possibly the culturing of cells with mechanical stimulation would all be important studies to elucidate whether these gels can serve as tissue engineering scaffolds in mechanically demanding applications.

Recently, Qin et al. cloned and expressed the full native resilin protein of *Drosophila* CG15920 gene from cDNA created from RNA extracted from *Drosophila melanogaster* pupa [187]. In addition, the authors cloned two genes encoding only the first exon alone (resilin) and the first two exons (resilin and the chitin-binding domain) into plasmids containing histidine fusion tags for purification purposes. The purified proteins derived from these two genes were used to

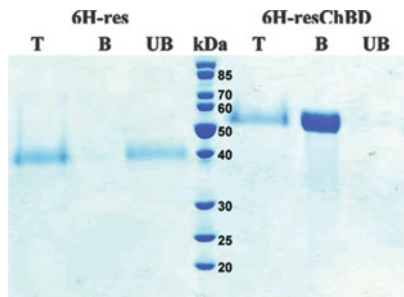


**Fig. 21** Chitin binding of 6×His-tagged resilin with chitin-binding domain (*6 H-resChBD*) as compared to 6×His-tagged resilin without chitin-binding domain (*6 H-res*). *T* total protein after affinity chromatography purification, *B* bound protein eluted from chitin beads, *UB* unbound protein. Reproduced from [187] with permission from The American Chemical Society, copyright 2009

demonstrate the efficacy of the R&R-2 chitin-binding domain. The results demonstrated that the resilin protein containing the domain bound strongly to chitin-coated beads while the resilin lacking the sequence showed no affinity (see Fig. 21). All of the genes were expressed using IPTG induction; the full length resilin was purified via heating and salt precipitation and the His-tagged gene products were purified using Ni-NTA purification. Full-length recombinant resilin, analyzed through FTIR and CD, exhibited the greatest degree of structure, both as soluble protein and in crosslinked gels. Approximately 60% of the protein was reported to adopt either helical, strand, or turn structure [187]. The full-length resilin was also crosslinked into a gel using horseradish peroxidase, and the mechanical properties of the polypeptide were probed via AFM. These constructs demonstrated similarly high resilience to recombinant resilin and other resilin-like polypeptides [187]. Despite modest differences between the recombinant resilins, it appears that they all exist largely in a disordered state, which would be expected from an ideal isotropic rubber.

Another group has looked into incorporating resilin-like sequences into a protein polymer that could be used as a biomaterial or for tissue engineering purposes. Lv et al. designed a *co*-block polypeptide combining resilin-like sequences with folded immunoglobulin-like domains in order to mimic the passive mechanical properties of muscle (see Fig. 22). The giant muscle protein, titin, is a complex molecular spring consisting of a series of immunoglobulin-like domains separated by largely unstructured sequences. Under high stretching forces, the immunoglobulin-like domains can unfold, dissipate energy, and prevent damage due to overstretching. The recombinant proteins produced by the authors mimicked the alternating structure of titin and, through the use of AFM techniques, they demonstrated the unfolding of immunoglobulin-like domains. Furthermore, the titin-mimetic polypeptide could be crosslinked into a hydrated biomaterial through a photochemical  $[\text{Ru}(\text{bpy})_3]^{2+}$  strategy. The resilin-like motifs provided the unstructured region and potential crosslinking sites, but whether the resilin served a mechanically important role is not clear [235].

The rec1-resilin protein has also seen application in other areas. The ability to control the organization of proteins to various surfaces is crucial in many biological

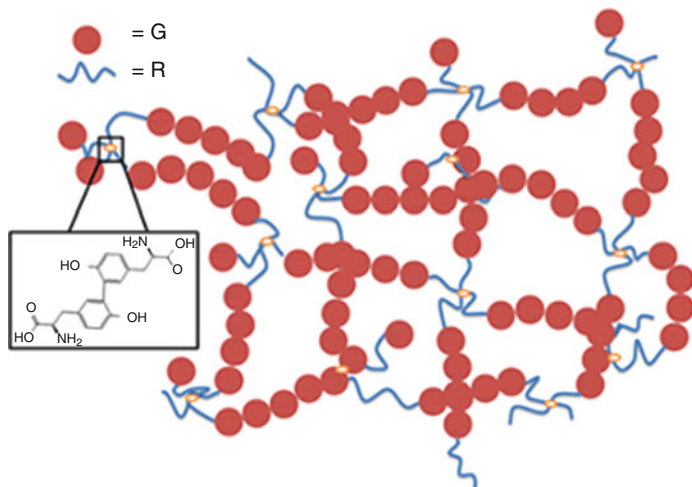
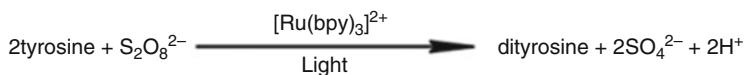


**Fig. 22** Photo-crosslinked titin-mimetic hydrogel, with the *circles* indicating the folded immunoglobulin-like domains and the *wavy lines* indicating the resilin-like domains. Reproduced from [235] with permission from Nature Publishing Group, copyright 2010

applications and in particular, clinical diagnostics [225]. Dutta et al. demonstrated that the assembly, structure, and morphology of adsorbed rec1-resilin could be tuned by altering the physical properties of the substrate surface, specifically by altering the pH and substrate hydrophilicity [225]. Truong et al. investigated the pH-dependent adsorption of rec1-resilin onto gold substrates via SPR and a quartz crystal microbalance with dissipation monitoring (QCM-D) [230]. It was shown that the recombinant resilin adsorbs to the gold substrate with different orientations and conformations, based upon varying electrostatic interactions that are influenced by the pH. The resilin could be induced to form compact or brush-like conformations; furthermore, these changes were completely reversible and fast. The authors attributed these properties to the dual phase transition behavior of rec1-resilin. These resilin-modified surfaces, and their demonstrated pH-responsiveness, could have potential applications in nanobiotechnology as a means to control cell adhesion and migration, or for creating a functional surface for biosensors [230].

## 4 Conclusions

Elastin is a structural protein with outstanding properties, and therefore it has inspired many investigations, with special interest in its elastomeric properties. This behavior can be mimicked with ELPs and these have found wide application in

bioengineering, biomedicine, and nanobiotechnology. It has been shown that the inverse phase transition of ELPs could be transferred to almost any type of material, such as biopolymers, small molecules, synthetic polymers, metals, and inorganic particles. A wide variety of applications for elastin-based polypeptides have been explored.

Similarly, resilin is a remarkable protein with characteristic resilience, high extensibility, and near-perfect rubber elasticity; it has demonstrated ability as an energy-storing material in numerous insect organs. Analysis of resilin gene products across an array of sources has demonstrated that although the resilin sequences can differ widely amongst insects, they maintain their useful mechanical behavior [188]. A small number of resilin-like polypeptides have been reported, with applications directed toward tissue engineering, composites, and surface modification. The development of new sequences will undoubtedly expand the toolbox and applications for biosynthetic resilins and resilin-like polypeptides.

## References

1. Mithieux SM, Weiss AS (2005) Elastin. In: Parry DAD, Squire JM (eds) *Fibrous proteins: coiled-coils, collagen and elastomers*. *Advances in protein chemistry*, vol 70. Elsevier Academic, San Diego, pp 437–461
2. Daamen WF, Veerkamp JH, van Hest JCM, van Kuppevelt TH (2007) *Biomaterials* 28:4378–4398
3. Foster JA, Bruenger E, Gray WR, Sandberg LB (1973) *J Biol Chem* 248:2876–2879
4. Gray WR, Sandberg LB, Foster JA (1973) *Nature* 246:461–466
5. Indik Z, Yeh H, Ornsteingoldstein N, Sheppard P, Anderson N, Rosenbloom JC, Peltonen L, Rosenbloom J (1987) *Proc Natl Acad Sci U S A* 84:5680–5684
6. Chen Z, Shin MH, Moon YJ, Lee SR, Kim YK, Seo JE, Kim JE, Kim KH, Chung JH (2009) *Exp Dermatol* 18:378–386
7. Sato F, Wachi H, Starcher BC, Murata H, Amano S, Tajima S, Seyama Y (2006) *Clin Biochem* 39:746–753
8. Vrhovski B, Weiss AS (1998) *Eur J Biochem* 258:1–18
9. Saunders NA, Grant ME (1984) *Biochem J* 221:393–400
10. Getie M, Schmelzer CEH, Neubert RHH (2005) *Proteins: Structure, Function and Bioinformatics* 61:649–657
11. Uitto J, Hoffmann HP, Prockop DJ (1976) *Arch Biochem Biophys* 173:187–200
12. Hinek A, Rabinovitch M (1994) *J Cell Biol* 126:563–574
13. Mecham RP (1991) *Ann N Y Acad Sci* 624:137–146
14. Rodgers UR, Weiss AS (2005) *Pathologie Biologie* 53:390–398
15. Reiser K, McCormick RJ, Rucker RB (1992) *FASEB J* 6:2439–2449
16. Moroy G, Ostuni A, Pepe A, Tamburro AM, Alix AJP, Hery-Huynh S (2009) *Proteins-Structure Function and Bioinformatics* 76:461–476
17. Senior RM, Griffin GL, Mecham RP, Wrenn DS, Prasad KU, Urry DW (1984) *J Cell Biol* 99:870–874
18. Urry DW, Parker TM (2002) *J Muscle Res Cell Motil* 23:543–559
19. van Hest JCM, Tirrell DA (2001) *Chem Commun* 19:1897–1904
20. Vrhovski B, Jensen S, Weiss AS (1997) *Eur J Biochem* 250:92–98
21. Urry DW, Long MM, Cox BA, Ohnishi T, Mitchell LW, Jacobs M (1974) *Biochim Biophys Acta* 371:597–602

22. Urry DW (1992) *Prog Biophys Mol Biol* 57:23–57
23. Chilkoti A, Dreher MR, Meyer DE (2002) *Adv Drug Deliv Rev* 54:1093–1111
24. Urry DW (1997) *J Phys Chem B* 101:11007–11028
25. Urry DW, Gowda DC, Parker TM, Luan CH, Reid MC, Harris CM, Pattanaik A, Harris RD (1992) *Biopolymers* 32:1243–1250
26. Meyer DE, Chilkoti A (2002) *Biomacromolecules* 3:357–367
27. McPherson DT, Xu J, Urry DW (1996) *Protein Expr Purif* 7:51–57
28. Schipperus R, Teeuwen RLM, Werten MWT, Eggink G, de Wolf FA (2009) *Appl Microbiol Biotechnol* 85:293–301
29. Sallach RE, Conticello VP, Chaikof EL (2009) *Biotechnol Prog* 25:1810–1818
30. Floss DM, Mockey M, Zanello G, Brosson D, Diogon M, Frutos R, Bruel T, Rodrigues V, Garzon E, Chevalere C, Berri M, Salmon H, Conrad U, Dedieu L (2010) *J Biomed Biotechnol* 2010:274346
31. Floss DM, Sack M, Arcalis E, Stadlmann J, Quendler H, Rademacher T, Stoger E, Scheller J, Fischer R, Conrad U (2009) *Plant Biotechnol J* 7:899–913
32. Cappello J, Crissman J, Dorman M, Mikolajczak M, Textor G, Marquet M, Ferrari F (1990) *Biotechnol Prog* 6:198–202
33. Meyer DE, Chilkoti A (1999) *Nat Biotechnol* 17:1112–1115
34. McDaniel JR, MacKay JA, Quiroz FG, Chilkoti A (2010) *Biomacromolecules* 11:944–952
35. Christensen T, Amiram M, Dagher S, Trabbic-Carlson K, Shamji MF, Setton LA, Chilkoti A (2009) *Protein Sci* 18:1377–1387
36. Chen JP, Hoffman AS (1990) *Biomaterials* 11:631–634
37. Chen JP, Yang HJ, Hoffman AS (1990) *Biomaterials* 11:625–630
38. Floss DM, Schallau K, Rose-John S, Conrad U, Scheller J (2010) *Trends Biotechnol* 28:37–45
39. Meyer DE, Trabbic-Carlson K, Chilkoti A (2001) *Biotechnol Prog* 17:720–728
40. Trabbic-Carlson K, Liu L, Kim B, Chilkoti A (2004) *Protein Sci* 13:3274–3284
41. Banki MR, Feng L, Wood DW (2005) *Nat Methods* 2:659–661
42. Ge X, Yang DSC, Trabbic-Carlson K, Kim B, Chilkoti A, Filipe CDM (2005) *J Am Chem Soc* 127:11228–11229
43. Wu WY, Fong BA, Gilles AG, Wood DW (2009) Recombinant protein purification by self-cleaving elastin-like polypeptide fusion tag. *Curr Protoc Prot Sci* 26.4: 21–18
44. Wu WY, Mee C, Califano F, Banki R, Wood DW (2006) *Nat Protoc* 1:2257–2262
45. Hu F, Ke T, Li X, Mao PH, Jin X, Hui FL, Ma XD, Ma LX (2010) *Appl Biochem Biotechnol* 160:2377–2387
46. Shimazu M, Mulchandani A, Chen W (2003) *Biotechnol Bioeng* 81:74–79
47. Ge X, Filipe CDM (2006) *Biomacromolecules* 7:2475–2478
48. Christensen T, Trabbic-Carlson K, Liu W, Chilkoti A (2007) *Anal Biochem* 360:166–168
49. Kim JY, Mulchandani A, Chen W (2003) *Anal Biochem* 322:251–256
50. Gao D, McBean N, Schultz JS, Yan YS, Mulchandani A, Chen WF (2006) *J Am Chem Soc* 128:676–677
51. Kim JY, Mulchandani A, Chen W (2005) *Biotechnol Bioeng* 90:373–379
52. Kim JY, O'Malley S, Mulchandani A, Chen W (2005) *Anal Chem* 77:2318–2322
53. Stiborova H, Kostal J, Mulchandani A, Chen W (2003) *Biotechnol Bioeng* 82:605–611
54. Lao UL, Mulchandani A, Chen W (2006) *J Am Chem Soc* 128:14756–14757
55. Kostal J, Mulchandani A, Chen W (2004) *Biotechnol Bioeng* 85:293–297
56. Lao UL, Kostal J, Mulchandani A, Chen W (2007) *Nat Protoc* 2:1263–1268
57. Kostal J, Mulchandani A, Chen W (2001) *Macromolecules* 34:2257–2261
58. Kostal J, Mulchandani A, Gropp KE, Chen W (2003) *Environ Sci Technol* 37:4457–4462
59. Lao UL, Chen A, Matsumoto MR, Mulchandani A, Chen W (2007) *Biotechnol Bioeng* 98:349–355
60. Pillai O, Panchagnula R (2001) *Curr Opin Chem Biol* 5:447–451
61. Patri AK, Majoros IJ, Baker JR (2002) *Curr Opin Chem Biol* 6:466–471

62. Teicher BA (2009) *Curr Cancer Drug Targets* 9:982–1004
63. Matsumura Y, Maeda H (1986) *Cancer Res* 46:6387–6392
64. Maeda H, Bharate GY, Daruwalla J (2009) *Eur J Pharm Biopharm* 71:409–419
65. MacKay JA, Chen MN, McDaniel JR, Liu WG, Simnick AJ, Chilkoti A (2009) *Nat Mater* 8:993–999
66. Hauck ML, Dewhirst MW, Bigner DD, Zalutsky MR (1997) *Clin Cancer Res* 3:63–70
67. Meyer DE, Kong GA, Dewhirst MW, Zalutsky MR, Chilkoti A (2001) *Cancer Res* 61:1548–1554
68. Meyer DE, Shin BC, Kong GA, Dewhirst MW, Chilkoti A (2001) *J Control Release* 74:213–224
69. Liu W, Dreher MR, Chow DC, Zalutsky MR, Chilkoti A (2006) *J Control Release* 114:184–192
70. Liu WE, Dreher MR, Furgeson DY, Peixoto KV, Yuan H, Zalutsky MR, Chilkoti A (2006) *J Control Release* 116:170–178
71. Dreher MR, Raucher D, Balu N, Colvin OM, Ludeman SM, Chilkoti A (2003) *J Control Release* 91:31–43
72. Furgeson DY, Dreher MR, Chilkoti A (2006) *J Control Release* 110:362–369
73. Dreher MR, Liu WG, Michelich CR, Dewhirst MW, Chilkoti A (2007) *Cancer Res* 67:4418–4424
74. McDaniel JR, Callahan DJ, Chilkoti A (2010) *Adv Drug Deliv Rev* 62:1456–1467
75. Bidwell GL, Davis AN, Fokt I, Priebe W, Raucher D (2007) *Invest New Drugs* 25:313–326
76. Bidwell GL, Fokt I, Priebe W, Raucher D (2007) *Biochem Pharmacol* 73:620–631
77. Tamsamani J, Vidal P (2004) *Drug Discov Today* 9:1012–1019
78. Bidwell GL, Davis AN, Raucher D (2009) *J Control Release* 135:2–10
79. Massodi I, Bidwell GL, Raucher D (2005) *J Control Release* 108:396–408
80. Bidwell GL, Raucher D (2005) *Mol Cancer Ther* 4:1076–1085
81. Massodi I, Moktan S, Rawat A, Bidwell GL, Raucher D (2010) *Int J Cancer* 126:533–544
82. Bidwell GL, Whitton AA, Thomas E, Lyons D, Hebert MD, Raucher D (2010) *Peptides* 31:834–841
83. Bidwell GL, Raucher D (2010) *Adv Drug Deliv Rev* 62:1486–1496
84. Dreher MR, Simnick AJ, Fischer K, Smith RJ, Patel A, Schmidt M, Chilkoti A (2008) *J Am Chem Soc* 130:687–694
85. Simnick AJ, Valencia CA, Liu RH, Chilkoti A (2010) *ACS Nano* 4:2217–2227
86. Torchilin VP (2007) *Pharm Res* 24:1–16
87. Lee TAT, Cooper A, Apkarian RP, Conticello VP (2000) *Adv Mater* 12:1105
88. Kim W, Thevenot J, Ibarboure E, Lecommandoux S, Chaikof EL (2010) *Angew Chem Int Ed* 49:4257–4260
89. Fujita Y, Mie M, Kobatake E (2009) *Biomaterials* 30:3450–3457
90. Sallach RE, Wei M, Biswas N, Conticello VP, Lecommandoux S, Dluhy RA, Chaikof EL (2006) *J Am Chem Soc* 128:12014–12019
91. Reguera J, Lagaron JM, Alonso M, Reboto V, Calvo B, Rodriguez-Cabello JC (2003) *Macromolecules* 36:8470–8476
92. Herrero-Vanrell R, Rincon AC, Alonso M, Reboto V, Molina-Martinez IT, Rodriguez-Cabello JC (2005) *J Control Release* 102:113–122
93. Bessa PC, Machado R, Nurnberger S, Dopler D, Banerjee A, Cunha AM, Rodriguez-Cabello JC, Redl H, van Griensven M, Reis RL, Casal M (2010) *J Control Release* 142:312–318
94. Bette H, Liu W, Zalutsky MR, Chilkoti A, Kraus VB, Setton LA (2006) *J Control Release* 115:175–182
95. Shamji MF, Whitlatch L, Friedman AH, Richardson WJ, Chilkoti A, Setton LA (2008) *Spine* 33:748–754
96. Shamji MF, Chen J, Friedman AH, Richardson WJ, Chilkoti A, Setton LA (2008) *J Control Release* 129:179–186

97. Liu WG, MacKay JA, Dreher MR, Chen MN, McDaniel JR, Simnick AJ, Callahan DJ, Zalutsky MR, Chilkoti A (2010) *J Control Release* 144:2–9
98. Adams SB, Shamji MF, Nettles DL, Hwang P, Setton LA (2009) *J Biomed Mater Res B Appl Biomater* 90B:67–74
99. Na K, Jung J, Lee J, Hyun J (2010) *Langmuir* 26:11165–11169
100. Megeed Z, Haider M, Li DQ, O'Malley BW, Cappello J, Ghandehari H (2004) *J Control Release* 94:433–445
101. Hatefi A, Cappello J, Ghandehari H (2007) *Pharm Res* 24:773–779
102. Greish K, Araki K, Li DQ, O'Malley BW, Dandu R, Frandsen J, Cappello J, Ghandehari H (2009) *Biomacromolecules* 10:2183–2188
103. Gustafson J, Greish K, Frandsen J, Cappello J, Ghandehari H (2009) *J Control Release* 140:256–261
104. Greish K, Frandsen J, Scharff S, Gustafson J, Cappello J, Li DQ, O'Malley BW, Ghandehari H (2010) *J Gene Med* 12:572–579
105. Gustafson JA, Price RA, Greish K, Cappello J, Ghandehari H (2010) *Mol Pharm* 7:1050–1056
106. Langer R, Vacanti JP (1993) *Science* 260:920–926
107. Nettles DL, Chilkoti A, Setton LA (2010) *Adv Drug Deliv Rev* 62:1479–1485
108. Betre H, Setton LA, Meyer DE, Chilkoti A (2002) *Biomacromolecules* 3:910–916
109. Betre H, Ong SR, Guilak F, Chilkoti A, Fermor B, Setton LA (2006) *Biomaterials* 27:91–99
110. Haider M, Cappello J, Ghandehari H, Leong KW (2008) *Pharm Res* 25:692–699
111. McHale MK, Setton LA, Chilkoti A (2005) *Tissue Eng* 11:1768–1779
112. Lim DW, Nettles DL, Setton LA, Chilkoti A (2007) *Biomacromolecules* 8:1463–1470
113. Lim DW, Nettles DL, Setton LA, Chilkoti A (2008) *Biomacromolecules* 9:222–230
114. Trabbic-Carlson K, Setton LA, Chilkoti A (2003) *Biomacromolecules* 4:572–580
115. Nettles DL, Kitaoka K, Hanson NA, Flahiff CM, Mata BA, Hsu EW, Chilkoti A, Setton LA (2008) *Tissue Eng Part A* 14:1133–1140
116. Nettles DL, Haider MA, Chilkoti A, Setton LA (2010) *Tissue Eng Part A* 16:11–20
117. Welsh ER, Tirrell DA (2000) *Biomacromolecules* 1:23–30
118. Heilshorn SC, DiZio KA, Welsh ER, Tirrell DA (2003) *Biomaterials* 24:4245–4252
119. Heilshorn SC, Liu JC, Tirrell DA (2005) *Biomacromolecules* 6:318–323
120. Di Zio K, Tirrell DA (2003) *Macromolecules* 36:1553–1558
121. Liu JC, Heilshorn SC, Tirrell DA (2004) *Biomacromolecules* 5:497–504
122. Liu JC, Tirrell DA (2008) *Biomacromolecules* 9:2984–2988
123. Ayres L, Vos MRJ, Adams PHHM, Shklyarevskiy IO, van Hest JCM (2003) *Macromolecules* 36:5967–5973
124. Reiersen H, Clarke AR, Rees AR (1998) *J Mol Biol* 283:255–264
125. Ayres L, Koch K, Adams PHHM, van Hest JCM (2005) *Macromolecules* 38:1699–1704
126. Fernandez-Trillo F, Dureault A, Bayley JPM, van Hest JCM, Thies JC, Michon T, Weberskirch R, Cameron NR (2007) *Macromolecules* 40:6094–6099
127. Fernandez-Trillo F, van Hest JCM, Thies JC, Michon T, Weberskirch R, Cameron NR (2008) *Chem Commun* 2008:2230–2232
128. Fernandez-Trillo F, van Hest JCM, Thies JC, Michon T, Weberskirch R, Cameron NR (2009) *Adv Mater* 21:55–59
129. Roberts SK, Chilkoti A, Setton LA (2007) *Biomacromolecules* 8:2618–2621
130. Conrad RM, Grubbs RH (2009) *Angew Chem Int Ed* 48:8328–8330
131. Lemieux V, Adams PH, van Hest JCM (2010) *Chem Commun (Camb)* 46:3071–3073
132. Teeuwen RLM, Zuilhof H, de Wolf FA, van Hest JCM (2009) *Soft Matter* 5:2261–2268
133. Teeuwen RLM, van Berkel SS, van Dulmen THH, Schoffelen S, Meeuwissen SA, Zuilhof H, de Wolf FA, van Hest JCM (2009) *Chem Commun* 2009:4022–4024
134. Schoffelen S, van Eldijk MB, Rooijackers B, Raijmakers R, Heck AJR, van Hest JCM (2011) *Chem Sci* 2:701–705
135. Nath N, Chilkoti A (2001) *J Am Chem Soc* 123:8197–8202

136. Hyun J, Lee WK, Nath N, Chilkoti A, Zauscher S (2004) *J Am Chem Soc* 126:7330–7335
137. Huang HC, Korias P, Parker SM, Selby L, Megeed Z, Rege K (2008) *Langmuir* 24:14139–14144
138. Alvarez-Rodriguez R, Alonso M, Girotti A, Reboto V, Rodriguez-Cabello JC (2010) *Eur Polym J* 46:643–650
139. Alvarez-Rodriguez R, Arias FJ, Santos M, Testera AM, Rodriguez-Cabello JC (2010) *Macromol Rapid Commun* 31:568–573
140. Bennet-Clark HC (2007) *J Exp Biol* 210:3879–3881
141. Weis-Fogh T (1960) *J Exp Biol* 37:889–907
142. Moore J, Overhill R (2001) *An introduction to the invertebrates*. Cambridge University Press, Cambridge
143. Anderesen SO, Weis-Fogh T (1964) In: Beament J, Treherne JE, Wigglesworth VB (eds) *Advances in insect physiology*, vol 2. Academic, London, pp 1–65
144. Andersen SO (2003) In: Shewry PR, Tatham AS, Bailey AJ (eds) *Elastomeric proteins: structures, biomechanical properties, and biological roles*. Cambridge University Press, Cambridge, pp 259–278
145. Bailey K, Weis-Fogh T (1961) *Biochim Biophys Acta* 48:452
146. Jensen M, Weis-Fogh T (1962) *Philos Trans R Soc Lond B Biol Sci* 245:137
147. Bennet-Clark HC (1963) *J Exp Biol* 40:223–229
148. Rice MJ (1970) *Nature* 228:1337–1338
149. Edwards HA (1983) *J Exp Biol* 105:407
150. Hermann HR, Willer DE (1986) *Int J Insect Morphol Embryol* 15:107–114
151. Young D, Bennet-Clark HC (1995) *J Exp Biol* 198:1001–1020
152. Skals N, Surlykke A (1999) *J Exp Biol* 202:2937–2949
153. Scott JA (1970) *Pan-Pac Entomol* 46:225
154. Nahirney PC, Forbes JG, Morris HD, Chock SC, Wang K (2006) *FASEB J* 20:2017–2026
155. Govindarajan S, Rajulu GS (1974) *Experientia* 30:908–909
156. Fonseca PJ, Bennet-Clark HC (1998) *J Exp Biol* 201:717–730
157. Bennet-Clark HC (1997) *J Exp Biol* 200:1681–1694
158. Gorb SN (1999) *Naturwissenschaften* 86:552–555
159. Haas F, Gorb S, Blickhan R (2000) *Proc R Soc Lond B Biol Sci* 267:1375–1381
160. Haas F, Gorb S, Wootton RJ (2000) *Arthropod Struct Dev* 29:137–146
161. Frazier SF, Larsen GS, Neff D, Quimby L, Carney M, DiCaprio RA, Zill SN (1999) *J Comp Physiol A* 185:157–172
162. Neff D, Frazier SF, Quimby L, Wang RT, Zill S (2000) *Arthropod Struct Dev* 29:75–83
163. Niederegger S, Gorb S (2003) *J Insect Physiol* 49:611–620
164. Gorb SN (1996) *J Morphol* 230:219–230
165. Federle W, Brainerd EL, McMahon TA, Holldobler B (2001) *Proc Natl Acad Sci U S A* 98:6215–6220
166. Rothschild M, Schlein Y, Parker K, Neville C, Sternber S (1973) *Sci Am* 229:92
167. Rothschild M, Schlein Y, Sternber S, Parker K (1972) *Nature* 239:45
168. Burrows M (2009) *J Exp Biol* 212:2881–2883
169. Bennet-Clark HC, Lucey ECA (1967) *J Exp Biol* 47:59–76
170. Rothschild M, Schlein J (1975) *Philos Trans R Soc Lond B Biol Sci* 271:457
171. Rothschild M, Schlein J, Parker K, Neville C, Sternberg S (1975) *Philos Trans R Soc Lond B Biol Sci* 271:499
172. Bennet-Clark HC (1975) *J Exp Biol* 63:53–83
173. Burrows M, Shaw SR, Sutton GP (2008) *BMC Biol* 6:16
174. Gorb SN (2004) *Arthropod Struct Dev* 33:201–220
175. Burrows M (2010) *J Exp Biol* 213:469–478
176. Alexander RM, Bennet-Clark HC (1977) *Nature* 265:114–117
177. Varman AR (1980) *Experientia* 36:564
178. Varman AR (1981) *Journal of the Georgia Entomological Society* 16:11–13



179. Sannasi A (1970) *Experientia* 26:154
180. Burrows M (2009) *BMC Biol* 7:17
181. Lombardi EC, Kaplan DL (1993) *Mater Res Soc Symp Proc* 292:3–7
182. Ardell DH, Andersen SO (2001) *Insect Biochem Mol Biol* 31:965–970
183. Nielsen H, Engelbrecht J, Brunak S, von Heijne G (1997) *Protein Eng* 10:1–6
184. Rebers JE, Riddiford LM (1988) *J Mol Biol* 203:411–423
185. Rebers JE, Willis JH (2001) *Insect Biochem Mol Biol* 31:1083–1093
186. Andersen SO, Hojrup P, Roepstorff P (1995) *Insect Biochem Mol Biol* 25:153–176
187. Qin GK, Lapidot S, Numata K, Hu X, Meirovitch S, Dekel M, Podoler I, Shoseyov O, Kaplan DL (2009) *Biomacromolecules* 10:3227–3234
188. Andersen SO (2010) *Insect Biochem Mol Biol* 40:541–551
189. Andersen SO (1963) *Biochim Biophys Acta* 69:249
190. Andersen SO (1963) *Acta Chem Scand* 17:869
191. Andersen SO, Kristens B (1963) *Acta Physiol Scand* 59(suppl 213):15
192. Andersen SO (1964) *Biochim Biophys Acta* 93:213–215
193. Weis-Fogh T (1961) *J Mol Biol* 3:648
194. Andersen SO (1966) *Acta Physiol Scand* 66(suppl 263):1–81
195. Andersen SO (1966) *Federation Proc* 25:715
196. LaBella F, Keeley F, Vivian S, Thornhill D (1967) *Biochem Biophys Res Commun* 26:748
197. LaBella F, Waykole P, Queen G (1968) *Biochem Biophys Res Commun* 30:333–338
198. Raven DJ, Earland C, Little M (1971) *Biochim Biophys Acta* 251:96–99
199. Devore DP, Gruebel RJ (1978) *Biochem Biophys Res Commun* 80:993–999
200. Garciacastineiras S, Dillon J, Spector A (1978) *Science* 199:897–899
201. Nomura K, Suzuki N, Matsumoto S (1990) *Biochemistry* 29:4525–4534
202. Gross AJ, Sizer IW (1959) *J Biol Chem* 234:1611–1614
203. Aeschbach R, Amadoè R, Neukom H (1976) *Biochim Biophys Acta Protein Structure* 439:292–301
204. Kristensen BI (1966) *J Insect Physiol* 12:173–176
205. Kristensen BI (1968) *J Insect Physiol* 14:1135–1138
206. Neville AC (1963) *J Insect Physiol* 9:265–272
207. Coles GC (1966) *J Insect Physiol* 12:679
208. Gosline J, Lillie M, Carrington E, Guerette P, Ortlepp C, Savage K (2002) *Philos Trans R Soc Lond B Biol Sci* 357:121–132
209. Amsden B (2007) *Soft Matter* 3:1335–1348
210. Brostow W (2007) In: Mark JE (ed) *Physical properties of polymers handbook*. Springer, New York, pp 443–444
211. Weis-Fogh T (1961) *J Mol Biol* 3:520
212. Rubinstein M, Colby RH (2006) *Polymer physics*. Oxford University Press, Oxford
213. Elliott GF, Huxley AF, Weis-Fogh T (1965) *J Mol Biol* 13:791
214. Kim W, Conticello VP (2007) *Polym Rev* 47:93–119
215. Tatham AS, Shewry PR (2002) *Philos Trans R Soc Lond B Biol Sci* 357:229–234
216. Urry DW, Hugel T, Seitz M, Gaub HE, Sheiba L, Dea J, Xu J, Parker T (2002) *Philos Trans R Soc Lond B Biol Sci* 357:169–184
217. Hayashi CY, Lewis RV (1998) *J Mol Biol* 275:773–784
218. Hayashi CY, Lewis RV (2001) *Bioessays* 23:750–756
219. Nairn KM, Lyons RE, Mulder RJ, Mudie ST, Cookson DJ, Lesieur E, Kim M, Lau D, Scholes FH, Elvin CM (2008) *Biophys J* 95:3358–3365
220. Tamburro AM, Panariello S, Santopietro V, Bracalello A, Bochicchio B, Pepe A (2010) *Chembiochem* 11:83–93
221. Rauscher S, Baud S, Miao M, Keeley FW, Pomes R (2006) *Structure* 14:1667–1676
222. Kiick KL (2007) *Polym Rev* 47:1–7
223. Charati MB, Ifkovits JL, Burdick JA, Linhardt JG, Kiick KL (2009) *Soft Matter* 5:3412–3416

224. Dudek DM, Gosline JM, Michal CA, Depew TA, Elvin C, Kim M, Lyons R, Dumsday G (2009) *Integr Comp Biol* 49:E50
225. Dutta NK, Choudhury NR, Truong MY, Kim M, Elvin CM, Hill AJ (2009) *Biomaterials* 30:4868–4876
226. Elvin CM, Carr AG, Huson MG, Maxwell JM, Pearson RD, Vuocolo T, Liyou NE, Wong DCC, Merritt DJ, Dixon NE (2005) *Nature* 437:999–1002
227. Kim M, Elvin C, Brownlee A, Lyons R (2007) *Protein Expr Purif* 52:230–236
228. Lyons RE, Lesieur E, Kim M, Wong DCC, Huson MG, Nairn KM, Brownlee AG, Pearson RD, Elvin CM (2007) *Protein Eng Des Sel* 20:25–32
229. Lyons RE, Nairn KM, Huson MG, Kim M, Dumsday G, Elvin CM (2009) *Biomacromolecules* 10:3009–3014
230. Truong MY, Dutta NK, Choudhury NR, Kim M, Elvin CM, Hill AJ, Thierry B, Vasilev K (2010) *Biomaterials* 31:4434–4446
231. Studier FW (2005) *Protein Expr Purif* 41:207–234
232. Tamburro AM, Bochicchio B, Pepe A (2003) *Biochemistry* 42:13347–13362
233. Li L, Teller S, Clifton RJ, Jia X, Kiick KL (2011) *Biomacromolecules* 12:2302–2310
234. Chow DC, Dreher K, Trabbic-Carlson, Chilkoti A (2006) *Biotechnol Prog* 22:638–646
235. Lv S, Dudek DM, Cao Y, Balamurali MM, Gosline J, Li HB (2010) *Nature* 465:69–73

# Self-Assembled Polypeptide and Polypeptide Hybrid Vesicles: From Synthesis to Application

Uh-Joo Choe, Victor Z. Sun, James-Kevin Y. Tan, and Daniel T. Kamei

**Abstract** The development of nanoscale drug delivery vehicles is an exciting field due to the ability of these vehicles to improve the pharmacokinetic and pharmacodynamic properties of existing therapeutics. These vehicles can improve drug effectiveness and safety by providing benefits such as increased blood circulation, targeted delivery, and controlled release. With regard to the building blocks, amphiphilic polypeptide and polypeptide hybrid (i.e., a macromolecule comprised of a polypeptide and another type of polymer) systems have been recently investigated for their abilities to self-assemble into vesicles. Advances in synthesis methodologies have allowed the development and characterization of many different amphiphilic polypeptide and polypeptide hybrid systems. In this review, we will discuss these vesicle-forming materials in terms of their synthesis, processing, and characterization. In addition, current efforts to use them for drug delivery purposes will be discussed.

**Keywords** Drug delivery · Encapsulation · Polymer · Polypeptide · Vesicle

## Contents

1	Introduction .....	119
2	Synthesis of Polypeptide Materials .....	121
2.1	Solid-Phase Peptide Synthesis .....	121
2.2	Protein Engineering .....	122
2.3	NCA Polymerization .....	122
3	Vesicle Processing Techniques .....	124
3.1	Direct Dissolution .....	124
3.2	Dual Solvent Method .....	126

4	Characterization of Vesicle Formation and Biocompatibility .....	127
4.1	Microscopy .....	127
4.2	Light Scattering, Polarization, and Zeta Potential .....	127
5	Cytotoxicity, Encapsulation, and Delivery .....	129
6	Concluding Remarks .....	131
	References .....	132

## Abbreviations

3D	Three-dimensional
AFM	Atomic force microscopy
Asp	$\alpha,\beta$ -Aspartic acid
Asp-AP	$\alpha,\beta$ -Aspartamide
CD	Circular dichroism
DLS	Dynamic light scattering
DMF	Dimethylformamide
DMSO	Dimethyl sulfoxide
DOX	Doxorubicin
EPR	Enhanced permeability and retention
HVT	High vacuum technique
ICG	Indocyanine green
K <sub>60</sub> L <sub>20</sub>	Poly(L-lysine) <sub>60</sub> - <i>block</i> -poly(L-leucine) <sub>20</sub>
LSCM	Laser scanning confocal microscopy
MeOH	Methanol
mPEG	Methoxy-poly(ethylene glycol)
NCA	$\alpha$ -Amino acid- <i>N</i> -carboxyanhydride
NCL	Native chemical ligation
NIRF	Near-infrared fluorescence
PAMAM	Polyamidoamine
PBLG	Poly( $\gamma$ -benzyl L-glutamate)
PEG	Poly(ethylene glycol)
PICsome	Polyion complex-based vesicle
PLGA	Poly(L,D-lactic- <i>co</i> -glycolic acid)
PMLG	Poly( $\gamma$ -methyl L-glutamate)
PolyDOX	Doxorubicin-loaded hyaluronan- <i>block</i> -poly( $\gamma$ -benzyl glutamate) vesicle
PSar	Poly(sarcosine)
R <sub>60</sub> L <sub>20</sub>	Poly(L-arginine) <sub>60</sub> - <i>block</i> -poly(L-leucine) <sub>20</sub>
R <sub>G</sub>	Radius of gyration
R <sub>H</sub>	Hydrodynamic radius
SCFC	Subtiligase-catalyzed fragment condensation
SEM	Scanning electronic microscopy
siRNA	Small interfering RNA
SLS	Static light scattering
SPPS	Solid-phase peptide synthesis
TEM	Transmission electron microscopy

TFA	Trifluoroacetic acid
THF	Tetrahydrofuran
TMS	Trimethylsilyl
tRNA	Transfer RNA

## 1 Introduction

Vesicles composed of synthetic lipids (liposomes) or polymers (polymersomes) have been quite successful in delivering drugs both *in vitro* and *in vivo*. These nanoscale drug delivery vehicles have improved current therapeutics by providing benefits such as protection from degradation inside the body, increased circulation time, targeted delivery to decrease toxic side effects, and controlled release of drugs to widen the therapeutic window. Liposomes have been extensively studied for their ability to deliver DNA into cells [1], and two formulations of doxorubicin (DOX) encapsulated in liposomes have been approved for clinical use [2]. DOXIL, an FDA-approved DOX formulation encapsulated in PEGylated liposomes, is currently being used in the treatments of ovarian cancer and Kaposi's sarcoma. Myocet, a non-PEGylated liposomal DOX, is approved in Europe and Canada for the treatment of metastatic breast cancer, in combination with cyclophosphamide. Polymersomes, although still in the research phase, offer certain advantages over liposomes, such as greater chemical diversity with regard to composition and the potential to be more stable and highly functionalized [3]. For example, Discher and coworkers were able to encapsulate both hydrophilic and hydrophobic drugs inside polymersomes and showed enhanced therapeutic efficacy *in vivo* over the drugs in free form [4]. Although delivery of drugs with liposomes and polymersomes have met with some success, there is still room for improvement in the field of drug delivery, especially since many therapeutics, such as small interfering RNA (siRNA), still lack a suitable delivery option [5].

In regards to drug delivery, the investigation of self-assembled vesicles comprised of amino acids is relatively new, but has been gaining popularity. Since the amino acid building blocks are naturally occurring, these vesicles have the potential to be nontoxic and nonimmunogenic. The availability of various natural and synthetic residues also suggests that these materials can be tailored to exhibit a wide variety of chemical properties. In addition, recent advances in polymerization techniques have led to precise control over the length of the polypeptides, leading to more customization and uniformity. Most importantly, polypeptides have an inherent ability to adopt stable secondary structures, which allows them to self-assemble into precisely defined structures, such as vesicles. We are using the term "polypeptide" in this review to refer to polymers consisting of 20 or more amino acids, which is consistent with definitions found in the literature [6–8]. In addition, the term "polypeptide hybrid" is used in this review to refer to a macromolecule comprised of a polypeptide and another type of polymer, where the polypeptide portion plays a role in the formation of the vesicular structures. Accordingly, liposomes or polymersomes conjugated to an oligopeptide (less than 20 amino acids) are not

included in this review. Moreover, although the self-assembly of peptides into vesicles was first reported in 1996 with helical oligopeptides [9] and many studies have been performed using oligopeptide-based vesicles [9–16], this review will not include vesicles formed from oligopeptides.

Historically, after the development of oligopeptide-based vesicles, several groups developed and characterized vesicles using polypeptide hybrid systems consisting of polypeptide and synthetic polymer blocks [17–19]. Soon thereafter, vesicles formed entirely from polypeptides, such as poly(L-lysine)-*b*-poly(L-leucine) and poly(L-lysine)-*b*-poly(L-glutamate), were developed [20, 21]. This review will focus on recent developments in the formation of vesicles composed of polypeptide hybrid or polypeptide systems, as well as the potential promise of these systems as effective drug delivery vehicles. A specific example of a polypeptide-based vesicle is shown in Fig. 1, where the hydrophobic segment is  $\alpha$ -helical and the hydrophilic segment is a random coil.

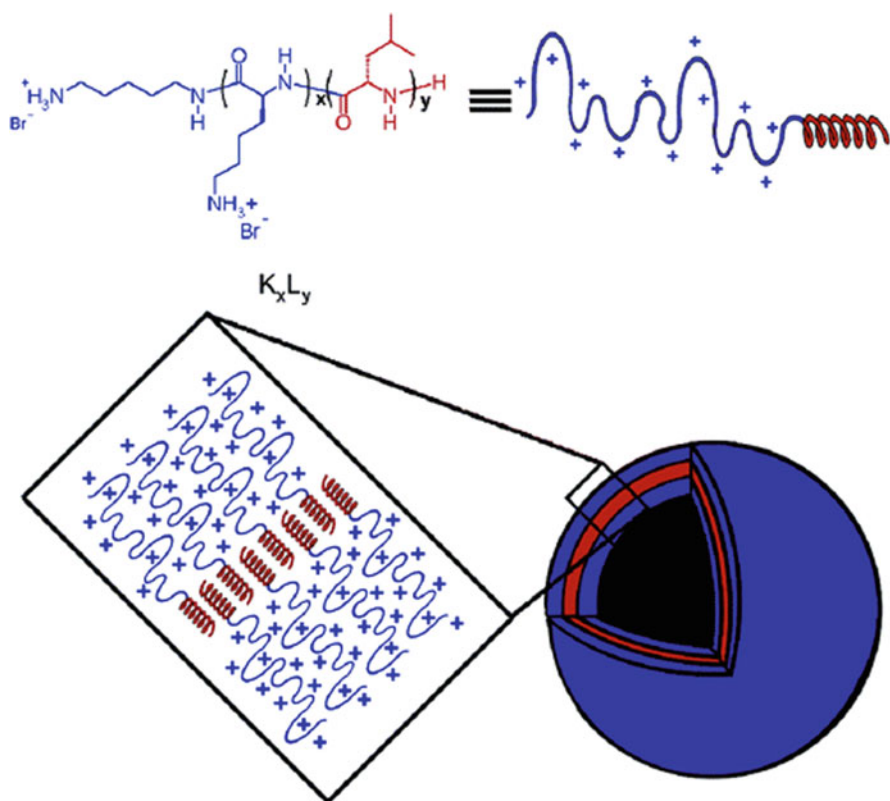


**Fig. 1** Vesicle construct formed from poly(L-lysine)-*b*-poly(L-leucine) polypeptides ( $K_xL_y$ ), where the poly(L-leucine) block corresponds to the  $\alpha$ -helical hydrophobic segments and the poly(L-lysine) block corresponds to the random coil hydrophilic segments. Note that this is one specific example and not all vesicle constructs have  $\alpha$ -helical and random coil blocks. Moreover, the amphiphilic copolymer can be comprised of either a pure block copolypeptide or a macromolecule consisting of a polypeptide and another type of polymer. Adapted from [20] with permission. Copyright 2010 American Chemical Society

## 2 Synthesis of Polypeptide Materials

The preparation of polypeptide and polypeptide hybrid vesicles with predictable properties begins with proper synthesis of a primary structure. This section focuses on three different classes of procedures that are used to synthesize polypeptides. Although conjugation between the polypeptide and non-polypeptide blocks to form polypeptide hybrids is discussed briefly with the third class of synthesis procedures (Sect. 2.3), more detailed information regarding the synthesis and generation of polypeptide hybrid macromolecules are reviewed elsewhere [22–26].

### 2.1 Solid-Phase Peptide Synthesis

Solid-phase peptide synthesis (SPPS) is a useful method for preparing oligopeptides and polypeptides up to approximately 50 amino acid residues in length [26–28]. In this method, an amino acid is covalently linked to a resin (solid bead) and a peptide chain is then assembled onto the amino acid. Once the peptide is synthesized, the peptide chain is cleaved from the resin by a mixture of reagents, one reagent being trifluoroacetic acid (TFA). The main principle behind this process is repeated steps of coupling and deprotection for every amino acid addition. Briefly, a resin-anchored amino acid with a free amine group is coupled to a single amine-protected amino acid, producing a single dipeptide. The protected amine of the new dipeptide is then deprotected, revealing a new free amine, upon which a new amino acid can be added for coupling, and this process continues. Because each amino acid can be added one at a time, primary sequences of oligopeptides and polypeptides can be prepared with precise control. Even though a high yield (~99%) is associated with each amino acid addition step of SPPS, the final yield of the entire polypeptide can become quite low for large amino acid chain lengths (~60% for 50 amino acids compared to ~37% for 100 amino acids) because there is a certain percentage of chains that acquire a defect at each step [26]. Due to this exponential increase in defects with increasing chain length, the concentration of polypeptides containing defects will increase as the number of amino acids increases [29, 30]. Thus, the application of SPPS has been limited to synthesizing long chains of block copolypeptides of ~50 amino acids [31].

Over the past 15 years, selective chemical or enzymatic ligation methods have been developed to address this limitation and combine polypeptides formed by SPPS. One method is the native chemical ligation (NCL) method, where an unprotected synthetic polypeptide segment with a C-terminal  $\alpha$ -thioester is reacted in a chemoselective manner with another unprotected polypeptide segment containing an N-terminal cysteine residue [32]. Because the ligation technique requires a cysteine group at the N-terminus, polypeptides lacking this amino acid at this position will first need to add a cysteine. This addition, however, may disrupt the polypeptide construct. Other methods that improve upon the drawbacks of NCL

are enzymatic ligation techniques, one of them being the subtiligase-catalyzed fragment condensation (SCFC) method. Unlike NCL, SCFC only requires a free N-terminal amino group, which removes the need for an N-terminal cysteine residue [33]. In this case, the enzyme subtiligase is used to catalyze the condensation reaction selectively between an activated polypeptide ester segment and a second polypeptide segment with a free N-terminal amino group, forming the ligation. Thus, polypeptide blocks of approximately 50 amino acids, formed by SPPS, can be ligated by NCL or SCFC to generate even longer polypeptide chains with higher overall yields [31].

## 2.2 Protein Engineering

Recombinant DNA technology can also be used to design genes that encode for proteins with desired features [34]. The gene can be incorporated into a plasmid, which is then used to transform a bacterial host such as *Escherichia coli*. Finally, the production of the desired amino acid polymer is performed by the host with a precisely defined sequence and near absolute monodispersity [29, 35].

An early challenge for protein engineering was the limitation of the polypeptide to the 20 naturally occurring amino acids, making it difficult to incorporate synthetic functional groups such as alkenes and alkynes [36, 37]. However, new molecular biology techniques now allow the incorporation of non-natural amino acids. A thorough review on this topic of incorporating non-natural amino acids in protein engineering can be found in a review by Beatty and Tirrell [38]. Although protein engineering has primarily been used to synthesize oligopeptides for the formation of peptide vesicles [12–14], this approach could be used in the future to synthesize polypeptides.

## 2.3 NCA Polymerization

The most general and frequently used method to synthesize long chains of block copolypeptides for vesicle assembly is successive ring opening polymerizations of  $\alpha$ -amino acid-*N*-carboxyanhydride (NCA) monomers [18, 20, 21, 39–51]. NCA monomers are readily prepared from commercially available amino acids, most commonly through direct phosgenation [52].

The first step of NCA polymerization is usually accomplished by the use of nucleophilic initiators. These initiators can be alkoxides, alcohols, amines, transition metals, and even water [53, 54]. In order to synthesize a copolymer diblock, the polymerization of the second block and its connection to the previously formed block are performed in a single process. This is achieved by initiating the polymerization of the second NCA monomer using the first homopolypeptide as a macroinitiator. Precipitation and purification processes follow to isolate the



block copolypeptides. To synthesize polypeptide hybrids where synthetic polymers are combined with homopolypeptide sequences, typically the synthetic polymer block is first synthesized using controlled polymerization methods, followed by NCA polymerization using the synthetic polymer block as a macroinitiator [18, 55, 56].

Commonly, NCA monomers with ionic functional side chains are initially protected to avoid side reactions. Once polymerization is complete, a deprotection process is used to free these functional groups, such as amine groups from lysine and carboxylic groups from glutamate or aspartate. Other protecting agents exist, but amine groups are typically protected with benzyloxycarbonyl groups and later removed by 33% hydrobromic acid in acetic acid. In contrast, carboxylic groups are generally protected by benzyl groups and removed by potassium hydroxide [57].

Primary amines, which are more nucleophilic than basic, are the most commonly used initiators for the polymerization of NCA monomers. The *n*-hexylamine molecule is a popular choice among several research groups for initiation of polymerization of the first block of the block copolypeptides [21, 41, 43]. Once the first block is synthesized, the primary amine in the N-terminus of this block is used to initiate the synthesis of a new block. Lecommandoux's research group has used this initiator to synthesize block copolypeptides of poly(L-glutamic acid)-*b*-poly(L-lysine) that formed pH-responsive vesicles. Jing and coworkers also used this approach to synthesize poly(L-lysine)-*b*-poly(L-phenylalanine) polypeptides, which also formed vesicles. Kono and coworkers used the primary amine located at the focal point of a polyamidoamine (PAMAM) dendron to initiate the ring-opening polymerization of  $\epsilon$ -benzyloxycarbonyl-L-lysine NCA monomers [49]. The resultant PAMAM dendron-poly(L-lysine) block copolymer formed monodisperse vesicles. In addition, Forster's group used amine-functionalized polybutadiene to initiate synthesis of the polypeptide portion of the polybutadiene-*b*-poly(L-glutamate) polymer, which was also found to self-assemble into stable vesicles [18].

Deming and coworkers used transition metal complex initiators to synthesize a series of poly(L-lysine)-*b*-poly(L-leucine) block copolypeptides, of which the poly(L-lysine)<sub>60</sub>-*b*-poly(L-leucine)<sub>20</sub> (K<sub>60</sub>L<sub>20</sub>) polymer was found to form stable vesicles [20]. Jan's group also employed this method to synthesize the poly(L-lysine)<sub>200</sub>-*b*-poly(L-glycine)<sub>50</sub> block copolypeptide, which also formed vesicles [48]. The sizes of these poly(L-lysine)<sub>200</sub>-*b*-poly(L-glycine)<sub>50</sub> vesicles, irrespective of the vesicle processing method, could be controlled by cycling the pH of the external solution between 7 and 11. Although transition metals can be toxic, cytotoxicity results have demonstrated that polypeptides synthesized with this approach can be purified to remove trace metal ions and are reasonably noncytotoxic after extensive dialysis [44].

Recently, Schlaad and coworkers used amine hydrochloride salts as initiators for NCA polymerization [58]. Huang and Chang also used this method to synthesize the polypeptide segment of the block copolymer poly(*N*-isopropylacrylamide)-*b*-polylysine, which could self-assemble into vesicles [59]. The Hadjichristidis group employed the use of a high vacuum technique (HVT) to allow the use of amine initiators for the living polymerization [34]. Schue's laboratory was also able to significantly reduce the side reactions of the NCA polymerization to only 1% by lowering the reaction temperature to 0 °C [60]. Moreover, Lee and coworkers

demonstrated that, by adding hydrochloric acid to a primary amine initiator, the resulting initiator was able to begin the living polymerization of poly(L-glutamic acid)-*b*-poly(L-phenylalanine). This block copolypeptide was found to self-assemble into pH-responsive vesicles [61]. In addition, Cheng and Lu recently reported a controlled NCA polymerization using *N*-trimethylsilyl (TMS) amines [62, 63]. The researchers demonstrated that this polymerization could be performed with a variety of *N*-TMS amines containing different functional groups, which could be used to further modify the polypeptide.

A unique copolypeptide was also synthesized by Kros and coworkers, who combined a block of poly( $\gamma$ -benzyl L-glutamate) (PBLG) with poly(ethylene glycol) (PEG) through a unique complexation [64]. Specifically, the PBLG block, synthesized through NCA polymerization, was ligated with a coiled-coil peptide sequence (called peptide *E*), which itself was synthesized through SPPS. They then conjugated a hydrophilic peptide sequence (called peptide *K*) to PEG. Upon complexing peptide *E* with the complementary sequence *K*, the PBLG-*E*/*K*-PEG suspension formed vesicles. These researchers also discovered that the PBLG-*E* polypeptides could form vesicles on their own if the polypeptides were initially solubilized by detergent micelles in aqueous buffer, followed by dialysis to dilute the detergent concentration [65]. This process transformed the mixed micelles into vesicles in an aqueous solution. A unique graft polypeptide was also synthesized by Tian's group, whereby a PBLG block was grafted with PEG to create a PBLG-*g*-PEG polymer [66]. By tuning the degree of grafting and the composition of the common solvent, these graft polymers were able to form different structures, such as vesicles, spindle-like micelles, and spherical micelles. This work corresponded to the first time a graft copolymer with the polypeptide as the backbone molecule was able to self-assemble into vesicles.

### 3 Vesicle Processing Techniques

Amphiphilic polypeptides that are synthesized with appropriate ratios of hydrophilic to hydrophobic blocks can form ordered vesicular shapes. Although many polypeptides can self-assemble into vesicles when simply dissolved in the correct solvent, others require more processing steps. This section provides an overview of the techniques that have been developed to process various polypeptide and polypeptide hybrid systems into vesicles.

#### 3.1 *Direct Dissolution*

Many polypeptide-based materials are able to self-assemble into vesicles when directly dissolved into the appropriate solvent. In fact, this method was used to form some of the earliest polypeptide vesicles in the literature. Lecommandoux and

coworkers studied polypeptide and polypeptide hybrid systems that self-assembled into pH-responsive vesicles. They synthesized a series of polypeptide hybrids, including polybutadiene-*b*-poly(L-glutamic acid) and polyisoprene-*b*-poly(L-lysine). When these hybrid macromolecules were directly dissolved in aqueous solution, vesicles were formed that could change size with changes in pH [45, 67, 68]. The group also synthesized vesicles composed of poly(L-glutamic acid)-*b*-poly(L-lysine), which also formed vesicles by direct dissolution and could respond to changes in pH [21, 45, 67].

Recently, Kataoka and coworkers developed a novel micron-sized vesicle with a membrane comprised of polyion complexes, also called a PICSome, using the direct dissolution method [56]. The PICsomes could be formed in aqueous media through self-assembly of oppositely charged block copolymers, using PEG-*b*-poly( $\alpha,\beta$ -aspartic acid) [PEG-poly(Asp)] as the anioner and PEG-*b*-poly((5-aminopentyl)- $\alpha,\beta$ -aspartamide) [PEG-poly(Asp-AP)] as the cationer. Similarly to Lecommandoux's pH-responsive vesicles, these PICsomes could also reversibly respond to changes in pH [69]. Although the PICsomes maintain their vesicular structures at pH 7.4, they dissociate into small particles at or below pH 5.7. Increasing the pH back to 7.4 or above restores the vesicular structures, and this transition is reversible. Interestingly, by simply changing the partner of the PEG-poly(Asp) from PEG-poly(Asp-AP) to the homocationer poly(Asp-AP), the authors showed that this new combination allowed nanometer-sized vesicle formation with controllable sizes ranging from 100 to 400 nm (Fig. 2) [70]. Other groups have also adopted direct dissolution to prepare vesicles from polypeptides (diblock and triblock) and polypeptide hybrids [18, 39, 40, 47, 48, 61, 71].

The advantage of the direct dissolution method is its simplicity. Systems that form vesicles under this method are easily dissolved in aqueous solution, unlike many other systems that form irregular aggregates due to strong hydrophobic interactions. Also, since the aqueous environment is relatively mild, this method

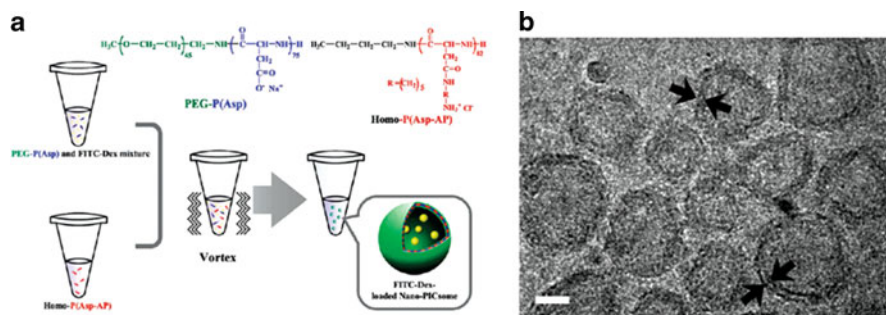


**Fig. 2** PICsomes formed from oppositely charged building blocks. (a) Chemical structures of the hybrid polypeptides for PICsomes and scheme of the PICsome preparation. (b) Cryo-TEM image of 100-nm-sized PICsomes (scale bar: 50 nm). *Arrows* indicate vesicle walls. Adapted from [70] with permission. Copyright 2010 American Chemical Society

allows the encapsulation of biologically active materials, such as proteins and DNA, with a low risk of denaturation. However, this method does not work with all block copolypeptide systems. For instance, when block copolypeptides containing poly(L-leucine) blocks are dissolved in water, hydrogels or aggregates of no particular shape were observed [20]. Solvation in water also usually produces smaller vesicles of 50–200 nm in diameter, although large micron-sized vesicles were reported for poly(L-lysine)-*b*-poly(L-phenylalanine) [43]. Although these vesicles were shown to be stable for up to 2 months, they were found to lose their vesicular structure when relatively low concentrations of sodium chloride (10 mM) were present, making them difficult to be used for *in vivo* applications.

### 3.2 Dual Solvent Method

Researchers studying polypeptide and polypeptide hybrid systems have also processed vesicles using two solvents. This method usually involves a common organic solvent that solubilizes both blocks and an aqueous solvent that solubilizes only the hydrophilic block. The two solvents can be mixed with the polypeptide or polypeptide hybrid system at the same time or added sequentially. The choice of organic solvent depends heavily upon the properties of the polypeptide material, and commonly used solvents include dimethylformamide (DMF) [46, 59], methanol (MeOH) [49], dimethyl sulfoxide (DMSO) [50, 72], and tetrahydrofuran (THF) [44, 55]. Vesicles are usually formed when the organic solvent is slowly replaced with an aqueous solution via dialysis or removed through evaporation; however, some vesicles have been reported to be present in the organic/aqueous mixture [49].

This dual solvent method is suitable for polypeptides with a block that does not dissolve easily in aqueous solution due to being hydrophobic or having a hydrophobic segment. For instance,  $K_{60}L_{20}$  and poly(L-arginine)<sub>60</sub>-*b*-poly(L-leucine)<sub>20</sub> ( $R_{60}L_{20}$ ) block copolypeptides synthesized using transition metal-mediated NCA polymerization were previously assembled into vesicular structures with this method [20, 44]. The poly(L-leucine) block in this material is very difficult to dissolve due to the  $\alpha$ -helical hydrophobic region, which only swells in organic solvents such as THF and DMF. The organic solvents used in this method, however, can be removed with careful and exhaustive dialysis to minimize and remove their cytotoxic effects. In a recent report, Kros and coworkers were able to dissolve poly( $\gamma$ -benzyl L-glutamate)<sub>36</sub>-*b*-E(EIAALEK)<sub>3</sub>-NH<sub>2</sub>, which is a rigid polypeptide, using the surfactant sodium cholate to form micelles. The surfactant was then slowly removed via dialysis to yield vesicles [65]. Since some surfactants are significantly milder than organic solvents, this method represents an approach to direct encapsulation of sensitive biomacromolecules.

## 4 Characterization of Vesicle Formation and Biocompatibility

Many techniques used in other fields have been adapted to visualize and characterize vesicles composed of polypeptide and polypeptide hybrid systems. This section will describe these different approaches.

### 4.1 Microscopy

The most direct way of visualizing vesicle formation is through microscopy. Vesicle sizes typically range from  $10^2$  to  $10^4$  nm, thus electron microscopy techniques provide the best method for visualization. Both scanning electronic microscopy (SEM) and cryo-transmission electron microscopy (TEM) techniques are frequently used to characterize vesicles with diameters as small as 20 nm [40, 56, 64, 73]. Unfortunately, these techniques do not always allow for the best three-dimensional (3D) characterization. For surface and 3D studies, atomic force microscopy (AFM) has been used. However, Jing and coworkers reported that their poly(L-lysine)<sub>53</sub>-*b*-poly(L-phenylalanine)<sub>12</sub> vesicles collapsed upon AFM sample preparation, citing the possible escape of water from the vesicle core [43]. Other groups [55, 74, 75] did not report this problem, but in those instances, longer hydrophobic chains were used that may have prevented water from leaving.

Laser scanning confocal microscopy (LSCM) can also be a useful tool in characterizing the vesicle shape and interior, whether by labeling the polypeptides themselves via conjugation of a fluorescent dye or by encapsulating a fluorescent molecule inside of the vesicles [20, 39, 43, 44, 47, 48]. This method is particularly beneficial when a biologically relevant molecule is being delivered because the fluorescence can be visualized within live cells for a qualitative measure of uptake efficiency and endocytic trafficking [44, 50]. Although LSCM does not have as high a resolution as SEM or TEM, the advantage of LSCM is its ability to filter out unfocused signal, thus allowing the distinction between cellular uptake and mere association with the cellular membrane. This is particularly important if the cargo delivered within the vesicles has no way of entering the cell on its own. Specifically, Deming and coworkers used LSCM to visualize the delivery of a hydrophilic cargo, Texas-Red-labeled dextran, by a polypeptide vesicle that had the ability to enter cells (Fig. 3).

### 4.2 Light Scattering, Polarization, and Zeta Potential

Scattering experiments can be performed to help determine the size and shape of the vesicles without the need for the extensive sample preparation required for electron microscopy and AFM. Dynamic (DLS) and static light scattering (SLS) are widely used to determine the size and possible shape of vesicle systems [40, 42, 48, 49, 51,

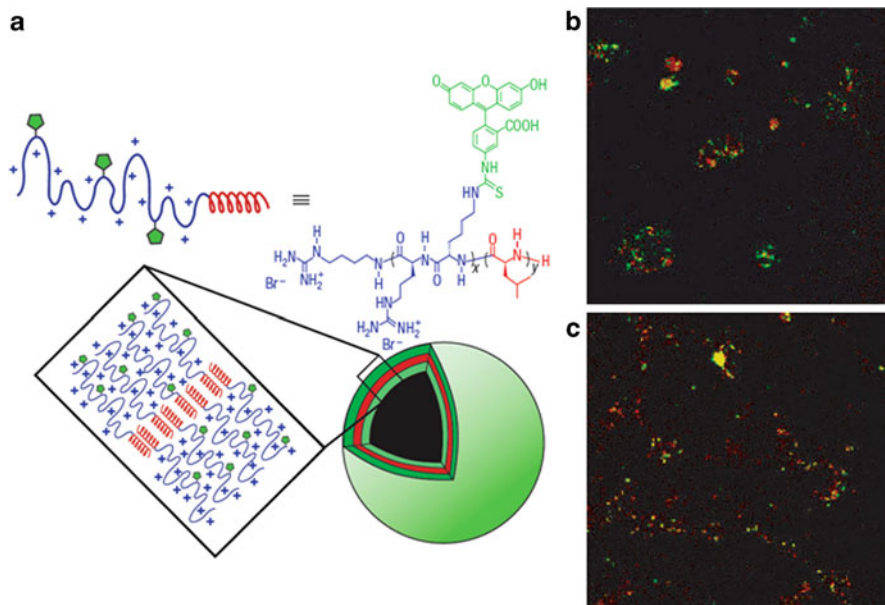


**Fig. 3** Polypeptide vesicle with endocytosis capability. (a) Vesicles formed from poly(L-arginine)<sub>60</sub>-*b*-poly(L-leucine)<sub>20</sub>. The poly(L-arginine) block provides an added cell-penetrating feature to the vesicles. (b, c) LCSM images of internalized vesicles (*green*) containing Texas-Red-labeled dextran (*red*) in (b) epithelial and (c) endothelial cells. Colocalization of the vesicles and Texas-Red-labeled dextran appears as a *yellow* fluorescent signal. Adapted from [44] with permission. Copyright 2007 Macmillan Publishers

56, 61, 64, 72, 73, 75, 76]. DLS and SLS experiments provide the hydrodynamic ( $R_H$ ) and gyrosopic ( $R_G$ ) radii of the vesicles, respectively. A linear angular dependence of  $R_H$  implies a spherical shape, and if the value for  $R_H$  is greater than a few times the predicted polypeptide length, a hollow spherical shape indicative of a vesicle can be assumed. Further confirmation can be obtained by noting the  $R_G/R_H$  ratio. Hollow spheres will have a ratio close to 1, whereas uniform spheres (micellar-like structures) and random coil conformations have ratios close to 0.774 and 1.50, respectively [77]. Small-angle neutron or X-ray scattering experiments can also be performed to further characterize the vesicles [67, 72].

Circular dichroism (CD) experiments can provide valuable data pertaining to the conformation of the peptides within the vesicles [48, 49, 51, 64, 75, 78]. It is common for hydrophobic or uncharged hydrophilic blocks to form  $\alpha$ -helical conformations in aqueous solution, whereas charged hydrophilic blocks tend to form random coils. CD is especially useful for the study of stimuli-responsive vesicles in which a change in polypeptide conformation is caused by the stimulus. Lecommandoux and coworkers, for example, have demonstrated that both blocks of their poly(L-glutamic acid)-*b*-poly(L-lysine) vesicles undergo a change from an  $\alpha$ -helical to a random coil conformation with a change in pH [45, 67]. CD was also

employed to observe pH-triggered structural shifts in other diblock and triblock polypeptide and polypeptide hybrid systems [40, 42, 47].

Measuring the zeta potential of the polypeptide or polypeptide hybrid vesicle has recently been widely used to characterize the surface charge of the vesicle [64]. The zeta potential describes the electrostatic potential near the surface of the particle. Higher absolute values of the zeta potential confer better particle stability because the particles will resist aggregation. Particles with zeta potentials ranging from +40 to +60 (or -40 to -60) mV are accepted as having good colloidal stability, whereas particles with zeta potentials ranging from +30 to +40 (or -30 to -40) mV are moderately stable. Lastly, particles with zeta potentials with absolute values lower than 30 mV will start showing instability, i.e., the particles will begin to coagulate. For example, Lee's group synthesized a poly(L-glutamic acid)-*b*-poly(L-phenylalanine) block copolypeptide that self-assembled into vesicles [61]. These vesicles were found to have negative zeta potentials below -30 mV at pH 7, which indicated moderate stability and ionization of the glutamate block. However, when the surrounding pH was dropped to pH 4, the zeta potential values ranged between -10 and -12 mV, indicating that the glutamate amino acids were being protonated. The resulting neutral amino acids therefore decreased the electrostatic repulsions between the vesicles, which were previously providing colloidal stability.

## 5 Cytotoxicity, Encapsulation, and Delivery

Although the field is still relatively new and only a handful of groups have started investigating polypeptide and polypeptide hybrid vesicles for drug delivery, there has been an increase in recent reports demonstrating that these vesicles are able to encapsulate biologically relevant molecules and deliver them to cells and animals, without causing toxicity towards cells and tissues. In this section, we will discuss the progress made in this area.

Kataoka's group was able to encapsulate myoglobin inside the hydrophilic core of their PICsomes [79]. In the same study, they showed that the 100 nm PICsomes have a long in vivo circulation time in the bloodstream of mice, comparable to typical long-lived liposomes and polymersomes. More recently, Lecommandoux's group encapsulated DOX into their hyaluronan-*b*-poly( $\gamma$ -benzyl glutamate) vesicle system to take advantage of hyaluronan's ability to bind to CD44 for cancer targeting [50] (Fig. 4). When administered intravenously into a mouse model for cancer, the encapsulated DOX had better tumor shrinking properties due to the combined effects of controlled release, targeting ability of hyaluronan, and the enhanced permeability and retention (EPR) effect of the vesicles [80]. They also showed that the empty vesicles were nontoxic using in vitro cytotoxicity assays, where 90% of the cells were viable at copolymer concentrations up to 650  $\mu\text{g/mL}$ . In addition to DOX, Lecommandoux's group was able to encapsulate docetaxel, a hydrophobic anticancer drug, into the hydrophobic membrane of the same

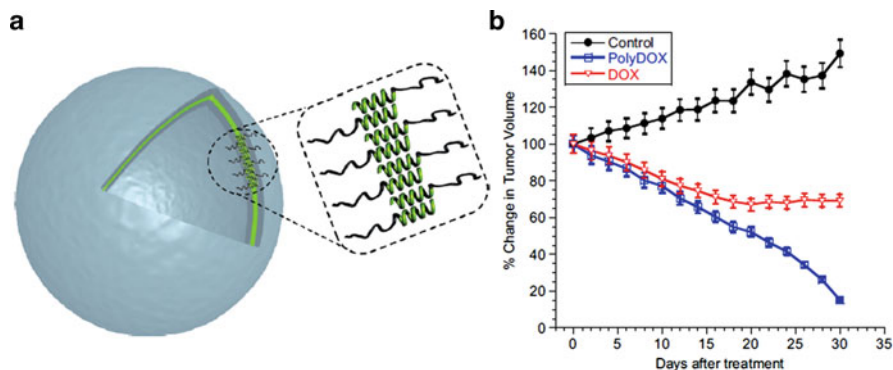


**Fig. 4** Polypeptide hybrid vesicle that was used to load DOX. (a) Representation of the hyaluronan-*b*-poly( $\gamma$ -benzyl glutamate) vesicle. Adapted from [50] with permission. Copyright 2009 American Chemical Society. (b) Tumor regression data after administration of free DOX and DOX-loaded hyaluronan-*b*-poly( $\gamma$ -benzyl glutamate) vesicles (*PolyDOX*). Reprinted from [80] with permission. Copyright 2010 Elsevier

vesicles, showing the versatility of these vesicles in loading different drugs [81]. Compared to free docetaxel, these docetaxel-loaded vesicles showed high *in vitro* cytotoxicity, especially towards cells that express high levels of CD44 receptors, demonstrating the vesicle's ability to target the receptor.

Uchegbu and coworkers have studied the complexation and delivery of DNA using a unique poly(amino acid)-based polymer vesicle. A polymer of either poly(L-lysine) or poly(L-ornithine) was functionalized with methoxy-poly(ethylene glycol) (mPEG) and hydrophobic palmitic acid chains to synthesize an amphiphilic triblock of either mPEG-*b*-poly(L-lysine)-*b*-palmitoyl or mPEG-*b*-poly(L-ornithine)-*b*-palmitoyl. Vesicles formed from these polymers were complexed with DNA and showed improved transfection *in vitro* over poly(amino acid) complexed with DNA or DNA alone [82].

Pure polypeptide vesicles have also been used for encapsulation and delivery of biologically relevant material, but with limited success. Kimura's group has reported the encapsulation of fluorescein isothiocyanate (FITC)-labeled dextran within their vesicles formed from a copolymer composed of poly(sarcosine) (PSar) and poly( $\gamma$ -methyl-L-glutamate) (PMLG) (Fig. 5) [41]. Sarcosine is an amino acid found in muscle and can be degraded to glycine by sarcosine dehydrogenase. They also labeled their vesicles with the near-infrared fluorescence (NIRF) probe, indocyanine green (ICG) [41], and showed that the labeled vesicles are retained within mouse tumors due to the EPR effect [83] of tumor vasculature.

The Jing group investigated their poly(L-lysine)-*b*-poly(L-phenylalanine) vesicles for the development of synthetic blood, since PEG-lipid vesicles were previously used to encapsulate hemoglobin to protect it from oxidation and to increase circulation time. They extended this concept and demonstrated that functional hemoglobin could be encapsulated into their vesicles. The same polypeptide material was also used to complex DNA, which caused the vesicles to lose their



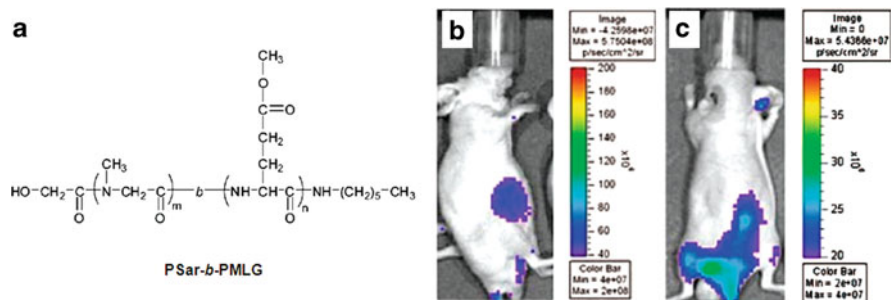


**Fig. 5** Polypeptide vesicles demonstrate the ability to utilize the EPR effect. (a) Chemical structure of the amphiphilic block polypeptide PSar-*b*-PMLG. (b) Fluorescence image using fluorescently labeled PEG. Fluorescence is not observed in the cancer site although accumulation is observed in the bladder. (c) Fluorescence image using ICG-labeled vesicles, showing evidence of vesicle accumulation due to the EPR effect. Adapted from [41] with permission. Copyright 2008 American Chemical Society

spherical shape and form irregular aggregates of less than  $2\ \mu\text{m}$  [43]. Encapsulation of DNA inside polypeptide vesicles has also been reported by Hadjichristidis's group [74]. Moreover, Deming and coworkers were able to employ poly(L-arginine) as both a structural component of the  $R_{60}L_{20}$  vesicles and as a cell-penetrating moiety to transport Texas-Red-labeled dextran into both endothelial and epithelial cell cultures (Fig. 3) [44]. The vesicles were also shown to be relatively noncytotoxic to T84 and HULEC-5A cells. The endocytosis mechanism and intracellular trafficking pathway of these vesicles were further investigated [84]. Macropinocytosis was found to be the dominant mechanism for endocytosis. Immunostaining experiments demonstrated that the vesicles enter early endosomes but not lysosomes, suggesting that they recycle back to the cell surface. This last finding suggests that incorporating a mechanism for endosomal disruption into the polypeptide vesicles would improve their release into the cytoplasm.

## 6 Concluding Remarks

The field of polypeptide and polypeptide hybrid vesicles is steadily growing. Using polypeptides to form vesicles is vastly interesting, since the vesicles are stable, can be tailored to incorporate a variety of functions, and have the potential to exhibit good biocompatibility. The aqueous core of vesicles also allows isolation of the interior environment from the bulk solution, which if combined with proper release mechanisms could greatly enhance the delivery of hydrophilic therapeutics. The delivery of therapeutics with these systems are just starting to emerge, demonstrating the potential for this new class of materials as effective drug carriers.

**Acknowledgments** The authors would like to thank the support of the Department of Defense Prostate Cancer Research Program under award number W81XWH-09-1-0584, the National Science Foundation DMR 0907453, and the UCLA Specialized Program of Research Excellence in Prostate Cancer P50 CA092131-08.

## References

1. Felgner PL, Ringold GM (1989) *Nature* 337:387
2. Leonard RC, Williams S, Tulpule A, Levine AM, Oliveros S (2009) *Breast* 18:218
3. Discher DE, Ahmed F (2006) *Annu Rev Biomed Eng* 8:323
4. Ahmed F, Pakunlu RI, Brannan A, Bates F, Minko T, Discher DE (2006) *J Control Release* 116:150
5. Nguyen T, Menocal EM, Harborth J, Fruehauf JH (2008) *Curr Opin Mol Ther* 10:158
6. Garrett R, Grisham CM (2010) *Biochemistry*. Thomson Brooks/Cole, Belmont
7. Thornton JM, Barlow DJ (1991) In: Hider RC, Barlow DJ (eds) *Polypeptide and protein drugs*. Ellis Horwood, Chichester, p 9
8. Lodish HF (2008) *Molecular cell biology*. W.H. Freeman, New York
9. Imanishi Y, Fujii K, Miura Y, Kimura S (1996) *Supramol Sci* 3:13
10. Fujita K, Kimura S, Imanishi Y, Rump E, Ringsdorf H (1997) *Adv Biophys* 34:127
11. Kimura S, Muraji Y, Sugiyama J, Fujita K, Imanishi Y (2000) *J Colloid Interface Sci* 222:265
12. van Hell AJ, Costa CI, Flesch FM, Sutter M, Jiskoot W, Crommelin DJ, Hennink WE, Mastrobattista E (2007) *Biomacromolecules* 8:2753
13. van Hell AJ, Crommelin DJ, Hennink WE, Mastrobattista E (2009) *Pharm Res* 26:2186
14. van Hell AJ, Fretz MM, Crommelin DJ, Hennink WE, Mastrobattista E (2010) *J Control Release* 141:347
15. Samyn P, Ruhe J, Biesalski M (2010) *Langmuir* 26:8573
16. Nishikawa H, Morita T, Sugiyama J, Kimura S (2004) *J Colloid Interface Sci* 280:506
17. Caillol S, Lecommandoux S, Mingotaud AF, Schappacher M, Soum A, Bryson N, Meyrueix R (2003) *Macromolecules* 36:1118
18. Kukula H, Schlaad H, Antonietti M, Forster S (2002) *J Am Chem Soc* 124:1658
19. Gebhardt KE, Ahn S, Venkatachalam G, Savin DA (2008) *J Colloid Interface Sci* 317:70
20. Holowka EP, Pochan DJ, Deming TJ (2005) *J Am Chem Soc* 127:12423
21. Rodriguez-Hernandez J, Lecommandoux S (2005) *J Am Chem Soc* 127:2026
22. Robson Marsden H, Kros A (2009) *Macromol Biosci* 9:939
23. Gauthier MA, Klok HA (2008) *Chem Commun (Camb)* 2008: 2591
24. Koeller KM, Wong CH (2000) *Chem Rev* 100:4465
25. Seeberger PH, Haase WC (2000) *Chem Rev* 100:4349
26. Lutz JF, Borner HG (2008) *Prog Polym Sci* 33:1
27. Chan WC, White PD (2000) *Fmoc solid phase peptide synthesis: a practical approach*. Oxford University Press, New York
28. Kent SB (1988) *Annu Rev Biochem* 57:957
29. Klok HA (2002) *Angew Chem Int Ed Engl* 41:1509
30. Plaque S, Muller S, Briand JP, Van Regenmortel MH (1990) *Biologicals* 18:147
31. Dawson PE, Kent SB (2000) *Annu Rev Biochem* 69:923
32. Muir TW, Dawson PE, Kent SB (1997) *Meth Enzymol* 289:266
33. Braisted AC, Judice JK, Wells JA (1997) *Meth Enzymol* 289:298
34. Aliferis T, Iatrou H, Hadjichristidis N (2004) *Biomacromolecules* 5:1653
35. Lowik DWPM, Ayres L, Smeenk JM, Van Hest JCM (2006) *Peptide Hybrid Polym* 202:19
36. Noren CJ, Anthonycahill SJ, Griffith MC, Schultz PG (1989) *Science* 244:182
37. van Hest JC, Tirrel DA (2001) *Chem Commun (Camb)* 2001(19):1897

38. Beatty KE, Tirrell DA (2009) In: Kohrer C, RajBhandary UL (eds) *Nucleic acids and molecular biology*. Springer, Berlin, p 127
39. Sun J, Huang Y, Shi Q, Chen X, Jing X (2009) *Langmuir* 25:13726
40. Tian Z, Li H, Wang M, Zhang AY, Feng ZG (2008) *J Polym Sci A Polym Chem* 46:1042
41. Tanisaka H, Kizaka-Kondoh S, Makino A, Tanaka S, Hiraoka M, Kimura S (2008) *Bioconjug Chem* 19:109
42. Cai QJ, Chan-Park MB, Lu ZS, Li CM, Ong BS (2008) *Langmuir* 24:11889
43. Sun J, Chen X, Deng C, Yu H, Xie Z, Jing X (2007) *Langmuir* 23:8308
44. Holowka EP, Sun VZ, Kamei DT, Deming TJ (2007) Polyarginine segments in block copolypeptides drive both vesicular assembly and intracellular delivery. *Nat Mater* 6:52
45. Checot F, Rodriguez-Hernandez J, Gnanou Y, Lecommandoux S (2007) *Biomol Eng* 24:81
46. Yang ZG, Yuan JJ, Cheng SY (2005) *Eur Polym J* 41:267
47. Bellomo EG, Wyrsta MD, Pakstis L, Pochan DJ, Deming TJ (2004) *Nat Mater* 3:244
48. Gaspard J, Silas JA, Shantz DF, Jan JS (2010) *Supramol Chem* 22:178
49. Harada A, Nakanishi K, Ichimura S, Kojima C, Kono K (2009) *J Polym Sci A Polym Chem* 47:1217
50. Upadhyay KK, Le Meins JF, Misra A, Voisin P, Bouchaud V, Ibarboure E, Schatz C, Lecommandoux S (2009) *Biomacromolecules* 10:2802
51. Sigel R, Losik M, Schlaad H (2007) *Langmuir* 23:7196
52. Lagrille O, Danger G, Boiteau L, Rossi JC, Taillades J (2009) *Amino Acids* 36:341
53. Kricheldorf HR (1987)  $\alpha$ -Amino acid N-carboxyanhydrides and related heterocycles. Springer, Berlin
54. Blout ER, Karlson RH (1956) *J Am Chem Soc* 78:941
55. Le Hellaye M, Fortin N, Guilloteau J, Soum A, Lecommandoux S, Guillaume SM (2008) *Biomacromolecules* 9:1924
56. Koide A, Kishimura A, Osada K, Jang WD, Yamasaki Y, Kataoka K (2006) *J Am Chem Soc* 128:5988
57. Greene TW, Wuts PGM (1999) *Protective groups in organic synthesis*. Wiley, New York
58. Dimitrov I, Schlaad H (2003) *Chem Commun (Camb)* 2003:2944
59. Huang CJ, Chang FC (2008) *Macromolecules* 41:7041
60. Vayaboury W, Giani O, Cottet H, Deratani A, Schue F (2004) *Macromol Rapid Commun* 25:1221
61. Kim MS, Dayananda K, Choi EY, Park HJ, Kim JS, Lee DS (2009) *Polymer* 50:2252
62. Lu H, Cheng J (2007) *J Am Chem Soc* 129:14114
63. Lu H, Cheng J (2008) *J Am Chem Soc* 130:12562
64. Marsden HR, Handgraaf JW, Nudelman F, Sommerdijk NAJM, Kros A (2010) *J Am Chem Soc* 132:2370
65. Marsden HR, Quer CB, Sanchez EY, Gabrielli L, Jiskoot W, Kros A (2010) *Biomacromolecules* 11:833
66. Cai C, Lin J, Chen T, Tian X (2010) *Langmuir* 26:2791
67. Checot F, Brulet A, Oberdisse J, Gnanou Y, Mondain-Monval O, Lecommandoux S (2005) *Langmuir* 21:4308
68. Checot F, Lecommandoux S, Klok HA, Gnanou Y (2003) *Eur Phys J E Soft Matter* 10:25
69. Kishimura A, Liamsuwan S, Matsuda H, Dong W, Osada K, Yamasaki Y, Kataoka K (2009) *Soft Matter* 5:529
70. Anraku Y, Kishimura A, Oba M, Yamasaki Y, Kataoka K (2010) *J Am Chem Soc* 132:1631
71. Atmaja B, Cha JN, Marshall A, Frank CW (2009) *Langmuir* 25:707
72. Schatz C, Louguet S, Le Meins JF, Lecommandoux S (2009) *Angew Chem Int Ed Engl* 48:2572
73. Holowka EP, Deming TJ (2010) *Macromol Biosci* 10:496
74. Iatrou H, Frielinghaus H, Hanski S, Ferderigos N, Ruokolainen J, Ikkala O, Richter D, Mays J, Hadjichristidis N (2007) *Biomacromolecules* 8:2173
75. Gil GO, Losik M, Schlaad H, Drechsler M, Hellweg T (2008) *Langmuir* 24:12823

76. Pencer J, Hallett FR (2003) *Langmuir* 19:7488
77. Burchard W (1983) *Light scattering from polymers*. Springer, Berlin, p 1
78. Schneider AS, Schneider MJ, Rosenheck K (1970) *Proc Natl Acad Sci USA* 66:793
79. Kishimura A, Koide A, Osada K, Yamasaki Y, Kataoka K (2007) *Angew Chem Int Ed Engl* 46:6085
80. Upadhyay KK, Bhatt AN, Mishra AK, Dwarakanath BS, Jain S, Schatz C, Le Meins JF, Farooque A, Chandraiah G, Jain AK, Misra A, Lecommandoux S (2010) The intracellular drug delivery and anti tumor activity of doxorubicin loaded poly( $\gamma$ -benzyl L-glutamate)-*b*-hyaluronan polymersomes. *Biomaterials* 31(10):2882
81. Upadhyay KK, Bhatt AN, Castro E, Mishra AK, Chuttani K, Dwarakanath BS, Schatz C, Le Meins JF, Misra A, Lecommandoux S (2010) *Macromol Biosci* 10:503
82. Brown MD, Schatzlein A, Brownlie A, Jack V, Wang W, Tetley L, Gray AI, Uchegbu IF (2000) *Bioconj Chem* 11:880
83. Maeda H (2001) *Adv Drug Deliv Rev* 46:169
84. Sun VZ, Li Z, Deming TJ, Kamei DT (2011) *Biomacromolecules* 12:10

# Peptide-Based and Polypeptide-Based Hydrogels for Drug Delivery and Tissue Engineering

Aysegul Altunbas and Darrin J. Pochan

**Abstract** Bio-inspired materials chemistry is an interdisciplinary field in which biological functions and structures are used as inspirations to construct a wide variety of new synthetic materials and devices. Peptide sequences that provide structural, mechanical, chemical, or biological function can be borrowed from nature and fused into synthetic poly(amino acid) chains without replicating the entire natural biomolecular sequence. Supramolecular self-assembly of such rationally designed peptidic sequences is emerging as a promising route to novel biofunctional materials. This chapter highlights recent progress in bio-inspired peptide and polypeptide hydrogels that have potential biomedical and pharmaceutical applications. The focus is on synthetic or biosynthetic poly(amino acid) hydrogels based on  $\alpha$ -helical coiled-coils,  $\beta$ -sheets, dipeptides, peptide amphiphiles, elastin-like peptides, and on hybrids of organic polypeptides or polymers functionalized with peptides.

**Keywords** Biomaterial · Drug delivery · Hydrogel · Peptide · Polypeptide · Self-assembly · Tissue engineering

## Contents

1	Introduction .....	137
1.1	Hydrogel Biomaterials: Tools for Tissue Engineering and Drug Delivery .....	139
1.2	Nature of Crosslinks in Hydrogels .....	141
1.3	Molecular Self-Assembly .....	143
2	Peptide Hydrogels Through Biologically Inspired Self-Assembly .....	144
2.1	Hydrogels Based on $\alpha$ -Helical Coiled-Coil Structures .....	144
2.2	Hydrogels Based on $\beta$ -Sheet Structures of Peptides and Polypeptides .....	146

---

A. Altunbas and D.J. Pochan (✉)

Department of Materials Science and Engineering, University of Delaware, 201 DuPont Hall,  
Newark, DE 19716, USA

e-mail: [aysegul@udel.edu](mailto:aysegul@udel.edu); [pochan@udel.edu](mailto:pochan@udel.edu)

2.3	Hydrogels Based on $\beta$ -Sheet Structures of Short Dipeptides .....	152
2.4	Hydrogels Based on Peptide Amphiphiles .....	153
2.5	Elastin-Like Polypeptide-Based Hydrogels .....	155
2.6	Organic-Inorganic Hybrid Materials .....	157
3	Polymer-Peptide Conjugates .....	157
4	Conclusions .....	159
	References .....	160

## Abbreviations

2D	Two-dimensional
3D	Three-dimensional
A	Alanine
Ac	Acetyl
ATRP	Atom transfer radical polymerization
Boc	<i>tert</i> -Butoxycarbonyl
C	Cysteine
D	Aspartic acid
E	Glutamic acid
ECM	Extracellular matrix
ELP	Elastin-like peptide
F	Phenylalanine
Fmoc	9-Fluofluorenylmethoxycarbonyl
G	Glycine
H	Histidine
I	Isoleucine
K	Lysine
L	Leucine
N	Asparagine
P	Proline
PA	Peptide amphiphile
PAA	Poly(acrylic acid)
PEG	Polyethylene glycol
PEO	Polyethylene oxide
PVA	Poly(vinyl alcohol)
Q	Glutamine
R	Arginine
S	Serine
SPPS	Solid-phase peptide synthesis
T	Threonine
V	Valine
W	Tryptophan
Y	Tyrosine

## 1 Introduction

Bio-inspired materials chemistry is an interdisciplinary field in which biological motifs and functions are used to construct a wide variety of synthetic materials and devices with designed properties [1]. Several of the most well-known examples of biomimicry in materials design include the fabric hook-and-loop fastener named Velcro, which was inspired from tiny hooks found at the ends of burr spines; industrial water-repelling coatings inspired by superhydrophobic lotus leaves; and antibacterial and friction-reducing surfaces based on the shape and texture of shark skin [2–4]. Biomimetic strategies are being applied in biomedical fields in which bio-inspired materials, biological molecules, and living cells can be used in combination to grow new tissues [5]. For example, tissue engineering biomaterials are being designed to mimic the ability of natural, native extracellular matrix (ECM) components [6]. In living tissue, ECM helps regulate cell fate with specific molecular cues. These cues are presented to cells from an intricately interwoven mesh material of highly hydrated proteoglycans (negatively charged carbohydrate chains with covalently bound glycosaminoglycans) and fibrous proteins such as collagen, elastin, laminin, and fibronectin. Variations in the composition and arrangement of the ECM macromolecules give rise to an amazing diversity of forms and functions within different types of tissues. Analysis of ECM macromolecules has identified a variety of active sequences that are responsible for distinct functions, providing molecular sequences that can be adopted for inclusion in designed materials. Two of the most well-known cell adhesion and ECM motifs employed in the preparation of synthetic tissue engineering scaffolds are arginine–glycine–aspartic acid (RGD) and elastin-mimetic pentapeptides. RGD was identified as a common cell binding domain found in many cell binding proteins in the ECM and blood (e.g., fibronectin, vitronectin, osteopontin, collagens, thrombospondin, and fibrinogen) [7]. Elastin is a major structural protein component of ECM that is responsible for imparting extensibility and elastic recoil to connective tissues found in arterial blood vessels, lung parenchyma, elastic ligaments, and skin [8]. The RGD sequence is recognized by over 20 known integrins and promotes cell adhesion, spreading, and growth. Correspondingly, scientists have incorporated RGD into a vast array of polymeric gels and surfaces on which desired cells are forced to bind, spread, and proliferate [9], sometimes despite the chemistry of the synthetic hydrogel material [e.g., poly(ethylene glycol)] that, without RGD, actually prevents cell or protein adhesion [10, 11]. While sequences such as RGD play a role in cell adhesion and function, other sequences, such as elastin-like peptides, play a more indirect role in cell behavior by modulating the mechanical properties of ECM and tissue. Elastin-mimetic peptides are mainly utilized to enable control over the mechanical properties and phase transition behavior of block copolymers.

As described above, protein domains that provide discrete biological cues (e.g., cell binding) or mechanical properties (e.g., expansion or contraction with temperature changes) can be borrowed from nature and designed into synthetic polypeptides or joined with other polymers to provide bio-inspired function in new

materials. In this chapter, we will discuss the design of hydrogel materials that use the same peptide chemistry as proteins for the underlying hydrogel network or for the functionalization of synthetic organic molecules to produce synthetic peptide hybrid hydrogel systems. Some of these materials contain natural protein sequences for a desired function. Other materials use peptide and polypeptide molecules that are inspired by natural sequences but are de novo designed. Both natural and de novo designed molecules enable the preparation of functional biomaterials.

Although the prime focus of this chapter involves recent research efforts for the preparation of peptide and polypeptide hydrogels, some of the basic principles employed as synthetic routes for construction of small peptides, polypeptides, and polymer-peptide hybrids will also be introduced briefly. Detailed information about synthetic routes for the preparation of such materials can be found elsewhere [12–15]. With regard to short peptides (smaller than approximately 50 amino acids), solution-phase and solid-phase peptide synthesis (SPPS) provide good control over the length and structure of a peptide chain, yet the length of the peptide chains are practically limited to 10 and 40 amino acids, respectively. Although success with SPPS depends highly on the sequence, preparation of amino acid chains containing more than 40 residues has not been routinely employed because purification becomes difficult and isolated yields are reduced [16]. In solution-phase peptide synthesis, amino acids are dissolved in organic solvents and the reaction proceeds through stepwise addition of amino acids to a growing chain. The growth is facilitated through coupling and decoupling of either the N- or C-terminus, depending on the appropriate choice of protecting/deprotecting agents. SPPS reactions can proceed through the N-termini if the C-terminus of the peptide is anchored to a solid resin support. Depending on the resin, peptide synthesis can proceed from N- to C-terminal or from C- to N-terminal. After growth, the peptide can be cleaved off the resin, followed by deprotection of side chains and purification of the crude peptide with liquid chromatography. New side chain protection strategies have minimized deleterious side reactions that yield peptides with less than the desired lengths [17]. When one is interested in synthesizing a polypeptide with length greater than ~50 amino acids, one must look to polymerization reactions, either synthetic or biological. *N*-Carboxyanhydride polymerization is commonly used for the preparation of homopolypeptides as well as block copolymers [18]. Recently, Kramer and Deming reported living polymerizations of glycosylated lysine *N*-carboxyanhydrides to produce well-defined, high molecular weight homopolymers as well as block and random copolymers [19]. Biosynthetic methods utilizing the expression of polypeptides by organisms such as yeast or *Escherichia coli* have enabled precise control over structure, monomer sequence, and molecular mass of polypeptides [20]. This technique is mostly used for the preparation of proteins with complex primary sequence (i.e., amino acid sequence along the chain). Although biosynthetic routes were initially limited to the 20 naturally occurring amino acids, incorporation of unnatural amino acids into genetically engineered proteins is currently feasible [21, 22].



Besides the chemistry to produce peptide or polypeptide sequences, there is a diverse array of synthetic methods to incorporate additional functional domains into peptides, polypeptides, or synthetic polymeric materials such as amino acid coupling or divergent and convergent peptide incorporation [13, 18]. Such modifications enable various types of site-specific modifications at or near physiological pH [23]. Divergent methods can be accomplished in several ways as synthetic routes towards more complex peptide–polymer hybrids. Some methods are similar to SPPS techniques because the coupling reactions progress on a polymer chain attached to a resin. For example, amine-functionalized polymers can be anchored to the resin from which the peptide part can be subsequently grown [24]. This coupling method provides substantial control over the molecular weight and polydispersity of block copolymer systems. Conjugation can also proceed thorough atom transfer radical polymerization (ATRP) from resin-supported peptides [25]. Similarly, ATRP of polymer monomers using an initiator-modified peptide in solution has also been achieved [26]. Convergent assembly methods involve splicing of separately synthesized intermediate fragments into one macromolecule for the formation of the target structure [18].

Once synthesized, assemblies of such synthetic and biosynthetic molecules facilitate the preparation of various types of hydrogels with tailored functionalities, compositions, and topologies for biomaterials use. The success of hydrogels as biomaterials is not solely dependent on the chemical composition of the molecules building up the network. In addition, the hydrogel network formed and its inherent structure (e.g., network mesh size that directly affects molecular diffusion into and out of the hydrogel) and mechanical properties (e.g., stiffness, elasticity) also play key roles in the physical and biological properties of the hydrogel [27].

### ***1.1 Hydrogel Biomaterials: Tools for Tissue Engineering and Drug Delivery***

Hydrogels have a high water content and are physically rigid, three-dimensional (3D), crosslinked networks formed from polymer, peptides, or polypeptides [28] of natural or synthetic origin. The high water content of hydrogels, controllable pore size and morphology, controllable mechanical properties, and diverse underlying chemistry provides for various applications in tissue engineering and drug delivery [29]. In fact, in current hydrogel biomaterial research, almost every aspect of hydrogel research falls under the rubric of tissue engineering, drug delivery, or a combination of the two areas.

High water content and a porous morphology, especially in 3D systems, are crucial to allow fast diffusion of nutrients, drugs, and waste. The diffusion of small molecules and proteins within and out of hydrogel matrices is the key to the use of hydrogels as drug delivery vehicles. Drug-infused hydrogel matrices are used to induce therapeutic intervention for specific cellular functions by controlled release

of encapsulated drugs (small molecules, peptides, or macromolecules). Methods to construct drug delivery vehicles can be as simple as physical entrapment of the drug through noncovalent association of the drug to the scaffold through physical bonds, or as complicated as immobilization of the drug with covalent bonds to the hydrogel constituent network chains. Covalent immobilization can be accomplished either through the use of side-chain grafting or, in the case of peptides and polypeptides, direct incorporation of the drug into the primary sequence if the drug is a peptide. Delivery systems in which the drug is physically entrapped are the most straightforward in the sense that the drug release can be modified by the mesh size of the network that restricts the diffusion-mediated release of the encapsulated drug. Strategies involving covalent grafting and direct incorporation of the drug into the polypeptide chain rely on network degradation to release the therapeutic agents [30].

Tissue engineering scaffolds aim to restore the function of diseased, injured or aging cells, tissues and organs [31–33]. To accomplish these goals, tissue engineering strategies focus on controlling hydrogel morphology, mechanical properties, and biochemical cues. Ultimately, the materials will be used in intimate contact with cells and, in many cases, *in vivo*. Cell culture is fundamental to the study of tissue engineering, whereby cells are cultured on two-dimensional (2D) or in 3D tissue engineering scaffolds to observe cell function and material cytocompatibility *ex vivo*. *In vitro* cell culture has been performed widely on 2D surfaces, a standard for typical *in vitro* cell culture. However, it has been demonstrated that cells behave more natively when cultured in 3D environments [34, 35]. As the native environment for cells in living systems is a complex structural and functional framework of 3D ECM components, any attempt to draw rigorous conclusions based on 2D studies would be inadequate. Hence, tissue engineering scaffolds where cells experience 3D environments on which they can attach, proliferate, migrate, and differentiate are being investigated heavily, along with 2D systems. A diverse range of natural and synthetic polymer hydrogels have been suggested as tissue engineering scaffolds. Examples of some widely used synthetic polymers are poly(vinyl alcohol) (PVA), polyethylene oxide (PEO) and poly(acrylic acid) (PAA) in addition to polypeptides. It is also important to note hybrid hydrogels, where the structure can be composed of peptidic as well as synthetic domains. Natural hydrogel-forming polymers are polysaccharides (alginate, agarose, dextran, chitosan) and proteins (collagen, gelatin, fibrin). The use of naturally derived materials as biomaterials is limited because they can elicit inconsistent or unwanted biological responses. They can also pose challenges if it is necessary to tune mechanical properties independently from the biochemical properties.

In contrast to these polymer and natural products, the peptide and polypeptide hydrogels allow the design and engineering of new, well-defined materials. For example, self-assembling peptides can be designed to form hydrogels with a well-defined nanostructure of ~3–10 nm diameter fibrils, similar in size and morphology to the fibrillar ECM components. Also, the display of biochemical cues on thin, well-defined fibrils for cells encapsulated within nanoporous 3D structures can build well-defined microenvironments. The specific placement of chemistry along

the constituent peptides or polypeptide chains allows biological functionality similar to the natural ECM, as well as biomimicry by actual use of natural sequences within rationally designed molecules. The design of peptidic and polypeptidic hydrogels is not limited to chemical functionality. Stiffnesses of ECM in different tissues varies widely within the body, e.g., the elastic modulus of bone tissue can be as stiff as  $\sim 18,000$  Pa whereas brain tissue can be as soft as  $\sim 2,500$  Pa [36]. Correspondingly, recent studies have revealed that matrix elasticity has a profound effect on the behavior of anchorage-dependent cells [37]. Successful interactions of cells and their scaffolds therefore require control over mechanical properties so that biophysically well-defined microenvironments can be created. Physical, covalent, and combinations of the two types of crosslinks in peptidic and polypeptidic systems mediate preparation of a wide variety of stiffnesses, depending on the desired properties of the final hydrogel material.

Materials used as tissue engineering scaffolds or drug delivery vehicles are diverse. In this chapter, we will concentrate on recent peptide- and polypeptide-based hydrogel systems. Hydrogels that are composed solely of synthetic or hydrocarbon high molecular weight polymers of synthetic [38–40] or natural [41, 42] origin, and bio-inspired peptides or polypeptides [43–47] that do not form hydrogels are beyond to scope of this chapter therefore the reader is directed elsewhere [48–51].

## ***1.2 Nature of Crosslinks in Hydrogels***

Knowledge of the nature of crosslinking in hydrogel networks is essential for determining the mechanical properties of materials and in considering the material for a particular application. An ideal hydrogel scaffold, as a candidate for a biomedical application, has to be self-supporting (i.e., rigid enough to sustain itself and any payload). Scaffolds with tunable mechanical stiffness to maintain cells in a 3D environments, i.e., comparable in elasticity to a cell's natural environment, are essential for regulation of cell phenotype, cell adhesion, and cell gene expression [37].

Chemical hydrogels are covalently crosslinked systems that provide definition of material properties when crosslinked *ex vivo*. Chemical hydrogels can be less well-defined when crosslinked *in vivo*, where the biological environment can affect the reactants before and during crosslinking. Covalent hydrogel networks are primarily responsive to their environment relative to the constituent chemistry of the hydrogel molecular chemistry. For example, they can absorb large quantities of water when synthesized with significantly hydrophilic chemistry, causing the network to swell in solution without dissolving. The degree of swelling is defined as the ratio of sample volume in the swollen, equilibrium state to the volume in dry state. Swelling and the content of water retained are largely dependent on the hydrophilicity of the polymer chains and crosslinking density. Common preparation of covalently crosslinked polymer hydrogels for biological applications involve bifunctional

monomers and UV radiation or redox-initiated chemistry. Radicals formed during the polymerization reaction, unreacted monomers, UV radiation, and the high polymerization exotherm experienced as a result of polymerization can be damaging to cells in cases where cells are to be homogeneously encapsulated within the network or a polymerizing hydrogel in neighboring living tissue. Covalent crosslinking of chemical hydrogel networks is a common method of producing hydrogels from synthetic polymers, but is also used in the formation of peptidic or polypeptidic hydrogels, either to form the underlying network structure or to further tune the properties of a physical hydrogel network.

In physical hydrogels, the hydrogel network is held together by physical rather than covalent chemical interactions. These physical interactions are diverse (e.g., molecular entanglements, hydrogen bonding,  $\pi$ -stacking, van der Waals, hydrophobic, ionic and electrostatic) and make physical hydrogels responsive to environmental changes (ionic strength, temperature, pH and/or stress). So, although physically crosslinked hydrogels display much less stiffness and strength than chemically crosslinked hydrogels, these systems can display responsiveness to environmental cues that can be used as a biomaterial tool. An example of this biological responsiveness being used as a biomaterial tool is the ability to design solid, preformed peptide hydrogels that can be implanted *in vivo* via syringe injection, whereby the scaffolds display similar mechanical properties before and after shear. This shear-thinning property of the solid peptide hydrogel requires appropriate flow properties that facilitate shear-thinning (i.e., the hydrogel flows like a low viscosity solution) upon application of a proper shear stress to the hydrogel, followed by immediate recovery into a solid once the stress is removed [52]. Identical material properties before and after syringe injection become crucial if homogeneous encapsulation of the payload (therapeutics or cells) within the hydrogel is required. The ability of the material to withstand possible local *in vivo* forces right after syringe delivery is also vital.

The desire to achieve optimal control over hydrogels is always a trade-off between various design parameters. One can design around limitations by combining physical and chemical crosslinks in hydrogels [53, 54]. Recently, Hartgerink and coworkers demonstrated a 60-fold increase in storage modulus by covalent linkage of self-assembled nanofibers through disulfide bond formation [55]. Examples of systems where chemical and physical crosslinks coexist are also prevalent in nature, e.g., the ECM protein, elastin, is composed of an ordered assembly of the monomeric elastin into a polymeric network in which juxtaposed lysine residues form covalent crosslinks to stabilize the polymer network [56].

Hydrogels made from peptides and polypeptides can involve physical or chemical interactions, or a combination of both. Nature frequently uses a combination of relatively weak, noncovalent associations in combination with covalent interactions [57]. Using peptides and polypeptides as the underlying tools to make gels provides systems that primarily rely on assembly, with subsequent covalent chemistry (if any) to define the final network. For example, covalent bonds through selective crosslinking of lysine residues in biomolecules has been carried out with variety of reagents, including glutaraldehyde, bis(imidoesters) and *N*-hydroxysuccinimide

esters of bifunctional carboxylic acids [58]. Examples of hydrogels made from peptides or polypeptides that are exclusively covalently crosslinked constitute, by far, the minority. Examples of physical, chemical, or combination physical/chemical hydrogel networks will be discussed in Sect. 2. First, we will describe molecular self-assembly, a process vital in natural, living systems [59]. Self-assembly provides an excellent strategy for generation of precisely defined and hierarchically ordered physical hydrogels [60].

### ***1.3 Molecular Self-Assembly***

Nature combines simple building blocks for making complicated architectures, at lengths ranging from nano- to macroscale [59, 61]. In modern materials production, technology has enabled a high degree of control over order on the nanoscale with conventional, top-down, methods such as photolithography. However intricately detailed structures in the lower nanometer length scales (<10 nm) are the domain of bottom-up methods such as molecular self-assembly.

Molecular self-assembly is the association of molecules into defined structures by noncovalent, intermolecular interactions through hydrogen bonding, coulombic, van der Waals, and/or electrostatic interactions. The supramolecular structure achieved through the assembly of smaller building blocks is not simply a result of random aggregation but, rather, specific intermolecular interactions that can result in exact nanostructure as well as hierarchical order on larger length scales. (For a comprehensive tutorial on directionality, specificity, reversibility, and complexity of molecular interactions in self-assembling systems the reader is directed elsewhere [57]).

Reversibility of relatively weak and noncovalent molecular associations facilitates disassembly in response to changes in the environment (e.g., remodeling of the ECM, depolymerization of actin filaments etc.). However, instances of irreversible molecular associations are also prevalent in nature. For example, bundles of  $\beta$ -sheet fibrils (i.e., amyloids) generate insoluble, protein aggregates that are deposited in tissues commonly associated with Alzheimer's disease. Amyloidosis represents an interesting example in which the fine line between typical healthy assembly and unhealthy self-aggregation is crossed [62]. The order, biological functions, material properties, and reversibility/irreversibility obtained in supramolecular systems is heavily dependent on the molecular building blocks as well as the environment. In the rest of the chapter, we will discuss various studies where peptide and polypeptide primary structure and solution conditions dictate molecular structure (e.g.,  $\beta$ -sheet secondary structure) and intermolecular assembly into hydrogels. Peptide and polypeptide design offers a particularly powerful opportunity for intermolecular, bottom-up assembly hydrogels [63]. Careful analysis of the natural domains that dictate the structure and biological functions of natural proteins have been used in the design and synthesis of engineered materials. The aim is to simplify or mimic an actual protein sequence by capturing salient

features of naturally occurring domains. For example,  $\beta$ -hairpins with short connecting loops (1–5 residues) [64, 65], helices that can adopt stable secondary structures [66, 67], and factors that stabilize helical folding patterns [68, 69] have been identified in protein structures [63]. Such conformational motifs are being used in the design of synthetic or biosynthetic peptides and polypeptides. These types of designs will be discussed in Sect. 2.

## 2 Peptide Hydrogels Through Biologically Inspired Self-Assembly

### 2.1 Hydrogels Based on $\alpha$ -Helical Coiled-Coil Structures

The coiled-coil protein superstructure is one that is being studied thoroughly as a motif to be used in peptide and polypeptide hydrogel design. This motif is observed frequently in nature and is crucial to the formation of many natural biomaterials. A prominent example is found in blood clots. Studies on the mechanism of blood clot formation have revealed a set of events that occur after injury to a blood vessel. Fibrinogen, a soluble plasma protein, is converted into fibrin monomer upon activation by the protease thrombin. The fibrin monomer is a long chain that connects three domains via coiled-coil linkers. Activation triggers the polymerization of fibrin monomers into branched networks of fibrin fibers [70]. The insoluble fibrin network, together with platelets and red blood cells, forms the blood clot (thrombus). The ability of a blood clot to withstand high shear forces has attracted great scientific interest. The bundle-like structure of fibrin fibers has been reported to be a major contributor to the remarkable elastic properties of fibrin gels [71]. Large extensibility properties of fibrin fibers have also highlighted the contributions of coiled-coil unfolding for up to a twofold strain [70, 72]. A recent study has investigated the unique hierarchical architecture and physical origin of mechanical strength of fibrin gels in detail [71].

The characteristic coiled-coil motifs found in proteins share an  $(abcdefg)_n$  heptad repeat of polar and nonpolar amino acid residues (Fig. 1). In this motif, positions a, d, e, and g are responsible for directing the dimer interface, whereas positions b, c, and f are exposed on the surfaces of coiled-coil assemblies. Positions a and d are usually occupied by hydrophobic residues responsible for interhelical hydrophobic interactions. Tailoring positions a, d, e, and g facilitates responsiveness to environmental conditions. Two or more  $\alpha$ -helix peptides can self-assemble with one another and exclude hydrophobic regions from the aqueous environment [74]. Seven-helix coiled-coil geometries have also been demonstrated [75].

Many examples exist of using this protein motif to construct hydrogels from protein or peptide assembly. For example, Dong et al., reported elongated fibrils with diameters as small as 4 nm by incorporation of charged amino acids in the

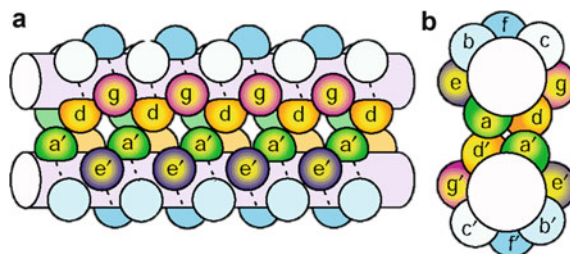


**Fig. 1** (a) Side and (b) top view of a parallel two-stranded coiled-coil based on heptad sequence repeat (*abcdefg*). Residues at positions *a*, *d*, *e* and *g* form the interface between  $\alpha$ -helices in a coiled coil structure. Prime notations are used to distinguish analogous positions in the two helices; for example, *a* and *a'* are analogous positions. Reproduced from Fong et al. [73]; licensee BioMed Central Ltd. copyright 2004 (<http://genomebiology.com/2004/5/2/R11>)

peripheral *b*, *c*, and *f* positions of blunt-ended coiled-coil peptides [74]. This was achieved by associations of 21 amino acid peptides at low pH values and at relatively high peptide concentrations. Hydrogelation was observed at pH  $\sim$  3.5 at 1 wt% (mg/mL).

Leucine zipper domains, where *a* and *d* in the heptad repeat are leucine or nonpolar residues, are common structural motifs that were originally identified in the amino acid sequences of several DNA binding proteins. The side chains of repeating leucine residues are recognized as long, stable projections from the  $\alpha$ -helix that interdigitate with those of a second helix, which causes the two helices to dimerize. This naturally occurring process has been incorporated into various hydrogel designs to allow reversible association of different polypeptides through environmentally responsive physical crosslinks [76–78]. Previously, Tirrell's group reported gelation of the AC<sub>10</sub>A triblock protein, where A is a leucine zipper-type coiled-coil domain and C<sub>10</sub> is a hydrophilic random coil polypeptide [AGAGAGPEG]<sub>10</sub> (where A is alanine, G glycine, P proline, and E glutamic acid). Studies have revealed fast erosion rates of hydrogels due to the strong tendency of the chains to form loops in addition to the small aggregation number of A zipper end groups and transient associations of the A domains [79]. To decrease erosion rates, triblock proteins with dissimilar helical coiled-coil endblocks that do not associate with each other were prepared. This strategy successfully reduced erosion rates in aqueous environments by more than 100-fold [80]. The ability to tailor transient associations in  $\alpha$ -helix coiled-coils has also been suggested as a strategy to trigger recognition events in electrostatically compatible heterodimers [81].

In another study, the original repetitive C<sub>10</sub>, (AGAGAGPEG)<sub>10</sub>, center was reconstructed into nine repeats of AGAGAGPEG with three distributed repeats of the RGD sequence. The new triblock protein, composed of acidic and basic terminal domains in addition to the reconstructed central block, has been shown to support adhesion, spreading, and polarization of human fibroblast cells [82]. Triblock polypeptides that facilitate antibody binding have also been reported [83].

Control over degradation rates of materials in biological systems is crucial because enzymatic degradation or hydrolysis can compromise the mechanical properties of the system. As discussed earlier, covalently crosslinked hydrogels (e.g., photo-crosslinked hydrogels) in general are systems where the network architecture is stabilized with permanent junctions. AC<sub>10</sub>-Polyethylene glycol (PEG)-acrylate and AC<sub>10</sub>RGD-PEG-acrylate were used to prepare physical hydrogels with additional photo-crosslinkable capability [84]. The C<sub>10</sub> domain was also decorated with an RGD group to enhance cell attachment to the hydrogels. Hydrogels were covalently crosslinked in cell culture media upon exposure of the photo-crosslinkable acrylates to UV light in the presence of a photoinitiator. The junction points formed through leucine zipper aggregation are physical and are believed to allow reversible opening and closing of 3D cell migration paths so that cells can migrate constitutively independent of hydrogel degradation [84].

One of the mechanisms of inducing coiled-coil assembly, instead of an overall solution stimulus, is mixing-induced self-assembly. Mixing-induced self-assembly of two 28-amino acid  $\alpha$ -helical peptides have been reported [77, 78, 80, 85]. Formation of thick, highly ordered, offset fibrils from strongly interacting, de novo coiled-coil-based self-assembling chains resulted in precipitates but no gelation. Replacement of strongly interacting residues in the b and c positions of the coiled-coil to form domains with weaker interacting residues led to the formation of physical hydrogels with smaller and more flexible bundles of thinner fibers [86]. In addition, these hydrogels of self-assembling fibers present only short hydrophobic methyl side chains of alanine residues on their outer surfaces and, thus, displayed reinforced interfibrillar interactions through hydrophobic crosslinks. The hydrophobic, interfibrillar interactions impart thermoresponsive behavior to the hydrogels, causing them to become stronger with increasing temperature. These hydrogels were used as substrates for the growth and differentiation of rat adrenal pheochromocytoma (PC12) cells. The two-component gelation strategy suggests a simple way to generate chemically defined tissue engineering scaffolds and eliminates the need for environmental triggers. Other studies that demonstrate two-component gelation strategies based on interactions of  $\beta$ -sheet forming peptides will be discussed in Sect. 2.2. For information on  $\alpha$ -helix-based biomaterials published before 2006, the reader is directed to a review by Woolfson and Ryadnof [87].

## ***2.2 Hydrogels Based on $\beta$ -Sheet Structures of Peptides and Polypeptides***

Just like in coiled-coils,  $\beta$ -sheet secondary structure (Fig. 2) is ubiquitous in natural examples and in proteins and biomaterials. Alzheimer's disease is characterized by fibrillar amyloid plaques in the cerebral parenchyma. The insoluble amyloid fibrils are predominantly formed upon conformational switching of the 42 amino acid



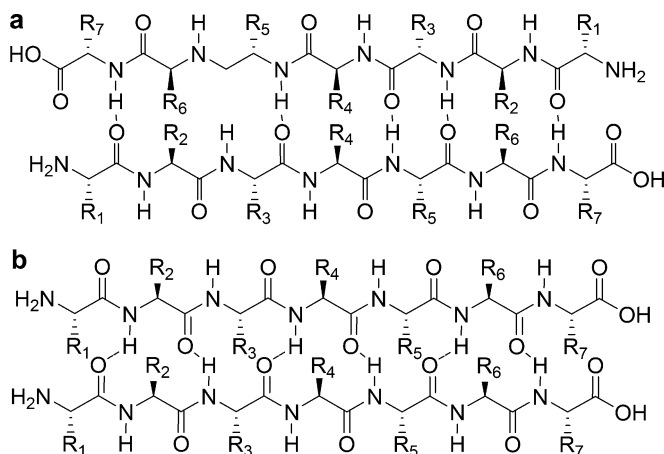


**Fig. 2** (a) Antiparallel and (b) parallel  $\beta$ -sheet structures of two peptide chains connected by hydrogen bonds

amyloid  $\beta$ -peptide ( $A\beta$ ) from  $\alpha$ -helix or random coil to a  $\beta$ -sheet structure [88]. The common feature of amyloid fibrils is the alignment of hydrogen bonded  $\beta$ -strands perpendicular to the fibril axis.  $\beta$ -Sheet structure is also observed in natural proteins such as silk fibroin [89–91]. Repetitive GAGAGS, GAGAGY, and GAGAGVGY sequences have been found to be responsible for the formation of antiparallel  $\beta$ -sheets in the spun fibers [92].

The use of the  $\beta$ -sheet motif in designed materials from designed molecules goes back to 1975, when research on the genetic code suggested that polypeptides in which hydrophilic and hydrophobic amino acids alternate tend to form  $\beta$ -sheets with one hydrophobic and one hydrophilic surface via self-assembly in aqueous solutions [93, 94]. This trend was observed with poly(EA), poly(YE), poly(KF), and poly(VK) [93]. A similar finding came in the 1990s, when these periodicities of polar and nonpolar residues in self-assembling oligomeric peptides were recognized as the major determinant of peptide  $\beta$ -sheet secondary structure [95].  $\beta$ -Sheet hydrogels have also been observed with much shorter dipeptides. We will be discussing the self-assembly of such dipeptides in Sect. 2.3.

There are many recent examples of the use of  $\beta$ -sheet structure to form fibril-rich materials, particularly hydrogels. Work by Aggeli et al. has highlighted the ability of transmembrane domains found in IsK protein [96] to assemble into  $\beta$ -sheet molecular tapes in solvents such as methanol or 2-chloroethanol. Domains K24 and K27 are amongst the first segments of native proteins to be synthesized and self-assembled into viscoelastic gels with  $\beta$ -sheet structures. K24, whose primary structure is (NH<sub>2</sub>-KLEALYVLGFFGFFTLGIMLSYIR-COOH), represents residues 41–67 of IsK, without the residues 47–49, and K27 represents residues 41–67 of IsK [97]. Gelation where K24 is found in  $\beta$ -sheet conformation ( $\geq 70\%$ ) was achieved in moderately polar solvents such as methanol with  $25 < \epsilon_r < 68$  (where  $\epsilon_r$  is the dielectric constant). No gelation was observed with solvents outside

this window because  $\beta$ -sheets were either not sufficiently soluble or the peptide was found predominantly in helical form ( $\epsilon_r < 15$ ). To achieve gelation in more polar solvents such as water, peptides with more hydrophilic and thus soluble  $\beta$ -sheets were investigated. Lys $\beta$ -21 [98], which is another naturally occurring motive, formed  $\beta$ -sheet-rich hydrogels in solvents with a broader range of polarities ( $\epsilon_r > 30$ ).

In 1993, Zhang et al. observed salt-induced peptide assembly into  $\beta$ -sheets with EAK16-II (AEAEAKAKAEAEAKAK), a 16-residue peptide motive originating from the yeast protein zotin [99, 100]. Since then, a number of ionic-complementary self-assembling peptides have been developed. Other peptides by Zhang and coworkers, which were designed to form hydrogels under physiological conditions, include RADA16-I [101, 102], (RADA)<sub>4</sub>, and RAD16-II (RARADADAR-ARADADADA). Such oligopeptide hydrogels prepared by the spontaneous assembly of self-complementary ionic bonds have been suggested as tissue engineering scaffolds for the culture of a wide variety of cell types [103, 104]. Others have developed stimuli-responsive release of encapsulated salts from liposomes to prepare hydrogels rich in  $\beta$ -sheet fibrils [105]. The water-soluble, 16-amino acid FEK-16, (FEFEFKFK)<sub>2</sub>, was found to undergo  $\alpha$ -helix-to- $\beta$ -sheet transition at concentrations above 10  $\mu$ M. Additional millimolar concentrations of NaCl or CaCl<sub>2</sub> were reported to induce this transition. Temperature- or light-sensitive liposomes were used to release CaCl<sub>2</sub> at physiological temperatures or when exposed to tissue-penetrating near-infrared light for triggered hydrogelation of the FEK-16 peptide.

If properly designed, peptides can be made to intermolecularly assemble into  $\beta$ -sheet-rich hydrogels only after proper intramolecular folding in response to an environmental trigger. A class of  $\beta$ -sheet peptides, namely  $\beta$ -hairpins, that can form hydrogels after intramolecular folding and intermolecular assembly is triggered by changes in external stimulus such as increases in pH [106], salt ion concentration [107], or temperature [108] has been developed by the Schneider and Pochan laboratories (Fig. 3). One of the de novo designed peptides presented by these research groups is MAX1. MAX1, whose sequence is (VK)<sub>4</sub>-V<sup>D</sup>PPT-(KV)<sub>4</sub>-CONH<sub>2</sub>, has a tetrapeptide turn sequence in the middle of two strands of alternating valine and lysine residues [107, 109]. MAX1 is readily soluble in aqueous, low ionic strength solutions (pH  $\sim$  5.5–7.4). At pH  $\leq$  10, most of the lysine residues are protonated, which results in charge repulsion between lysine residues along the peptide strands. In turn, the charge repulsion causes the peptide to adopt a random coil conformation and be freely soluble in solution. Self-assembly of the peptides into well-defined, fibrillar structures is initiated upon folding of the random coil peptides into a  $\beta$ -hairpin conformation. Peptide folding into a  $\beta$ -hairpin can be achieved either by an increase in ionic strength [107], which produces charge screening on the lysine residues, or by an increase in pH [106] (pH  $\sim$  9) that causes deprotonation of lysine residues [110]. Also, raising the temperature has been found to trigger folding by inducing dehydration of the nonpolar residues, which causes hydrophobic collapse [108]. The folded peptide is of amphiphilic character and displays its hydrophobic valine and hydrophilic lysine residues on opposite faces of

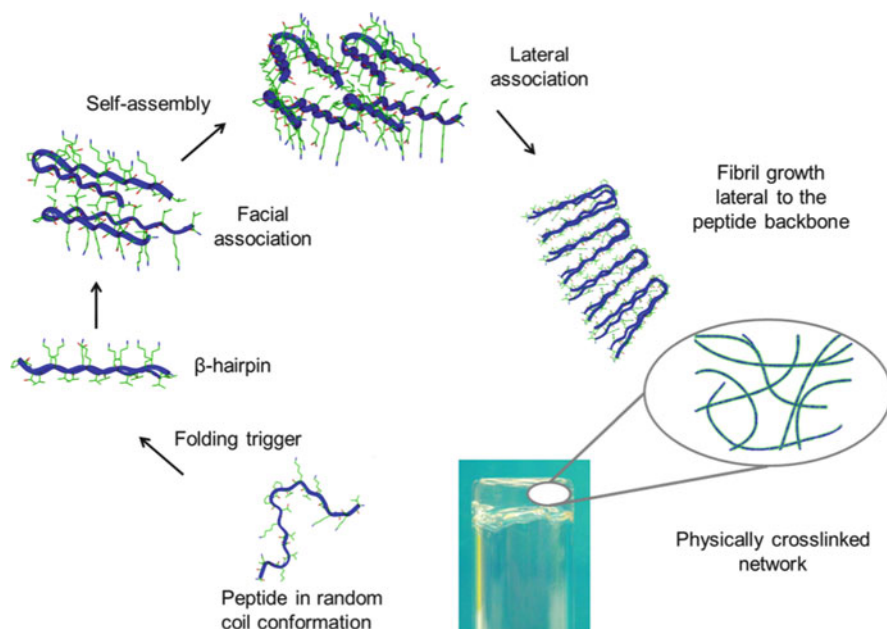


**Fig. 3** Triggered folding of MAX1 or MAX8 peptide yields a facially amphiphilic  $\beta$ -hairpin. Facial hydrophobic associations between  $\beta$ -hairpins yield  $\beta$ -sheet bilayers. Intermolecular interactions through side chain hydrophobic associations (valine side chains) among these bilayers and hydrogen bonding lateral to the peptide backbone gives rise to the formation of fibrils. Assembly-defect induced branching and physical entanglements among peptide fibrils (lysine side chains) yield a self-supporting hydrogel

the  $\beta$ -hairpin. Intramolecular hydrogen bonding stabilizes the  $\beta$ -hairpin. The valine faces of two  $\beta$ -hairpins collapse through hydrophobic interactions to form a  $\beta$ -sheet sandwich that undergoes intermolecular interactions through side chain hydrophobic associations between these bilayers and through hydrogen bonding lateral to the peptide backbone. These intermolecular interactions cause the assembly of fibrils [111]. Physical entanglements among peptide fibrils and fibril branching [112] yield a rigid, fibrillar network. Complete  $\beta$ -sheet transformation and hydrogelation for a 0.5 wt% MAX1 system (0.5 mg MAX1/100  $\mu$ L of hydrogel at physiological conditions) requires  $\sim$ 30 min [113]. The need for faster gelling systems is essential for homogeneous 3D cell encapsulation and potential tissue engineering applications. Therefore, MAX8 was designed by making a point substitution of a lysine residue on the 15th position of MAX1 with a glutamic acid, which resulted in an overall charge decrease to yield faster gelation kinetics under physiological conditions [113, 114]. The reduction of overall charge to be screened during peptide folding thus imparts faster gelation kinetics with complete  $\beta$ -sheet transformation in under 1 min at physiological conditions [113]. Gelation kinetics in such systems can also be manipulated by the ionic strength of the medium, temperature, and peptide concentration. For example, the average storage modulus ( $G'$ ) of  $\beta$ -hairpin

hydrogels, assembled in a 150 mM NaCl buffer at pH 7.4 and 25°C, varies from ~40 (0.5 wt%) to 2,080 Pa (2.0 wt%) for MAX1 and ~415 (0.5 wt%) to 4,800 Pa (2.0 wt%) for MAX8 – the faster folding and assembly providing for the more highly crosslinked, stiffer hydrogel network.

The self-supporting nature of the  $\beta$ -hairpin physical hydrogels facilitates cell culture on 2D and in 3D situations. Hydrogels of the MAX1 and MAX8 peptides have been used for the *in vitro* culture of a variety of cells, and both have proven to be cytocompatible [115–117]. Fast gelation kinetics, especially observed with MAX8 peptide at pH 7.4, 37°C and 160 mM ionic strength medium, enables homogeneous encapsulation of living mammalian cell or drug payloads in 3D within the hydrogel. MAX1 hydrogels have also been linked to antibacterial properties. The high density of lysine groups exposed on MAX1 fibril surface have been reported to disrupt the bacteria's negatively charged surface without causing any damage to mammalian cell membrane [118]. Such biocompatible, self-assembling peptide systems hold promise because the peptide structure can be manipulated to introduce specific biochemical functionalities [53]. In addition, macromolecule self-diffusion and bulk release studies with MAX1 and MAX8 hydrogels have indicated macromolecule mobility within and release out of the gels [119]. This proves an important point because porous hydrogels that allow transport of nutrients and metabolites are ideal candidates for tissue engineering and drug delivery scaffolds. The average mesh sizes reported vary from ~22 to 49 nms for 0.5–2.0 wt% MAX1 networks and ~18 to 30 nm for 0.5–2.0 wt% MAX8 networks. Thus, the mesh size can be modulated by varying the concentration of the peptides or altering peptide sequence [119].

A final property of the  $\beta$ -hairpin hydrogels to be pointed out is their ability to shear-thin and flow but immediately reheel back into a solid that is almost identical to the pre-sheared material. This makes MAX1 and MAX8 injectable hydrogel solids since solid hydrogels made from either peptide are highly responsive to mechanical shear. Yan et al. recently elucidated mechanisms of shear-thinning and subsequent self-healing properties of MAX1 and MAX8 peptide hydrogels via characterization of the systems during and after flow [117]. Figure 4a displays the gel restoration kinetics of 2 wt% MAX1 hydrogels after shear-thinning the hydrogels for 5, 40, and 120 s at constant rate (1,000/s) with oscillatory rheology. The figure demonstrates that the recovery of mechanical properties of hydrogels is dependent on the length of shear duration. The figure also compares shear-thin recovery behavior of 2 wt% MAX1 hydrogels after syringe injection to behavior observed during rheometer-induced shear treatment and confirms that the observed shear-thinning and rehealing after flow is representative of authentic bulk gel properties. The study also revealed that the solid hydrogel network is fractured into domains that allow the gel to flow like a low viscosity solution under shear stress (Fig. 4b). Upon removal of the shear stress, the fractured domains rapidly percolate into a network, allowing the gel to immediately display solid-like properties and eventually restore its initial strength. Self-healing properties of the peptide hydrogels after shear-thinning facilitate local delivery of gel–cell constructs via syringe. It was observed that shear-thin delivery of MAX8 had no effect on

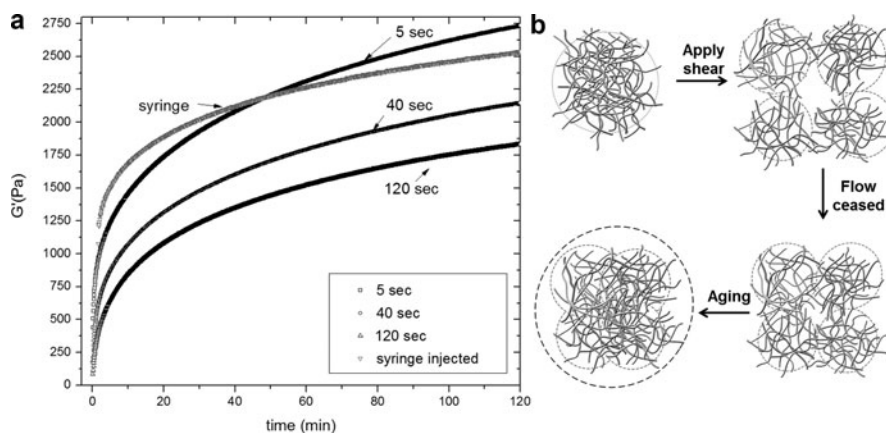


**Fig. 4** (a) Gel restoration kinetics: storage modulus,  $G'$ , restored as a function of time after shearing three 2 wt% MAX1 gels formed on the rheometer (pH 7.4, 50 mM bis tris propane buffer, 400 mM NaCl at 20°C) at a constant shear rate of 1,000/s for 5 (squares), 40 (circles) and 120 s (up triangles), respectively. The figure also compares gel restoration kinetics of 2 wt% MAX1 gel subjected to shear induced by syringe injection (grey down triangles) with respect to the shear in the rheometer. MAX1 hydrogel was injected through a 26 gauge needle onto the rheometer and measurement of  $G'$  as a function of time was performed immediately. (b) Network structure evolution of  $\beta$ -hairpin peptide-based hydrogels (MAX1 or MAX8) during shear-thinning and recovery processes. Under shear, the gel network is fractured into domains that allow the gel to flow. Once the shear has ceased, these domains immediately percolate into a network leading to the immediate recovery of a solid gel response after cessation of shear. Gel rigidity close to values prior to shear is recovered via fibrillar network relaxation at the boundaries between previously fractured domains

encapsulated cell viability and distribution [113, 117]. Control over gelation kinetics, gel stiffness, homogeneous encapsulation of living cells and drug payloads, localized injectable delivery, and controlled release of therapeutics, in addition to the potentially non-inflammatory properties [115] of these hydrogels makes them strong candidates for biomedical applications and biotechnology.

These favorable shear flow and rehealing properties are being studied in other systems. For example, another hydrogel that shows rapid recovery from shear-induced breakdown is prepared by the co-assembly of peptides Ac-WK-(VK)<sub>4</sub>-amide and Ac-EW-(EV)<sub>4</sub>-amide [120]. Upon mixing the two mutually attractive but self-repulsive decapeptides at low concentrations (0.25 wt%), viscoelastic hydrogels with nanofibrillar morphologies and rich in  $\beta$ -sheet conformations were observed. Mixed self-assembly of peptidic molecules to form hydrogels is a strategy used by others to form hydrogels. For example, Hartgerink and coworkers produced 3D networks by electrostatic attractions of positively and negatively charged peptide amphiphiles (PAs) [121]. We will discuss self-assembly of PAs involving a single type of molecule in Sect. 2.4. Also recently, the Heilshorn group reported a two-component, molecular recognition gelation strategy based on interactions of the  $\beta$ -sheet-forming WW domains [122] and proline-rich peptides that enable cell encapsulation [123]. The hydrogel has been shown to support cell

proliferation, differentiation, and neurite extension. The recombinantly synthesized chains are composed of multiple repeats of each association domain linked together by random-coil hydrophilic spacers. The design is based on associations that are not prevalent in the extracellular environment, thus yielding reproducibly gelling materials that present the advantage of not being influenced by changes in composition of the surrounding environment. It is proposed that variations in the molecular-level design of the two components can be used to tune the association stability and hydrogel viscoelasticity. Engineered polypeptides for forming hydrogels seem promising because biologically functional modules can be directly incorporated into the design so that macromolecular design with molecular level precision can be achieved.

### 2.3 Hydrogels Based on $\beta$ -Sheet Structures of Short Dipeptides

All of the  $\beta$ -sheet-rich hydrogels just discussed result from the assembly of oligopeptides up to polypeptides, all with amino acid lengths of greater than five amino acids. However, gelation has also been achieved with much shorter dipeptides. The feasibility of such systems for commercial application is good from a synthesis point of view as dipeptides are short and relatively cheaper to synthesize than longer oligopeptides [18]. Aromatic components conjugated to short peptide sequences mediate self-assembly by enforcing  $\pi$ -stacking (stacking of aromatic rings) interactions. As mentioned previously, amyloid-like fibril formation was also observed with short Boc (*tert*-butoxycarbonyl) and Fmoc (9-fluorenylmethoxycarbonyl) dipeptides. Fmoc dipeptides undergoing gelation was first reported by Vegners et al. in a study where Fmoc-LD, Fmoc-AD, and Fmoc-ID formed viscoelastic gels upon a heating (100°C) cooling (60°C) cycle of the peptide solutions in water [124]. Fmoc-A<sub>2</sub> hydrogels have also been reported to gel upon lowering environmental pH to 3. Also, Fmoc-<sup>D</sup>A<sup>D</sup>A gel (where <sup>D</sup>A refers to *D*-alanine) was found to undergo gel–sol transition upon binding to Vancomycin (Van) through strong ligand–receptor interactions, whereas Fmoc-<sup>L</sup>A<sup>L</sup>A was left unaffected.[125] The gel–sol transition is explained by the high affinity of Van to <sup>D</sup>A<sup>D</sup>A via four to five hydrogen bonds, in addition to interruption of the  $\pi$  stacking of fluorenyl groups by the biphenyl moiety on Van.

Significant progress with dipeptides has been achieved when gelation of Fmoc-F<sub>2</sub> was achieved at physiological pH. Hydrogels prepared with Fmoc-F<sub>2</sub> [126–128] and with 50:50 (mol/mol) Fmoc-F<sub>2</sub>:Fmoc-G<sub>2</sub> [126] have been used as 2D and 3D scaffolds for cells *in vitro*. Uljin and coworkers proposed interlocking through lateral  $\pi$ -stacking of four twisted antiparallel  $\beta$ -sheets with Fmoc-F<sub>2</sub> peptides [129]. Strong, noncovalent interactions through  $\pi$ -stacking of the  $\beta$ -sheet peptide nanotubes formed significantly rigid hydrogels [128]. The common cell binding motive RGD was also utilized to prepare Fmoc-RGD tripeptides. The self-assembled nanofibers display the RGD sequences at the fiber surface, which makes the bioactive domain readily available to surrounding cells [130].

Xu and coworkers designed a number of dipeptide hydrogelators where the aromatic motif was selected as the naphthyl group (Nap) due to the presence of clinically approved drug molecules that contain the naphthalene fragment [131]. Biocompatibility of hydrogels prepared with Nap-GG, Nap-G<sup>D</sup>A, Nap-GA or Nap-GS was tested with HeLa cells. All four hydrogels displayed near 100% cell survival after culture for 24 h. For Nap-GA, it was proposed that hydrogen bonding between dipeptides together with  $\pi$ -stacking of the naphthyl groups cooperatively result in supramolecular nanofibers that lead to 3D hydrogels.

## 2.4 Hydrogels Based on Peptide Amphiphiles

As mentioned in the Introduction, one is not exclusively limited to peptide chemistry when designing hydrogel materials that contain peptide functionality. Hybrid molecules that are part peptide and part organic functionality provide powerful tools for assembly of hydrogels. PAs are self-assembling molecules that form cylindrical micelle nanofibers [132]. The nanofibers assemble into interwoven, viscoelastic 3D hydrogels when a sufficient concentration is reached. The PA molecules are composed of a hydrophobic alkyl tail, a short peptide block capable of forming hydrogen bonds with other peptide segments through intermolecular interactions, a short block that is relatively hydrophilic to impart water solubility in addition to pH and salt responsiveness, and a short bioactive headgroup. Self-assembly of the PAs are triggered by either changes in pH to neutralize residues or addition of ions into the medium to screen charge repulsions. Under appropriate conditions, hydrophobic collapse of long alkyl tails forms the fiber core, and the peptide segments are displayed on the outside in the form of a  $\beta$ -sheet or  $\alpha$ -helix. Self-assembling PAs have gained a lot of attention because consistent nanostructures and biochemical functionality can easily be engineered into these systems. The Stupp laboratory has developed various PAs that self-assemble into high-aspect ratio nanofibers that form hydrogel networks. The PAs can also be crosslinked by formation of disulfide bonds under oxidizing conditions through incorporation of cysteine residues along the peptide block [133] or by UV irradiation of incorporated diacetylene groups in the hydrophobic block [134, 135]. The peptide sequence adjacent to the alkyl chain, which is mostly a  $\beta$ -sheet-promoting sequence, can be changed into bulky, more hydrophilic residues such as SLSLGGG instead of AAAAGGG to slow down gelation kinetics to allow a longer time frame for injection of the materials without clogging a syringe [136]. The ability to modify the peptide sequence that is exposed on the surface facilitated the use of these PAs as bioactive scaffolds for various applications. Peptide epitopes such as RGDS [133, 136–138] and IKVAV [139] have been incorporated into PAs to enhance cell adhesion to the self-assembled nanofibers. IKVAV, which is naturally found in laminin, was used for neural attachment, migration, and neurite outgrowth. A cytotoxic, cationic  $\alpha$ -helical (KLAKLAK)<sub>2</sub> (“KLAK”) peptide was also conjugated into the PAs to induce cancer cell death by membrane disruption [140].

Without any purposeful alignment, hydrogels normally display a high degree of isotropy with randomly oriented fibers or fibrils. Recently, strings of aligned peptide amphiphile nanofibers were prepared and used to direct the orientation of human mesenchymal stem cells (hMSCs) in 3D environments [141]. The peptide amphiphile,  $V_2A_3E_3(CO_2H)$  and a  $C_{16}$  alkyl chain at the peptide's N-terminus, was self-assembled in water into long cylindrical, worm-like nanofibers that crosslink into a gel in ionic medium. Heating of the nanofiber suspension caused assembly of individual nanofibers into plaque-like sheets, and subsequent cooling resulted in an aligned liquid-crystalline phase of nanofiber bundles. The significance of this work is the anisotropic rupture of plaques into aligned bundles on cooling and the ability to crosslink these anisotropic nanofibers in ionic medium to create 3D environments for encapsulated cells [142].

Finally, just as in the case of pure peptide nanofibrils, the specific cylindrical nanostructure of the assembled PA molecules provides the opportunity for specific display of chemical functionality. This display can, in turn, be used to design a hydrogel system with a specific biological function. For example, vascular endothelial growth factor (VEGF) and fibroblast growth factor (FGF) are heparin-binding growth factors for vascular endothelial cells and fibroblasts that are able to induce angiogenesis (formation of new blood vessels from pre-existing ones) in vivo [143, 144]. Some earlier methods employed to control angiogenesis in tissue engineering involved matrices in which the matrix–heparin microstructure on the molecular scale was not well defined, which limited a clear understanding of how heparin was geometrically displayed for the recruitment of growth factors [145]. Self-assembling PAs with strong heparin binding affinity have been recently suggested as a biomimetic strategy to produce angiogenic matrixes [145]. The heparin-binding consensus sequence [146] XBBBXXBX (where B is a basic amino acid and X is a hydrophobic amino acid) was used as a model to design the peptide LRKCLGKA [145]. Heparin is used as a mediator to trigger the self-assembly process by changing the  $\alpha$ -helical peptide to a  $\beta$ -sheet conformation, leading to the formation of cylindrical nanostructures. It is proposed that these rigid cylindrical morphologies are superior to conventional polymer chains in growth factor recruiting due to the fact that the Brownian motion would be minimized, opposing cell signaling and the entropic cost associated with the ligand–receptor binding.

Gelation in peptide gel formers does not only depend on amino acid sequence, chain length, and peptide concentration but also depends on chain conformation [147]. Deming and coworkers investigated diblock copolypeptides ( $K_xL_y$  and  $K_xV_y$ ) with hydrophobic domains that can adopt either  $\alpha$ -helix [poly( $^L$ L)],  $\beta$ -sheet [poly( $^L$ V)], or random coil conformations. Although not PA molecules in the sense that they are small-molecule peptides attached to a hydrophobic aliphatic tail, the block copolypeptides are PAs in the sense that they are large amphiphiles with pure peptidic chemistry. Random conformation was achieved by using racemic leucine in the hydrophobic block (equal portions of L- and D-leucine). Gelation at low concentration of the PAs was observed in samples with strong hydrophobic associations as a result of the ordered packing of  $\alpha$ -helical or  $\beta$ -strand segments.



Such hydrogels have been suggested to be suitable for biotechnological applications (DNA delivery vehicles, cell encapsulation) [28]. Recently, amphiphilic diblock copolypeptide hydrogels of  $K_{180}L_{20}$  were used in an *in vivo* study where the hydrogels were injected into the mouse forebrain. Evaluation of samples displayed substantial tissue integration with little or no detectable toxicity in the central nervous system [148].

## 2.5 *Elastin-Like Polypeptide-Based Hydrogels*

While the PA and block copolypeptides mentioned above are excellent examples of peptide or polypeptide hydrogel formers using biological chemical functionality, namely amino acids, to form assembled structures, other hydrogels draw their inspiration much more specifically from a particular natural protein. For example, the mammalian elastic protein, elastin, is a major protein component of the connective tissues including vascular wall and is responsible for keeping the tissues flexible. Recombinant techniques have enabled the preparation of monodisperse complex macromolecules in an easy way and, thus, the synthesis of polymers with elastin-inspired sequences in the polypeptide or polypeptide-synthetic hybrid. The naturally occurring motive (VPG-Xaa-G) is common to all elastin-like polypeptides (ELPs), where Xaa is termed the guest residue and can be any of the naturally occurring amino acids with the exception of proline [149]. Due to their biocompatibility, ELPs have been proposed for a series of drug delivery and tissue engineering applications [150]. Elastin displays thermoresponsive behavior that allows control over the thermal transition temperature ( $T_t$ ) by changing hydrophobicity, molecular weight, and concentration of the polypeptide. ELPs are water-soluble at temperatures below their characteristic  $T_t$ . When the temperature is raised above the  $T_t$  the ELPs undergo a phase transition into an aggregated state. This aggregated state can be used to form crosslinks to form a network and/or a responsive system for delivery. The strategy for drug delivery in such systems is to adjust the  $T_t$  of the polypeptide so that it lies between body temperature and the hyperthermic temperature applied. The ELP will circulate freely at normal body temperature but will aggregate and thus become localized once external temperature is applied to raise the intended tissue above the ELP's  $T_t$ . The thermoresponsive behavior of the pentapeptide is observed not only with polypeptides but also with a single repeat of VPGVG [151]. Research on ELPs is predominantly with linear macromolecules because the synthesis of linear polypeptides with SPPS or recombinant methods is straightforward. There has also been interest in using ELPs as pendant groups on polymer chains in a versatile approach to producing thermally responsive triblock copolymers [152]; however, the hydrogel-forming capabilities of these polymers have not been mentioned [18]. Substitution of the fourth residue in the pentapeptide with different amino acids facilitates chemical modifications such as crosslinking or peptide functionalization of ELPs [153]. Placement of a hydrophobic amino acid in the fourth position was found to cause conformational

changes from random coil to repetitive type II  $\beta$ -turns at temperatures below 37°C [154]. However, placement of a charged amino acid, like glutamic acid, on the same position did not alter chain conformation [154–156]. In a recent study, thermally responsive and crosslink-stabilized micelles were prepared with recombinant amphiphilic diblock copolymers tailored with cysteine-containing domains in between the blocks [157]. An increase in temperature above 10°C induced conformational changes in the hydrophobic block from random coil to type II  $\beta$ -turns. This thermoresponsive, reversible conformational change triggered the self-assembly and resulted in the formation of micelles. Cysteine residues in between the blocks facilitated stabilization of the micelles through disulfide crosslinking. The hydrophobic core promotes encapsulation of hydrophobic drugs for drug delivery applications. Again, these are not hydrogelation systems but use the ELP thermoresponsiveness of ELP protein segments to induce assembly and provide potential function.

In a recent study, the dependency of mechanical properties and chondrogenesis on the frequency of reactive lysine residues and molecular weight of various ELP hydrogels was investigated [158]. The crosslinking density, which is dependent on the frequency of the reactive lysine residues, was observed to be a powerful determinant factor of both mechanical properties and biological outcomes when compared to the molecular weight of the uncrosslinked ELPs chains. Thermoresponsive behavior of ELPs and chemical conjugation methods were combined to design thermally targeted drug carriers for the delivery of antitumor agents. Strategies involved conjugation of the chemotherapeutic agent doxorubicin (Dox) to ELP through an acid-labile hydrazine bond that aimed to promote release of the drug in the low pH environment once inside the squamous carcinoma cells (FaDu) [159].

For increased cell permeability of the ELP–drug conjugates, Tat-ELP-GFLG-Dox was recently used in an *in vitro* setting for its potent cytotoxic effects towards MES-SA, uterine sarcoma cells [160]. The Tat peptide, originally derived from HIV-1 Tat protein (Tat), was conjugated to ELP for its cell penetrating ability. The cleavable (by lysosomal proteases) tetrapeptide linker, GFLG, and the C-terminal cysteine residue were used for the attachment of drugs to the macromolecule. Tropoelastin, the soluble monomer of elastin, is also a versatile building block for the construction of biomaterials with potential for diverse applications in elastic tissues [161]. Kaplan and coworkers reported a protein blend system based on silkworm fibroin and recombinant human tropoelastin that promotes mesenchymal stem cell attachment and proliferation [162]. Silk fibroin is a semicrystalline fibrous protein with  $\beta$ -sheet crystals that provides mechanical strength to tropoelastin. Varying  $\beta$ -sheet crystal content in the physical polymer blends removes the need for chemical crosslinking due to hydrogen bonding between silk fibroin and tropoelastin. At a mass mixing ratio of 25:75 (silk:tropoelastin), the tropoelastin formed a bicontinuous interpenetrating network that suggested future use for biomedical applications as hydrogels.

## 2.6 Organic–Inorganic Hybrid Materials

Biomimicry also entails co-existence of hard and soft materials as nature is replete with organisms in which certain proteins have the ability to template inorganic materials [163]. In this respect, polycationic peptides [163], polymer–peptide hybrids [164], and block co-polypeptides [165] have been used to catalyze formation of silica into various morphologies. Ideally, the peptidic nanostructure and material would then display synergistic properties of the peptidic nanostructure and the inorganic material. In an attempt to mimic bone tissue, Hartgerink et al. integrated phosphorylated serine residues into peptide amphiphiles to direct templated mineralization of hydroxyapatite on self-assembled  $\beta$ -sheet fibers [133]. The controlled precipitation of minerals in 3D could lead to biomimetic materials that promote bone formation. This strategy could be used to repair fractures and reconstruct joints [166]. Templated growth has been observed in self-assembled  $\beta$ -sheet peptide fibrils [167, 168] and PAs [169] that catalyze polymerization of silica onto fiber surfaces. Construction of such organic–inorganic hybrid networks can improve mechanical properties. For example, scaffolds with about three orders of magnitude greater stiffness have been observed after sol–gel processing of self-assembled peptide hydrogels [167]. A route in which dynamic supramolecular self-assembly of  $\beta$ -sheet peptides and silica deposition on the surface of fibrils act synergistically has also been reported [170].

## 3 Polymer–Peptide Conjugates

Progress on physiologically benign conjugation techniques has enabled addition of thermal responsiveness and biological and chemical recognition to otherwise inert synthetic polymers by the addition of peptidic sequences. Poly(ethylene glycol) (PEG) and PEO are oligomers of low (<20,000 g/mol) and high (>20,000 g/mol) molecular weight ethylene oxide, respectively. PEGylation is a commonly employed method to reduce immunogenicity and enhance solubility, stability and circulation of peptides, proteins, or antibodies. PEG hydrogels that are not derivatized with functional peptides are usually poor substrates for adhesion in tissue culture studies for tissue engineering applications. Although this poor adhesion has proven to be beneficial in reducing postoperative adhesions in animal models, PEG hydrogels provide a platform for the incorporation of synthetic adhesion peptides to permit biospecific tissue resurfacing [171]. Conventional methods used for incorporation of peptide sequences into the PEG hydrogel involve functionalizing the N-terminus of the peptide sequence with an acrylate moiety (*N*-hydroxysuccinimidyl), facilitating the rapid copolymerization of the adhesion peptide with the PEG mono- or diacrylate upon photoinitiation [171]. For example, short peptide sequences inspired by the fibrin coiled-coil were used to prepare triblock peptide–PEG–peptide bioconjugates that self-assembled into viscoelastic hydrogels

[172]. Amino acid substitutions on the native  $\gamma_{52-88}$ KI peptide, coiled-coil domain of human fibrin were able to stabilize the coiled-coil formation. These substitutions were targeted to the positions that compose the interface between coiled-coil strands while the solvent-exposed residues were left unperturbed. This strategy aimed at reducing the likelihood of immunogenicity for future in vivo application of these materials. In contrast to PEG block copolymers with end blocks that are not used for directed assembly, PEG copolymers with coiled-coil protein motives aim to enhance intermolecular interactions and control over the assembly conditions [85, 173].

Some studies involving in vivo applications of RGD-containing surfaces have reported some challenges such as limited selectivity for integrins and conformational differences of peptides exposed on surfaces compared to the native ECM ligand [174]. Consequently, some of the recent efforts to overcome these limitations involve presentation of the cell binding motifs with either cyclic or oligomeric peptides presenting multiple arms. Modifications of surface chemistries exposed on the materials are vital for controlling the biological activity of adsorbed proteins by directing protein adsorption and conformation [174]. The presence of functional motives seems to be as important as the architecture of the scaffold and presentation of the functional domains, especially under complex in vivo conditions. Other matrix-derived adhesive peptide sequences like RGD, IKVAV, LRE, PDSGR, YIGSR, DGEA (a sequence derived from collagen type I), and combinations of these have been covalently attached to linear PEG chains for creating 3D hydrogel environments for the encapsulation of pancreatic islet cells [175].

Overall, cell adhesion, migration, and proteolytic degradation are highly important issues in colonization of biomaterials by cells. To create multifunctional 3D environments for cells, end-functionalized multiarm PEG macromers have been crosslinked with a variety of oligopeptides. Integrin-binding sites and substrates for matrix metalloproteinases (MMP) have been incorporated into synthetic hydrogels to render adhesion and MMP-mediated invasion into hydrogel networks [176].

As discussed earlier, the suitability of mechanical properties of scaffolds relative to target cells has been recognized as one of the driving factors in stem cell lineage specificity [177]. Mechanical properties (storage moduli) of self-assembling systems are usually limited to  $\sim 10$  kPa [178] because such systems lack chemical crosslinks. We have described some of the methods employed recently to improve the mechanical properties of self-assembling peptide or polypeptide systems. Motivated to create bioactive hydrogels with enhanced mechanical properties, an injectable, thermosensitive poly(organophosphazene)-peptide conjugate was prepared through a covalent amide linkage between the carboxylic acid-terminated poly(organophosphazene) and a peptide, GRGDS, in the presence of isobutyl chloroformate as the activator [179]. The thermoresponsive poly(organophosphazene) domain of the conjugate facilitated subcutaneous injection of rabbit MSCs at room temperature into a nude mouse. The aqueous polymer-peptide conjugates displayed sol-gel transition at body temperature. The viscoelastic xenografts facilitated osteogenesis in rabbit MSCs. While polymers can provide responsiveness to peptides as in the previous example, the presence of peptides in

polymer–peptide hybrids can also impart environmental responsiveness to polymers. *N*-(2-Hydroxypropyl)methacrylamide (HPMA) was prepared by attaching coiled-coil forming peptides to a linear water-soluble polyHPMA backbone. Peptides of different lengths that adopt coiled-coil motifs facilitated control over the preparation of 3D hydrogels by nonspecific hydrophobic association and specific spatial recognition of coiled-coil motifs [180–182].

Besides contributors as bioactive elements, peptides have been also utilized to direct architectural properties of polymers. However, the structures obtained as a result of self-assembly cannot be solely attributed to the peptide domain. PEO-F<sub>4</sub>-OEt and PEO-V<sub>4</sub>-OEt conjugates represent a good example of this phenomenon, whereby PEO length was found to have a profound effect on the outcome of the self-assembly of PEO-F<sub>4</sub>-OEt but not on PEO-V<sub>4</sub>-OEt [183]. Self-assembly into nanotubes, fibers, and wormlike micelles was affected by various PEO lengths. Formation of antiparallel  $\beta$ -sheets have been observed with shorter PEO blocks whereas aromatic stacking becomes predominant with longer PEO blocks. Due to the stronger propensity of valine side chains to form  $\beta$ -sheets, the length of the PEO group did not affect the formation of aggregates with  $\beta$ -sheet and random coil conformation, thus gelation with PEO-V<sub>4</sub>-OEt samples with various PEO lengths was not achieved.

## 4 Conclusions

Many innovative methods have been suggested for tissue engineering scaffolds and drug delivery vehicles, as demonstrated by the body of work discussed herein. Every system has its own unique preparation conditions, degradation rates, gel strength etc. that is designed for a solution in a particular biomedical application. Some challenges remain regarding clinical ease of use and applicability.

One of these challenges is to improve the injectability of the system to facilitate minimally invasive delivery of the constructs. Traditional polymeric hydrogels are predominantly designed to be injected as free-flowing solutions and to solidify into a chemically crosslinked gel within the body through various mechanisms. The low-viscosity polymer solution therefore can leak to surrounding tissues during the time needed for gelation. *Ex vivo* gelled polymer solutions on the other hand would require surgical transplantation but would then not be able to fit into an ill-defined defect. Thermosensitive block copolymers have the risk of syringe clogging during injection if the gelation temperature is not tailored properly or polymer concentration is too high. Gelation with injectable self-assembling hydrogels on the other hand is achieved through noncovalent, physical crosslinking that gives the hydrogel the ability to flow as a low viscosity solution under shear. Due to the nature of the physical forces that form the network, the hydrogels can subsequently recover their pre-shear mechanical properties upon removal of the shear force. However, not all fibrillar peptide and polypeptide hydrogels are shear-thinning and subsequently

rehealing. More work must be done in order to elucidate general design parameters to engineer this property into new systems.

Control over degradation rates that facilitate appropriate time frames for clearance of the scaffold or delivery vehicle from the body is also an important issue. These properties depend highly on the desired application; scaffolds loaded with cells or drugs may require slowly degrading materials for long-term applications. Other important concerns for new peptide and polypeptide gels include biodistribution profiles and clearance from the body. Elimination of toxic degradation products also needs consideration. Finally, although some peptide hydrogels provide control over ligand type and density, they fail to recreate molecular level spatial organization of natural ECM. Hence, another goal for current research in regenerative medicine involves exact control over spatial organization of components in 3D because this would enable mimicking the highly complex microarchitecture of ECM. Peptides, polypeptides, and conjugates or hybrids provide excellent opportunities to push forward into new hydrogel research in order to tackle the challenges described above.

## References

1. Dujardin E, Mann S (2002) Bio-inspired materials chemistry. *Adv Mater* 14:775–788
2. Bhushan B, Jung YC (2011) Natural and biomimetic artificial surfaces for superhydrophobicity, self-cleaning, low adhesion, and drag reduction. *Prog Mater Sci* 56:1–108
3. Foo CWP, Huang J, Kaplan DL (2004) Lessons from seashells: silica mineralization via protein templating. *Trends Biotechnol* 22:577–585
4. Sundar VC, Yablon AD, Grazul JL et al (2003) Fibre-optical features of a glass sponge – some superior technological secrets have come to light from a deep-sea organism. *Nature* 424:899–900
5. Murphy WL, Mooney DJ (2002) Molecular-scale biomimicry. *Nat Biotechnol* 20:30–31
6. Pradhan S, Farach-Carson MC (2010) Mining the extracellular matrix for tissue engineering applications. *Regen Med* 5:961–970
7. Ruoslahti E, Pierschbacher MD (1987) New perspectives in cell-adhesion - RGD and integrins. *Science* 238:491–497
8. Keeley FW, Bellingham CM, Woodhouse KA (2002) Elastin as a self-organizing biomaterial: use of recombinantly expressed human elastin polypeptides as a model for investigations of structure and self-assembly of elastin. *Philos Trans R Soc Lond B Biol Sci* 357:185–189
9. Mitra A, Mulholland J, Nan A et al (2005) Targeting tumor angiogenic vasculature using polymer-RGD conjugates. *J Control Release* 102:191–201
10. Burdick JA, Anseth KS (2002) Photoencapsulation of osteoblasts in injectable RGD-modified PEG hydrogels for bone tissue engineering. *Biomaterials* 23:4315–4323
11. VandeVondele S, Voros J, Hubbell JA (2003) Rgd-grafted poly-L-lysine-graft-(polyethylene glycol) copolymers block non-specific protein adsorption while promoting cell adhesion. *Biotechnol Bioeng* 82:784–790
12. Amblard M, Fehrentz J, Martinez J et al (2005) Peptide synthesis and applications. In: Howl J (ed) *Springer protocols*. Humana Press, Totowa
13. Gauthier MA, Klok HA (2008) Peptide/protein-polymer conjugates: synthetic strategies and design concepts. *Chem Commun* 23:2591–2611

14. Guzman F, Barberis S, Illanes A (2007) Peptide synthesis: chemical or enzymatic. *Electron J Biotechnol* 10:279–314
15. Kiick KL (2007) Biosynthetic methods for the production of advanced protein-based materials. *Polym Rev* 47:1–7
16. Bray BL (2003) Large-scale manufacture of peptide therapeutics by chemical synthesis. *Nat Rev Drug Discov* 2:587–593
17. Nilsson BL, Soellner MB, Raines RT (2005) Chemical synthesis of proteins. *Annu Rev Biophys Biomol Struct* 34:91–118
18. Adams DJ, Topham PD (2010) Peptide conjugate hydrogelators. *Soft Matter* 6:3707–3721
19. Kramer JR, Deming TJ (2010) Glycopolypeptides via living polymerization of glycosylated-l-lysine n-carboxyanhydrides. *J Am Chem Soc* 132:15068–15071
20. Top A, Kiick KL (2010) Multivalent protein polymers with controlled chemical and physical properties. *Adv Drug Deliv Rev* 62:1530–1540
21. van Hest JCM, Tirrell DA (2001) Protein-based materials, toward a new level of structural control. *Chem Commun* 19:1897–1904
22. Wang L, Xie J, Schultz PG (2006) Expanding the genetic code. *Annu Rev Biophys Biomol Struct* 35:225–249
23. Tiefenbrunn TK, Dawson PE (2010) Chemoselective ligation techniques: modern applications of time-honored chemistry. *Biopolymers* 94:95–106
24. Reynhout IC, Lowik D, van Hest JCM et al (2005) Solid phase synthesis of biohybrid block copolymers. *Chem Commun* 602–604
25. Mei Y, Beers KL, Byrd HCM et al (2004) Solid-phase atp synthesis of peptide- polymer hybrids. *J Am Chem Soc* 126:3472–3476
26. Loschonsky S, Shroff K, Worz A et al (2008) Surface-attached pdmaa-grgdsp hybrid polymer monolayers that promote the adhesion of living cells. *Biomacromolecules* 9:543–552
27. Peppas NA, Huang Y, Torres-Lugo M et al (2000) Physicochemical, foundations and structural design of hydrogels in medicine and biology. *Annu Rev Biomed Eng* 2:9–29
28. Nowak AP, Breedveld V, Pakstis L et al (2002) Rapidly recovering hydrogel scaffolds from self-assembling diblock copolypeptide amphiphiles. *Nature* 417:424–428
29. Wichterle O, Lim D (1960) Hydrophilic gels for biological use. *Nature* 185:117–118
30. Romano NH, Sengupta D, Chung C et al (2010) Protein-engineered biomaterials: nanoscale mimics of the extracellular matrix. *Biochim Biophys Acta* 1810:339–349
31. Freed LE, Engelmayr GC, Borenstein JT et al (2009) Advanced material strategies for tissue engineering scaffolds. *Adv Mater* 21:3410–3418
32. Langer R (2000) Biomaterials in drug delivery and tissue engineering: one laboratory's experience. *Acc Chem Res* 33:94–101
33. Lanza RP, Langer R, Vacanti J (2007) Principles of tissue engineering. Academic, San Diego
34. Burdick JA, Vunjak-Novakovic G (2009) Engineered microenvironments for controlled stem cell differentiation. *Tissue Eng A* 15:205–219
35. Tibbitt MW, Anseth KS (2009) Hydrogels as extracellular matrix mimics for 3d cell culture. *Biotechnol Bioeng* 103:655–663
36. Liu WF, Chen CS (2005) Engineering biomaterials to control cell function. *Mater Today* 8:28–35
37. Tse JR, Engler AJ (2010) Preparation of hydrogel substrates with tunable mechanical properties. In: Bonifacino JS (ed) *Current protocols in cell biology*. Wiley, Somerset
38. Bettinger CJ, Weinberg EJ, Kulig KM et al (2006) Three-dimensional microfluidic tissue-engineering scaffolds using a flexible biodegradable polymer. *Adv Mater* 18:165–169
39. Bowman CN, Kloxin CJ (2008) Toward an enhanced understanding and implementation of photopolymerization reactions. *AIChE J* 54:2775–2795
40. Green JJ, Langer R, Anderson DG (2008) A combinatorial polymer library approach yields insight into nonviral gene delivery. *Acc Chem Res* 41:749–759
41. Yamamoto M, Tabata Y, Ikada Y (1999) Growth factor release from gelatin hydrogel for tissue engineering. *J Bioact Compat Polym* 14:474–489

42. Young S, Wong M, Tabata Y et al (2005) Gelatin as a delivery vehicle for the controlled release of bioactive molecules. *J Control Release* 109:256–274
43. Farmer RS, Kiick KL (2005) Conformational behavior of chemically reactive alanine-rich repetitive protein polymers. *Biomacromolecules* 6:1531–1539
44. Hirano Y, Mooney DJ (2004) Peptide and protein presenting materials for tissue engineering. *Adv Mater* 16:17–25
45. Lamm MS, Sharma N, Rajagopal K et al (2008) Laterally spaced linear nanoparticle arrays templated by laminated beta-sheet fibrils. *Adv Mater* 20:447–451
46. Liu S, Kiick KL (2008) Architecture effects on the binding of cholera toxin by helical glycopolypeptides. *Macromolecules* 41:764–772
47. Sharma N, Top A, Kiick KL et al (2009) One-dimensional gold nanoparticle arrays by electrostatically directed organization using polypeptide self-assembly. *Angew Chem Int Ed* 48:7078–7082
48. Collier JH, Messersmith PB (2004) Self-assembling polymer-peptide conjugates: nanostructural tailoring. *Adv Mater* 16:907–910
49. Hamley IW, Ansari A, Castelletto V et al (2005) Solution self-assembly of hybrid block copolymers containing poly(ethylene glycol) and amphiphilic beta-strand peptide sequences. *Biomacromolecules* 6:1310–1315
50. Hentschel J, Krause E, Borner HG (2006) Switch-peptides to trigger the peptide guided assembly of poly(ethylene oxide)-peptide conjugates into tape structures. *J Am Chem Soc* 128:7722–7723
51. Minh KN, Lee DS (2010) Injectable biodegradable hydrogels. *Macromol Biosci* 10:563–579
52. Yan CQ, Pochan DJ (2010) Rheological properties of peptide-based hydrogels for biomedical and other applications. *Chem Soc Rev* 39:3528–3540
53. Rughani RV, Branco MC, Pochan D et al (2010) De novo design of a shear-thin recoverable peptide-based hydrogel capable of intrafibrillar photopolymerization. *Macromolecules* 43:7924–7930
54. Sallach RE, Cui W, Wen J et al (2009) Elastin-mimetic protein polymers capable of physical and chemical crosslinking. *Biomaterials* 30:409–422
55. Aulisa L, Dong H, Hartgerink JD (2009) Self-assembly of multidomain peptides: sequence variation allows control over cross-linking and viscoelasticity. *Biomacromolecules* 10:2694–2698
56. Miao M, Cirulis JT, Lee S et al (2005) Structural determinants of cross-linking and hydrophobic domains for self-assembly of elastin-like polypeptides. *Biochemistry* 44:14367–14375
57. Grzybowski BA, Wilmer CE, Kim J et al (2009) Self-assembly: from crystals to cells. *Soft Matter* 5:1110–1128
58. McMillan RA, Conticello VP (2000) Synthesis and characterization of elastin-mimetic protein gels derived from a well-defined polypeptide precursor. *Macromolecules* 33:4809–4821
59. Alberts B, Bray D, Lewis J et al (1994) *Molecular biology of the cell*. Garland, New York
60. Kopecek J, Yang JY (2009) Peptide-directed self-assembly of hydrogels. *Acta Biomater* 5:805–816
61. Whitesides GM, Boncheva M (2002) Beyond molecules: self-assembly of mesoscopic and macroscopic components. *Proc Natl Acad Sci* 99:4769–4774
62. Merlini G, Bellotti V (2003) Molecular mechanisms of amyloidosis. *N Engl J Med* 349:583–596
63. Gunasekaran K, Ramakrishnan C, Balaram P (1997) Beta-hairpins in proteins revisited: lessons for de novo design. *Protein Eng* 10:1131–1141
64. Blanco FJ, Jimenez MA, Herranz J et al (1993) Nmr evidence of a short linear peptide that folds into a beta-hairpin in aqueous-solution. *J Am Chem Soc* 115:5887–5888
65. Haque TS, Little JC, Gellman SH (1994) Mirror-image reverse turns promote beta-hairpin formation. *J Am Chem Soc* 116:4105–4106



66. Barlow DJ, Thornton JM (1988) Helix geometry in proteins. *J Mol Biol* 201:601–619
67. Presta LG, Rose GD (1988) Helix signals in proteins. *Science* 240:1632–1641
68. Lyu PC, Liff MI, Marky LA et al (1990) Side-chain contributions to the stability of alpha-helical structure in peptides. *Science* 250:669–673
69. Oneil KT, Degradó WF (1990) A thermodynamic scale for the helix-forming tendencies of the commonly occurring amino-acids. *Science* 250:646–651
70. Liu W, Jawerth LM, Sparks EA et al (2006) Fibrin fibers have extraordinary extensibility and elasticity. *Science* 313:634–634
71. Piechocka IK, Bacabac RG, Potters M et al (2010) Structural hierarchy governs fibrin gel mechanics. *Biophys J* 98:2281–2289
72. Brown AEX, Litvinov RI, Discher DE et al (2007) Forced unfolding of the coiled-coils of fibrinogen by single molecule afm. *Biophys J* 92:L39–L42
73. Fong JH, Keating AE, Singh M (2004) Predicting specificity in bZIP coiled-coil protein interactions. *Genome Biol* 5:R11
74. Dong H, Paramonov SE, Hartgerink JD (2008) Self-assembly of alpha-helical coiled coil nanofibers. *J Am Chem Soc* 130:13691–13695
75. Liu J, Zheng Q, Deng YQ et al (2006) A seven-helix coiled coil. *Proc Natl Acad Sci* 103:15457–15462
76. Landschulz WH, Johnson PF, McKnight SL (1988) The leucine zipper – a hypothetical structure common to a new class of DNA-binding proteins. *Science* 240:1759–1764
77. Petka WA, Harden JL, McGrath KP et al (1998) Reversible hydrogels from self-assembling artificial proteins. *Science* 281:389–392
78. Wang C, Stewart RJ, Kopecek J (1999) Hybrid hydrogels assembled from synthetic polymers and coiled-coil protein domains. *Nature* 397:417–420
79. Shen W (2005) Structure, dynamics, and properties of artificial protein hydrogels assembled through coiled-coil domains. California Institute of Technology, Pasadena
80. Shen W, Zhang KC, Kornfield JA et al (2006) Tuning the erosion rate of artificial protein hydrogels through control of network topology. *Nat Mater* 5:153–158
81. Ryan SJ, Kennan AJ (2007) Variable stability heterodimeric coiled-coils from manipulation of electrostatic interface residue chain length. *J Am Chem Soc* 129:10255–10260
82. Mi LX, Fischer S, Chung B et al (2006) Self-assembling protein hydrogels with modular integrin binding domains. *Biomacromolecules* 7:38–47
83. Cao Y, Li HB (2008) Engineering tandem modular protein based reversible hydrogels. *Chem Commun* 4144–4146
84. Liu B, Lewis AK, Shen W (2009) Physical hydrogels photo-cross-linked from self-assembled macromers for potential use in tissue engineering. *Biomacromolecules* 10:3182–3187
85. Vandermeulen GWM, Tziatzios C, Duncan R et al (2005) Peg-based hybrid block copolymers containing alpha-helical coiled coil peptide sequences: control of self-assembly and preliminary biological evaluation. *Macromolecules* 38:761–769
86. Banwell EF, Abelardo ES, Adams DJ et al (2009) Rational design and application of responsive alpha-helical peptide hydrogels. *Nat Mater* 8:596–600
87. Woolfson DN, Ryadnov MG (2006) Peptide-based fibrous biomaterials: some things old, new and borrowed. *Curr Opin Chem Biol* 10:559–567
88. Makin OS, Atkins E, Sikorski P et al (2005) Molecular basis for amyloid fibril formation and stability. *Proc Natl Acad Sci* 102:315–320
89. Hayashi CY, Shipley NH, Lewis RV (1999) Hypotheses that correlate the sequence, structure, and mechanical properties of spider silk proteins. *Int J Biol Macromol* 24:271–275
90. Parkhe AD, Seeley SK, Gardner K (1997) Structural studies of spider silk proteins in the fiber. *J Mol Recognit* 10:1–6
91. Slotta U, Hess S, Spiess K et al (2007) Spider silk and amyloid fibrils: a structural comparison. *Macromol Biosci* 7:183–188
92. Matsumoto A, Chen J, Collette AL et al (2006) Mechanisms of silk fibroin sol-gel transitions. *J Phys Chem B* 110:21630–21638

93. Brack A, Orgel LE (1975) Beta-structures of alternating polypeptides and their possible prebiotic significance. *Nature* 256:383–387
94. Brack A, Spach G (1981) Multiconformational synthetic polypeptides. *J Am Chem Soc* 103:6319–6323
95. Xiong HY, Buckwalter BL, Shieh HM et al (1995) Periodicity of polar and nonpolar amino-acids is the major determinant of secondary structure in self- assembling oligomeric peptides. *Proc Natl Acad Sci* 92:6349–6353
96. Aggeli A, Bell M, Boden N et al (1997) Engineering of peptide beta-sheet nanotapes. *J Mater Chem* 7:1135–1145
97. Aggeli A, Bell M, Boden N et al (1997) Responsive gels formed by the spontaneous self-assembly of peptides into polymeric beta-sheet tapes. *Nature* 386:259–262
98. Yang JJ, Pitkeathly M, Radford SE (1994) Far-uv circular-dichroism reveals a conformational switch in a peptide fragment from the beta-sheet of hen lysozyme. *Biochemistry* 33:7345–7353
99. Zhang SG, Lockshin C, Herbert A et al (1992) Zuoitin, a putative z-DNA binding- protein in *saccharomyces-cerevisiae*. *EMBO J* 11:3787–3796
100. Zhang SG, Holmes T, Lockshin C et al (1993) Spontaneous assembly of a self- complementary oligopeptide to form a stable macroscopic membrane. *Proc Natl Acad Sci* 90:3334–3338
101. Semino CE, Kasahara J, Hayashi Y et al (2004) Entrapment of migrating hippocampal neural cells in three-dimensional peptide nanofiber scaffold. *Tissue Eng* 10:643–655
102. Semino CE, Merok JR, Crane GG et al (2003) Functional differentiation of hepatocyte-like spheroid structures from putative liver progenitor cells in three- dimensional peptide scaffolds. *Differentiation* 71:262–270
103. Holmes TC, de Lacalle S, Su X et al (2000) Extensive neurite outgrowth and active synapse formation on self-assembling peptide scaffolds. *Proc Natl Acad Sci* 97:6728–6733
104. Zhang SG (2002) Emerging biological materials through molecular self-assembly. *Biotechnol Adv* 20:321–339
105. Collier JH, Hu BH, Ruberti JW et al (2001) Thermally and photochemically triggered self-assembly of peptide hydrogels. *J Am Chem Soc* 123:9463–9464
106. Schneider JP, Pochan DJ, Ozbas B et al (2002) Responsive hydrogels from the intramolecular folding and self-assembly of a designed peptide. *J Am Chem Soc* 124:15030–15037
107. Ozbas B, Kretsinger J, Rajagopal K et al (2004) Salt-triggered peptide folding and consequent self-assembly into hydrogels with tunable modulus. *Macromolecules* 37:7331–7337
108. Pochan DJ, Schneider JP, Kretsinger J et al (2003) Thermally reversible hydrogels via intramolecular folding and consequent self- assembly of a de novo designed peptide. *J Am Chem Soc* 125:11802–11803
109. Rajagopal K, Ozbas B, Pochan DJ et al (2005) Self-assembled hydrogels from beta- hairpin peptides: tuning responsiveness and bulk material properties by peptide design. *Biopolymers* 80:487–487
110. Kretsinger JK, Haines LA, Ozbas B et al (2005) Cytocompatibility of self-assembled ss-hairpin peptide hydrogel surfaces. *Biomaterials* 26:5177–5186
111. Rajagopal K, Ozbas B, Pochan DJ et al (2006) Probing the importance of lateral hydrophobic association in self-assembling peptide hydrogelators. *Eur Biophys J Biophys Lett* 35:162–169
112. Yucl T, Micklitsch CM, Schneider JP et al (2008) Direct observation of early-time hydrogelation in beta-hairpin peptide self-assembly. *Macromolecules* 41:5763–5772
113. Haines-Butterick L, Rajagopal K, Branco M et al (2007) Controlling hydrogelation kinetics by peptide design for three-dimensional encapsulation and injectable delivery of cells. *Proc Natl Acad Sci* 104:7791–7796
114. Rajagopal K, Lamm MS, Haines-Butterick LA et al (2009) Tuning the ph responsiveness of beta-hairpin peptide folding, self-assembly, and hydrogel material formation. *Biomacromolecules* 10:2619–2625

115. Haines-Butterick LA, Salick DA, Pochan DJ et al (2008) In vitro assessment of the pro-inflammatory potential of beta-hairpin peptide hydrogels. *Biomaterials* 29:4164–4169
116. Hule RA, Nagarkar RP, Altunbas A et al (2008) Correlations between structure, material properties and bioproperties in self-assembled beta-hairpin peptide hydrogels. *Faraday Discuss* 139:251–264
117. Yan CQ, Altunbas A, Yucel T et al (2010) Injectable solid hydrogel: mechanism of shear-thinning and immediate recovery of injectable beta-hairpin peptide hydrogels. *Soft Matter* 6:5143–5156
118. Salick DA, Kretsinger JK, Pochan DJ et al (2007) Inherent antibacterial activity of a peptide-based beta-hairpin hydrogel. *J Am Chem Soc* 129:14793–14799
119. Branco M, Wagner N, Pochan D et al (2009) Release of model macromolecules from self-assembling peptide hydrogels for injectable delivery. *Biopolymers* 92:318–318
120. Ramachandran S, Tseng Y, Yu YB (2005) Repeated rapid shear-responsiveness of peptide hydrogels with tunable shear modulus. *Biomacromolecules* 6:1316–1321
121. Niece KL, Hartgerink JD, Donners J et al (2003) Self-assembly combining two bioactive peptide-amphiphile molecules into nanofibers by electrostatic attraction. *J Am Chem Soc* 125:7146–7147
122. Macias MJ, Gervais V, Civera C et al (2000) Structural analysis of ww domains and design of a ww prototype. *Nat Struct Biol* 7:375–379
123. Foo C, Lee JS, Mulyasmita W et al (2009) Two-component protein-engineered physical hydrogels for cell encapsulation. *Proc Natl Acad Sci* 106:22067–22072
124. Vegners R, Shestakova I, Kalvinsh I et al (1995) Use of a gel-forming dipeptide derivative as a carrier for antigen presentation. *J Pept Sci* 1:371–378
125. Zhang Y, Gu HW, Yang ZM et al (2003) Supramolecular hydrogels respond to ligand-receptor interaction. *J Am Chem Soc* 125:13680–13681
126. Jayawarna V, Ali M, Jowitt TA et al (2006) Nanostructured hydrogels for three-dimensional cell culture through self-assembly of fluorenylmethoxycarbonyl-dipeptides. *Adv Mater* 18:611–614
127. Liebmann T, Rydholm S, Akpe V et al (2007) Self-assembling fmoc dipeptide hydrogel for in situ 3d cell culturing. *BMC Biotechnol* 7:88
128. Mahler A, Reches M, Rechter M et al (2006) Rigid, self-assembled hydrogel composed of a modified aromatic dipeptide. *Adv Mater* 18:1365–1370
129. Smith AM, Williams RJ, Tang C et al (2008) Fmoc-diphenylalanine self assembles to a hydrogel via a novel architecture based on pi-pi interlocked beta-sheets. *Adv Mater* 20:37–41
130. Zhou M, Smith AM, Das AK et al (2009) Self-assembled peptide-based hydrogels as scaffolds for anchorage-dependent cells. *Biomaterials* 30:2523–2530
131. Yang ZM, Liang GL, Ma ML et al (2007) Conjugates of naphthalene and dipeptides produce molecular hydrogelators with high efficiency of hydrogelation and superhelical nanofibers. *J Mater Chem* 17:850–854
132. Anderson JM, Andukuri A, Lim DJ et al (2009) Modulating the gelation properties of self-assembling peptide amphiphiles. *ACS Nano* 3:3447–3454
133. Hartgerink JD, Beniash E, Stupp SI (2001) Self-assembly and mineralization of peptide-amphiphile nanofibers. *Science* 294:1684–1688
134. Lowik D, Shklyarevskiy IO, Ruizendaal L et al (2007) A highly ordered material from magnetically aligned peptide amphiphile nanofiber assemblies. *Adv Mater* 19:1191–1195
135. Stendahl JC, Rao MS, Guler MO et al (2006) Intermolecular forces in the self-assembly of peptide amphiphile nanofibers. *Adv Funct Mater* 16:499–508
136. Niece KL, Czeisler C, Sahni V et al (2008) Modification of gelation kinetics in bioactive peptide amphiphiles. *Biomaterials* 29:4501–4509
137. Beniash E, Hartgerink JD, Storrie H et al (2005) Self-assembling peptide amphiphile nanofiber matrices for cell entrapment. *Acta Biomater* 1:387–397
138. Bull SR, Guler MO, Bras RE et al (2005) Magnetic resonance imaging of self-assembled biomaterial scaffolds. *Bioconjug Chem* 16:1343–1348

139. Silva GA, Czeisler C, Niece KL et al (2004) Selective differentiation of neural progenitor cells by high-epitope density nanofibers. *Science* 303:1352–1355
140. Standley SM, Toft DJ, Cheng H et al (2010) Induction of cancer cell death by self-assembling nanostructures incorporating a cytotoxic peptide. *Cancer Res* 70:3020–3026
141. Zhang SM, Greenfield MA, Mata A et al (2010) A self-assembly pathway to aligned monodomain gels. *Nat Mater* 9:594–601
142. Deming TJ (2010) Regenerative medicine noodle gels for cells. *Nat Mater* 9:535–536
143. Burgess WH, Maciag T (1989) The heparin-binding (fibroblast) growth-factor family of proteins. *Annu Rev Biochem* 58:575–606
144. Leung DW, Cachianes G, Kuang WJ et al (1989) Vascular endothelial growth-factor is a secreted angiogenic mitogen. *Science* 246:1306–1309
145. Rajangam K, Behanna HA, Hui MJ et al (2006) Heparin binding nanostructures to promote growth of blood vessels. *Nano Lett* 6:2086–2090
146. Cardin AD, Weintraub HJR (1989) Molecular modeling of protein- glycosaminoglycan interactions. *Arteriosclerosis* 9:21–32
147. Lamm MS, Rajagopal K, Schneider JP et al (2005) Laminated morphology of nontwisting beta-sheet fibrils constructed via peptide self-assembly. *J Am Chem Soc* 127:16692–16700
148. Yang CY, Song BB, Ao Y et al (2009) Biocompatibility of amphiphilic diblock copolypeptide hydrogels in the central nervous system. *Biomaterials* 30:2881–2898
149. Betre H, Ong SR, Guilak F et al (2006) Chondrocytic differentiation of human adipose-derived adult stem cells in elastin-like polypeptide. *Biomaterials* 27:91–99
150. Arias FJ, Reboto V, Martin S et al (2006) Tailored recombinant elastin-like polymers for advanced biomedical and nano(bio)technological applications. *Biotechnol Lett* 28:687–695
151. Reiersen H, Clarke AR, Rees AR (1998) Short elastin-like peptides exhibit the same temperature-induced structural transitions as elastin polymers: implications for protein engineering. *J Mol Biol* 283:255–264
152. Ayres L, Vos MRJ, Adams P et al (2003) Elastin-based side-chain polymers synthesized by atp. *Macromolecules* 36:5967–5973
153. Nettles DL, Chilkoti A, Setton LA (2010) Applications of elastin-like polypeptides in tissue engineering. *Adv Drug Deliv Rev* 62:1479–1485
154. Yamaoka T, Tamura T, Seto Y et al (2003) Mechanism for the phase transition of a genetically engineered elastin model peptide (vp<sub>gig</sub>)(40) in aqueous solution. *Biomacromolecules* 4:1680–1685
155. Luan CH, Harris RD, Prasad KU et al (1990) Differential scanning calorimetry studies of the inverse temperature transition of the polypentapeptide of elastin and its analogs. *Biopolymers* 29:1699–1706
156. Urry DW, Trapani TL, McMichens RB et al (1986) N-15 nmr relaxation study of inverse temperature transitions in elastin polypentapeptide and its cross-linked elastomer. *Biopolymers* 25:S209–S228
157. Kim W, Thevenot J, Ibarboure E et al (2010) Self-assembly of thermally responsive amphiphilic diblock copolypeptides into spherical micellar nanoparticles. *Angew Chem Int Ed* 49:4257–4260
158. Nettles DL, Haider MA, Chilkoti A et al (2010) Neural network analysis identifies scaffold properties necessary for in vitro chondrogenesis in elastin-like polypeptide biopolymer scaffolds. *Tissue Eng A* 16:11–20
159. Dreher MR, Raucher D, Balu N et al (2003) Evaluation of an elastin-like polypeptide-doxorubicin conjugate for cancer therapy. *J Control Release* 91:31–43
160. Bidwell GL, Fokt I, Priebe W et al (2007) Development of elastin-like polypeptide for thermally targeted delivery of doxorubicin. *Biochem Pharmacol* 73:620–631
161. Wise SG, Mithieux SM, Weiss AS (2009) Engineered tropoelastin and elastin-based biomaterials. *Adv Protein Chem Struct Biol* 78:1–24
162. Hu XA, Wang XL, Rnjak J et al (2010) Biomaterials derived from silk-tropoelastin protein systems. *Biomaterials* 31:8121–8131

163. Kroger N, Deutzmann R, Sumper M (1999) Polycationic peptides from diatom biosilica that direct silica nanosphere formation. *Science* 286:1129–1132
164. Kessel S, Thomas A, Borner HG (2007) Mimicking biosilicification: programmed coassembly of peptide-polymer nanotapes and silic. *Angew Chem Int Ed* 46:9023–9026
165. Cha JN, Stucky GD, Morse DE et al (2000) Biomimetic synthesis of ordered silica structures mediated by block copolypeptides. *Nature* 403:289–292
166. Spoerke ED, Anthony SG, Stupp SI (2009) Enzyme directed templating of artificial bone mineral. *Adv Mater* 21:425–430
167. Altunbas A, Sharma N, Lamm MS et al (2010) Peptide-silica hybrid networks: biomimetic control of network mechanical behavior. *ACS Nano* 4:181–188
168. Meegan JE, Aggeli A, Boden N et al (2004) Designed self-assembled beta-sheet peptide fibrils as templates for silica nanotubes. *Adv Funct Mater* 14:31–37
169. Yuwono VM, Hartgerink JD (2007) Peptide amphiphile nanofibers template and catalyze silica nanotube formation. *Langmuir* 23:5033–5038
170. Pouget E, Dujardin E, Cavalier A et al (2007) Hierarchical architectures by synergy between dynamical template self-assembly and biomineralization. *Nat Mater* 6:434–439
171. Hern DL, Hubbell JA (1998) Incorporation of adhesion peptides into nonadhesive hydrogels useful for tissue resurfacing. *J Biomed Mater Res* 39:266–276
172. Jing P, Rudra JS, Herr AB et al (2008) Self-assembling peptide-polymer hydrogels designed from the coiled coil region of fibrin. *Biomacromolecules* 9:2438–2446
173. Vandermeulen GWM, Tziatzios C, Klok HA (2003) Reversible self-organization of poly(ethylene glycol)-based hybrid block copolymers mediated by a de novo four-stranded alpha-helical coiled coil motif. *Macromolecules* 36:4107–4114
174. Petrie TA, Garcia AJ (2009) Extracellular matrix-derived ligands for selective integrin binding to control cell function. In: Puleo DA (ed) *Biological interactions on materials surfaces*. Springer, New York
175. Weber LM, Hayda KN, Haskins K et al (2007) The effects of cell-matrix interactions on encapsulated beta-cell function within hydrogels functionalized with matrix-derived adhesive peptides. *Biomaterials* 28:3004–3011
176. Lutolf MP, Lauer-Fields JL, Schmoedel HG et al (2003) Synthetic matrix metalloproteinase-sensitive hydrogels for the conduction of tissue regeneration: Engineering cell-invasion characteristics. *Proc Natl Acad Sci* 100:5413–5418
177. Engler AJ, Sen S, Sweeney HL, Discher DE (2006) Matrix elasticity directs stem cell lineage specification. *Cell* 126:677–689
178. Jung JP, Jones JL, Cronier SA et al (2008) Modulating the mechanical properties of self-assembled peptide hydrogels via native chemical ligation. *Biomaterials* 29:2143–2151
179. Chun C, Lim HJ, Hong KY et al (2009) The use of injectable, thermosensitive poly(organophosphazene)-RGD conjugates for the enhancement of mesenchymal stem cell osteogenic differentiation. *Biomaterials* 30:6295–6308
180. Wu K, Yang JY, Konak C et al (2008) Novel synthesis of hpma copolymers containing peptide grafts and their self-assembly into hybrid hydrogels. *Macromol Chem Phys* 209:467–475
181. Yang JY, Xu CY, Kopeckova P et al (2006) Hybrid hydrogels self-assembled from hpma copolymers containing peptide grafts. *Macromol Biosci* 6:201–209
182. Yang JY, Xu CY, Wang C et al (2006) Refolding hydrogels self-assembled from n-(2-hydroxypropyl)methacrylamide graft copolymers by antiparallel coiled-coil formation. *Biomacromolecules* 7:1187–1195
183. Tzokova N, Fernyhough CM, Butler MF et al (2009) The effect of peo length on the self-assembly of poly(ethylene oxide)-tetrapeptide conjugates prepared by “click” chemistry. *Langmuir* 25:11082–11089

# Index

## A

Activated monomer (AM), 4  
Amido-amidate nickelacycles, 7  
Amine initiators, 5  
Amine-hydrochloride initiators, 11  
Amino acids, 1  
*N*-2-(Aminoethyl)-3-aminopropyltrimethoxysilane, 93  
 $\beta$ -Amyloid, 43, 146  
Arginine–glycine–aspartic acid (RGD), 137  
Arthropod cuticle, resilin, 94  
Artificial extracellular matrix (aECM), 91  
Aspartimides, 36  
ATRP, 93, 139

## B

Bait peptides, 64  
Biomaterials, 135  
Biomimicry, 137, 154, 157  
Block copolymers, 1  
Block copolypeptides, 14  
Blood, synthetic, 130  
Bone morphogenetic proteins (BMPs), 89

## C

Cell-penetrating peptide (CPP), 87  
Co-assembly, 27  
Collagen, 102  
Copolypeptides, 14  
Core–shell CdSe/CdS nanoparticles, 16  
Cu(I)-catalyzed azide-alkyne cycloaddition click chemistry, 93  
Cyclisation, 36  
Cytotoxicity, 129

## D

Deprotection, 19, 34, 121  
Dicyclohexylcarbodiimide (DCC), 32  
Diketopiperazines, 36  
Dipeptides, 152  
Dityrosine, 99  
DNA delivery, 130  
Docetaxel, 129  
DOX-loaded hyaluronan-*b*-poly( $\gamma$ -benzyl glutamate), 130  
Doxorubicin, 85, 119, 129  
Drug delivery, 84, 117, 135  
Drug depots, 89

## E

Elastin, 71, 73, 155  
Elastin-binding protein (EBP), 74  
Elastin-derived peptides (EDP), 76  
Elastin-like polypeptides, 71, 155  
Encapsulation, 117, 129, 140  
Enhanced permeability and retention (EPR), 129

## F

Fibrils, mixed, 46  
Fibrinogen, 144  
Fibroblast growth factor (FGF), 107, 154  
9-Fluorenylmethoxycarbonyl (Fmoc) group, 32  
Fluorescein isothiocyanate (FITC), 130  
Fmoc-RGD tripeptides, 152  
Functionalization, 27

## G

Glutenin, 102  
Group-transfer polymerization (GTP), 13

**H**

Hemoglobin, encapsulated, 130  
 Hexafluoroisopropanol, 60  
 Hexamethyldisilazane (HMDS), 12  
 Hyaluronan, 129  
 Hydrogels, 135, 139
 

- crosslinks, 141
- elastin-like polypeptide-based, 155
- PEG, 157
- peptide amphiphiles, 153
- self-healing, 150
- $\beta$ -sheet, 152

 Hydrogen bonds, 147  
 1-Hydroxy-7-azabenzotriazole (HOAt), 32  
 1-Hydroxybenzotriazole (HOBt), 32  
*N*-(2-Hydroxypropyl)methacrylamide (HPMA), 159  
*N*-Hydroxysuccinimide (HOSu), 32  
 Hyperthermia, 86

**I**

Immobilization, 140  
 Indocyanine green (ICG), 130  
 Insulin fibrils, 50  
 Inverse transition cycling (ITC) purification, 81  
 Isocyanocarboxylates, 10

**L**

Liposomes, 119  
 Lysyl oxidase, 76

**M**

Matrix metalloproteinases (MMP), 158  
 Membrane translocating sequence (MTS), 87  
 Microfibrils, 75  
 Molecular dynamics, 27  
 Molecular self-assembly, 143  
 Monodansylcadaverine, 62  
 mPEG-*b*-poly(L-lysine)-*b*-palmitoyl, 130  
 Muscle, 108

**N**

Nanocarriers, 88  
 Native chemical ligation (NCL), 121  
 Native extracellular matrix (ECM), 137  
*N*-carboxyanhydrides (NCAs), 1, 122, 138,  
 Nickelacycle initiators, 7

**O**

Organic–inorganic hybrids, 157  
 Oxazolone, 34

**P**

PAMAM dendron-poly(L-lysine) block, 123  
 PEGylation, 157  
 Peptide amphiphiles (PAs), 151  
 Peptide piperidines, 36  
 Peptide-diacetylene  $\beta$ -sheet, 59  
 PICsomes, 129  
 Poly(amino acid) hydrogels, 135  
 Poly( $\beta$ -benzyl-L-aspartate), 20  
 Poly( $\gamma$ -benzyl-L-glutamate) (PBLG), 8, 124  
 Poly(ethylene glycol) (PEG), 8, 53, 124  
 PolyHIPE, 93  
 Poly(hydroxyalkyl glutamines), water-soluble, 17  
 Poly(*N*-isopropylacrylamide)-*b*-polylysine, 123  
 Poly(L-lysine)-block-poly(L-cysteine) block copolypeptides, 15  
 Poly(sarcosine), 130  
 Poly(VPGVG), 78  
 Polymer–peptide conjugates, 157  
 Polymerization, 1–22, 92, 93, 119, 122–124, 126, 138, 139, 142, 144, 157  
 Polymers, 117  
 Polymersomes, 119  
 Polypeptides, 1
 

- elastomeric, 71
- resilin-like, 94
- side-chain-functionalized, 16

 Proline, to hydroxyproline, 74  
 Protein engineering, 122

**Q**

Q11, 55

**R**

Resilin, 71, 94  
 Resilin-like polypeptides, 71  
 ROMP, 93

**S**

Self-assembly, 27, 135, 143
 

- hierarchical, 37

 Shear flow, 151

Silk-elastin-like polypeptide (SELPs), 90  
Silk fibroin, 56, 98, 147, 156  
Solid-phase peptide synthesis (SPPS), 27, 30,  
121, 138  
Stimulus-responsive biopolymer, 93  
Subtiligase-catalyzed fragment condensation  
(SCFC), 122  
Swelling, 141

**T**

Tissue engineering, 90, 135, 139  
TMS-amine initiators, 14

Transglutaminase, 62  
Transition metal initiators, 6  
Trifluoroacetic acid (TFA), 121  
Trimethylsilyl dimethylcarbamate (TMSCD), 13  
 $\beta$ -[Tris(hydroxymethyl)phosphino]propionic  
acid (THPP), 91  
Tropoelastin, 72, 73

**V**

Vascular endothelial growth factor (VEGF),  
107, 154  
Vesicles, drug delivery, 117, 139